Development of tests and methods of analysis for multi-factor ageing, degradation monitoring and/or lifetime modelling of an electrical insulation system of electrical motors (used in electric vehicle)

Pawel Piotr Pietrzak

THÈSE

En vue de l'obtention du

DOCTORAT DE L'UNIVERSITÉ DE TOULOUSE

Délivré par :

Institut National Polytechnique de Toulouse (Toulouse INP)

Discipline ou spécialité :

Génie Electrique

Présentée et soutenue par :

M. PAWEL PIOTR PIETRZAK

le vendredi 6 octobre 2023

Titre :

Mise au point de méthodes d'essais et d'analyse permettant le test-multi-contraintes, le suivi du vieillissement et/ou la modélisation de durée de vie du système d'isolation employé dans les moteurs électriques utilisés dans

---

Ecole doctorale :

Génie Electrique, Electronique, Télécommunications (GEETS)

Unité de recherche :

Laboratoire Plasma et Conversion d'Energie (LAPLACE)

Directeurs de Thèse :

M. PASCAL MAUSSION

M. DAVID MALEC

Rapporteurs :

MME LUCIA FROSINI, UNIVERSITA DEGLI STUDI DI PAVIA

M. STEPHANE DUCHESNE, UNIVERSITE D'ARTOIS

Membres du jury :

M. HUBERT RAZIK, UNIVERSITE LYON 1, Président

M. ANTOINE PICOT, TOULOUSE INP, Invité(e)

M. DAVID MALEC, UNIVERSITE PAUL SABATIER, Membre

M. PASCAL MAUSSION, TOULOUSE INP, Membre

M. TAHAR HAMITI, NIDEC PSA EMOTORS, Membre

Abstract

Keywords: electic motor, insulation system, lifetime, ageing, modelling, prognostic

The growing concern for human generated negative impact on the environment pushes us into development of new technologies that would reduce that impact. One of the proposed solutions is to transform the road transportation. We could shift from using vehicles with thermal motors – directly burning fossil fuels – into electrical vehicles. An electric motor embarked into an electric car is impacted by many degrading factors during its lifetime. Among them high and fluctuating temperature, mechanical vibrations, environmental factors like humidity. Modern electric vehicle's motor is driven by an inverter. The motor is subjected to high frequency PWM voltage. All those factors have some impact on the lifetime of the Electrical Insulation System (EIS) of the motor. To assure optimal and cost-effective life cycle of the electric vehicle, there is a great interest to develop appropriate methods of testing. Methods that would provide information during both design and exploitation phases for prediction of lifetime.

The thesis explores the different factors with some more attention to cycling that is a degrading factor that have not been exhaustively studied so far. The existing methods for dealing with cycling are described, the impact of cycling was also studied experimentally. The impact of voltage, frequency and temperature was studied for twisted pairs in Partial Discharge accelerated tests. The voltage and frequency cycling did not confirm existence of such impact in the conditions of the experiment. It remains to be determined whether such an impact exists. On the other hand, there was a significant impact on the temperature cycling with higher amplitudes of temperature variation.

The last chapter of the thesis focuses on lifetime prognostic methods. An attempt at finding a degradation indicator is made. The Design of Experiments methodology is applied to PDIV evolution tests. A model of that evolution for multi-factor ageing tests is created. The model has some success in extrapolating the PDIV evolution in time but also between the levels of aging factors.

Résumé

Mots-clés : moteur electrique, system d'isolation, duree de vie, vieillissement, modélisation, pronostic

L'inquiétude croissante concernant l'impact négatif de l'homme sur l'environnement nous pousse à développer de nouvelles technologies qui permettraient de réduire cet impact. L'une des solutions proposées consiste à transformer le transport routier. Nous pourrions passer de l'utilisation de véhicules à moteur thermique - brûlant directement des combustibles fossiles - à des véhicules électriques. Un moteur électrique embarqué dans une voiture électrique est soumis à de nombreux facteurs de dégradation au cours de sa durée de vie. Parmi eux, les températures élevées et fluctuantes, les vibrations mécaniques et les facteurs environnementaux comme l'humidité. Le moteur d'un véhicule électrique moderne est piloté par un onduleur. Le moteur est soumis à une tension PWM à haute fréquence. Tous ces facteurs ont un impact sur la durée de vie du système d'isolation électrique (EIS) du moteur. Pour assurer un cycle de vie optimal et rentable du véhicule électrique, il y a un grand intérêt à développer des méthodes d'essai appropriées. Des méthodes qui fourniraient des informations pendant les phases de conception et d'exploitation pour la prédiction de la durée de vie.

La thèse explore les différents facteurs avec une attention particulière au cyclage qui est un facteur de dégradation qui n'a pas été étudié de manière exhaustive jusqu'à présent. Les méthodes existantes pour faire face au cyclage sont décrites, l'impact du cyclage a également été étudié expérimentalement. L'impact de la tension, de la fréquence et de la température a été étudié pour les paires torsadées dans des tests accélérés de décharge partielle. Le cyclage en tension et en fréquence n'a pas confirmé l'existence d'un tel impact dans les conditions de l'expérience. Il reste à déterminer si un tel impact existe. Par contre, il y a eu un impact significatif sur le cycle de température avec des amplitudes de variation de température plus importantes.

Le dernier chapitre de la thèse se concentre sur les méthodes de pronostic de durée de vie. Une tentative de trouver un indicateur de dégradation est faite. La méthodologie des plans d'expériences est appliquée aux tests d'évolution de la PDIV. Un modèle de cette évolution pour les tests de vieillissement multi-facteurs est créé. Le modèle a un certain succès dans l'extrapolation de l'évolution de la PDIV dans le temps mais aussi entre les niveaux des facteurs de vieillissement.

Podziękowania

Firstly, I would like to direct sincerest thanks to the members of the PhD defence jury: the reviewers, Mrs Lucia Frosini and Mr Stéphane Duchesne and the examinator Mr Hubert Razik. Thank you for agreeing to devout your time and technical expertise to the reading and reviewing of my PhD thesis manuscript and to be members of the jury.

Then, I would like to thank the people that directed me in my efforts of preparing this thesis. I thank Pascal Maussion, the director, David Malec, the co-director, Tahar Hamiti, the co-director from Emotors, Antoine Picot, Philippe Manfé, Loucif Benmamas and Richard Moore. They provided me with this opportunity and lead me along the way. They had patience and support for me when tough times came and I was ready to give up. They demanded from me when I was failing to demand from myself, and they thought of me better than I thought of myself at times. I am grateful for that.

I would like to express my thanks to those that came before me (scientifically). I thank Farah Selmeh and Mateusz Szczepański, the thesis was built on the foundations that they have laid with their doctoral work. Here, I also thank my friend Andrea Al Haddad, with whom I had the pleasure of cooperating on some experimental parts of this thesis.

I am grateful to all the people that I interacted with and that helped me during this almost four years in Laplace, the CODIASE group members, the MDCE group members, the technical and administrative staff at ENSEEIHT and UPS parts of Laplace. I would also thank the people of JV Emotors in Carrieres-sous-Poissy for the hospitality they offered me during my few visits there.

The thing that always made going back to the lab worth it, were the people, the friends I made and the atmosphere they created there. I would like to thank them all. To name some: my office mates, Quentin, Gregoire and Rashad, the ones than already left the lab, the doctors, Andrea, David, Joseph, Mohsin, Wojciech and the ones that are still there, Youssef, Abdulrahman, Lucas, Corentin, Lucien, Mattis, Paul, Alessandro, Evelise, Igor, Ryan, Daouda, Saif, Tara, Tania, Adrien, Jeremy and all the others that I failed to mention.

My thanks go also to my friends back in Poland and elsewhere, Agnieszka and Adam, Marta and Karol, Kasia and Michał, Anastazja and Wojciech, Jakub, Bartosz, and Artur. For being there for me when I come back and for keeping in touch when I am away.

I would like to address great thanks to my aunt Maria, without her I would not be in France, I am grateful for her continuous support and advice throughout the thesis. Many thanks to all my family, my sister Ania, my brother-in-law Adam and my parents, Ewa and Przemysław for their love and unwavering support of my decisions even if it meant me being far away.

Table of Contents

General Introduction

The thesis takes upon the task of investigating new ways to test and diagnose the insulation of electrical machines destined for electrical vehicles. Specifically, the investigated methods – of testing and analysing the results - are multi-factor ones. It is important to predict the lifetime while considering all the possible causes of ageing. After the initial period of bibliographic research and familiarisation with the topic, the two main axes of the research crystalised. First one was the cycling, it was discovered that the cyclic change of ageing factor had been far from being exhaustively investigated. In the scope of this thesis, multi-factor, including cycling, ageing experiments were performed. A method of evaluating the impact of cycling in cycling ageing tests is described and used. The second research axis is establishing a multi factor model of insulation degradation tracing by PDIV measurements.

The research topic was formulated in cooperation between LAPLACE (Laboratoire Plasma et Conversion d'Energie) and JV Nidec Stellantis. The research activities adhered to CODIASE (Commande et Diagnostique de Systèmes Electromécaniques) and MDCE (Matériaux Diélectriques en Conversion d'Energie). Most of the experiments were conducted in Laplace facilities which are part of the UPS (Université Paul Sabatier), most of the office hours were spent in Laplace located at ENSEEIHT (Ecole Nationale Supérieure d'Electronique, d'Electrotechnique, d'Informatique, d'Hydraulique et des Télécommunications).

The thesis is composed of four chapters, the titles and brief descriptions of their contents are included below.

Chapter 1: State of art on insulation ageing

The first chapter contains the context of the thesis as well as some basic knowledge in the topic of electrical machines and electrical insulation systems. The industrial context of electrical motors for electrical vehicles requires enumeration of various ageing factors that such equipment experiences as well as the test methods of them that are currently used in practice. The chapter finishes with a short section on multi-factor ageing testing techniques and modelling methods.

Chapter 2: Cycling tests for electrical machines, state of the art, analysis methods

The second chapter covers the state of art in cycling tests and modelling. It was concluded that the cycling for low-voltage machines was not a topic investigated at large. The research and standards on various kinds of cycling are nevertheless covered. The last section covers the methods of modelling the cyclic impact of the ageing factors.

Chapter 3: Cycling impact on ageing of twisted pairs and stators

The third chapter describes multi-factor cycling experiments that were done during the thesis. Firstly, a thorough investigation of the impact of various kinds of cycling on the lifetime of twisted-pair samples is described. The second part is dedicated to thermal ageing of stators of electrical machines for electric vehicles.

Chapter 4: Degradation of magnet wire modelling by PDIV evolution data

Finally, the fourth chapter covers long term experiments with multi-factor degradation tracing. The aged samples are twisted pairs. The factors imposed and controlled are voltage, voltage frequency and temperature. The value measured periodically is the PDIV. The collected data on PDIV evolution is the fitted onto models. Multiple experimental points of different combinations of ageing factors levels (following Design of Experiments method) permit to construct a predictive model of PDIV evolution.

Chapter 1.
State of the art on electrical insulation aging

1.1 Introduction

This chapter informs the reader on the background of the problems tackled during this PhD thesis. The title of the thesis lists multiple themes, namely development of multi-factor tests, analysis methods for them, ageing monitoring and lifetime modelling. All those themes are considered in the context of insulation in electrical machines for the future electric vehicles. The themes were established in cooperation with an industrial partner: the Joint Venture between Nidec and PSA (now Stellantis) by the name of Emotors. Therefore, the chapter contains some information about the research requirements from the industrial side of things.

The chapter covers the context that informs the decisions concerning the research made later. The first section contains the information on the company and their products under development. The developed motors are permanent magnet synchronous machines. Some basic information about this kind of electrical machine was included. Next sections focus on the electrical insulation systems (EIS). There are parts on materials commonly used in low-voltage electrical machines and on elements of an EIS. Then, the ageing factors and failure mechanisms resulting from those factors are discussed. The next part enumerates the procedures developed for testing of the insulation and the kinds of samples that are used for the tests. The final part presents in broad strokes the current state of the art on ageing and lifetime modelling with a focus on multi-factor methods.

1.2 Industrial context: Nidec-Leroy Somer, Stellantis, Emotors

This PhD thesis was achieved with support from JV (joint venture) Nidec PSA Emotors. The company is co-owned by Nidec Leroy Somer and Stellantis. Stellantis at the time of the start of the thesis was still PSA Peugeot Citroen but over the course of the thesis in 2021 merged with Fiat Chrysler to form Stellantis. Nidec is a company that designs and manufactures electrical machines. They are based in Japan. In recent years they acquired a French company of a similar profile - Leroy Somer based in Angouleme. PSA is a French car manufacturer, Fiat Chrysler, an Italo American one. After the merge in 2021 they formed Stellantis and placed fourth in the world in terms of market share of car manufacturers.

At the start of this doctoral process, PSA had one electric vehicle in commercial offer, but it was only the platform that was their own. The motor was outsourced or rather bought from a different company. The world that we live in now pushes us to pursue cleaner

technologies. The existing political incentives, both on the consumer and the producer side, promote development of low emission cars. The two mother companies brought to life the JV Emotors with the objective of developing their own line of electrical motors. More precisely, Stellantis has the goal to produce more than five million cars per year in 2030. The Stellantis side brought the automotive competence, the savoir-faire on how to make cars. They are able to define the operational conditions of the traction chain and the requirements posed on a motor to fulfil its mission. Nidec Leroy Somer brought electrical machine competences. They provide expertise on motor design, topology, performance and the control. An important part of the design of a machine is its insulation system. An adequately designed insulation assures longevity and safety of the machine.

At the time of writing of this thesis the first production line was already launched. The JV offers multiple solutions targeting different types of mobility. In their catalogue they offer a motor for Battery Electric Vehicle (BEV) or Fuel Cell Electric Vehicle (FCEV), a motor for Hybrid Plug-in Electric Vehicle (HPEV) and one for Mild Hybrid Electric Vehicle (MHEV).

1.2.1 400V Electric Vehicle e-Drive for BEV or FCEV

The motor dedicated for fully electric mobility where the electricity if supplied whether from a battery pack or from a fuel cell stack. It is a 6-pole Permanent Magnet Synchronous Motor. It can provide power between 60 kW up to 250 kW. The product consists of both the machine as well as the inverter driving the motor. Both are encapsulated in one compact casing (Figure 1-1).

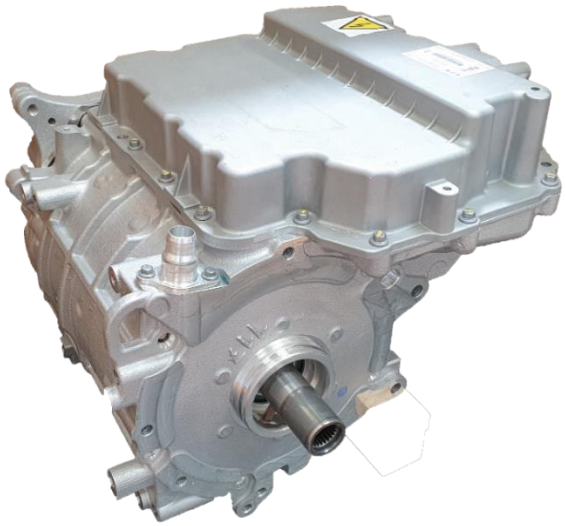

Figure 1-1 400V Electric Vehicle e-Drive. [1]

1.2.2 400V Plug-in Hybrid Electric Vehicle e-Drive

The motor dedicated for PHEV is a smaller machine outputting from 60 kW up to 120 kW of power. The Plug-in Hybrid requires charging of its battery from an outside source. Unlike in a full hybrid where the battery, apart from regenerative breaking, can be recharged by the internal combustion engine. The visualisation in Figure 1-2 shows the inverter, the permanent magnet rotor and the stator.

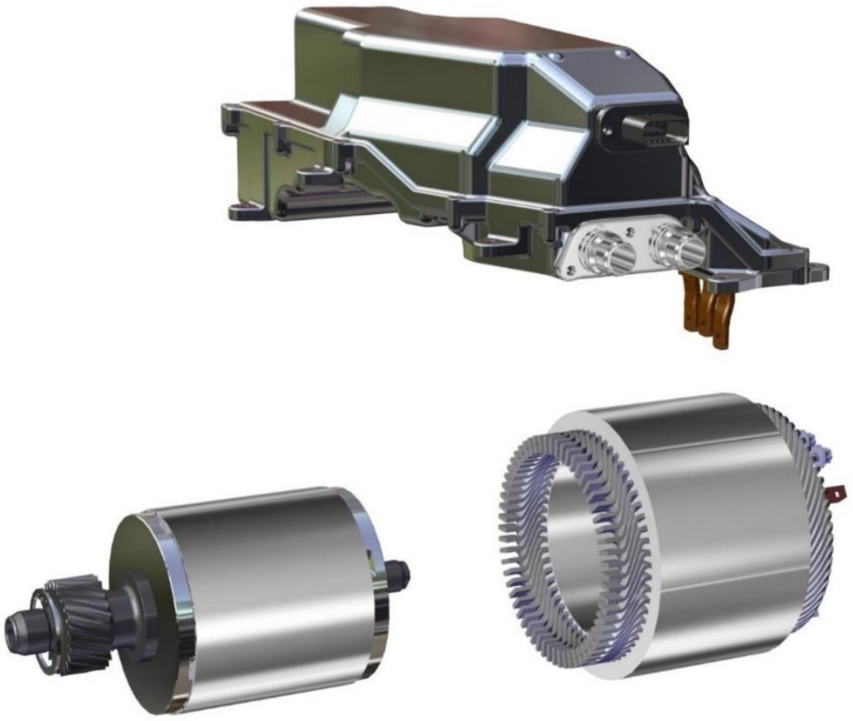

Figure 1-2 400V Plug-in Hybrid Electric Vehicle e-Drive. [1]

1.2.3 48V e-Drive for Mild Hybrid and Electric Vehicle

The smallest offered motor is a permanent magnet machine supplied by voltage of 48 V. It is dedicated for Mild Hybrid, where hybridisation is much less pronounced. The car does not have an electric-only propulsion mode. The motor is there to assist start-stop cycles of internal combustion engine in, for example, dynamic urban driving. The motor shown in Figure 1-3 can achieve power from 6 kW to 30 kW.

Figure 1-3 48V e-Drive for Mild Hybrid and Electric Vehicle. [1]

1.3 Synchronous Electric Motor for an Electrical Vehicle

A synchronous electric machine is a machine with a winding on the stator and windings or permanent magnets in the rotor. The Emotors machines make use of permanent magnets on the rotor, hence rotor winding insulation system is not discussed. The most common design of an electrical machine consists of three phases. The phases are fed with sinusoidal current (or current approximating the sinusoid). The currents between phases are spaced by 120 degrees on electrical phasor diagram. The phase shift between the three windings and strategic distribution of phases in the slots creates rotating magnetic field. The poles of the magnets in the rotor have no choice but to follow the rotating field to align with the rotating magnetic poles of the stator.

The rotational speed of the motor is thus linked directly to the rotational speed of the magnetic field created by the stator. For an application in an electric car, the interest is obviously to be able to control the speed. Historically a synchronous motor could have been controlled by a frequency changer where a physical change of circuit shifted between different number of primary winding's turns and different possible frequencies. Nowadays, all electric car motors are driven by an inverter. An inverter is a DC/AC static converter. The converter in an electric car is fed by the DC bus voltage sourced by a battery pack and outputs an alternating current. The control consists of instructions to the semiconductor switches in the inverter about the sequence and time of switching between open and closed states. What that means is that the inverter can seamlessly change the frequency of the current fed into the motor's windings and control the rotational speed of the rotor.

One way to classify electrical machines is by the form of the winding wire. We can distinguish two categories: random-wound and form-wound windings (shown in Figure 1-4).

In the first case, the position of an individual wire in a slot is not controlled or known, hence random. On the contrary, in form-wound windings, the position of each turn is perfectly known. When putting coils of copper into a slot of a machine we have an interest in dividing the wire cross-section as much as possible. That is because of the skin effect. When we run alternating current through a wire the flow will concentrate on the outer parts of the section of a conductor, the skin. That is also dependant on the frequency of the current. If we divide one conductor into multiple turns, we lose the core parts of section that would anyway be lost to the skin effect. It is one of the factors that leads to prevalence of the random-wound scheme in smaller machines. We gain the surface by fighting the skin effect but, on the other hand, the slot filling factor worsens. Some section must be taken by the enamel on each individual turn. Also, the round wires, when packed together, will leave some empty spaces in between them. A random-wound machine was historically wound by hand, recently it can be automatised in various degrees. Still, it is more time-consuming process and less process-capable than the winding of a form-wound machine.

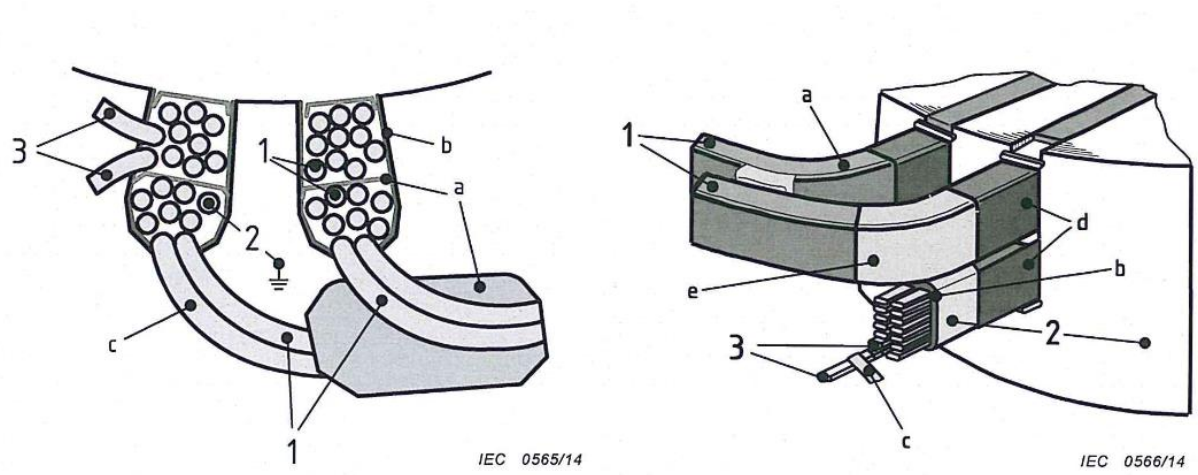

Figure 1-4 Random wound (left) and form wound (right) slots of a stator [2]

The form-wound scheme was more popular in bigger machines like the hydro plant generators. The size of the slot works against using enormous numbers of very thin wires. If the diameter were to be increased the fill factor would suffer significantly. Additionally, in a bigger machine with a sufficiently deep slot the magnetic field is ununiformly distributed in the radial direction. That causes unequal induction in the wires deeper in the slot and those closer to the slot surface. In order to prevent the axial current that would result from such a potential difference a setup called Roebel bar is applied [3]. All the rectangular wires assembled in the bar traverse the slot at an angle so that the average depth in the slot is equal for all. The form-found wire assures an excellent filling factor. The trend for machines dedicated for electric vehicles, which compared to generators, are small machines, is to wound them with rectangular wire. It turned out that it is possible to highly automatise the process. The wire is formed into a shape called ‘hairpin’ (shown in Figure 1-5). Packets of such hairpins can be placed into the slots of a stator and welded on the other side. Compared

to the winding process of a random-wound machine a lot of time is saved. This opens other engineering problems, for example one must assure proper and repetitive welding that does not damage the insulation.

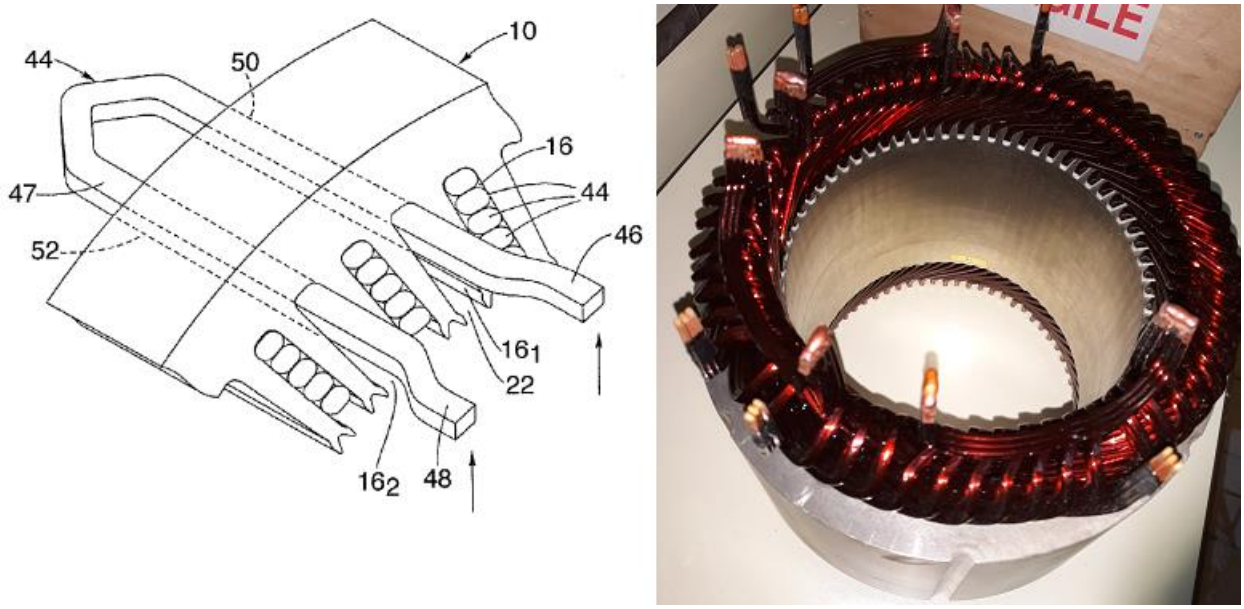

Figure 1-5 A diagram of a hairpin formed wire inserted into a slot of a stator.[4]

The distribution of phases in the stator varies. One of the possibilities is to have two different phases in a slot where two phases meet. This results in smoother rotating magnetic field. In some cases, two different phases occur in one slot. That has some consequences for the insulation system, namely, the inter-turn insulation is at the same time the inter-phase insulation.

1.4 Electrical Insulation System of an Electric Machine

1.4.1 Dielectric materials in a low-voltage electric machine.

Electrical insulation in an electric machine comes in many forms, among them the enamel, insulating paper and tapes, impregnation resin. Depending on the destination, the insulation part is made of a material that assures fulfilment of its function during its designed lifetime.

The enamel is a layer of polymer stuck to a conducting wire. The process of covering a wire dedicated as a magnet wire in an electric machine is an integral part of manufacturing of said wire. The common materials for enamel are polyesterimide (PEI), polyamideimide (PAI) and polyimide (PI). They have different mechanical properties, chemical resistances and thermal endurance.

Table 1-1 Organic polymers used for electric machine magnet wire enamel [5] [6].

Material name	**Shortcut name**	**Temperature Index**	**Specifics**
Polyurethane	PUR	155 180	Not for high current of high temperature applications Solderable
Polyester	PES	150 185	Not good for high moisture applications
Polyesterimide	PEI	180 200	Improved thermal properties compared to polyester
Polyamide imide	PAI	200 220	Resistant to high temperature, good mechanical properties Resistant to chemicals and moisture
Polyimide	PI	240	Resistant to high temperatures Resistant to continuously high operating temperatures and intermittent severe overloads
Polyimide/Polyamide-imide	PI/PAI	260	Very resistant to high temperatures
Nano-filled polyimide	PI	280	

The paper comes in form of sheets or rolls resembling actual cellulose paper. They are often composites of layers of various insulating materials (often referred by their commercial names Nomex, Kapton, Mylar). Nomex is a meta-aramid, it is flame and heat resistant (can withstand temperature up to 370 °C) and have good chemical resistance. Kapton is a polyimide film, it can operate in a very wide range of temperatures (-269 °C to 400 °C) but is somewhat lacking in mechanical durability and ages poorly when exposed to humidity. Mylar is a name for polyethylene terephthalate (PET) film, characterised by high tensile strength and good dimensional and chemical stability.

The enamel is typically an organic resin. The resin is the last part of the insulation system to be introduced into the electric machine. Once all the other parts are set in their places the stator is impregnated. The techniques vary but the main interest of all of them is that the resin has to penetrate all the spaces in the machine slots in order to leave a minimum amount of air bubbles areas. After the resin is introduced, it is cured with elevated temperature and as a result it solidifies. Three primary materials are commonly used as the

impregnation of low-voltage machine [7]. Epoxy based, polyester-based and polyesterimide-based. Polyester-based are easy to introduce in between the insulation parts. They have worse mechanical properties, are more brittle and are weaker dielectrically at high temperatures. The epoxy-based liquids are more viscous which makes it more problematic to introduce them into the machine. They have excellent mechanical properties and chemical resistance. Polyesteramides liquids have similar properties to the polyester-based but have better thermal properties at high temperatures. Resins with micro and nano particles mixed in show additional properties. Certain nano particles were demonstrated to help to endure PDs and lengthen lifetime of the insulation by an order of magnitude. Alternatively, instead of impregnation, the self-bonding magnet wire can be used. In that technology, the turn-to-turn wire is coated with additional layer of material, which, upon introduction of heat or solvent, bonds with adjacent turns.

1.4.2 The elements of Electrical Insulation System

An Electrical Insulation System (EIS) of an electrical machine consists of multiple parts. One way to divide the insulation is by its function as in what are the two objects that it separates. In this logic we have the turn-to-turn insulation, phase-to-phase insulation, phase-to-ground insulation and the impregnation.

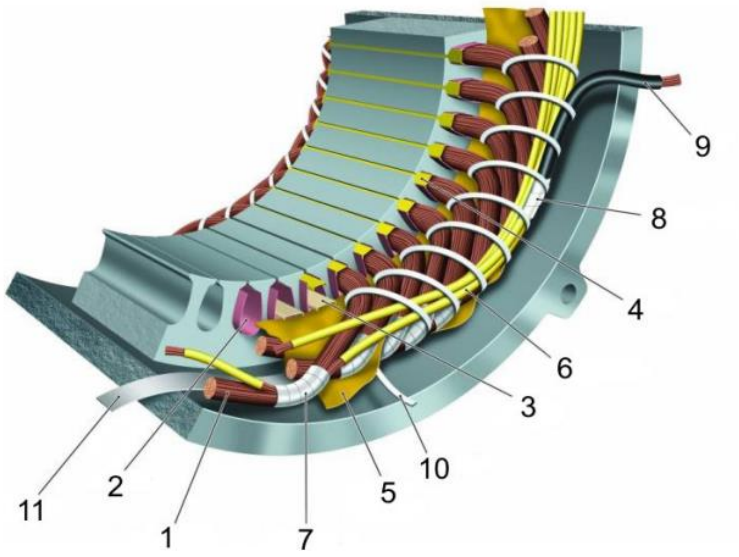

Figure 1-6 Overview of materials in a low-voltage insulation system (random wound winding): 1 turn insulation, 2 slot liner, 3 slot separator, 4 wedge, 5 phase separator, 6 lead sleeving, 7 coil-nose tape, 8 connection tape, 9 cable, 10 tie cord, and 11 bracing [7].

1.4.2.1 The turn-to-turn insulation

The turn-to-turn insulation assures separation between the wires of one coil. In theory turns of the same coil should be at the same electrical potential but it is not true for

transients, change of voltage propagates with a delay. If one or multiple turns were to be shorted there would be less current over section of the slot which would result in some imbalance in the magnetic field generation. Also, the shorting contact point could be a resistance choke point generating excess heat, further aggravating the problem. The separation between turns is assured by enamel on the wires and, to some extent, by the impregnation.

1.4.2.2 The phase-to-phase insulation

The phase-to-phase insulation separates different phases. In a typical three-phase machine there are 120 electrical degrees between any two phases. If one phase is at its peak value one of the others has an opposite polarity. Hence, there is a significant difference in potential between phases. Wires carrying different phases cross paths in the end-winding space but also if the design calls for it, two different phases share one slot. As shown in Figure 1-6 the random-wound machine is equipped with phase separator tape (5) and slot liner (3) to tackle the mentioned insulation needs. However, in case of a form-wound low-voltage machines it is common practice to skip those two elements. The end-windings rigidness assures that there remains a gap between them. On the other hand, the contact in a shared slot means that the phase-to-phase insulation is of the same properties as turn-to-turn insulation, the enamel supported by impregnation.

1.4.2.3 The phase-to-ground insulation

The phase-to-ground insulation creates a barrier between the windings and the stator's iron. There is also no separation between the stator and the motors casing, for the possibility of a short to the ground the motor requires a ground fault monitoring system, otherwise may pose a risk to the user. The separation between the magnet wires and the slot walls exists in the first place as the enamel on the wire. It is then strongly reinforced by the slot liner, the insulating paper covers all the surface of every slot.

1.4.2.4 The impregnation

The impregnation is the last part of the insulation system of an electric machine. When it comes to the qualification from above it adds to insulation of each of the mentioned separation configurations. The impregnating resin, apart from the insulating function, serves as mechanical support and heat removal path improvement. The solidified resin holds the windings in place and absorbs their vibration. The conductors carrying current are subjected to Lorenz force oscillating radially with twice the frequency of the current injected by the inverter. The current running through the windings creates heat (Joule's losses). Some machines are cooled down by liquid that circulates in small canals inside the copper wires [8], shown in Figure 1-7. However, in most cases the heat has to be pushed through layers of

insulation into the stator or the end-winding where the cooling system evacuates it. Hence, it is important that the resin has sufficient thermal conduction properties. Thermal Conductivity of epoxy resin is about 0.2 W/mK, number that can be raised by mixing in various micro and nano particles.

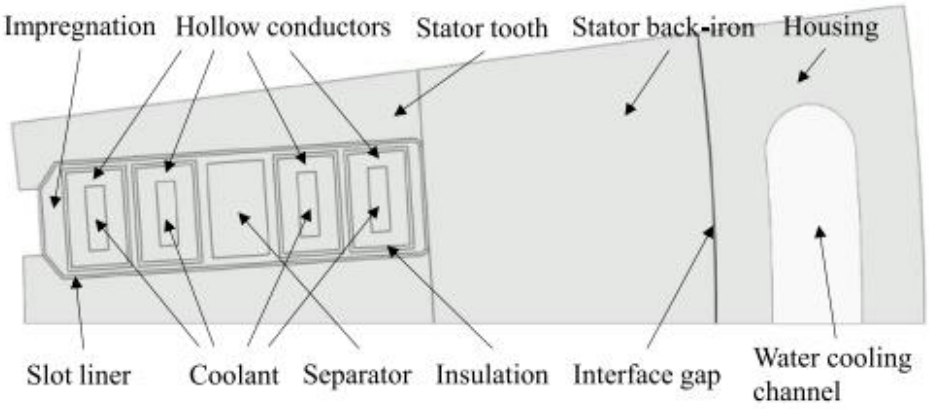

Figure 1-7 The hollow conductors with coolant that evacuates the heat created due to Joule's losses. [8]

1.5 Ageing factors of an Inverter-fed machine

A standard [9] provides an exhaustive summary of the failure mechanisms with the respective ageing factors responsible for their occurrence.

The ageing or degradation in an EIS is produced by:

- Processing, Manufacturing, Transport, Installation,
- Thermal, Electrical, Mechanical and Environmental Stress,
- Abuse, Accidents and Misapplication.

Some of the mentioned causes results in contamination or defects of the EIS. Under contamination there are impurities, particles, by-products, moisture and material incompatibilities. Among defects cavities, protrusions, cracks, missing components, wrinkles, processing errors and discontinuities are mentioned.

1.5.1 Electrical stress

The electrical stress takes various forms. There are Direct Current and Alternating Current. Often what applies to DC stress does not apply to AC stress. The AC may be a mains-fed system or an inverter-fed one with high frequency voltage, that also constitutes differences in mode of ageing [10] [11]. Within the bracket of electrical stress also transients are included. High switching frequency may cause overvoltage that result in partial discharge inception[12], [13].

The standard mentions the following results of electrical stress causing ageing and leading to a failure of an EIS:

- Intrinsic breakdown
- Surface, corona and partial discharges
- Absorption and conduction current
- Charge injection
- Water treeing
- Cavity formation and expansion, mechanical rupture

The modes are often interconnected. For example, it is marked that the absorption and conduction current may lead to a temperature rise in the insulation and add the effect of thermal ageing thus accelerating deterioration.

1.5.2 Thermal stress

There are multiple sources of heat in an electrical machine and a few specific for one dedicated for an electric vehicle. The current running through the windings causes resistive losses in the copper. The created rotating magnetic field causes eddy currents in the stator plates which also heat it up. The amount of heat created depends on the driving profile. Higher demand for power will naturally increase the temperature, a lot of start-stop cycles will add the thermo-mechanical aspect of thermal ageing. The electric vehicles are being designed for wide range of environments, they need to meet both the needs of sub-zero and hot weathers. The electric motor depends on its cooling system to evacuate the excess heat, problems with heat management on board of a car may lead to premature failure of an EIS.

The standard names the following results of ageing by thermal stress leading to a failure of an EIS:

- Change in state of the material: Melting, Vaporisation, Crystallisation, Re-crystallisation, Glass transition, Morphological changes.
- Chemical reactions and subsequent material modifications: Polymerisation, depolarisation, reduced mechanical properties, formation of hydrophilic compounds, formation of conducting compound, water absorption and others.
- Thermomechanical ageing leading to cracks and delamination.
- Modification of repartition of electrical stress due to changes in state and from.

1.5.3 Mechanical stress

An electric motor embedded in an electric vehicle has to withstand additional mechanical constraints. The machine and its EIS need to be tested for its endurance against the road conditions: the mechanical vibration and other mechanical stress that are connected with it.

The standard names the following results of ageing by mechanical stress leading to a failure of the EIS:

- Enhancement of electrical stress due to change of form by fatigue, rupture, creep of conductor, abrasion.
- Fatigue leading to cracks, delamination and loss of mechanical strength, loss of continuity of the insulation.
- Cracks and delamination leading to penetration by external contaminants.

1.5.4 Environmental stress

Among the environmental stresses that the standard mentioned are exposure to gasses, conducting or insulating liquids, pollution, radiation and mechanical stress. While more exotic stress like radiation is not particularly significant for electrical vehicles, humidity certainly is. The standard qualification tests of EIS require a cycle of exposure to moisture for this reason. The impact of humidity on ageing was researched [14] [15] in a context of its synergy with electrical stress. At higher humidity the PD magnitude was higher and the lifetime shortened.

Increased conductivity caused by environmental contamination results in temperature rise and modification of electric stress distribution. Water contamination leads to water treeing and in time to breakdown. Contamination of the surface leads to surface discharges, then erosion of the material, chemical reactions and material modifications. In summary, various environmental factors have many synergetic impacts on degradation and high potential of aggravating effects starting due to another stress factor.

1.6 Existing test methods and protocols

1.6.1 Test in the standards

The IEC standards propose a range of tests for electrical insulation. The actual processes relevant to a specific field (as for example low-voltage electrical machines and enamelled wires used in them) can be found across multiple documents. The standards are organised in a web of dependencies. The higher order standards describe generalities for whole category of materials or equipment, while additional parts give more precise guidelines how to test specific kind of objects.

The standards distinguish between procedures of Temperature Index (TI) attribution for Electrical Insulation Material (EIM) and Electrical Insulation Systems (EIS). The distinction is made in the standard defining the Thermal Classes [16]. The EIM are simpler, more basic objects like enamelled wires, insulating papers, while the EIS encompasses complex applications like electrical machines that may consist of multiple EIM. The standard

remarks that an EIS consisting of EIMs which TIs are known, does not automatically inherit their TI.

1.6.1.1 Electrical Insulation Materials

The general procedures for establishing the Temperature Index (TI) for EIM are described in IEC 60216-1 [17]. The standard establishes basic terms and various methods that can be chosen depending on specific situation. The different thermal classes are defined in other standards like [16]. They attribute a Thermal Class as a number. The number signifies the temperature in Celsius at which the material is supposed to survive for 20 000 h, in the most common case.

The number of samples, data points (data points being the temperatures at which the experiments take place) and heating methods are discussed. The standard requires that we do not extrapolate the TI more than 25 K. For example, if the supposed TI is 200 °C, the lowest temperature among the set of the chosen data points cannot be higher than 225 °C. As the heating method, heating in an oven or a climate chamber is proposed as a reliable and cost-effective mean.

The standard makes it clear that Thermal Endurance characteristics (so Temperature Index and Halving Interval – a rise in temperature that causes the lifetime to be halved) only make sense when they come with the information on the methodology of obtaining it. The standard recognises that the measured state of deterioration of the material may differ depending on the choice of the traced property. The standard considers three possibilities of establishing end-of-life criterion. The possibilities are the non-destructive test, the proof test and the destructive test.

The non-destructive tests are ones that measure a chosen property of the insulating material. The samples are taken out of the oven in between thermal exposure cycles, cooled down to ambient temperature and then the property is measured. The end-of-life of a sample is proclaimed when the measurement reaches a preconceived end-point criterion value. The property may be one that increases or decreases over the course of ageing. The end-of-life criterion is expressed as a percent of to the initial value. Figure 1-8 shows an example where the endpoint is set at 50% of the measured characteristic.

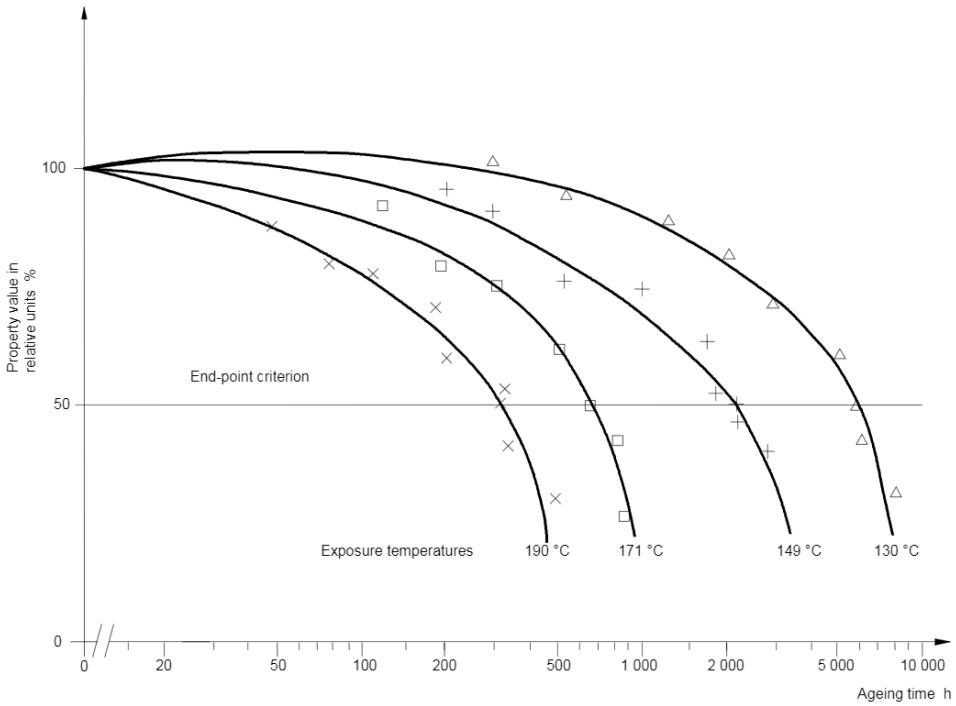

Figure 1-8 The end-point criterion example [17]. The standard shows an example data for four temperatures and evolution of the measurement in the non-destructive test paradigm of establishing the TI.

The proof test end-of-life model requires a pass-fail test done periodically on the samples. They are taken out of the oven and the test is administered. The ones that pass are put back in the oven, the ones that fail are considered at the end-of-life. The time between the last passed test and the failed one is recorded as the endpoint.

In the destructive test case, multiple sets of samples are aged together but some are removed earlier than others. After each ageing cycle one set of samples is removed from the oven, cooled down and a destructive test is administered. It may be a test like the Breakdown Voltage test. The voltage upon the material is gradually increased until the breakdown occurs. The voltage is recorded for each sample. The method requires significantly more samples than the two previous ones. Moreover, the data obtained in a destructive test are not compatible with the next step of TI attribution.

1.6.1.2 Enamelled wire

In order to obtain the TI of enamelled wires one would have to apply guidelines from standard 60172 [18]. The standard contains details on sample manufacturing, both for wires of a round section and those of a rectangular section. The samples undergo a voltage proof test before first thermal exposure. For round wire the voltage depends on the insulation thickness, for the rectangular one the value is arbitrarily set to 1000 V AC. The period between the proof tests during thermal ageing is specified depends on the ageing temperatures chosen.

Logically, the higher the temperature compared to estimated TI, the shorter the periods between measurements. Lifetime in higher temperature is shorter, so this way more points are obtained. The proof voltage depends on the insulation thickness as shown in Figure 1-9.

Table 2 – Proof voltage for round enamelled wire

Increase in diameter due to the insulation (mm)		Voltage (rms)
Over	Up to and including	
–	0,015	300
0,015	0,024	300
0,024	0,035	400
0,035	0,050	500
0,050	0,070	700
0,070	0,090	1 000
0,090	0,130	1 200

Table 4 – Proof voltage for tape-wrapped round and for enamelled or tape-wrapped rectangular wire

Increase in dimension due to the insulation (mm)		Voltage (rms)
Over	Up to and including	
0,035	0,050	300
0,050	0,065	375
0,065	0,080	450
0,080	0,090	550
0,090	0,100	650
0,100	0,115	700
0,115	0,130	750
0,130	0,140	800
0,140	0,150	850

Figure 1-9 Tables specifying the proof voltage during ageing tests for enamelled wires [18].

1.6.1.3 Electrical Insulation System of a Low-Voltage Machine

More relevant Thermal Endurance characteristics standard for the scope of this PhD thesis is the one that covers the methods for low-voltage EIS [19]. In principle the contents of the standard describing EIS evaluation are like those of EIM evaluation. They base on a comparison of the candidate EIS and an EIS proven in service. An important difference from EIM evaluation is that the EIS evaluation requires a pre-diagnostic exposure step. The samples after each thermal ageing period (called cycle in the standard) should be exposed to both mechanical stress and moisture before a diagnostic test. The mechanical stress is delivered by vibration table, it is an hour of sinusoidal vibrations at a frequency of 50 to 60 Hz and acceleration of about 1.5 g. The moisture exposition is done at a climate chamber for 48 hours at humidity of 95 to 100%. Subsequent voltage diagnostic test (or rather proof test if we follow the nomenclature of EIM process discussed above) is performed immediately after the samples are removed from the climate chamber.

The standard 60034-18-31 [20] proposes testing procedure for complete machines. The Thermal Endurance test serve the purpose of attributing a comparative characteristic of TI. These norms tackle the problem of testing machines to qualify them for use.

This particular part of the 60034-18-31 standard concerns machines with insulation system of type I, the ones that do not experience partial discharges during its normal operation. Overall, the standard subscribes to the idea of comparative evaluation. After obtaining a curve of relationship between temperature and time till the end-of-life that curve is compared to data from another system already validated in the field operation. What is meant by validation is that the data is supposed to be real ageing data, not accelerated ageing data.

The standard repeats the proposition of additional pre-stress in its protocol. There is an initial mechanical stress exposure, a vibration with frequency of 60 Hz, acceleration of 1.5 g and lasting one hour. Then the samples spend 48 h exposed to humidity of 95% to 100%. The standard proposes additional diagnostic measurements to trace the ageing. Insulation Resistance, Partial Discharge test, Dissipation Factor and Capacitance measurements are mentioned but the norm suggests that making any measurements of choice is possible. Subsequently comes the diagnostic test, the standard specifies voltage for AC high potential tests and impulse voltage test described in IEC 60034-15. At last, the samples are put in the oven for the thermal exposure. The exposure is done in cycles, predetermined periods that are separated by the breaks for diagnostic measurements. The temperature and length of each cycle are determined by tables in the standard. They are supposed to be chosen in a way that assures about 10 thermal exposure cycles. The end-of-life of a sample is pronounced when it fails the proof test.

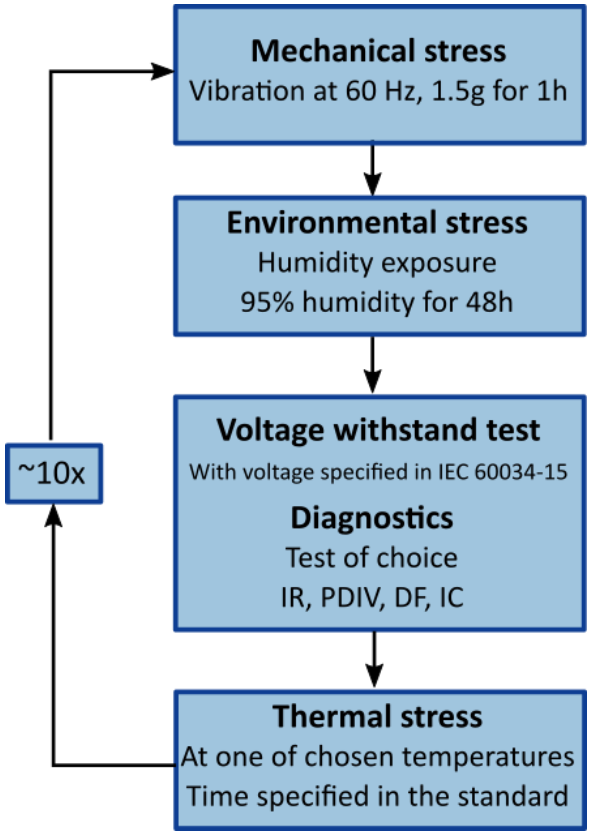

Figure 1-10 The test protocol for a type II EIS qualification test from IEC 60034-18-31

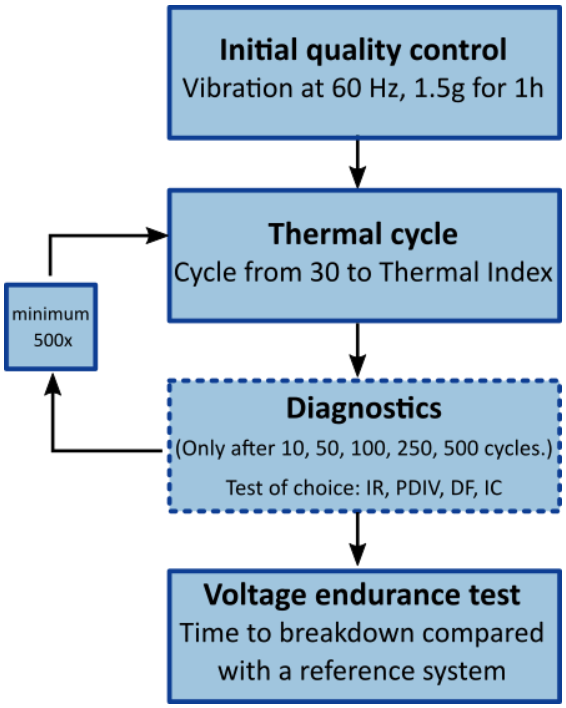

Figure 1-11 The test protocol for a type II EIS from IEC 60034-18-34 The cycling test.

Another interesting test protocol appears in Part 34 of the same standard. The test is dedicated for the form-wound machines with the type II insulation system. It is recognised that the insulation in such machines may undergo thermomechanical stress. A stress that appears during a change of temperature of EIS. The change causes a sheering stress between materials of different coefficients of thermal expansion. The standard is written with large machines, like hydro plant generators, in mind. It is sometimes assumed that the small size of low-voltage machines makes the thermomechanical forces insignificant as an ageing factor [21], [22].

The sequence of IEC 60034-18-34 consists of an initial quality test which singles out weaker samples that may be eliminated from the test. Then comes the cycling part, the samples are subjected to temperature rise from 30°C up to the Temperature Index. The process is shown in Figure 1-11.

1.6.2 Test samples

1.6.2.1 Electrical Insulation System and Electrical Insulation Material

One way to classify the samples for tests of an EIS of Electrical Machine is the complexity level. The more complex the sample the closer it emulates the real system. On the other hand, those complex samples pose a risk of producing less homogeneous populations. The dispersion of result widens the confidence interval and may make it harder to draw conclusions about the system. At the top of the complexity classification there are the

complete machines, the stator, the rotor with full EIS. One way of narrowing the confidence interval is to experiment with higher number of samples, but it is often not economically viable to use large number of stators for evaluating the insulation. Moreover, at the stage of design the final version of the EIS simply does not yet exist. The possible commonly used samples for EIS testing, aside from a stator, are: statorettes, motorettes, back-to-back sample and twisted pairs. The samples are described further in this section.

The choice of the test sample is dictated by what are we trying to establish, which part of insulation are we trying to evaluate. When it is the EIM that is tested what is typically needed is the characteristics like Thermal Endurance. It is performed by the manufacturer in order to provide the information for a designer. They need the information when they are making a decision on the material to choose for the insulation system being designed.

1.6.2.2 The turn-to-turn and phase-to-phase insulation

The simplest sample that one can think of when testing elements of an electrical machine system is a twisted pair for random-wound machine and a back-to-back sample for form-wound machines. They emulate the turn-to-turn insulation and, in the case of the systems where two phases meet in one slot or cross in the end-winding, the phase-to-phase insulation.

The twisted pairs (Figure 1-12) are commonly used in both standardised tests and in research. It is the base for thermal ageing tests in attribution of Thermal Class. Researchers extensively use twisted pairs in research for life prediction, stressing the samples thermally, mechanically and electrically. A lot of examples of research with twisted pairs was done in the domain of Partial Discharges.

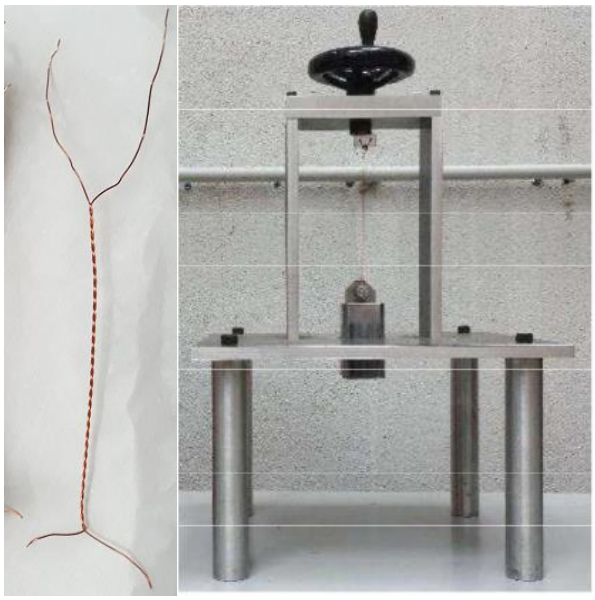

Figure 1-12 A twisted pair and the apparatus employed in its manufacturing.

The back-to-back sample for rectangular wire is established in the standard. However, the application of this kind of wire is somewhat of a new trend in low-voltage electric machines. There is a push for updates in standards in order to accommodate the lack of dedicated tests for low-voltage form-wound insulation systems [23] [24]. The back-to-back is normally wound by a tape in order to maintain the contact between the two wires that make up the sample. The method seems like something that would not result in good repeatability. It is hard to assure perfect flatness of the two surfaces or similar force during manual taping of the sample. No research on dispersion of such samples has been performed so far.

An alternative sample is one that is, instead of being held together by a tape, stuck between two metal plates. The metal plates have a number of holes where screws can fit though. The plates are screwed together with the pair in between, some measures have to be taken so that the contracting force is uniform and repeatable between samples. The alternative sample not only gives better control over manufacturing process but also adds the possibility of emulating the phase-to-ground part of insulation if some insulating paper is added between the wire and the metal plate.

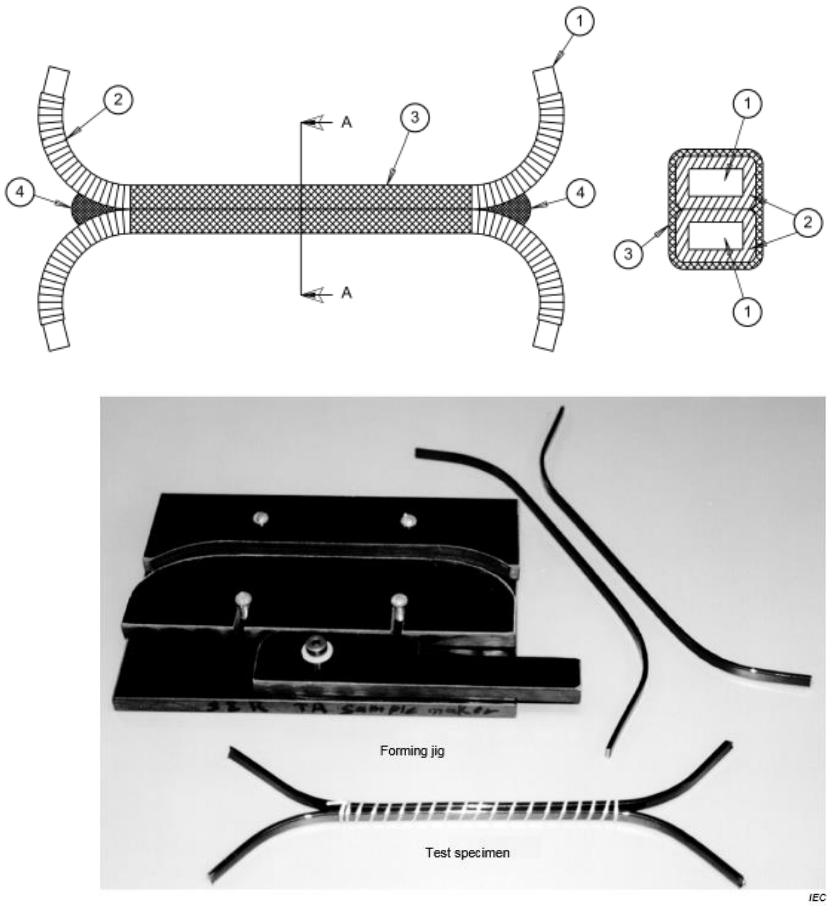

Figure 1-13 The back-to-back sample forming equipment and an example of a back-to-back sample stuck together with a tape [18]. 1 – the copper wire, 2 – the enamel, 3 – the tape for holding the two wires together, 4 – the separator at the PD vulnerable spot at the triple point.

Back-to-back sample was also used for high-voltage machines [25]. The thermo-mechanical ageing was applied and different cooling methods were compared. The bars were tested outside of any slot. It rose a question whether the bars being in a slot is not an important factor in both the process of cooling down and the occurrence of thermo-mechanical stress.

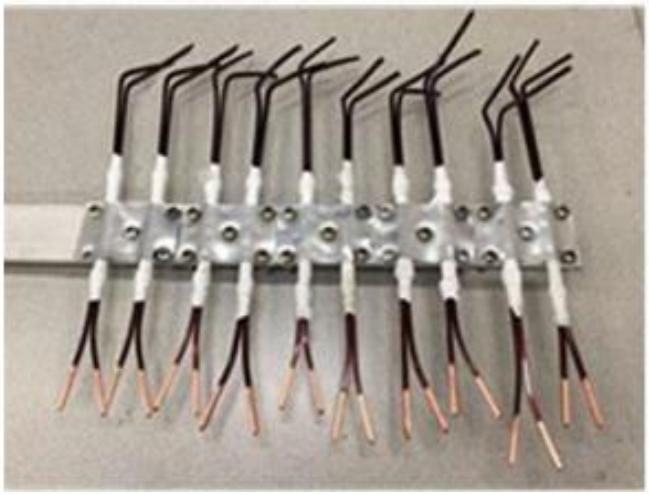

Figure 1-14 The back-to-back samples fixed on a metal band in order to apply mechanical vibration simultaneously with thermal factor. [24]

1.6.2.3 The phase-to-ground insulation

In order to include the phase-to-ground part of the insulation system, the experimental sample must consist of a part that emulates the presence of a stator. That is partially achieved in the aforementioned back-to-back sample but the standards and previous research have more to offer in this matter.

The nomenclature for the device is non-uniform across the literature. Three names are used interchangeably, some call them formette, some call them motorette while other call them statorette. The name formette applies mostly to setups with form-wound rectangular bar and formette is used for random-wound round wire samples. A formette and a motorette appear to be something farther away from a stator than a statorette. The formette gives a form to the insulation that it may have in a stator or a rotor, while a statorette inherits more stator characteristics like volume and material. A formette may be made of metal plates [20], while a statorette will tend to resemble a stator section [24]

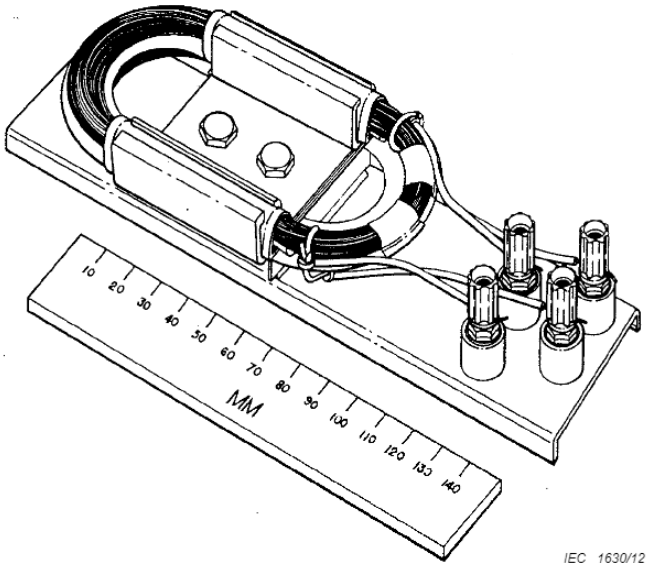

Figure 1-15 A motorette as described in IEC 60034-18-21 [26].

Figure 1-15 shows an example of a motorette proposed by the standard for testing insulation system parts for rotating inverter-fed electric machines. The device consists of two enamelled round wires wound into coils. The coils are separated one from another by a sheet of insulation. Also, each coil has a layer of insulating paper where it touches the slot. Alternatively, the standard describes a motorette for montage on a pole for DC machines.

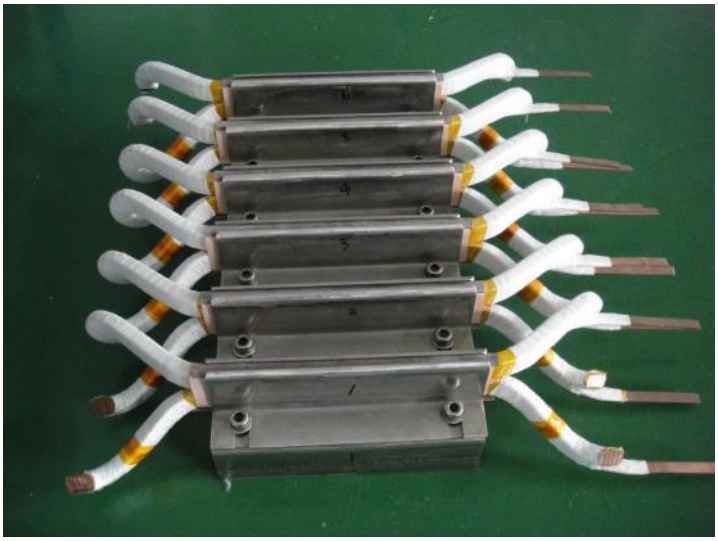

Figure 1-16 A formette for high-voltage form-wound machine qualification test [20].

The IEC 60034-18-31 describes the production details of a formette dedicated for thermal endurance evaluation of inverter-fed rotating machines. The standard proposes a device that emulates multiple conductive bars in their respective slots. Each bar belongs to a coil that spans two slots, thus the device has both phase-to-ground and phase-to-phase insulation. Part 32 of the same standard suggests that for electrical endurance evaluation each

slot should contain two independent bars rather than coils spanning two slots. Presumably for the reason that when voltage is applied between two bars there is a certainty that it is exactly the one sample that is tested and not its pair in another slot.

This kind of sample was used in research for multi-factor test [27]. It was observed that the simultaneous application of stressing factors yields more degradation when compared with single-stress tests or sequential multi-stress tests. A modified version of these samples was applied specifically to research thermo-mechanical ageing [28]. The samples were diagnosed with Dissipation Factor (DF) and Partial Discharge (PD) tests which did not show significant difference. Only comparison of delamination (the tap test, which consists of tapping the surface of the insulation to check whether it would flake off) and Breakdown Voltage. The DF and PD patterns were before found to be appropriate tests to evaluate the thermo-mechanical ageing [29] [30]. The sample in Figure 1-17 was used for the thermal cycling tests. The cycling caused delamination between the insulation and the copper. It was observed that even though the insulation system passed the proof test it was already totally delaminated in places. It points to inability of standard tests to appropriately qualify the EIS. A similar kind of sample was used for multi-factor tests [31]. It was concluded that the most ageing occurred at the end-winding region due to the manufacturing process manipulation.

Figure 1-17 An example of variation on the standard formette. The EIS is complete, the bars inside the slots are impregnated with resin. [30]

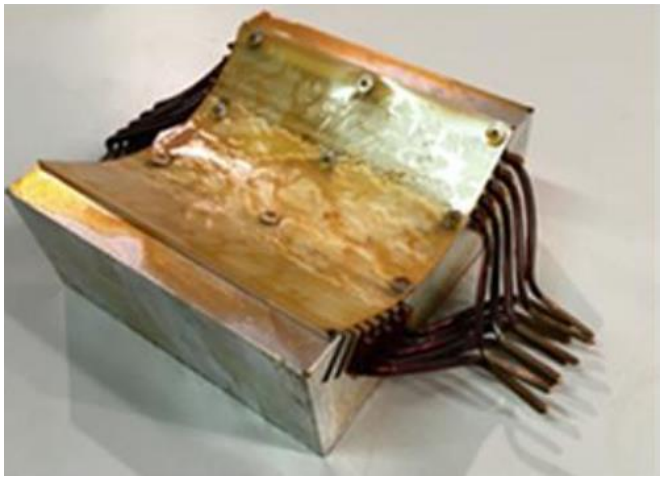

Figure 1-18 Statorette for low-voltage rectangular magnet wire, complete insulation system with slot paper and resin impregnation [24].

The final possibility is to use full stators for tests. With rising complexity of the sample, the dispersion of results also rises, whatever the measured value may be. When the scientific investigation is more basic it is more pertinent to use more basic samples such as twisted pairs. When the tests are conducted for the needs of the industry it is necessary to verify that an electrical machine is capable of sustaining the stress that it would encounter in its application.

1.7 Ageing modelling and prediction methods

The literature on low-voltage insulation ageing and lifetime estimation started appearing and growing with widespread introduction of inverters as a drive for electrical machines. A recent review of the literature reports tens of articles specifically on low-voltage inverter-fed insulation appear yearly and the number is on the rise [32]. The review divides the literature into categories that show the current state of affairs and what the researchers were focusing on. The categories are Standards and Reviews, Classical Lifespan Estimation, Partial Discharges in Lifespan Estimation, Insulation Tests for Lifespan Estimation, Factors influencing Ageing, and Current (which combines articles from some other categories but are the most recent ones, there is modelling, PDIV measurements etc.). For each category the main themes were covered, and some findings were described. The review is an exhaustive resource on the state of the art in low-voltage machine ageing and the choice of categorization of the literature very pertinent, hence the coverage of ageing modelling will follow that example.

1.7.1 Multi-factor models and methods

The basic models for single factor ageing are mostly simple equations with empirically established parameters. Either Arrhenius equation for thermal ageing [33] [34] or inverse power equation for electrical ageing [35]. Multiple researchers tried to establish multi-factor model based on convolution of these equations [36] [37] [38] [39] [40] [41] [42] [43]. Even though the models differ between one another in implementational details the basic principles remain. The final models are empirical, the parameters are established through experiments. However, the parameters have some physical meaning, the activation energy signifies how much energy must be delivered so that the system enters another state. For example, with injection of energy the connections between polymers are severed. The synergy between the parameters has to be found again through experiments. What was a constant in an equation now becomes a function of another factor. The model works for a specific material for which the experiments were done. Question remains how well it can work for complex EIS consisting of multiple different materials, each having their own different set of parameters.

A PhD thesis [44] that this one greatly builds upon successfully applied Design of Experiments method in order to create multi-factor models for electrical insulation. A temporal factor of one hundred was achieved for lifetime prediction for multi-factor ageing with influence of Partial Discharges. Before that another thesis explored various methods for more broad spectrum of equipment in electrical engineering [45]. The methods include Design of Experiments, Surface Response and Regression Trees.

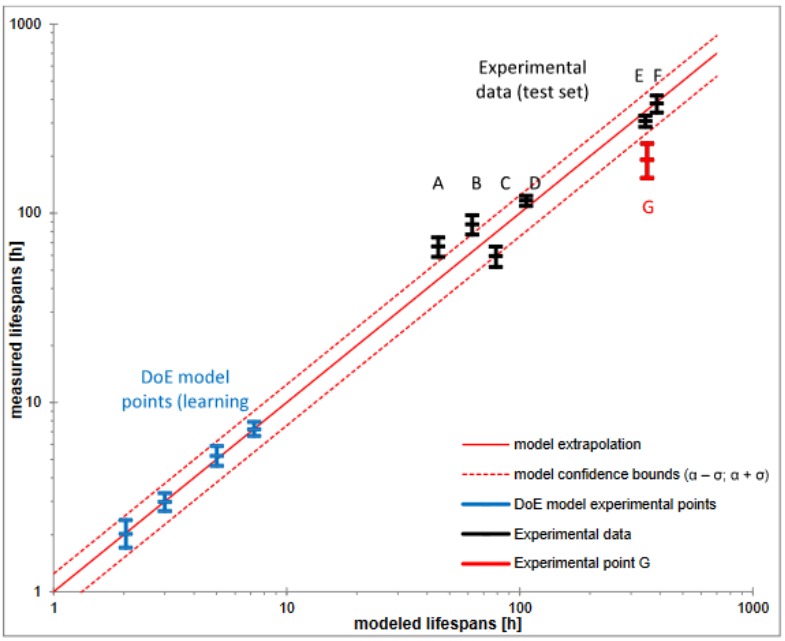

Figure 1-19 Results from illustrating extrapolation of DoE model [44]

The multi factor models created with Design of Experiments methods are one of the most popular multi-factor modelling for low-voltage machines [46] [47] [48] [49] [50] [51] [52] [53] [54]. The considered factors are temperature, voltage and inverter switching frequency. One study tries to incorporate rise rate and voltage spike proportion as factors by additionally using fuzzy logic in the modelling. It is common to choose the inverse power models for most of the lifetime-factor relations and exponential model for temperature. The examples use twisted pair, coated steel plates or polyimide film directly as samples. Multi-factor modelling for more complex samples is not being attempted.

1.7.2 Partial Discharge vs Lifetime Estimation

Extensive amount of research has been done on Partial Discharge influence on the insulation lifetime. That is despite the fact that the low-voltage machines' EIS falls into the category of type I where Partial Discharges are not expected to appear. It is argued that the lifetime of magnetic wires can be determined by observation of the PD generated [55]. The influence of the parameters of the impulse waveform like the rise time, the frequency, and the duty cycle on the Partial Discharge inception and lifetime of turn-to-turn isolation samples are investigated [56] [57] [58] [59]. In the tests performed it was found that PD generated by the

same voltage step of short rise time had greater magnitude than those of longer rise time (Figure 1-20). The overvoltage in different rise time cases was unsubstantial. Higher magnitude PD is more destructive to the insulation shortening its lifetime. It was also noted that tests performed with sinusoidal voltages on systems to be used with an inverter style voltage give overly optimistic estimation of lifetime.

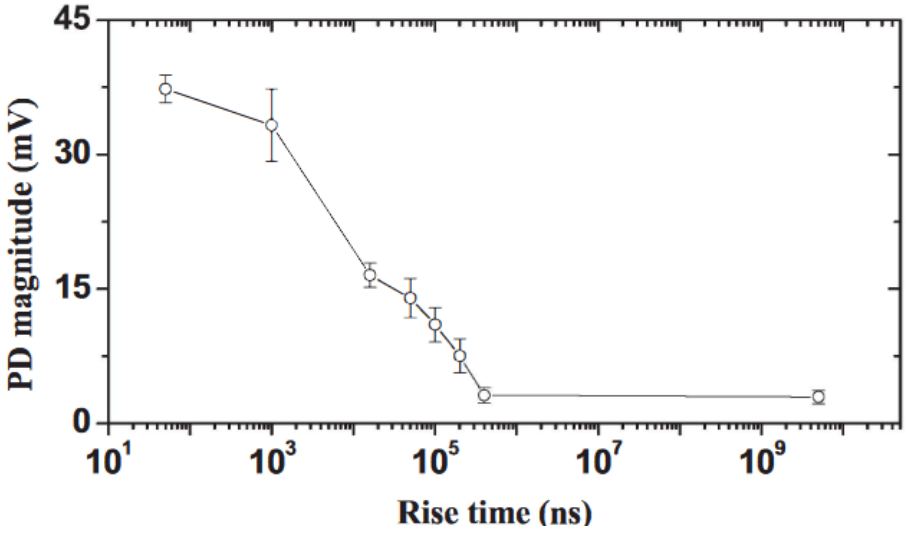

Figure 1-20 Measured PD magnitude in relation to rise time.[58]

1.7.3 Prognostic Methods Examples

The question of effective prediction of remaining lifetime based on diagnostic measurement is a topic of many research papers. While it is reasonable to content oneself with a general idea of a lifespan of a piece of equipment, there are some advantages in making that knowledge more precise. From the industrial and commercial point of view we need the cost of the additional measures related to prediction outweigh the cost related to unpredicted premature failure. The prediction methods may require additional, and even extensive, tests during the development phase and may require the installation of sensors. We need methods that can predict failure within reasonable bounds and at the same time minimise the cost of applying them. In the context of the EIS of electric vehicle motor, the prediction is particularly interesting. Failure of an electrical motor while on the road would be a major inconvenience and potentially even a danger.

A family of methods focusing on various measurements of currents present in the machine exists. Some monitor the current passing through the phases in order to establish how much charge leaked outside of the machine through the insulation, a complex model may be used to achieve this [60] . The interest of this method lies in the fact that the current is often already monitored for the purpose of machine control. A method for online lifetime prediction of a low voltage machine by observing the transient leakage current was developed [61] [62]. It was researched whether the evolution of the peak of the transient current during inverter commutation may be an indicator for lifetime (Figure 1-21). The same current were observed

in [63], [64] but the diagnosis of the ageing was concluded from changes in the spectrum of the transient currents.

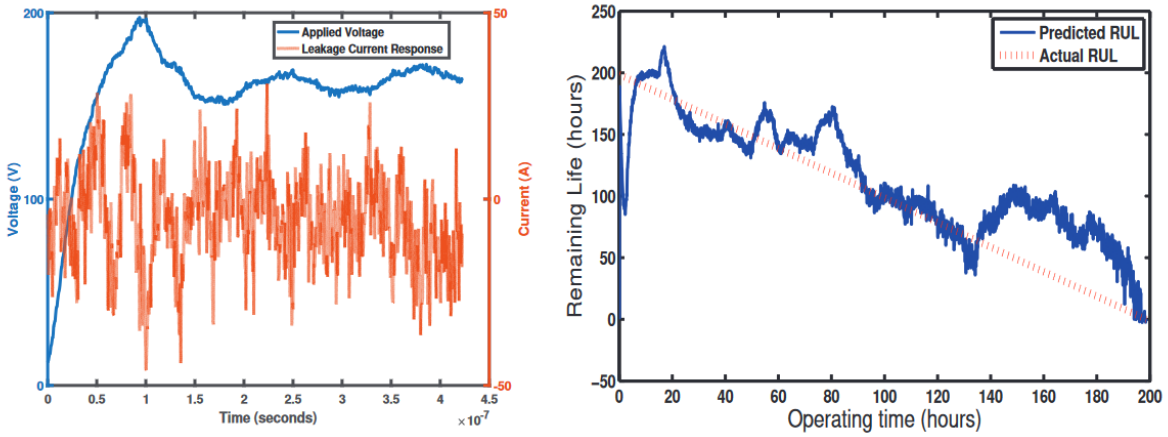

Figure 1-21 A measurement of the transient current during commutation (left) and a result of a Remaining Useful Lifetime (RUL) prediction based on evolution of that current (right)[61].

1.8 Conclusions

Research on insulation ageing in electrical machines is important as we are trying to make a transition from internal combustion engine to electrical motor in the automotive industry. The electrical insulation system is a weak link in the overall system of a motor. With the introduction of static converters new kind of stress was put upon the EIS – a square-wave PWM voltage. A risk of overvoltage and inception of Partial Discharges became a major focus of much of the research for electrical machines. In bigger, high voltage machines the insulation materials used are PD resistant, in lower voltage machines the PD are never expected to appear and Type I insulation system is applied.

EIS is relatively complex system composed of multiple elements performing different functions (turn-to-turn, phase-to-phase, phase-to-ground). The different layers are made of different materials and assembled in an array of industrial processes that themselves pose significant engineering challenge. Then, there are many factors that act destructively over time on the insulation when exposed to them (the electrical, thermal, mechanical, and environmental stresses). The factors have many modes of causing failure of the insulation and may interact with one another to aggravate the ageing process.

How to evaluate accurately the deterioration of an insulation system and how to predict its remaining lifetime remain open questions. There is no easy answer, some attempts are being made. Often, they require additional high-precision sensors or additional processing power which is not desirable in an industrial context, and more specifically in the automotive domain where each euro matters. Additional cost of applying those measurements would prevent them from being commercially viable. Another question is their accuracy. A versatile

and well proven method does not exist; margins of prediction stay wide and often specific to one material or application.

The tests existing in standards focus on product qualification. The question being answered is ‘If an average representative of a line of products can endure its envisioned lifetime?’ rather than ‘How long will this specimen last?’. The strategy is to compare the designed system to one already in operation.

The existing modelling techniques can cover the multi-factor aspect of ageing. However, so far, few researchers have tried to take into account the cyclical nature of a stressing factors in electrical machines for electrical vehicles and represent the impact in a model. The following chapter discusses the research into that very topic.

Chapter 2.

Cycling tests for electrical machines: state of the art of testing and analysis methods

2.1 Introduction

Electrical machines rarely work in a static domain. The load changes, the conditions vary. The way we use electrical machines in electrical vehicles consists of many periodical changes. In a scope of one trip (displacement from point A to point B) – a car would encounter many instances where speed, torque and load change. The road may be flat, slope upward or downward. In a city, with its traffic lights and where congestion is a common occurrence, multiple start-stop sequences would occur. The current flowing through the windings of the EM evolves dynamically according to the needs of the road and the driver. A rise in demand for power increases the current and consequently the heat losses cause rise in temperature. Sooner or later, the strain of the EM ends and the heat is evacuated. The machine underwent a thermal cycle. Moreover, in the usual case a vehicle is subjected the daily commuter's cycle. The car is used in the morning, it starts cold and the temperature quickly rises. After the commute is finished, the engine cools down and stays like that till the late afternoon. Then the city commuter needs to return home from work and the cycle repeats. An example of such a cycle included in Worldwide Harmonised Light Vehicle Test Procedure.

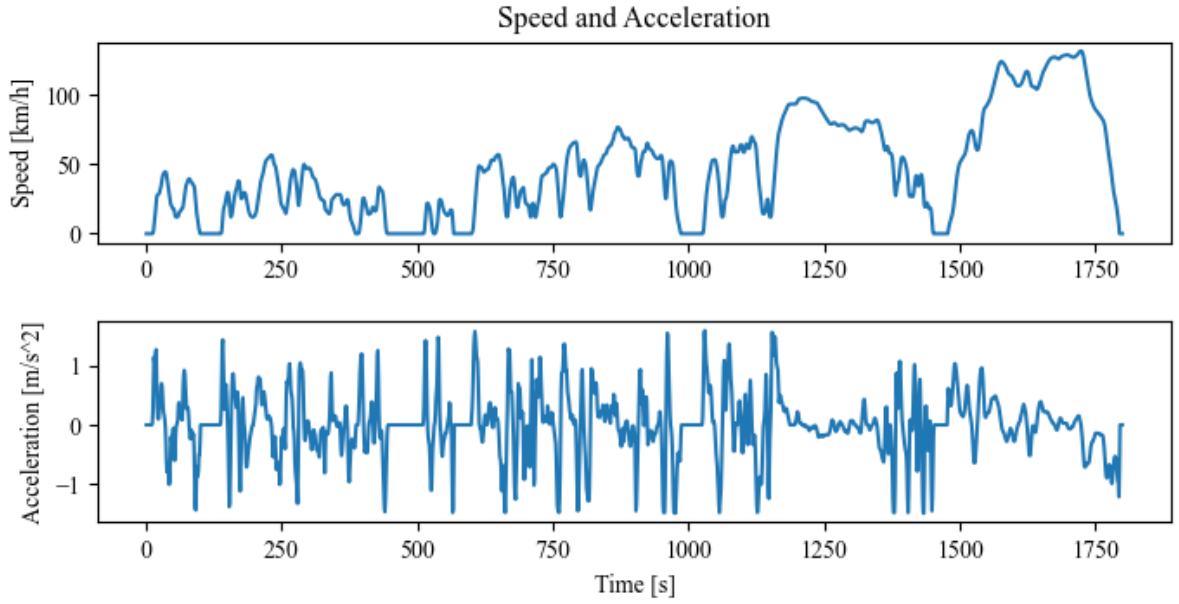

Figure 2-1Worldwide Harmonised Light Vehicle Test Procedure cycle profile.

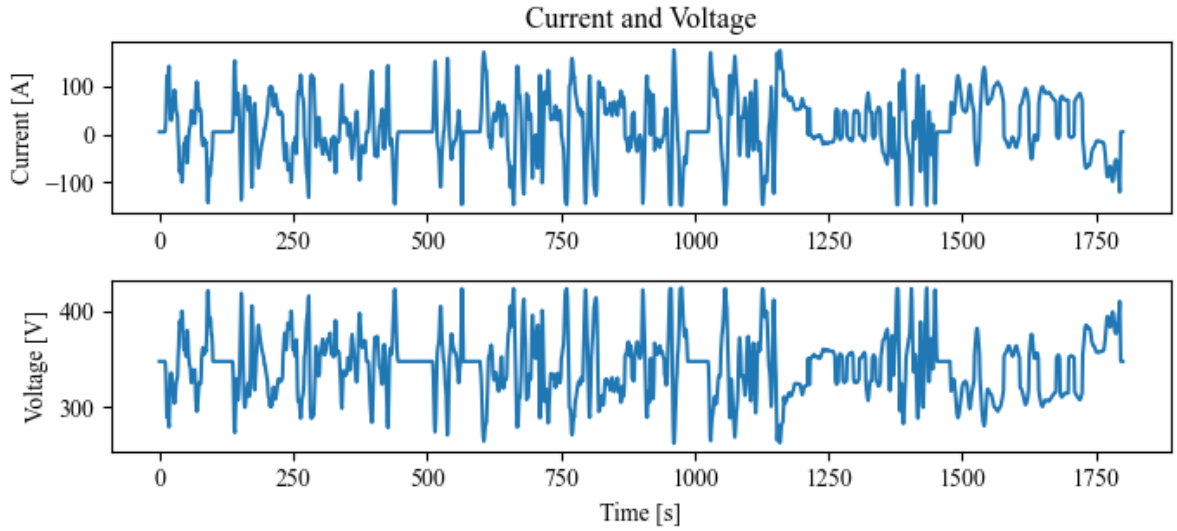

Figure 2-2 Values of current and voltage obtained from a simple EM model for WLTP profile.

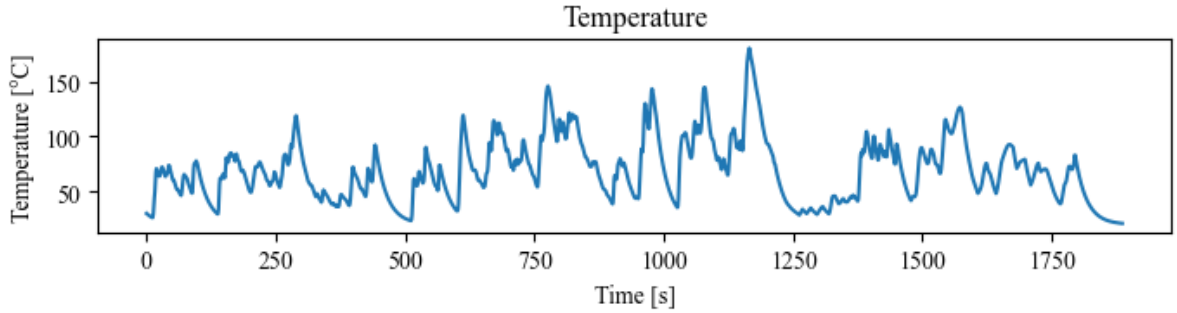

Figure 2-3 An example of winding temperature evolution obtained from a simple EM model.

Yet, the most common practice for testing in standards is based mostly on constant temperature tests which does not correspond to the type of constraints that a motor has to face.

This chapter explores the work done in the topic of cycling constraints on the electric motor. It involves a review of the literature and the standards in terms of cycling tests. The cycled factors and the cycling parameters are looked at. The last part focuses on existing models and methods to evaluate the relationship between cycling and ageing.

2.2 Cycling in the standards

[65] IEEE 1310 is the most utilized test form for high voltage form-wound machines. The norm stems from research done on qualification of hydro generators' EIS. Hydro generators experience frequent start-stop cycles where temperature rises rapidly from cold/ambient to high - close to Temperature Index of the material used [36]. Low-voltage machines due to smaller size and shorter conductors are said to be less susceptible to ageing mechanism of Coefficient of Thermal Expansion (CTE) mismatch of materials [66]. Standards for low voltage machines concerning cycling do not exist, yet it is interesting to

look at the procedures targeting larger machines. One can draw inspiration from the practices and, by getting an understanding of decisions made for those machines, avoid problems that were already solved.

Table 2-1 An example of a cycling protocol, IEEE 1310 standard.

Protocol element	**IEEE 1310 - Thermal cycling test**
Factor application	The heating is applied by running a high current through the winding. The cooling down is active: fans are forcing air at the samples.
Cycle's form	The standard informs on: • The factor boundaries: Lower temperature at 40 and higher at the Temperature Index of the material. • The hold time: no hold time, the heating or cooling switches to the opposite process as soon as the target temperature is achieved. • The slope of the changing factor: 2.5°C/min
Cycles' number	500 cycles
Samples and their number	The samples are machine bars in a kind of statorette that emulates the slots of a machine. At least four bars for the test and one additional bar for temperature control.
Sensors	The standard discusses placement of the temperature sensors. There should be a direct temperature measurement of the winding's copper. Meaning, that it should not be done though the insulation. Even a thin layer would make a difference, the copper temperature is higher than the temperature of the surface of insulation covering it [67].
Diagnostic tests.	The standard suggests a list of tests to be done. Electrical proof test, dissipation factor, dissipation factor tip-up, partial discharge measurement, physical dimensions measurements, tap test, surface resistivity. It is specified that the tests are to be done after 50, 100, 250 and 500 cycles to trace the changes in the measured values.
Post-cycling tests	As the tests designer does not predict the end of life after the designated number of cycles, there is a destructive test to be done after the cycling. The standard proposes either of the two: • Breakdown Voltage test – the bar's insulation is subjected to voltage that is gradually rising. The result of the test, the recorded value is the value of the highest voltage achieved before breakdown. • Voltage Endurance Test – the bar's insulation is subjected to a voltage that is a multiplication of its nominal value. The test lasts until the insulation's breakdown. The result of the test is the time until the breakdown. Both tests are themselves standardised.

IEEE 1310 is specifically a thermal cycling standard but some ideas from it may be generalised to other cycled factors. On this example we can distinguish a few elements that a standard may define for a cycling test. In this case they are the way of applying the factor, the form of the cycle, the number of cycles, the sample to be used and the number of samples, the sensors, the diagnostic tests to be done during the ageing and destructive tests to be done after the process if it is not destructive. The details of each of the elements mentioned are described in Table 2-1. IEC 60034-18-34 also covers thermo-mechanical cycling and in essence proposes the same method as described in IEEE 1310.

The standard since its publication in its current form is still subject of some discussion. [67] notices that cooling practices as presented in the standard are not sufficient for large bars or coils. It is also argued that thermocouple used for temperature measurement should be in direct contact with the measured copper bar which requires a measuring device that is capable of taking measurement of conductor under current. This situation is not possible in the EM of an EV. [68] studies discrepancy between ageing generated by a test and ageing from real operation. Cycling from the IEEE 1310 standard was applied to bars taken from a machine aged in service by about 10000 start-stop cycles. It was found that the standard cycling protocol created defects that did not appear in the operational lifetime. Also, it quickly propagates the ones that did appear during the lifetime. The authors argue that the test may produce results that do not correspond with the real operation of a system hence underplaying how reliable it is. One of the concerns is that in an effort to accelerate the ageing the specimens are subjected to temperatures close to Temperature Index which would not happen in most operational cases.

2.3 Cycling in the literature

A great compilation of existing works on thermal cycling was done in a review paper [69]. Factors that produce ageing and the ageing processes that occur in electrical machines are described. It was noted that the underlying exact mechanisms that cause the defects were not known at the time. The review compares many thermal cycling protocols performed in the literature. It cites cycling temperatures applied, heating (in an oven, by DC current or by AC current) and cooling (water cooling or forced air cooling) techniques and used slot models. Examples where additional constant stress factor, besides thermal cycling, was applied are presented. Examples of simultaneous stressing are given for constant thermal stress, electrical stress, humidity and mechanical bending.

Evaluation tests performed after or during accelerated ageing tests are enumerated: among them Dissipation Factor, PD tests, Voltage Endurance and Breakdown Voltage. The authors try to establish which tests correlate well with ageing in all the literature. The conclusion was that since many ageing mechanisms exist there is no single evaluation test that can detect all of them. The existence of thermomechanical ageing through thermal ageing is

recognized but its importance compared to other factors is hard to estimate from existing literature.

Nevertheless, the review focuses on high voltage mica-epoxy or mica-polyester hydro generator insulation. So far, no review focuses on low-voltage machine type EIS when it comes to cycling tests.

2.3.1 Significance of cycling – an example

Brugger et al. proposes a new method of thermally cycling hydro generators' stators insulation [70]. The novelty stems from the fact that they try to insulate the impact of thermal cycling from the deterioration caused by high temperature. They minimise the thermal ageing by placing the cycle range in low temperatures. Instead of reaching the Temperature Index of the insulation, as detailed in the relevant standard, the upper temperature was set to 100°C.

The performed cycle consisted of internal copper losses heating and forced air cooling. The bars were heated up from 30°C to 100°C which took about 200 s. When the winding reached the 100°C the current was shut off and ventilators cooled down the bars back to 30°C. That part of the cycle lasted about 1250 s. The cycle's form can be observed in Figure 2-4.

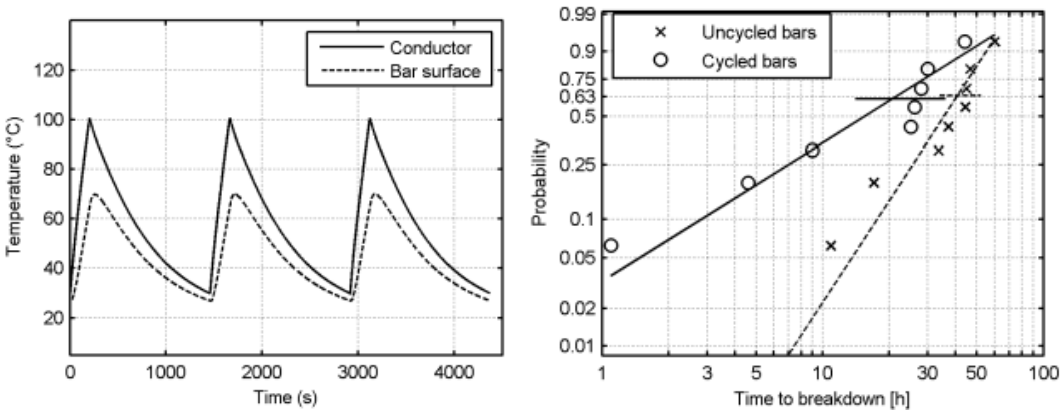

Figure 2-4 The cycle applied to hydrogenerator bars and the results of Voltage Endurance Tests of the cycled conductor bars and the bars from control group [70].

The presented research concerned a hydrogenator's bars experiencing nominal voltage of 10 kV during their lifetime. The insulation is a type II insulation system involving inorganic materials resistant to accelerated deterioration by partial discharges. The bars in this study were sourced from a generator decommissioned after years of operation. The bars themselves were not damaged nor experienced breakdown prior to the experiments. Among the sixteen bars used, eight were destined to undergo the thermal cycling; the eight remaining were the control group.

The test group of bars was subjected to 1500 cycles, the procedure lasted about 600 h. Some diagnostics were run periodically, the performed tests were the Dissipation Factor,

Dissipation Factor tip-up and Partial Discharge test that resulted with phase resolved partial discharge pattern. At the end of the planned number of cycles both groups of samples were put to a destructive test: the Voltage Endurance Test. A voltage of 3.5 times the nominal voltage was applied to the electrical insulation until breakdown.

The Weibull's distribution resulting from the final tests is show in Figure 2-4. It can be read from the graph that the scale parameter for the cycled group was about 20 h, while it was about 40 h for the control group. The authors state that the large uncertainty of the scale parameter prevented them from making conclusive statements about the significance of the difference between the groups.

Even though the study was inconclusive it is nevertheless important as it introduces the idea of decoupling the thermal ageing from the thermal cycling. It tried to solve the problem by eliminating the thermal deterioration as much as possible. Yet, that may be a problem in itself. The key to a good ageing test is proper acceleration. An accelerated ageing test is designed to speed up the process that in normal operation could last years. Here, the cycles, even though they are more condensed, do not represent a major accelerating factor.

2.3.2 Literature on cycling in numbers

We can imagine that there are multiple factors that can have a cyclic nature in the case of electrical machine insulation. There are factors like temperature but also voltage, mechanical strain, ambient humidity for open-air machines and some of those factors may have additional cycling impact. That additional impact would be a result of repetitive passing from one level of ageing factor to another. Consequently, there is some interest in the field of thermal cycling for electric machines. The interest in the other factors is virtually nonexistent, the few relevant examples will be mentioned here.

2.3.2.1 Electrical cycling

Electrical ageing, compared to thermal ageing, is considered to be a weak factor when the value of voltage is below the PDIV [71]. No standard exists where the fundamental of the voltage would change in time in a periodical manner. Yet, a cycling of this kind seems relevant as an EIS of an electrical machine in an electrical vehicle would undergo many changes of value of electric field during its lifetime.

The only kind of cycling that is explored in literature is the impact of Partial Discharges. In this kind of experiment the value of fundamental voltage does not evolve over time in a cyclic fashion but the insulation is subjected to high frequency repetitive voltage impulses. The phenomenon of impedance mismatch between the source, the inverter, and the system, the cables and the machine, causes an overvoltage which may be a result of undesired partial discharges.

In [10] the authors explore how different forms of PD inducing voltage impact the lifetime of the insulation. Twisted pairs are aged with square and sine waveforms at different frequencies. The results show little difference between the cases, while the frequency is the factor that dictates the lifetime. The author admits that the lack of any difference may be due to voltage value well above PDIV, lower values closer to PDIV may show different results.

Average lifetime (s) Shape parameter	**1 kHz**		**5 kHz**	
	Sinus	Square	Sinus	Square
50%	**41833** 9,64	**41395** 26,47	**7992** 16,71	**7952** 10,24
60%	**31820** 14,26	**30405** 6,31	**6162** 13,52	**6669** 7,8

Figure 2-5 Results of twisted pairs ageing in [10]. Lifetime (in seconds) similar between square-wave and sinusoidal form of voltage. The frequency is the factor deciding lifetime.

Another study in the area concludes that the square-wave voltage forms are more destructive than the sinusoidal forms [72]. The work challenges the assumption that type II EIS driven by inverter can be tested with sinusoidal form for PD detection. In their accelerated ageing test of medium voltage machines, they discovered that lifespan of samples under square-wave PD inducing voltage was a few times shorter than lifespan of samples aged with sinusoidal waveforms. On the other hand, there was no difference between two different rise times of the impulses of the square-wave voltage ageing.

A study investigating the effect of multi-level inverters [73], shows that PDIV of twisted pairs tested with two level commutation is lower than PDIV when the commutation is done in three levels. The multi-level inverters offer the reduction of voltage overshoot at machine terminals [74] but at the same time shift the reliability bottleneck from the electrical insulation to the inverter as the number of power electronics element is multiplied.

2.3.2.2 Mechanical cycling

Mechanical stress as a factor in insulation ageing is discussed in [75]. The stator winding bars were being continuously bent in a specially prepared test bench (shown in Figure 2-6). The bars were held on one end in three points to ensure rigid grip. On the other end, the bars were subjected to vibrations provided by a grip point there. Seven different levels of mechanical stress were applied – the levels were different amplitudes of vibrations. Similar experiment was held many years earlier [76]. In that case the bars were held in one place only, not in three as in the forementioned study. PD, PI or DF were deemed insufficient for mechanical ageing diagnostics. Experiment with varying strain levels of the bars. A model of strain to lifetime as inverse power law was found.

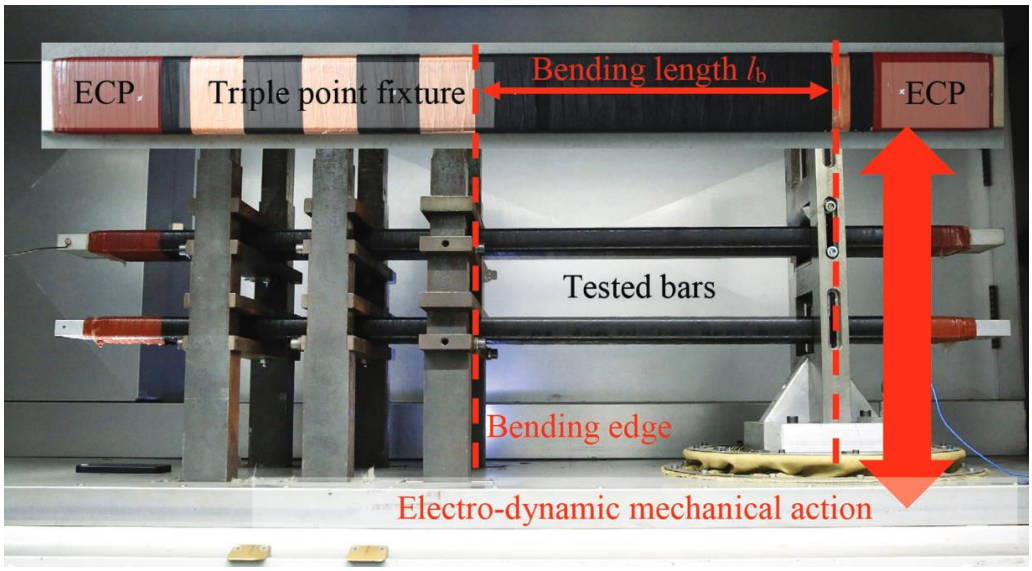

Figure 2-6 The test bench applying vibration to stator bars. [75]

Mechanical cycling in terms of the cycling defined in this work is hard to conceptualise. We would talk about changes in vibration amplitude in a periodic manner and whether that change has an additional detrimental effect. Mechanical vibrations are a factor in the process of ageing of in EIS. Firstly, in terms of the vibration linked to the electromagnetic forces appearing during normal operation. The reaction force on stator winding as a result of the rotor being pushed by the magnetic field has a cyclic nature. Similarly, the force between two parallel phase wires having periodically opposite and conforming current flow directions causes them to cyclically attract and push at each another. Secondly, for a motor dedicated for an electric vehicle, the vibration during driving caused by imperfections on the road or the motor itself, more rarely, in case of an unbalanced mechanical load. In the end, no research on specifically mechanical cycling was found. The distinction is subtle, which may be the reason why no one ever researched the question or it is simply not an important or even sensible factor.

2.3.2.3 Thermal cycling

Overall, sixty-four articles specifically talking about cycling of machines were found in the literature for this PhD thesis up to the year 2022 [10], [22], [25], [28]–[30], [36], [67]–[70], [72], [75]–[126]. That number contains the three examples of mechanical and electrical cycling covered in the sections above. Even those do not exactly fit the definition of cycling. All the rest of the literature found on cycling concerns thermal cycling. Among those there were about twenty examples of multi-factor ageing with two or more constant factors involved in the ageing process. The numbers and specific types of additional factors are shown in Figure 2-7.

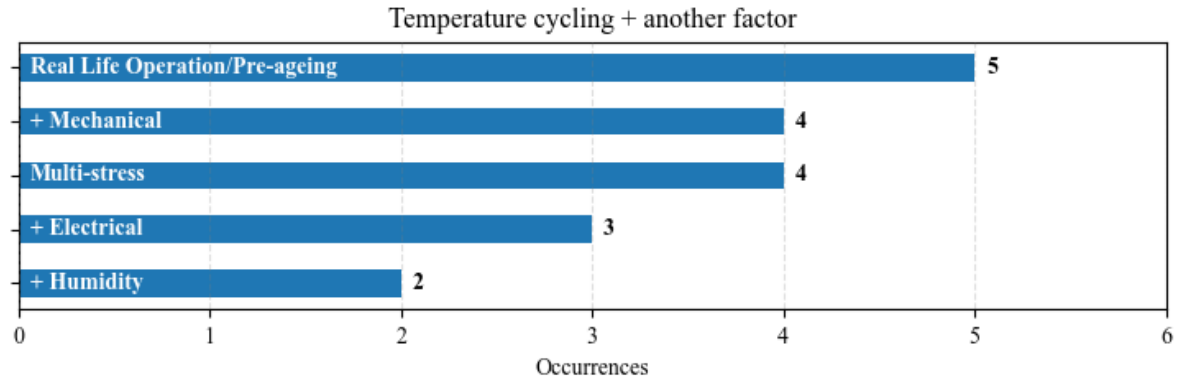

Figure 2-7 The number of articles concerning thermal cycling with simultaneous another factor or kind of ageing.

The literature treating cycling can be divided into two distinct categories: cycling on high-voltage machines and cycling on low-voltage machines. The former has longer history in terms of scientific interest, mainly due to research on the insulation of hydro-generators. The particular intermittent work pattern of many start-stop cycles made the question of cycling natural for this kind of EIS. When it comes to the low-voltage electric motors category, the research is much more recent. When a specific domain of application is mentioned, it is mostly motors used in various embedded platforms. The distribution of articles in the two categories is presented in Figure 2-8. The literature on the low-voltage machines, which are more interesting for the scope of this PhD thesis, is rather scarce.

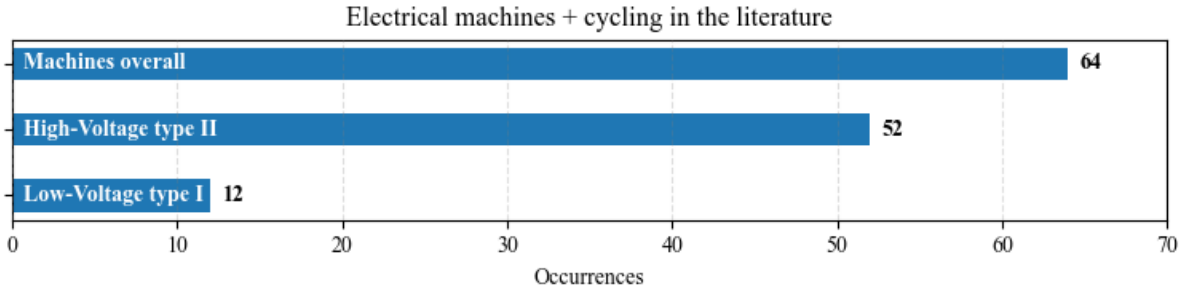

Figure 2-8 The number of articles treating cycling of different categories of machines.

Then, a large body of the articles is influenced (or outright is a commentary on) the standard IEEE 1310, described in detail in section 2.2. The method of introduction of the heat is a dividing aspect of the thermal cycling tests. Figure 2-9 shows the number of papers related to the two used methods. The standard makes a sensible argument that the heat introduction should be as similar to the method in a real-life operation as possible. For the windings of a stator of an electric machine that is the heat from copper losses and, in lesser extent, iron losses. The internal heating is said to induce more realistic temperature gradient in the different layers of an insulation system. Also, it has the ability to exhibit the potential hot spots caused by flaws in the design. Alternative method, the oven heating, introduces the heat

uniformly and from the outside of the insulation which is the opposite of the current heating. No research tries to explore the question whether ageing thermal tests in an oven and by forced current result in different deterioration of insulation materials.

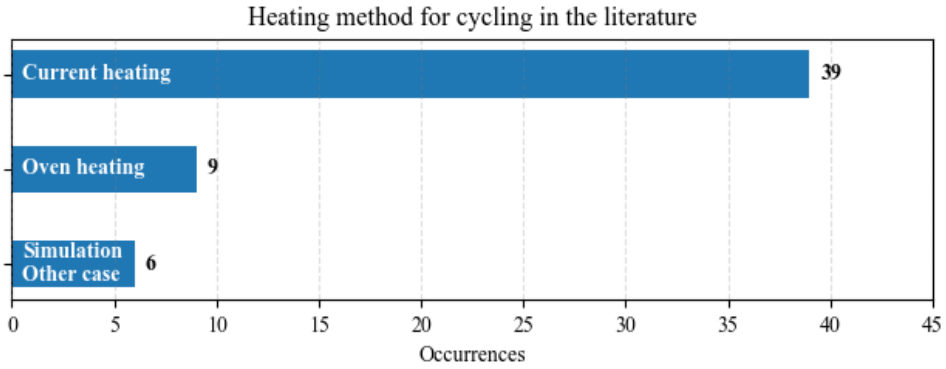

Figure 2-9 The number of articles on thermal cycling by method of heat delivery.

In order to try to draw meaningful conclusions from the cycling experiments the researchers monitor continuously certain value. The tests done during the cycling in the reviewed literature are presented in Figure 2-10. The amount of PD related tests is a consequence of high-voltage machines being in the spotlight of cycling research so far. The type II insulation is PD resistant hence the PD are not out of ordinary in nominal operation of those machines. We do not have the same conditions when it comes to type I low-voltage machines. Quite a few articles employed destructive tests at the end of cycling. It gives the idea that the applied cycling is not destructive enough to give the result in terms of time or number of cycles till the end-on-life.

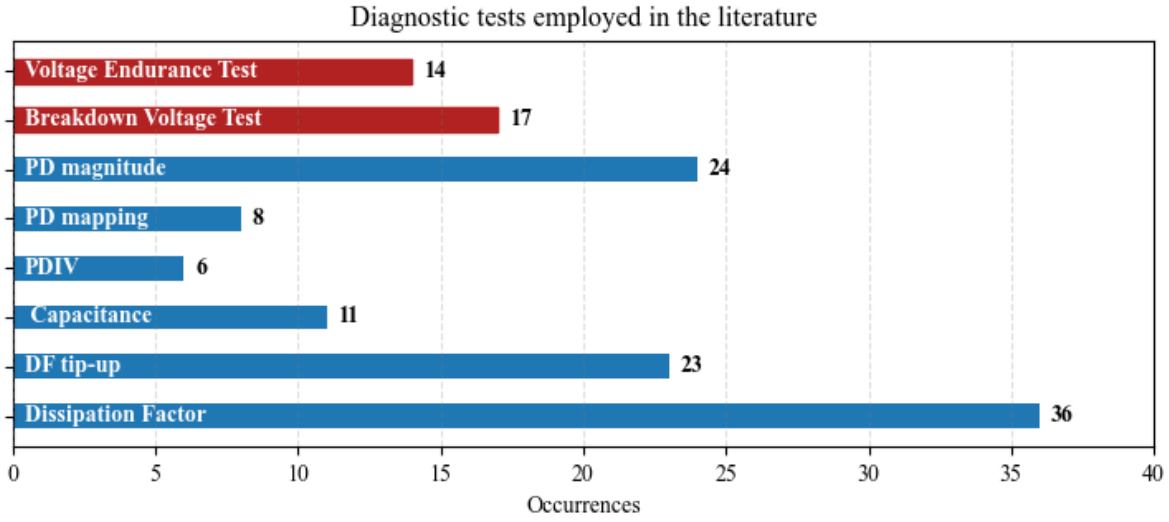

Figure 2-10 The tests performed during the thermal cycling, number of occurrences. In red the destructive tests used after some planned number of cycles to evaluate the ageing.

2.3.3 Low Voltage Electrical Machine EIS cycling

2.3.3.1 Test samples

Thermal cycling tests were performed on round magnet wire coils in [106] and [113]. Round magnet wire also appeared in [66] where it is wound on steel bars which represent stator teeth. In [127] and [114] a few different coil specimens were wound on interconnected mockup slots – motorettes. Full stators with round magnet wire were employed in [115], [121] and [122]. The two first examples had the wire loosely and randomly wound in the slots while in the last case the stators were also impregnated with epoxy. [123] performs thermal cycling on a fully assembled machine and [128] proposes a test bench for complex cycling tests on machines. [72] focuses on different kind of conductor, a rectangular one, the samples are two taped together rectangular enameled wires which are also impregnated with epoxy. In this case the materials used are said to be Type II insulation system for Medium Voltage application.

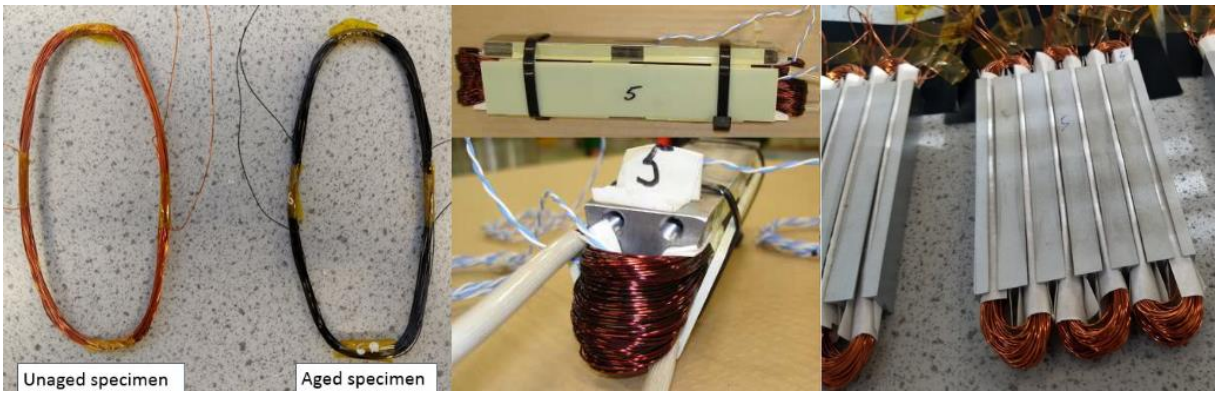

Figure 2-11 A range of low-voltage machine samples. From left to right, enamelled wire coils [106], windings on a single steel bar [66] and motorettes [127].

Even if the research on cycling of low-voltage machines is not a vastly covered domain, we found a good section of different kinds of samples. The samples used for experiments vary from the easiest, like twisted pairs, to the actual fully impregnated stators. In this sense the smaller kind of machines have an advantage over bigger high-voltage machines, it is relatively easier to obtain at least a few samples of full machines for tests.

2.3.3.2 Cycling protocols

Thermal cycling is the only kind of cycling that is treated in the literature. The word ‘cycling’ or ‘cycle’ appears often in terms of periods of constant factor level exposure. However, this kind of protocol does not fit into the definition of cycling that is considered for this thesis. In that case, the change of the factor itself is not regarded as a potential ageing factor.

When it comes to thermal cycling, most of the research done was performed at temperatures over TI (Temperature Index) of the insulation [106] [66] [127] [114] [115] [121] [123] [113]. An example of cycling profile shown in Figure 2-12. In the case of [106] the reason for choosing the levels was that they targeted research of brief overtemperatures in an aeronautical application. The most common reason for using high temperatures is to accelerate ageing and greatly reduce the lifetime. In [127] and [114] the standardized method for obtaining TI is applied – three constant temperature ageing tests are performed, Arrhenius model is fitted into the data and used for calculation of impact of cycling on lifetime.

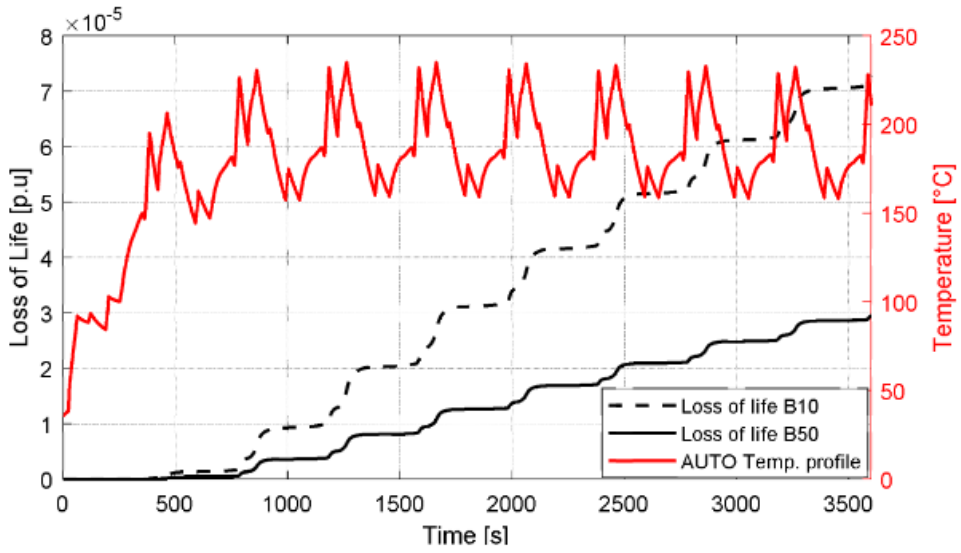

Figure 2-12 An example of cycling profile, the cycles at the range of high temperatures around TI. [127]

The preferred form of cycling is where the temperature rises to the chosen higher bound and then instantly drops to the chosen lower bound. All but one [122] of the articles on Low-Voltage thermal cycling employ internal current losses as heat source. The majority of cases use forced air for cooling. Among outliers are an experiment done on stators – the stators are cycled in a climate chamber from -50°C to 150°C [122] and one study that introduces a water cooling system for its samples [66].

2.3.3.3 Performed measurements

The diagnostic tests used for low voltage machine EIS, performed during cycling ageing vary. Some use High-Potential DC test [106] or High-Potential AC test [127] [114]. The test may be used as a pass or fail criterion only or leakage current through insulation may be recorded and traced [66]. Leakage current is monitored online [123], AC capacitance and Dissipation Factor are derived from that measurement. In [115] the Insulation Resistance was treated as an end-of-life criterion. Resistance falling below 1 GΩ was the threshold. PDIV appears as a way of tracing the ageing of the insulation. The values of PDIV are recorded before and after ageing [122] or measured cyclically during ageing [113]. Beside PDIV, the

PD are observed directly [72], phase-resolved PD maps are registered over time. In . [80] the author advises to use Breakdown Voltage Tests when the lifetime would be too long and a control group of unaged samples. In the end the breakdown test is performed, lowered breakdown voltage in the aged group would be indicative of deterioration.

2.3.3.4 Insights on cycling/Knowledge acquired in the research

It was found that PD activity is harder to identify in an square-wave voltage form than for a sine-wave voltage case [72]. The experiences were performed on rectangular conductors with mica-type insulation, taped together back-to-back and impregnated with epoxy. The PD signature overlaps with transients caused by the impulses. Some difference exists in ageing potential of sinewave and impulse voltage that incudes PD – the square-wave reduced the lifetime. Applying the Arrhenius' law to cycling can produce models of thermal ageing over a cycling profile [127][114]. The article does not go into impact of the cycling itself, evaluates only the theoretical number of cycles till the end-of-life. When treating experimental data of ageing, where there are multiple samples and a spread in their lifetimes, it is proposed to use the lifetime of the first to die rather than some middle value. The idea is targeted at critical applications. In a study of thermal cycling the samples were coils of magnet wire wound on the same stator, shown in Figure 2-13 [115]. The samples were heated up by copper losses in the wire. It was noted that it would be more logical to put the samples on separate stator emulators rather than a single piece of steel. The used configuration made controlling the temperature of individual samples difficult, when it was supposed to be different for different samples. Overall the thermal cycling of low voltage machines was found to be significantly reducing of the lifetime of the EIS [121][113].

Figure 2-13 A stator with six separate windings used for thermal cycling experiments. [115]

2.4 Cycling modelling

2.4.1 Thermal cycle shape impact

The question about the impact of the different kinds of cycles could also be considered for an insulation system. Almost no research exists on the topic, even though it seems a very pertinent question. When it comes to the larger machines and tests on conductor bars the current needed to heat them up is already considerable. There may be some practical and economic barriers to achieving faster cycles. In the case of smaller machines, the task poses less problems. Despite that, only one article was found that asks the question. One of them [113] tests multiple shapes of cycle and concludes that there is an important difference in the lifetime of the insulation [113].

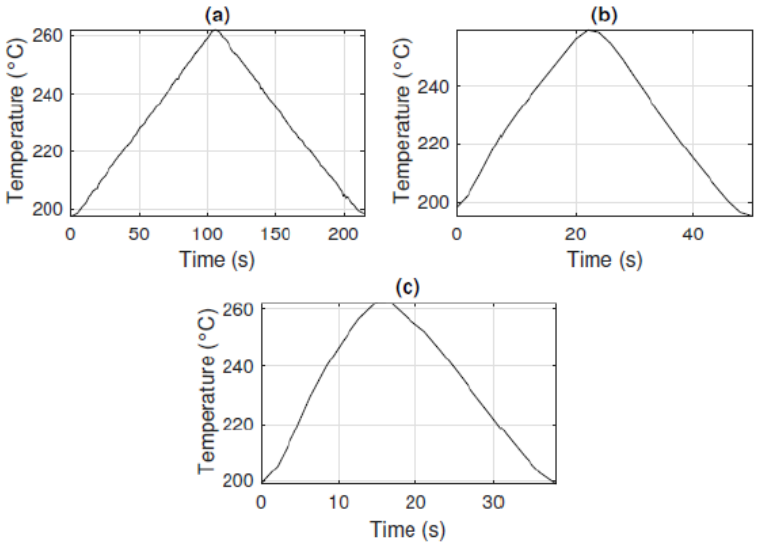

Fig. 2. Temperature profiles for (a) 0.5°C/s, (b) 2.5°C/s and (c) 4°C/s.

Figure 2-14 Different thermal cycles applied on enamelled wires wound into coils. Identical temperature range with varying cycle time, steeper heating and cooling ramps [113].

The study tries to quantify the impact of the heating rate, its ramping steepness on ageing. It involved coiled enamelled wires as the samples in the experiment. The coils were supplied with current that was able to heat them up quickly. The current could be adjusted in a way to have different rise rates. Cooling down of the samples was achieved by ventilators. The temperature range was chosen as between 200 °C to 260 °C. The high temperatures were connected to the aeronautical application that the study considered.

The three different cycling forms are shown in Figure 2-14. The different heating rates were 0.5 °C/s, 2.5 °C/s and 4 °C/s. The samples were cycled continuously for periods of 20h. Between the ageing periods they were cooled down to room temperature and their PDIV was measured. The end-of-life criterion was set at a level of PDIV recommended by a standard 60034-18-41. It was concluded that the lifetime for the worst-case slew rate was 50%

shorter than for the least steep ramp. The insulation undergoes the thermal ageing but also mechanical one due to the change of temperature. It was demonstrated that the shape of the cycle has an impact, but it is difficult to quantify.

2.4.2 The Coffin-Manson and Norris-Landzberg model

The Coffin-Manson model is dedicated to describing the mechanical fatigue resulting from thermal stress [129], [130]. Later the model was modified by Norris and Landzberg to include cycling frequency and maximum temperature [131]. The model is often applied to electronics to model solder crack growth due to thermal cycling [132]. It is expressed as follows:

$$N = Af^{-a}\Delta T^{-b}G(T_{max}) \quad (2.1)$$

Where N is the number of cycles to fail, A is a coefficient, f is the cycling frequency, ΔT is the temperature range of a cycle, a is a cycling frequency exponent, b is a temperature range exponent, G is the Arrhenius term evaluated for the maximum temperature of the cycle.

The model requires the knowledge of the activation energy of the insulation material. That adds the need to establish it experimentally before the model could be used in an application. Moreover, the model takes into account only the temperature ranges from the lowest to the highest temperature of the cycle. It is implied that there is only one kind of cycle. Even then the model does not distinguish between a cycle with a very steep change in temperature with some hold time and a gentler slope without the hold time. In case of the solder joints the distinction is important, the two kinds have different impact on the lifetime of the connection [132].

2.4.3 The Arrhenius' law

The basic form of the Arrhenius equation is as in (2.2):

$$k = Ae^{\frac{-E_a}{kT}} \quad (2.2)$$

where k is the rate constant, A is the pre-exponential factor, E_a is the activation energy, k is the gas constant and T is the temperature expressed in K.

The Arrhenius equation describes the relation between the rate of occurrence of a chemical reaction and the energy delivered to a system. In this case the energy being the amount of heat delivered, taken into account in the equation as the absolute temperature. The equation has a very wide range of applications. For us its importance lies in the fact that it models the ageing of insulating materials. The materials used as the enamel of windings, the insulating papers, the slot filling resin of electrical machines are usually organic or inorganic polymers, also ceramics in high-voltage machines. The bonds between polymers' chains

break over time. The more energy delivered, the faster the process. The electrical rigidity of the material deteriorates and the voltage that the insulation is capable of withstanding decreases. The process is relatively slow in room temperature, but the exponential nature of the equation means that in temperatures high enough the acceleration of the deterioration is high.

The Arrhenius equation, when the material's properties are known, can output the lifetime for a given temperature. When the temperature changes, as is the case in cycling, it is not obvious how to apply the equation. The easiest idea would be to apply the same equation to an average of the temperatures. But since the relation is not linear it could not be arithmetic average but some different method. Going further we could calculate the lifetime for each moment at each temperature of the thermal profile. That approach is known as Miner's Rule.

2.4.4 The Miner's rule and its applications

The Miner's rule, also known as Palmgren-Miner linear damage hypothesis was first introduced by Palmgren in the twenties, later popularised by Miner in the forties [133]. The most commonly cited form of Miner's rule is as in (2.3).

$$C = \sum \frac{n_i}{N_i} \tag{2.3}$$

where C is the cumulative damage, unitless, takes values from 0 to 1, where 0 is new and undamaged and 1 is the end-of-life, n_i is the number of cycles of type i experienced by the cycled object. N_i is the number of cycles of type i that the cycled object can sustain until breakdown.

The usage of the principle behind Miner's rule is often sourced back to an article by Huger et al. [134]. In the article, the usage of the linear damage accumulation hypothesis was inspired by work done on the topic of bearings' ageing. For winding insulation, the basic Arrhenius Model is transformed into a model based on a power function with a base of two. The rationale for it is that increasing the temperature which is acting upon an insulating material by 10 K, its lifetime is halved.

$$D_w(t) = \frac{1}{L_0} \int_0^t 2^{\frac{\max(\theta_{cu}(\tau)) - TI}{HIC}} d\tau \tag{2.4}$$

where D_w is the accumulated damage, L_0 is the overall lifetime at TI, TI is the Temperature Index, HIC is the Halving Interval Coefficient or half-life index, often approximated at 10 K, may be 8 K to 15 K, depending on the material and its TI, θ_{Cu} is the temperature profile measured at contact point with the winding copper.

That is a qualitative shift from the original Miner's rule. Originally, the number of cycles is used, here it is the time passed in the presence of a condition. We suppose we know

how many identical cycles it would take for an object to arrive at its end-of-life. We have that knowledge for multiple different cycles. Then we can calculate how different numbers of different cycles would deteriorate the cycled object. We do that by summing the fractions of number of cycles experienced divided by number of the same cycles till the end-of-life. The number of cycles can be replaced by time passed in a condition. The denominator of the fraction would be then replaced by the lifetime under solely this condition. That is what happened in (2.4). It integrates time differentials multiplied by how the lifetime at instantaneous temperature compares to lifetime at TI. Then the integral is divided by lifetime at TI giving a fraction describing how much lifetime was spent.

The Miner's rule hypothesizes linear damage accumulation without any influence of the initial stress condition. What it means is that the sequence of application of different stresses does not matter. The model does not take into account the state of health of the object at the moment of application of the stress. Which may or may not be an issue in the case of the insulating materials.

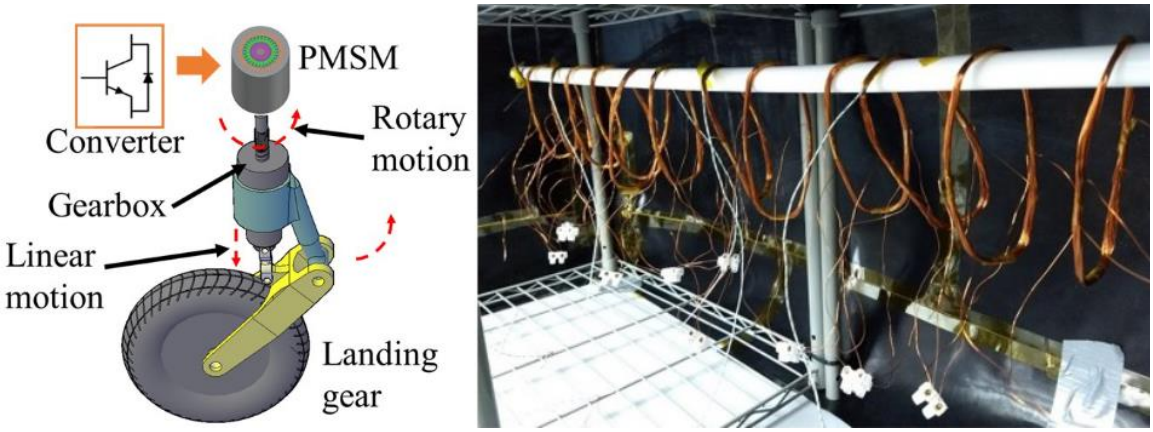

Figure 2-15 The landing gear and its actuator, a PMSM (left). The samples undergoing the thermal cycling corresponding to the operational profile of the landing gear (right). [106]

The next evolution on the application of Miner's rule to thermal cycling is an article on thermal overload of a helicopter landing gear actuator [106]. What differentiates this work from the one above is that here the ageing experiments were actually performed, it was not a simulation. The authors used coils of round-section enamelled wire to emulate stator windings (Figure 2-15. The method is applied for samples that were thermally cycled. The experiments last till electrical breakdown of all the samples. A model was derived that permitted calculation of loss of life depending on number of cycles. The basis for calculation of loss of life, called Life Fraction (LF) in the article, was as follows:

$$LF\left[\theta_j(t)\right] = \int_0^{\Delta t_j} \frac{dt}{L_0 \exp\left[B\left(\frac{1}{\theta_j(t)} - \frac{1}{\theta_0}\right)\right]} \tag{2.5}$$

where the Life Fraction is calculated for one cycle alone, $\theta_j(t)$ is the temperature profile of one cycle, B is a constant related to activation energy, θ_0 is the TI, and L_0 is lifetime at constant temperature of TI. The article offers a framework for the design of machines working with thermal overloads. It makes it possible to calculate how many cycles the insulation can sustain. However, the approach still assumed that the damage applied to the insulation is purely thermal, there is no component modelling the mechanical strain caused by the changes of temperature.

The lack of the thermo-mechanical ageing was covered in a paper on thermal cycling of full stators [121]. The study used stators of low-voltage EM winded with round-section enamelled wires.

$$LoL = \int \frac{dt}{L_0 e^{B\left(\frac{1}{T(t)}-\frac{1}{T_0}\right)}} + \sum_{i,j} \frac{N_{cycles}\left(\Delta T_i, T_{peak_j}\right)}{N_{i,j}} \qquad (2.6)$$

where LoL stands for Loss of Life, $T(t)$ is the temperature profile, B is a constant related to activation energy, T_0 is the TI, and L_0 is lifetime at constant temperature of TI. The second term introduces the impact of the cycles to the loss of life calculation. The different cycles are defined in terms of their amplitude ΔT_i, and peak temperature $T_{peak}j$. In the equation, it is assumed that the lifetime data for all the occurring cycles is known. $N_{i,j}$ is the number of cycles till breakdown of amplitude numbered i and peak temperature numbered j. The sum of fractions of certain types of cycles divided by the $N_{i,j}$ is the expression of the Miner's rule applied for cycling.

In fact, the article applied the Miner's rule twice. Once for pure thermal ageing considering the time spent at certain temperature during thermal cycling. For the second time it was applied for the cycling itself. The way it is supposed to work was that first the cycling experiments for different kinds of cycles are performed. Only one kind of cycle is performed on one set of samples, and the experiment ideally lasts till breakdown of all the samples. Then, with the first application of Miner's rule, the loss of life by thermal ageing is calculated. If then, the loss of life does not add up to unity, the remaining fraction of damage to the insulation is inscribed to the cycling. That fraction divided by the number of cycles is the damage done by one cycle.

Still, the method carries on the Miner's rule supposition that the sequence in which the of cycles or current state of the insulation is not a factor. It is an unexplored possibility that after sustaining some damage, whether thermal or thermomechanical, the insulation may respond differently to additional ageing. Also, as it was presented in the article, it is necessary to perform a specific experiment with a kind of cycle to use it in later calculations. The relationship between amplitude of cycle and loss of life was shown, but the fact that for each experiment only one stator sample was used makes it difficult to draw solid conclusions.

Another question that was asked by researchers dealing with cumulative damage models was which data should be used in determining coefficients of the ageing models. The activation energy in the Arrhenius model is established from three or more constant temperature ageing tests. According to the standard the tests require at least five samples per temperature in order to assure statistical significance. The lifetimes are fitted onto a distribution. The commonly used distribution is Weibull distribution. The scale parameter of that distribution is the point of highest probability for failure and corresponds to 63% of samples already arriving at the end-of-life. Those points are then used to fit the Arrhenius equation onto them. In a paper [127] authors argue that it is a better idea to choose different point at the distribution for certain applications.

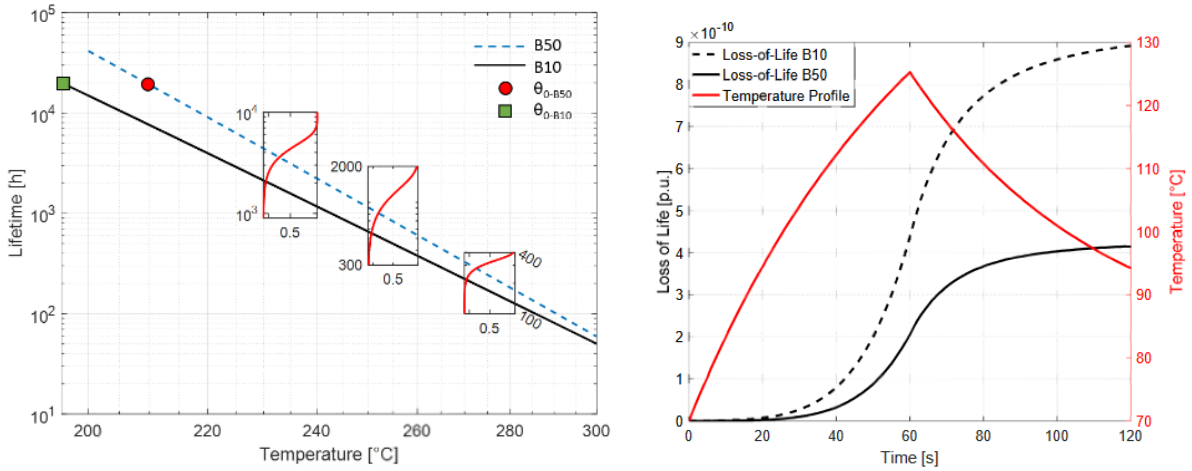

Figure 2-16 The loss of life or cumulative damage sustained by the insulation by applying one cycle. The comparison between using the ageing data differently, the B10 and B50 [127]. The left image shows two ways to fit the Arrhenius law, the right shows the resulting difference in loss of life calculation.

The scale parameter, when it is the lifetime that is distributed, is the time when 63% of the samples have arrived at the end-of-life. In [127] they made an argument that for critical applications, like avionics and other embarked cases, it is better to use more demanding criteria. We can consider the lifetime as the moment when 50% or even only 10% of samples have failed. This way we consider the worst-case scenario instead of the most probable. The impact of different choice on the cumulative damage calculation is shown in Figure 2-16. The different choices of lifetime points are denoted as B10 and B50 for 10% and 50% of dead samples in the trial.

The logical future modification of the method would be to include other factors in the cycling modelling. So far, cycling of any other factor than thermal is not well explored. Only one work which applies some form of cumulative damage method was found [135]. They applied the idea for High-Voltage DC cables. Electrical cycling considers the changes of DC load over time as the cycling. They used the Arrhenius equation to model thermal ageing and Inverse Power Model to model electrical ageing. They calculated the loss of life for cycling temperature while applying electric field. It was found that there is a synergy between

thermal ageing and electrothermal ageing. The conclusion is that the ageing temperature proposed by standards is not high enough to evaluate the case that includes also electric field applied to the insulation, which is an interesting finding also for electrical machines. However, so far, few researchers consider the question of multi-factor ageing.

The last example in this section is a study that includes the form of a cycle in its model [115]. The rationale behind the inclusion of rate of change was that the faster the temperature changes, the greater the temperature gradient and as a reason the mechanical strain. The same basic principles were used but a term for instantaneous change of temperature was added to the cumulative damage equation (2.7).

$$LoL = \int_{t_0}^{t_f} \frac{1}{L\big(T(t), v(t)\big)} dt \tag{2.7}$$

The *v(t)* is the derivative ot *T(t)*, the rate of change of temperature. Inside the lifetime model it is included as an inverse power model (2.9).

$$L_M = (1 + k|v|)^{-N} \tag{2.8}$$

where L_M is the thermomechanical lifetime, k and N are parameters of the impact of the thermal ageing.

The method was tested for six samples of round-section coil of wire wound on a stator. The samples were heated by running current in cycles reaching 285°C. A model taking into account only the thermal ageing predicted lifetime seven times longer than it actually was. Then based on the result of the experiment the parameters in (2.8) were calculated.

The approach differs from the on presented earlier where two terms were included in one cumulative damage equation. Here both thermal and thermomechanical ageing are included in one equation. The rate of change of temperature's impact on lifetime is modelled with an inverse power model which would require further research as the study does not present multiple points of data to confirm the model. It was shown that the impact of the rate of change of temperature has an impact on lifetime [113], hence the addition of it in the model is a step in a right direction.

2.4.5 Arrhenius-Miner approach

The section describes a complete process of applying the Arrhenius-Miner approach, compiled from different entries in literature. It involves the acquisition of static ageing data, finding the ageing law by fitting of Arrhenius curve, application of Miner's idea for thermal ageing, thermal cycling tests in order to utilise them in a model, second application of Miner's rule for the cycles themselves and the rainfall cycle counting for thermal profiles.

2.4.5.1 Acquisition of static ageing data.

The static thermal ageing is meant as the insulation's degradation purely due to the impact of constant temperature throughout the ageing process. A part of the standard practice in the Electrical Insulation System characterization is Temperature Index determination. Temperature Index is a temperature at which the system can survive for 20000 hours. For mica-epoxy insulation systems present in more massive, high voltage machines the value of TI is characterized up to 180°C. Low voltage machines' enamels of magnet wire are made up of materials of which TI goes up to 220°C or 240°C. The protocol of determining TI is described in standards [9] [26].

The samples are subjected to accelerated ageing tests. The standard specifies that at least three tests are required. The first set of samples is aged at the temperature of the projected TI plus 20°C and at two other temperatures, each augmented by another 20 degrees in reference to the previous one. For example, for a projected TI of 200°C the test temperature levels would be 220°C, 240°C and 260°C. The standard permits intervals of 10 K if there are more than three levels of temperature.

The Arrhenius' equation (2.3) is an empirical law that describes chemical reaction rate in relation to temperature. By acquiring a few data points one can determine activation energy which is a value characteristic for a given material. In the standard the result of such action is presented on the Thermal endurance graph. Logarithm of time in function of reciprocal value of temperature of the Arrhenius' equation is represented by a straight line, shown in Figure 2-17.

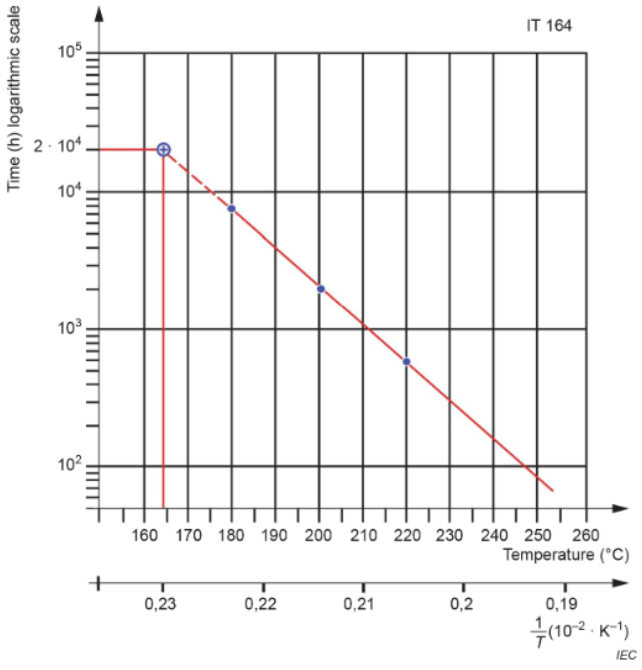

Figure 2-17 Thermal endurance graph [18]. The reciprocal-logarithmic scale shows the Arrhenius equation plot as a straight line.

The objective of the standards is to qualify a system rather than to evaluate it. The standards propose to compare a candidate system with a validated reference system of a known TI. The candidate system's Arrhenius law should be reasonably parallel to the reference law, which would indicate the same degradation process. The TI should be higher than that of the reference system.

The end-of-life criteria are not defined in the standard. It remains a point of discussion how to choose the end-of-life criterium, no concrete proposition for the measurements to be done during ageing. If a parameter, a chosen ageing indicator, is used as an end-of-life criterion, when it falls below 50% of initial value is considered the end of life [17]. Common practice is to wait until the breakdown of the insulation [136]. The end-of-life is pronounced when a sample fails a high-potential test or the leakage current exceeds some threshold in a test of this kind.

2.4.5.2 Finding the ageing law by fitting the Arrhenius curve.

The calculation of the three (or more) points required to establish the Arrhenius law is done with Weibull distribution. The distribution is fitted onto the ageing data, that would usually be the times till the end-of-life of the samples. From the five or more experimental points one number is distilled. By the standard, it is the scale parameter of Weibull distribution, the most probable time to failure or the time when 63% of the samples have arrived at the end-of-life. Once the scale parameters are calculated the expression of Arrhenius law is fitted onto the three (or more) data points as in Figure 2-17. The basic form of the Arrhenius equation is as in (2.9).

$$L = Ae^{\frac{-E_a}{kT}} \tag{2.9}$$

where L is the lifetime, T is the temperature, Ea is the activation energy, k is the Boltzmann constant and A a constant. The Arrhenius equation is often expressed with two constants A and B, that is when activation energy and Boltzmann constant are simplified to one constant B. Then, the equation takes the form as in (2.10).

$$L = Ae^{\frac{B}{T}} \tag{2.10}$$

In order to use linear regression methods, the equation (2.10) can be linearized by applying logarithm to both sides of the equation, the result is presented in (2.11).

$$\ln L = B\frac{1}{T} + \ln A \tag{2.11}$$

The equation expresses logarithm of lifetime as a linear function of reciprocal of temperature. That is why the Arrhenius Law is shown on a plot with logarithmic-reciprocal scale as a straight line in Figure 2-17. If the data were not conforming to the Arrhenius model the data would not form a straight line on reciprocal-log plot. Constants may be calculated

with the help of any optimization algorithm of choice. Once the constants are established, we have a model that relates the temperature with lifetime at that temperature.

2.4.5.3 Introduction of the Miner model, working principle

At this point the Miner's rule can be used. The Miner's rule is a simple cumulative damage model. It takes into account that different stress levels or cycles of different intensity would damage the object a different amount. It states that for each stress level there is a total number of cycles that the system can endure. When subjected to some number of cycles of a kind a fraction of the damage is added to the cumulated damage. That fraction is expressed as a few cycles undergone by total number of cycles of this kind to the end of life. When the cumulative damage reaches unity (1) the object's failure is expected. The expression of Miner's rule was shown in (2.3)

2.4.5.4 Application of Miner idea for thermal ageing

The Arrhenius law for insulation can be employed in Miner's rule as a base for establishing how many cycles at different stress levels it can endure. Yet, in this case we do not deal with cycles but in fact with time spent at that stress level. Temperatures are stress levels and the lifetimes in time units are the numbers of cycles till the end of life.

The lifetime of the insulation at any temperature can be calculated. When going over instantaneous values of temperature fractions of life lost are added to cumulative damage. The fraction is time spent at a level (in this case sampling time) by result of Arrhenius law for that level.

Even though the extrapolation from Arrhenius' equation necessary for TI determination should not be more than 25 K [137], when we apply it to lower temperatures its influence is often negligible. The added fractions of lost lifetime are so minuscule that the fact of excessive extrapolation should not be much of a problem.

2.4.5.5 Cyclic test, Arrhenius-Miner applied to the cyclic temperatures.

When thermal cycling comes into play in ageing tests, it was noticed by a few researchers that the loss of life from temperature exposure evaluated by Arrhenius law is not sufficient. The samples fail too early or much too early when only the Arrhenius-Miner procedure is applied. The cumulative damage at the actual end of life of cycled samples is lower than one. The remaining life is hence attributed to cycling itself.

2.4.5.6 Miner idea applied for the cycle impact evaluation.

Miner's rule can be applied another time in a different fashion. Whereas earlier it was applied to temperature levels as different cycles, this time it is applied to actual cycles. In fact, it is employed in a way closer to the intended use but combined with the influence of thermal ageing.

Ageing should be performed until the end of life with one and the same kind of cycle repeatedly. This way the amount of life lost can be attributed to some particular cycle. At the end-of-life amount of life lost from 'pure' thermal effect is calculated with Arrhenius-Miner method as described above. The remaining life unaccounted for, can be attributed to cycling. The amount of remaining life divided by number of identical cycles performed during the ageing gives an amount of lifetime lost by one cycle of this time.

If more kinds of tests with repeated identical cycles were to be done at an identical set of samples, one could imagine a model for how destructive different shapes of cycles are. As an example, cycle amplitude and maximum value can be taken as factors distinguishing cycles in terms of their degrading characteristics.

2.4.5.7 Rainflow cycle counting for thermal profiles

The final addition to the protocol of evaluation of cycling would be an algorithm for cycle counting. The Rainflow algorithm applied to a temporal profile of cycling counts the number of cycles and provides the amplitude and bounds of each one. Having constructed a model of how destructive different kinds of cycles are one can evaluate cumulative damage attributed to cycling of whichever profile. Provided that one has a proper way to discern cycles from said profile. The method was applied to power semiconductors [138].

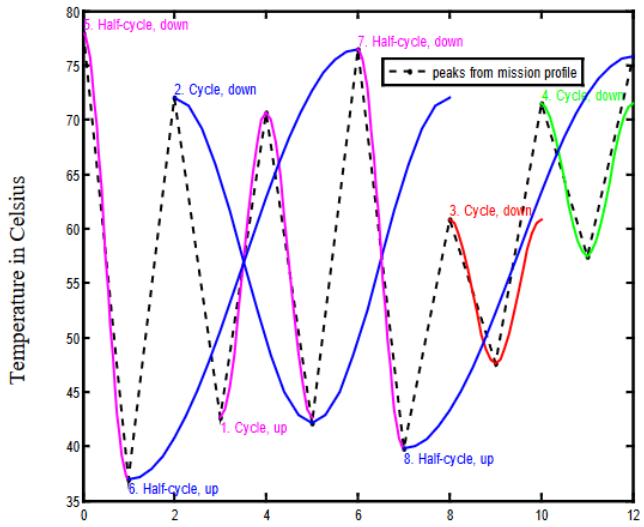

Figure 2-18 A temperature profile (dashed line) with cycles found with Rainflow method [138].

It would be extremely hard and expensive to have all possible cycles in a look-up table. That would require one experiment per cycle, where, in fact there is infinite space of possible cycles. What is more, some cycles, in low temperatures, would probably not accelerate the insulation ageing enough to achieve the results and the cycling impact in a reasonable time. For these reasons, one could imagine a protocol where only a few cycles are characterised in terms of their destructivity. Then, any other form of cycle's impact could be interpolated or extrapolated from the data for those key cycles. If we could define the significant parameters of a cycle that impact the lifetime of an EIS, we could design an experiment. The result of such would permit creation of a model liking those parameters with cycle's impact on insulation.

2.5 Conclusions

The chapter covers the different cycling tests methods for electrical machines. The first part of the chapter concerns standards on cycling. Standards offer one protocol for thermal cycling, which is widely used for accelerated ageing in experiments in the relevant literature. It regards the high-voltage type II machines but certain observations, like recommendation to use internal heating rather than external apply to tests on low-voltage type I machines. The lack of cycling standard for low voltage machines implies that the testing for them is mostly happening in constant values of stressing factors. Which may lead to underestimation of impact of real-life conditions on machines for applications where cycling occurs like electrical motors for electrical vehicles.

The second part of the chapter focuses on the literature on cycling in the context of EIS of the electrical machine. In the section, the lack of literature on any other kinds of cycling than thermal cycling is noted. Electrical or mechanical cycling when appears it has a different meaning than the cycling defined in this thesis – periodical change in ageing factor level. The commonly cited mechanism of deterioration of insulation during cycling is the result of mechanical strain. The force appears between layers of insulation and wire caused by temperature gradient and difference of thermal expansion coefficients. Within thermal cycling, aspects as cycle amplitude, temperature maximum and rise time are explored. It was shown that each of those cycling characteristics may have an impact on insulations lifetime.

The reason for testing of the electrical machines is to predict whether they can survive their designed lifetime. Whether the test is a qualification test after the manufacturing or a diagnostic test during its lifetime. In the second case, we would like to have ways to assess the state of the machine and reasonably predict the lifetime. Since cycling seem to be an important factor when it comes to machine ageing, we need such models that can incorporate that impact. The existing methods for evaluating such impact are described in the last section of this chapter.

The next chapter draws from the experience on cycling. The presented research was done to try to fill the existing gap of different kinds of cycling. It involved voltage cycling, voltage frequency cycling and that with multi-factor ageing.

Chapter 3.

Cycling impact on ageing of twisted pairs and stators.

3.1 Introduction

In this chapter, the results of applied cycling ageing tests and their analysis are presented. As already mentioned, cycling tests are not a common practice, especially for low voltage electrical machines. Few standards acknowledge the impact of cycling on lifetime of insulation, fewer propose any solutions for taking it into account. When cycling tests are considered, it is for big high-voltage machines, like hydro-generators. The tests are uniquely temperature cycling. In the scope of this PhD thesis original multiple cycling tests were performed with measurements of the impact of the cycling in mind. A range of different samples was used for this purpose from elementary samples to real objects such as stators. Different samples have different levels of complexity and present other challenges in experiment design. A twisted pair is easier to manufacture in abundance and offer a better reproducibility yet is further away in terms of build from the full system. A stator is the actual system, but it is hard to get access to an important number of samples. They are more costly and large numbers may simply not exist when the motor is in the early stages of development. Moreover, more effort is required to perform meaningful ageing routine on a stator – complexity of a test bench increases.

A considerable amount of research has been done on the topic of insulating materials ageing. The electrical insulation fault is one a major cause of an electrical machine failure [139]. The ability to model the degradation with respect to the stress factors and to predict and anticipate the breakdown are of dramatic importance and could lead to maintenance decisions. The sum of impacts of multiple factors defines the length of life of an EIS. Among those factors are generally voltage, temperature, mechanical vibrations and other various environmental stresses like humidity.

Well established models were developed for modeling the influence of constant factors on the lifetime. Some models consider one factor – temperature [33], some multiple factors[37], [39], [52], [140], some try to take into account also the interactions between factors – temperature, voltage and switching frequency [47], [50], [51]. These models are functions of constant factors' level; they do not deal with the operational characteristics of the stress, variability of the levels, conditions change over the course of operation which also may change periodically. At the same time, this mode of operation is the most frequent case and dominant in the electrical machines for electric or hybrid cars.

The process of evaluation of the EIS has to balance representativeness of the test, the time it takes to perform it and the cost. To derive information about a system's reliability or longevity, it must be tested in conditions resembling those of target application – be representative. On the other hand, the tests cannot last too long – the process has to be accelerated in some manner, usually by an increase in stress levels. The best practice so far proposes mostly to perform accelerated tests at constant levels [137] and extrapolate the results into lower levels where the system would operate (as shown in Figure 3-1). Established empirical models are employed for this purpose.

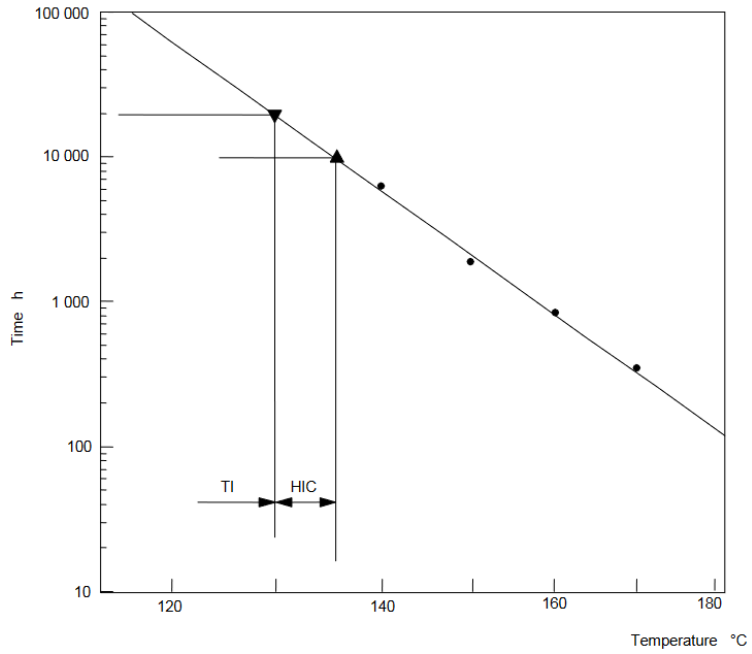

Figure 3-1 Dependence of insulation lifetime dependent on accelerated ageing. Results of constant stress ageing modelled and extrapolated [137]

Some work was done in the topic of thermal cycling [69]. The bulk of the work concerns hydro generators which experience many start-stop cycles during their lifetimes. Some of more recent research investigates thermal cycling in smaller machines [106], some try to quantify and model the impact of the thermal cycling on insulation system [121]. Rapidly changing temperature causes strain between insulation and copper due to thermal expansion coefficient mismatch (Figure 3-2). With time and many cycles, it may lead to delamination and consequently breakdown.

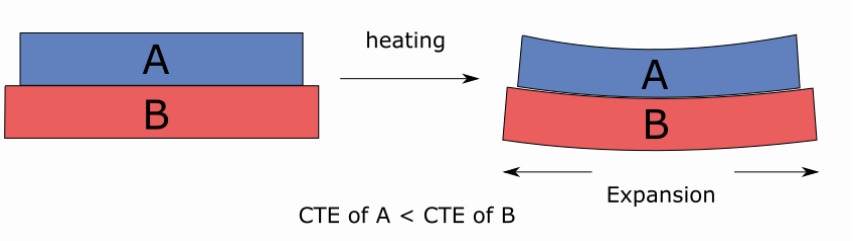

Figure 3-2 An illustration of the mechanism of appearance of shearing stress at the border of two materials of mismatched Coefficient of Thermal Expansion (CTE).

An electrical machine in an electric vehicle in its lifetime would typically experience many cycles of all possible factors, voltage, temperature, vibrations and humidity. The cycles would be both in the sense of seasonal or daily long cycles when used twice a day to commute and in a sense of shorter cycles when it comes to variability of route traffic. To our best knowledge no previous research investigates the existence of impact of voltage and frequency cycles on EIS of an electric motor.

The first part of this chapter presents a method to quantify the impact on lifetime of periodically changing stressing factors. Experimental setup emulates the output voltage of an inverter. Samples are twisted pairs of round enameled wires commonly used as low voltage electric motor winding. The ageing of the insulation is accelerated by imposing voltage high enough to impose partial discharges (PD). The latter parts of the chapter describe thermal cycling on stators and methods to quantify the results by referring them to constant temperature ageing tests.

3.2 Cycling of twisted pairs

3.2.1 Samples

In this experimental part, enameled wires of 0.5 mm in diameter are used. The enamel is polyimide, its temperature index is 240°C. The twisted pairs are prepared according to relevant standard [141]. (For a wire of diameter 0.5 mm it is 3.4 N of load and 16 turns.) The samples are manufactured in latex gloves and, before being placed in the oven, are cleaned with ethanol to reduce contamination. Indeed, it was demonstrated that if twisted pairs are exposed to dust, their lifetime is reduced [44]. The result shown in Figure 3-3.

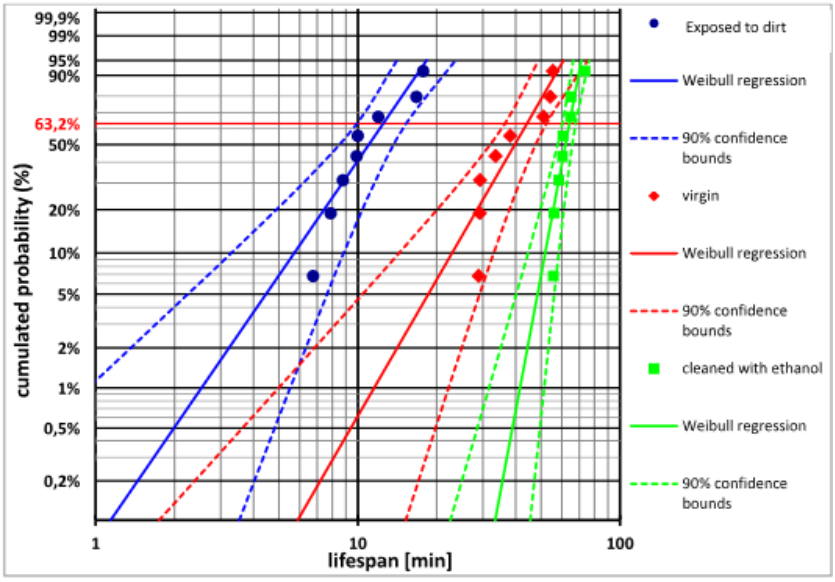

Figure 3-3 The impact on proper preparation of twisted pair samples on their lifetime [44].

Voltage amplitudes applied to the samples are well beyond Partial Discharge Inception Voltage (PDIV). In order to accelerate the tests, ageing is done with the impact of PD.

3.2.2 Test bench

The experimental part of this work profits from equipment prepared for previous research [47] [50]. The test bench (shown in Figure 3-4) permits to recreate voltage forms that are experienced by inverter-fed machines. It consists of two high voltage sources, a high voltage switch, a function generator and a dedicated counter. The sources provide voltage of opposite polarities but equal in value into the switch inputs. The switch which is gated with a signal from a function generator, outputs either the positive or the negative voltage value. This output is set onto the pairs through relays on one side. The other side is connected to the switch's ground. The relays are controlled by the counter. At the start of the experiment the relays are switched on and the counters begin to measure passage of time. When insulation of one of the pairs breaks down the switch detects the resulting overcurrent. The signal is passed to the counter which turns all the relays off and then tests every pair one by one to detect the broken one. Upon identification of the broken-down sample, its clock is stopped, its relay stays unconnected, and the operation is resumed for the remaining pairs.

Figure 3-4 The test bench, inverter style voltage emulator [44].

The test bench produces square-wave bidirectional voltage and permits to set the values of voltage amplitude and frequency. Temperature is also controlled as the samples are

kept in a climate chamber during the accelerated ageing. The climate chamber was chosen over the ovens, as a PD activity may increase the internal temperature of the oven [44].

3.2.3 Characterisation – single factor modelling

The insulation degrades at different rates at different stress levels. For describing the relationship between lifetime and voltage or frequency, an Inverse Power Law (1) is often used [35].

$$L(V) = k * V^{-n} \quad (3.1)$$

where L is the lifetime, V the applied voltage and k and n are model parameters. Similarly for frequency, expression (2) is commonly used [35]:

$$L(f) = l * f^{-m} \quad (3.2)$$

Where L is the lifetime, f the frequency and l and m are model parameters.

Tests at five levels of voltage and five levels of frequency were done. In tests where voltage was changed the frequency was kept at 4 kHz and temperature at 30°C. Where frequency changed, voltage was kept at 1 kV and temperature at 30°C. The same information is presented in Table 3-1. In each test 8 samples were tested. The choice of the values of voltage was dictated by the fact that for all the levels we need a voltage high enough to have PD activity and the resulting accelerated ageing. The frequency of 15 kHz is the upper capability of the high voltage switch.

Table 3-1 Factor levels for characterisation

Factor	**Stress levels**	**Fixed factors' levels**
Voltage	1, 1.1, 1.2, 1.3, 1.4 [kV]	Temperature (30°C) ; Frequency (4 kHz)
Frequency	1, 2.29, 4, 7, 15 [kHz]	Temperature (30°C) ; Voltage (1 kV)

The time until the end of life of the twisted pairs is considered to follow the Weibull's probability distribution. The analysis is done with accordance to the standard [142]. The model is established based on the scale parameters or the Weibull's α of the data sets. The two model parameters are found when a straight line is fitted on the data points on a log-log scale graph.

3.2.3.1 Cycling equivalence in constant stress

In order to evaluate the potential impact of periodic changes of stress level, we need to compare the cycling lifetime with a constant stress level lifetime. As a consequence, a form

of changing stress is needed that would, in theory, cause degradation of the material at the same rate if we assume that the cycling is not an additional ageing factor.

Some studies successfully attempt to apply Miner's rule and cumulative stress to insulation ageing [5, 6]. The Miner's rule at its basic form is often noted as (3.3):

$$C = \sum \frac{n_i \times S_i}{N_i \times S_i} \tag{3.3}$$

where C is the cumulative damage, n_i the number of cycles at stress S_i and N_i is the number of cycles at stress S_i till the end of life if only cycles of severity S_i are applied.

In principle the Miner's rule associates a value of degradation (a fraction of unity) to each kind of cycle or level of its severity. Then a prediction is made that the end of life would happen when the sum of degradation reaches unity. It can be understood as lifetime consumed per time that was spent at specific stress level, as in (3.4), an example for temperature.

$$C = \int \frac{1}{L(T(t))} dt \tag{3.4}$$

where $L(T)$ is lifetime at temperature T, dt is time spend at temperature T, which is a function of time in this case.

Table 3-2 Cycling factor ranges and constant equivalent values.

Factor	**Cycling stress levels**	**Equivalent constant stress level**
Voltage	0.95 kV - 1.45 kV	1.2 kV
	1.05 kV – 1.35 kV	1.2 kV
Frequency	2.29 kHz – 7 kHz	4 kHz

Table 3-2 discloses the chosen voltage and frequency ranges and corresponding equivalent constant stress levels. The upper and lower factor levels were calculated in accordance with equation (3.1) for voltage and (3.2) for frequency.

3.2.3.2 Characterization in function of frequency

Experimental results for ageing at different levels of frequency (set at a constant level) are presented in Figure 3-5. The inverse power model was fitted onto a Weibull's scale parameters of lifetimes of eight samples per trial. The model well describes the evolution of ageing in function of frequency (coefficient of determination $r^2 = 0.9962$). Especially good fit can be explained by the fact that frequency directly correlates with number of PD experienced by the insulation.

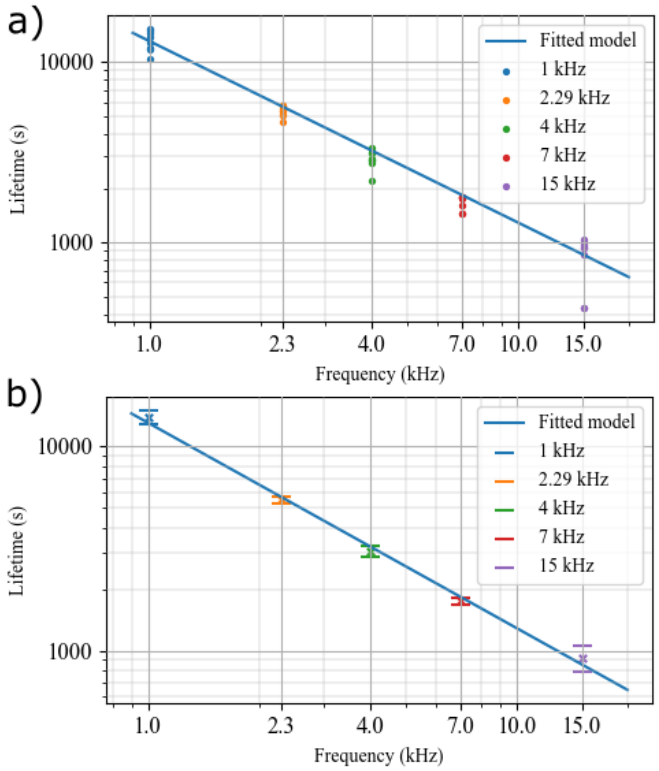

Figure 3-5 Sample lifetime in a function of imposed static frequency, log-log plot. (a) Every single experimental point and (b) Weibull scale parameters with 90% confidence intervals. Model (3.2) parameter values: l = 13061, m = 1.007

3.2.3.3 Characterization in function of voltage

Experimental results for ageing at different levels of voltage (set at a constant level) are presented in Figure 3-6. The inverse power model was fitted onto Weibull scale parameters of lifetimes of eight samples per trial. The model well describes the evolution of ageing in function of voltage (coefficient of determination $r^2 = 0.9686$).

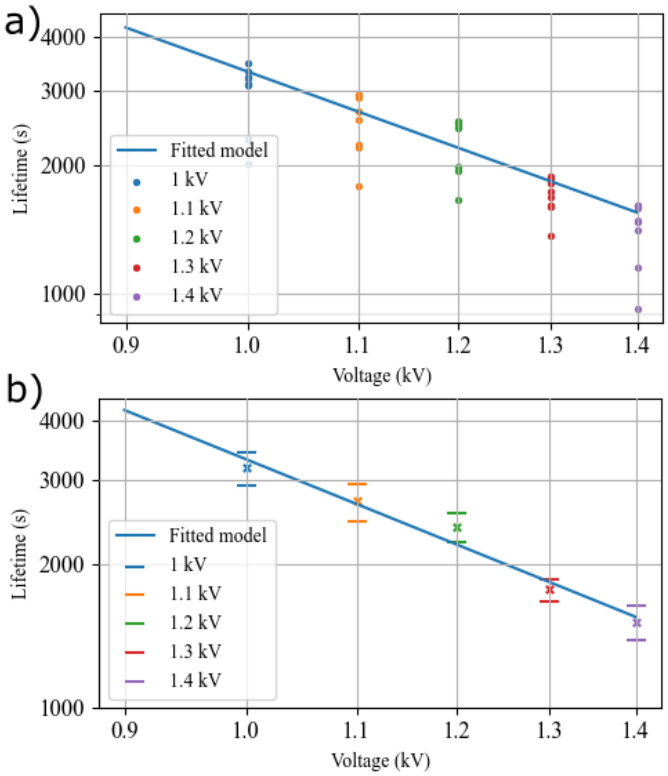

Figure 3-6 Sample lifetime in a function of imposed static voltage, log-log plot. (a) Every single experimental point and (b) Weibull scale parameters with 90% confidence intervals. Model (3.1) parameter values k = 3320 n = 2.256.

3.2.4 Voltage and frequency cycling of twisted pairs

Now that the impact of each of the factors was modelled separately by the characterization, we can proceed to the cycling tests and assessment of cycling impact.

Cycling is a periodic change of severity of one or several stressing factors. In this part, both voltage and frequency changes impacts are investigated. Voltage cycling was achieved by using a feature of voltage sources. The sources are controllable by a 0-10 V signal. When provided with a signal that informs the source that it is in remote control setting it blocks usage of knobs at the front panel. Instead, the output is a voltage between 0 and 3kV proportional to the control voltage. A signal generator provides a saw-tooth form voltage at levels proportional to the envisaged cycling. The resulting form can be observed in Figure 3-7.

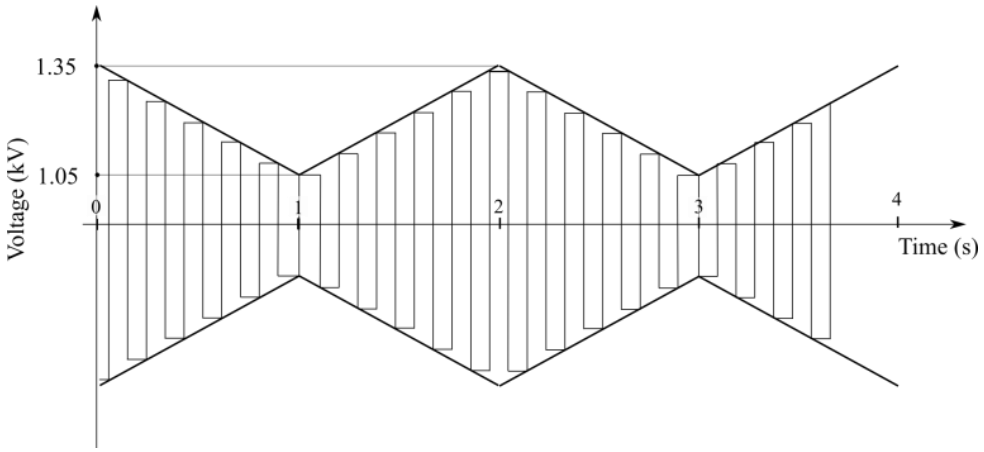

Figure 3-7 Voltage form of cycling - example. Saw-tooth form from signal generator (in bold line) and resulting square-wave form at the switch's output. (The switching period is grossly exaggerated for a better understanding.)

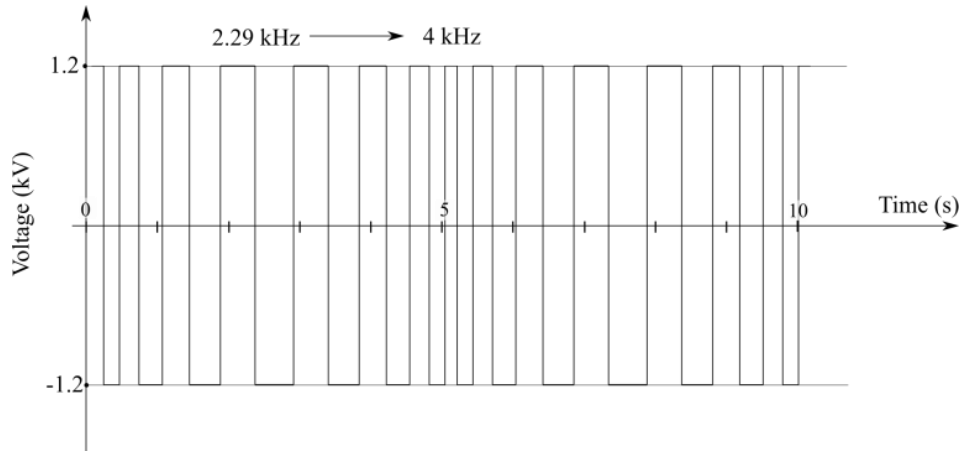

Figure 3-8 Frequency form of cycling - example. The switching frequency oscillates linearly between two values. (The switching period is grossly exaggerated for a better understanding.)

The frequency is changed by varying in time the gating signal of the switch. The signal generator with sweep over frequencies functionality provides a signal of linearly changing frequency. An example of such waveform is displayed in Figure 3-8.

Experiments with two different voltage cycling amplitudes and one frequency cycling amplitude were achieved. Obtaining two different amplitudes of cycling presented an opportunity to try to determine whether there is an impact of the cycle amplitude. For each cycling protocol a few different frequencies were tested, presented in Table 3-3. Cycle frequency means number of cycles per time unit.

Table 3-3 Cycling frequencies in cycling tests for voltage and frequency.

Factor	Stress levels	Cycling frequencies [Hz]
Voltage	0.95 kV – 1.45 kV 1.05 kV – 1.35 kV	0.1, 0.5, 1, 2, 4 0.1, 0.5, 1, 2, 4
Frequency	2.29 kHz – 7 kHz	0.03,0.06,0.12,0.24

Different cycling frequencies gave from 100 to 700 cycles during similar lifetime for variable frequency. In the case of voltage frequency, the different periods resulted in the number of cycles from 200 to 9000.

Figure 3-9, Figure 3-10 and Figure 3-11 present results of three different cycling protocols described in Table 3-3.

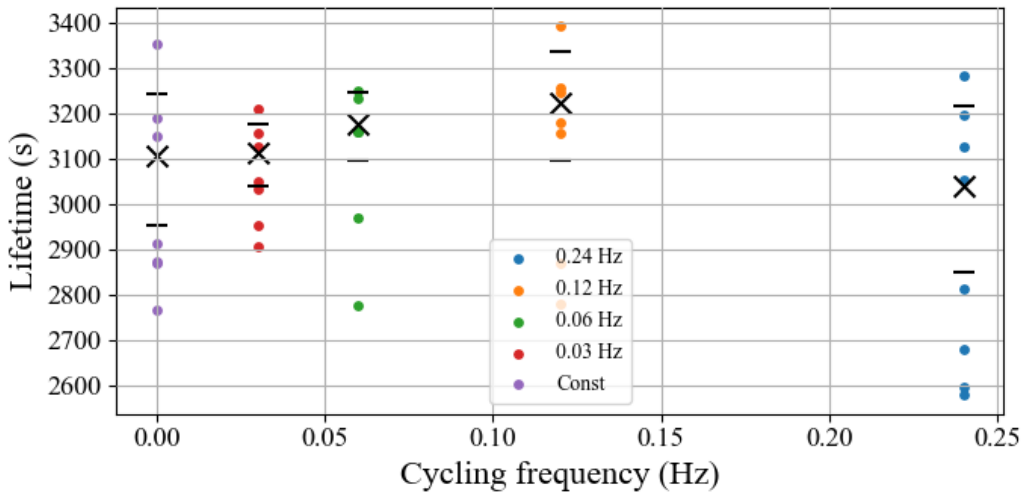

Figure 3-9 Lifetime versus cycling fundamental frequency. Amplitude from 2.29 MHz to 7 MHz.

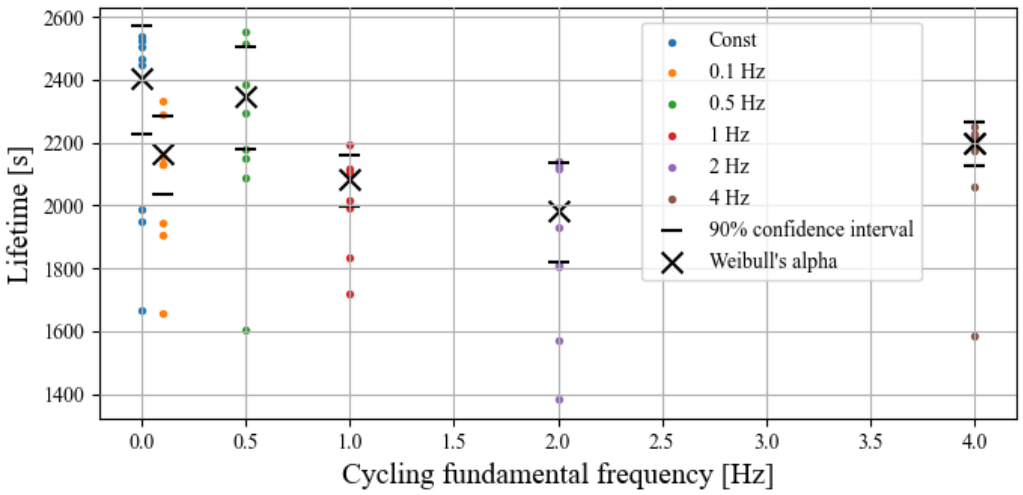

Figure 3-10 Lifetime versus cycling fundamental frequency. Voltage amplitude from 0.95 kV to 1.45 kV.

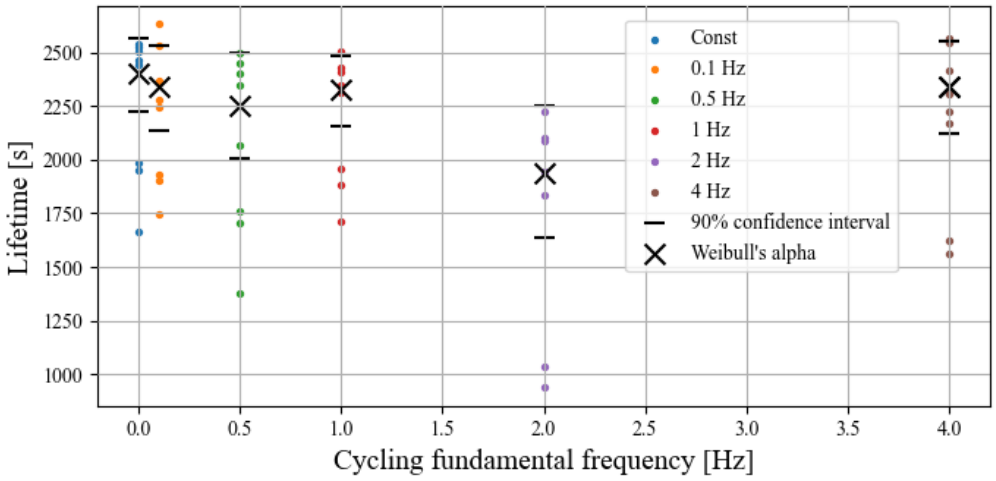

Figure 3-11 Lifetime versus cycling fundamental frequency. Voltage amplitude from 1.05 kV to 1.35 kV

Table 3-4 Cycled lifetime as percentage of constant stress lifetime.

Frequency cycling range 2.29 kHz - 7 kHz					
Cycling frequency [Hz]	0.03	0.06	0.12	0.24	
Percent of const lifetime [%]	100.2	102.2	103.7	97.8	
Voltage cycling range 1.05 kV - 1.35 kV					
Cycling frequency [Hz]	0.1	0.5	1	2	4
Percent of const lifetime [%]	90.0	93.1	83.9	82.4	91.4
Voltage cycling range 0.95 kV - 1.45 kV					
Cycling frequency [Hz]	0.1	0.5	1	2	4
Percent of const lifetime [%]	97.2	93.7	96.7	80.6	97.3

Table 3-4 quantifies the difference between constant stress lifetime and cycling cases – Weibull α of data sets are compared. For frequency cycling the numbers stay within 4% difference, there is no decrease or increase of lifetime with rising cycling frequency. In voltage cycling the differences reach 20%, still no decreasing or increasing trend is observed. Except for two measurements in Figure 3-10, at 1 Hz and 2 Hz, all the 90% confidence intervals for the data sets overlap. That overlapping prevents us from drawing any conclusions to any impact of applied cycling so far.

3.2.4.1 Conclusions on voltage and frequency cycling

In conditions used in this study and for the tested materials no significant difference is found between constant stress level accelerated ageing and periodically variable stress accelerated ageing. Static value ageing was compared with multiple numbers of cycles per lifetime for both frequency and voltage. Additionally, two amplitudes of change for voltage were tested. Both confidence intervals of constant case and cycling case overlap; no trend is observed when increasing cycling frequency.

The ageing tests on the twisted pairs were done with impact of PDs. In this case the PDs are the main cause for samples ageing leading to breakdown. The PD's destructivity is additionally accelerated with augmentation of voltage and frequency as the characterization part indicates. The choice to perform the tests at voltages so destructive to the insulation was to highly accelerate the process. It may be interesting to search for cycling impact under the PDIV level. Consequently, the tests will be longer and potential cycling impact more pronounced. Moreover, the same type of study should be carried out for other materials than twisted pairs, motorettes being the primary candidate.

3.2.5 Temperature cycling of twisted pairs

The performed temperature cycling test were treated separately. The voltage and frequency cycling required only minor changes to the tests bench compared to the characterisation protocol. It required the function generator controlling the frequency to be in a sweep mode, which changes the frequency linearly between chosen frequency values. The voltage cycling was added by fixing the high voltage source to a function generator outputting a triangular voltage signal. Chosen rates of change of factors permitted to apply multiple hundreds of cycles in a time of around an hour per test. When it comes to temperature the tests have to be done in a climate chamber to control both heating and cooling down phases. What is more, the fastest cycle with significant amplitude that the chamber can deliver, last about an hour. If the factor levels form characterisation were to remain the same in these tests, the samples would experience only one cycle in their lifetimes.

3.2.5.1 Test bench modification

In the preliminary tests the chosen cycle was between 0 °C and 31 °C (the middle point being 15 °C). The results of these tests are shown in Figure 3-12. The lifetime is almost linearly related to inverter frequency if the voltage is above PDIV. The commutation being the most fragile moment for PD to appear. By decreasing the frequency by one order of magnitude we can extend the lifetime from below an hour to over a day. Voltage was lowered but not significantly so that we stay above the PD inception voltage to accelerate the test.

Preliminary constant temperature tests were done for 0°C, 15°C and 31,7°C in order to try to establish a similar characteristic as for higher temperatures (results shown in Figure 3-12). Then a cycling from 0 °C to 31 °C was performed (The result also shown in Figure 3-12).

The temperature cycling was provided by a climate chamber. The twisted pairs were connected to the inverter emulator with constant value of voltage and frequency (1kV and 100 Hz) inside the chamber. The climate chamber temperature was programmable. The nominal value of temperature ramp for heating for this device is 2.5 K/min and 1.5 K/min for cooling. The chamber was launched to heat up to the initial temperature of the first cycle, then the electrical ageing and the thermal cycling were started simultaneously. Lifetime of each of the eight samples was recorded by the test bench. Number of cycles was recorded by the climate chamber. Number of cycles per hour was then deduced from the time passed by the chamber on cycling.

In Figure 3-12 it can be observed that the Weibull's alpha of the cycling is higher than that of the middle point at 15 °C but the confidence intervals overlap. In this sense the additional impact of cycling was not observed.

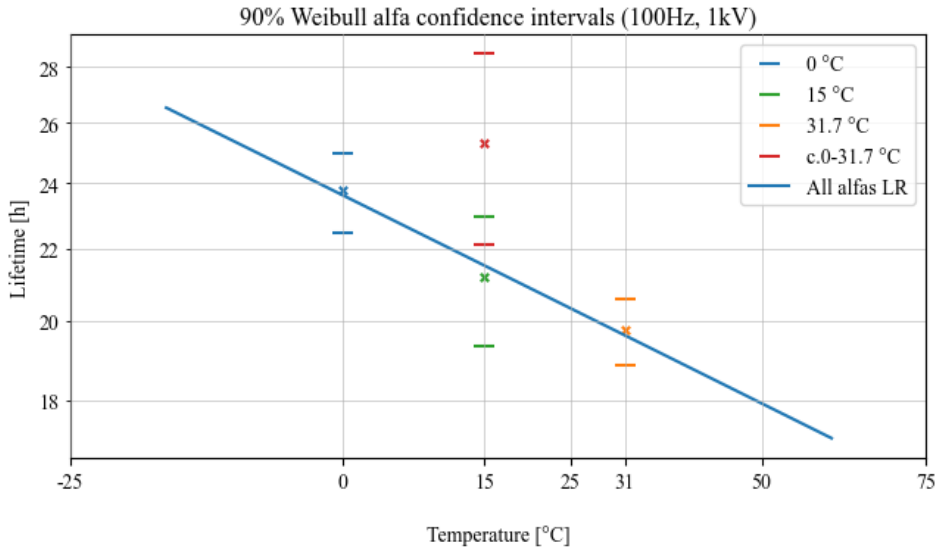

Figure 3-12 Weibull's α and confidence intervals for lifetimes of twisted pairs. Arrhenius' law fitted onto the constant temperature lifetime points (blue).

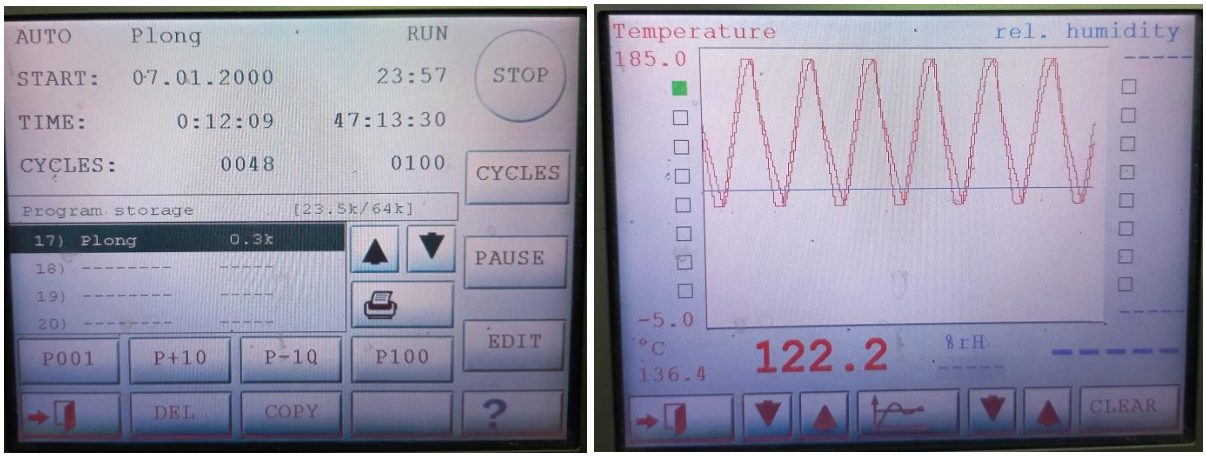

Figure 3-13 Example of a dashboard of the climate chamber with a program running.

It can be read in the left photo in the Figure 3-13, that in 47 hours and 1 minute the device went through 47 cycles. (The 48th started 12 minutes prior to the taking of the photo). In the same figure on the right the climate the 80-180 cycle is illustrated. The plot shows the set value over time and the measured temperature that follows it. It is the fastest possible cycle at this temperature and with this amplitude for this device.

3.2.5.2 Temperature cycling results.

In the next step amplitudes of 50 K and 100 K were chosen. It was decided that it would not be prudent to get too close to the enamel Thermal Index (i.e.: 240 °C) not to accelerate the ageing too much. The middle point was decided as 123 °C and that gave two intervals, from 100 to 150 °C and 80 °C to 180 °C. Both intervals have middle points at the 123 °C on the reciprocal scale. Thermal ageing is usually modelled with Arrhenius' curve. To

achieve equivalency between constant temperature test and Miner's rule calculated thermal impact, the middle temperature is chosen according to reciprocal scale. Figure 3-14 illustrates the placement of the middle point. The voltage remained at 1 kV to stay over the PDIV. The frequency was further decreased to 50 Hz to gain even more cycles in a lifetime of a sample.

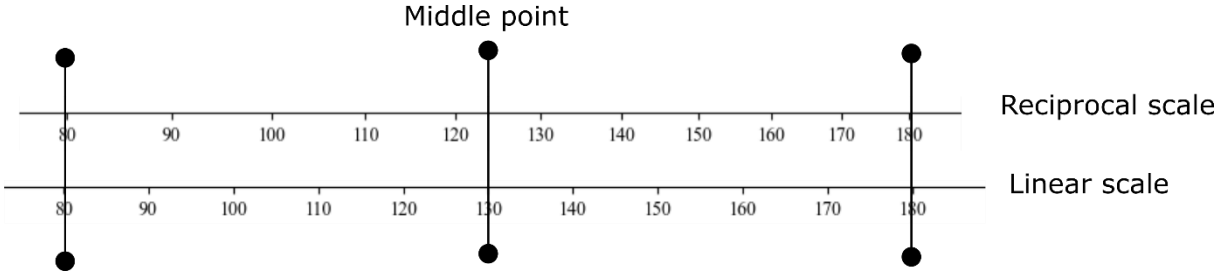

Figure 3-14 Comparison between reciprocal and linear scale. Middle point on reciprocal scale demonstrated.

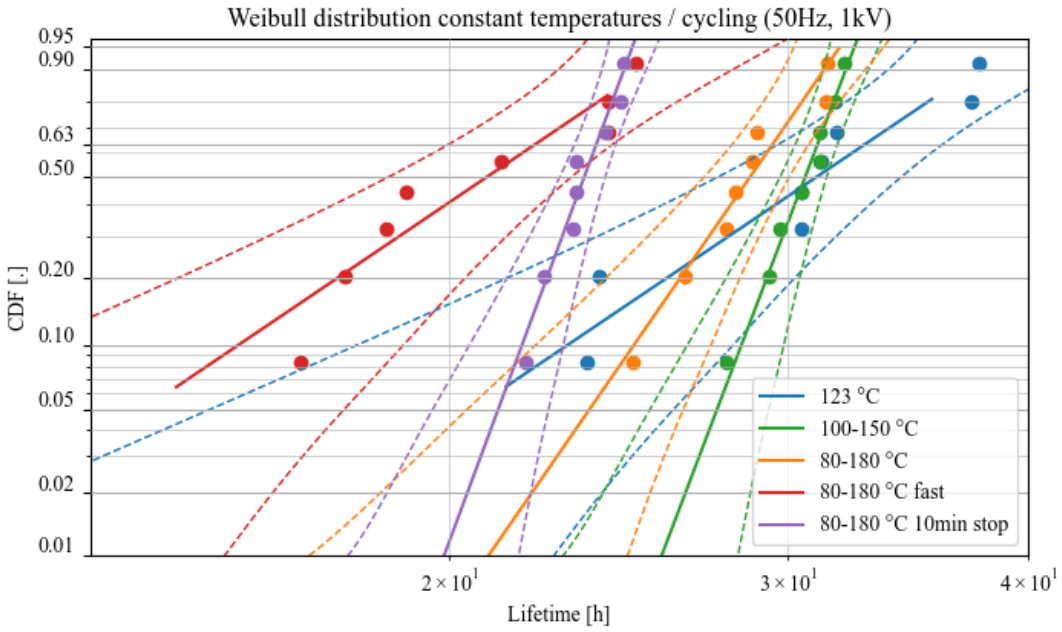

Figure 3-15 Experimental points and cumulative probability Weibull distributions for a few temperature cycling tests. The distributions are fitted onto the data, the confidence intervals are calculated according to the relevant standard.

Unfortunately, the result for constant temperature at 123 °C has more of a spread (the blue data points in Figure 3-15). There is no understandable reason behind that. One could speculate that in this regime only the heating mode of the climate chamber was used. The active cooling was never launched; hence the process differs from the cycling modes in this way. The fact that one of the cycling tests presents similar spread disqualifies this idea. For the purposes of analysis, the Weibull's α value is usually used. Also, for small number of samples the early samples are counted with penalising weights, they are considered premature end-of-life.

Table 3-5 Results of thermal cycling for various cycles.

Temperature range	Amplitude [K]	Cycles per hour	Dwell time	Lifetime [h]	Percentage of constant stress lifetime [%]
123 °C	-	-	-	32.9	100
100°C-150°C	50	0.93	-	31.0	94
80°C-180°C	100	0.83	-	29.4	89
80°C-180°C	100	1.01	-	22.1	67.1
80°C-180°C	100	0.75	10 min	23.8	73.2

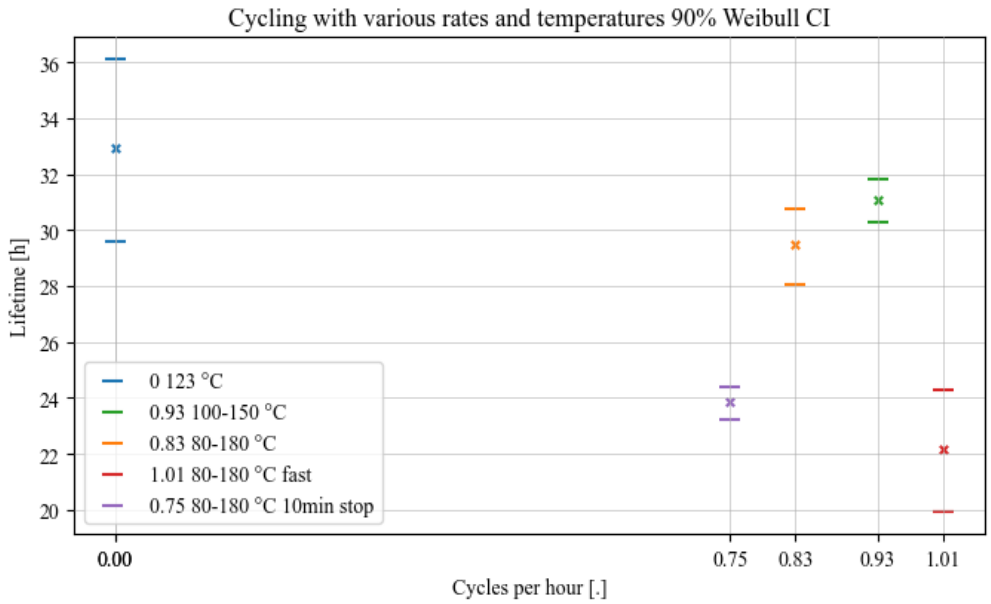

Figure 3-16 Weibull's α parameter with confidence intervals for tested cases. Constant temperature test in blue (as 0 cycles per hour). Compared cycling cases indexed by number of cycles per hour.

Confidence intervals of constant temperature test lifetimes and two first cycling tests overlap (visualised in Figure 3-16) – which would mean that this kind of cycling did not cause additional ageing. However, the constant temperature test has a wider confidence interval, perhaps if we acquired more data, we would be able to see a difference. The two subsequent tests were done at maximum achievable temperature change rate. Second of which had an additional dwell time at 80°C and 180°C of 10 min each. Intervals for those two tests overlap and are significantly lower than those of the other tests – impact of cycling can be claimed. The test without dwelling has more dispersion and its α Weibull value is lower. The samples in this experiment have higher cycling rate hence experience a few cycles more.

The primary suspected mechanism of degradation when it comes to thermal cycling is the difference of thermal expansion coefficient between two materials that constitute two adjacent layers. When heated up or cooled down rapidly one contracts or extends much more than the other. This process repeated multiple times can cause degradation and more specifically, delamination. In this experiment only the highest possible change rate produced shorter lifetimes. It points to a possibility that a threshold exists on the mechanism of thermo-mechanical degradation, which could be further investigated.

3.2.5.3 Design of Experiment for Thermal Cycling

Experiences from previous trials on thermal cycling led to the idea of performing a Design of Experiments type campaign. This time the points were chosen more scrupulously, and more care was put into obtaining the exact values of number of cycles per hour. Figure 3-17 presents the ageing runs performed in this experimental part. As before, each experiment consists of eight twisted pair samples.

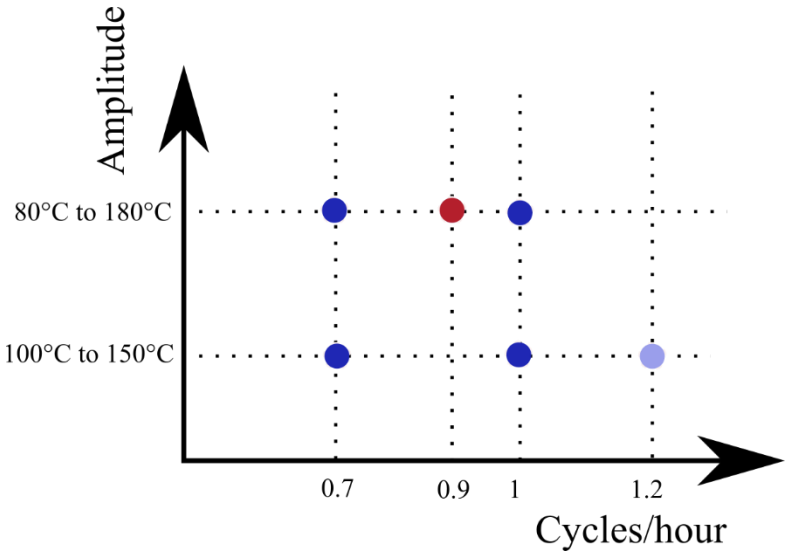

Figure 3-17 The experiment performed in this part. Dark blue points represent the points of the plan, the other ones are the results of improperly programmed climate chamber.

At that point in time the influence of change rate was not fully realised. The two factors that were considered are cycling temperature amplitude and number of cycles per hour. The two temperature amplitudes used before were preserved. The maximum number of 80°C - 180 °C cycles per hour is one. It was the natural higher level of this factor. Naturally, it is possible to do more cycles of lower amplitude. When the cycle 100°C - 150°C is performed with the same change rate as the fastest possible 80°C - 180 °C cycle we obtain 1.2 cycle per hour. The lower level of cycles per hour factor was chosen as 0.7.

Table 3-6 Cycling results, cycle details and resulting lifetime, comparison with equivalent constant stress lifetime.

Temperature range	**Amplitude [°C]**	**Cycles per hour**	**Lifetime [h]**	**Percentage of constant stress lifetime [%]**
123 °C	-	-	32.9	100
80°C-180°C	100	0.9	20.2	61.3
100°C-150°C	50	1	33.8	102.7
80°C-180°C	100	1	19.2	58.3
100°C-150°C	50	1.2	32.0	97.3
80°C-180°C	100	0.7	20.9	63.5
100°C-150°C	50	0.73	31.1	94.5

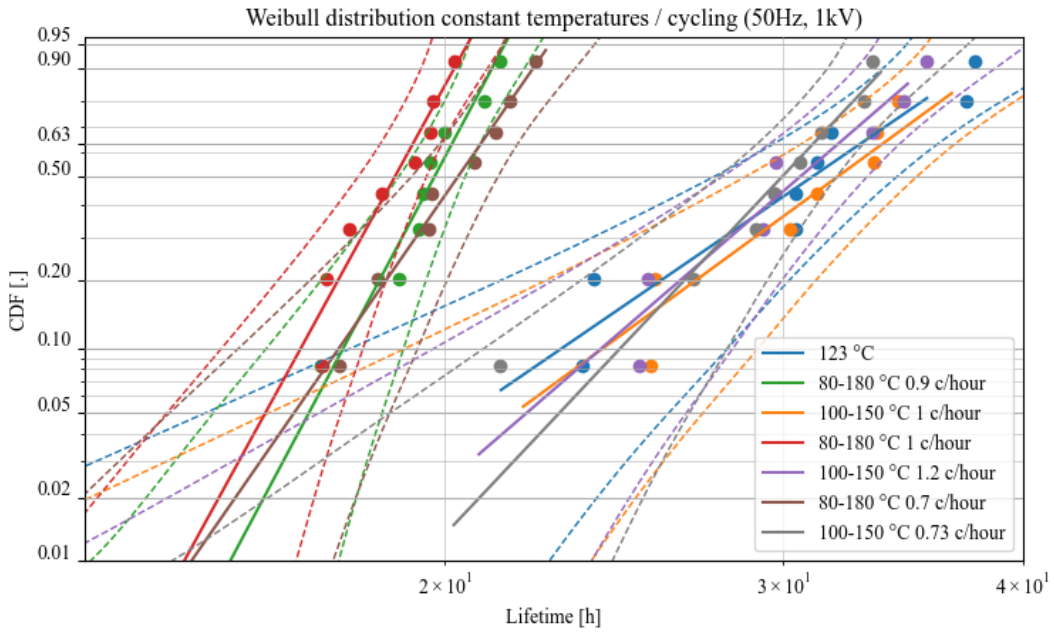

Figure 3-18 Measured lifetimes and fitted cumulative distributions on Weibull's plot.

What can be seen instantly from the combined ageing data of all the test cases is that there are two clear groups (Figure 3-18). One group of shorter lifetimes is the cycling of higher amplitude. What is more, the spread in this group differs significantly from the higher spread present among points of the other group. Within the second part of tests, the 100°C - 150°C cycling is grouped with the constant temperature ageing case. That means that the addition of this cycle does not appear clearly as a destructive factor. On the other hand, the

difference in spread for the other group may indicate presence of a different ageing mechanism. The lifetimes are also shorter.

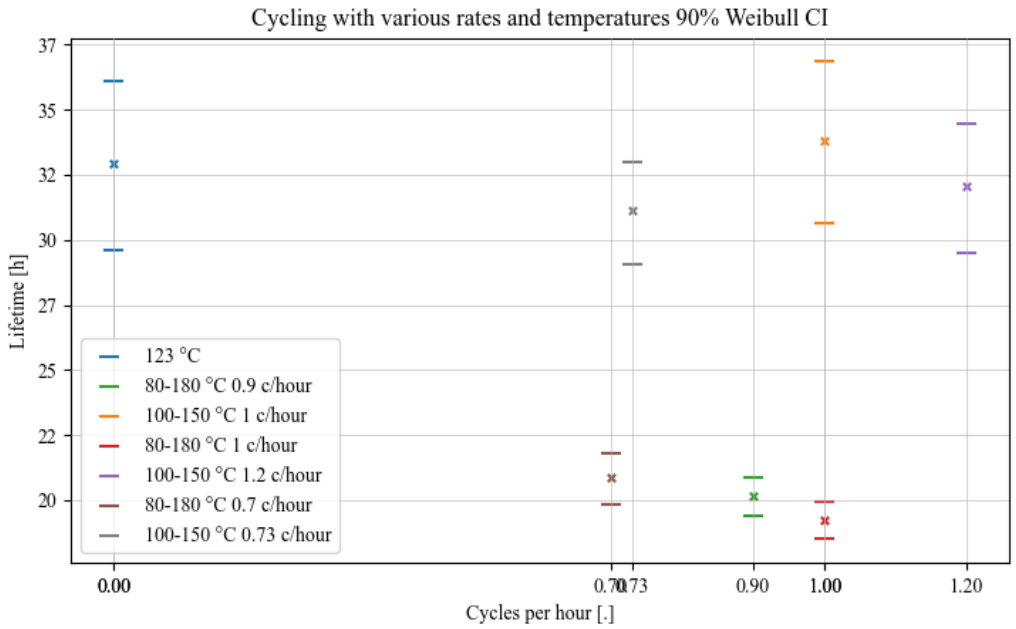

Figure 3-19 Weibull's α parameters with confidence intervals for tested cases. Constant temperature test in blue. Compared cycling cases indexed by number of cycles per hour.

Overlap of the confidence intervals of lifetimes for cycling with lower temperature amplitude and the constant temperature ageing can be observed in Figure 3-19. The other group of results, the large amplitude cycling is clearly distinct compared to the reference constant temperature test. Within the group slight decrease of lifetime with number of cycles can be observed – yet the confidence interval of points at 0.7 and 1 still do overlap.

The Arrhenius law, according to the standard, should be extrapolated only by about 20 °C away from the temperatures used to establish that law. Any further extrapolation may not by accurate. The hypothesis of equivalency between the constant temperature 123°C and the cycles assumes that the law extends even to lowest temperatures. It may well be that the observed difference in spreads and lifetimes is since the temperature approaches the TI of the material.

The experiment shows that the 80°C - 180°C cycle accelerates the breakdown of twisted pairs when PDs are present. The question whether it is really the thermomechanical ageing or simple influence of higher temperature requires additional tests at higher amplitude but with lower maximum point.

3.3 Active cycling vs passive cycling of a stator

Two identical and complete stators – with windings, insulating paper and impregnation – were available for experiments. The stators were prototypes manufactures in a quantity of a few samples for research purposes.

Figure 3-20 One of the two identical stator used in cycling tests.

The JV Emotors performed standardised accelerated ageing tests at constant temperatures on stators of this design. One of the objectives of the PhD thesis is to broaden the established testing procedure and propose multi-factor tests, including cycling as far as possible. In this case, beside the high temperature, close or beyond the TI, the insulation is subjected to relatively rapid changes of temperature. Comparing a test with the addition of cycling with constant temperature tests we can establish if there is an impact on the lifetime.

In this work, the terms passive and active thermal cycling are used. We define the passive thermal cycling as a heating situation where the heat source is external to the stator. It usually means that the stators are put into an oven (or a climate chamber) and the heat is transferred to them through the air in the chamber. The passive method heats up the sample from the outside to the inside. The temperature, provided a proper ventilation of the chamber, is quite uniform. Alternatively, if there is little circulation and the temperature is measured at only one point there is probability of variability of temperature in the volume.

Active thermal cycling is defined as the introduction of heat into the sample through injection of current into its copper conductors. High current is supplied in the windings and the resistance of the copper dissipates energy. In this method the uneven heat distribution is more representative of the real-world situation of, for example, an electrical machine in an automotive application.

The first test campaign on a stator was performed with passive heating - by an oven. It is a standard practice for product qualification, yet supposedly the active heating is more

representative of real-life situation. Henceforth, for the second trial the test bench was modified to accommodate injection of high currents into the stator and heat it that way. Significant difference between the two trials could demonstrate the need for changes in protocols for cycling tests. Still, the fact that one sample per method prevents from drawing strong conclusions.

3.3.1 Cycling form and performed tests

The cycling protocol was fixed as 12 h in 220 °C and 12 h at 40 °C. The temperature profile copied one used before in previous tests performed in an industrial context. That offered the possibility to compare obtained results with the previous ones.

The stators were tested twice a day with dielectric tester FI9015HT. Similarly, as with the temperature profile the test protocol was identical to the one performed in previous tests performed by Emotors. There were four different tests:

- Phase-to-phase insulation AC test at 300 V
- Phase-to-phase insulation DC test at 500 V
- Ground-to-phase insulation AC test at 1000 V
- Ground-to-phase insulation DC test at 2500 V

The voltage is gradually ramped up during a few seconds and then held for a few more. Table 3-7 shows the exact data.

Table 3-7 Test performed during cycling ageing on the stators.

	Voltage form	**Voltage [V]**	**Ramp-up time [s]**	**Holding time [s]**
Phase-to-phase	AC 50 Hz	300 (RMS)	5	3
	DC	500	5	15
Phase-to-ground	AC 50 Hz	1000 (RMS)	5	3
	DC	2500	5	10

The testing device returns either a pass or a failure for each test. Beside that it displays the leakage current measured at the end of the test. That current amplitude was recorded for each test. Each of three phase-to-phase combinations (1 with 2, 1 with 3 and 2 with 3) and the three phase-to-ground insulations were evaluated. One set of tests was done at 40 °C and another at 220 °C at least 4 hours after the start of the heating when the stator achieved thermal equilibrium. As long as the massive steel part of the stator does not properly heat up the wire and insulation inside would be significantly cooler than the insulation at end-winding.

The test was continued until all the diagnostic tests return a failure. Yet, the stator was considered to be failing as soon as one of the mentioned tests returns ‘failed’ result.

3.3.2 Test bench for passive cycling

The tests were carried out in an oven (Carbolite AX). The oven is equipped with programmable temperature regulator. Daily measurements did not require opening of the oven. That prevented the potential temperature shock or excessive contamination with the outside air. For that effect, for each of the phases and the ground there were wires on one end soldered onto terminals of the phases. The other ends were led to the outside through an opening in the oven. The setup presented in Figure 3-21. That assured electrical availability of the phases’ windings from the outside without opening the door.

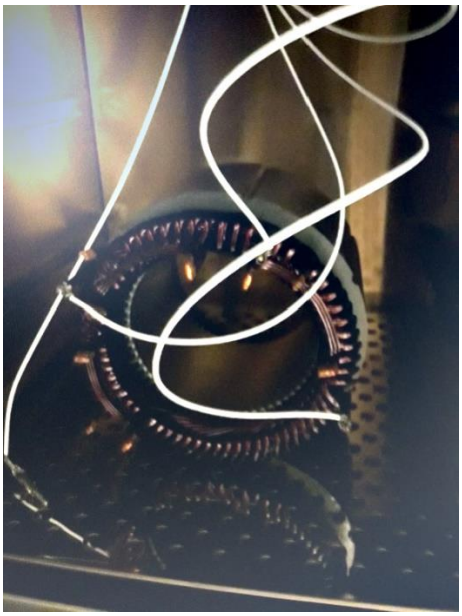

Figure 3-21 The stator in the oven’s chamber. The cables led to the outside that permit the measurements are visible.

3.3.3 Test bench for active cycling

Active cycling is defined here as cycling where the heat produced is inside the stator with copper losses. The process is more representative of an actual situation of a stator in an application. In the previous case of passive heating, the oven delivers heat to the stator from the outside and the temperature distribution is more uniform. Whereas when it is the winding that delivers heat in early instants of heating the copper arrives at high temperature and there is more of a gradient between wire and its insulation. To assure the most similar conditions to the passive test the active cycling was also performed in the same oven. The oven was there to insulate the sample – the stator – from the outside changing conditions, as much as it did for the previous passive test, as well as maintain the lower temperature bound of 40 °C while current is not supplied to the windings.

In order to heat up the stator it was supplied with current from 100 A to 150 A. An autotransformer connected to the grid supplied voltage through a primary winding of a transformer. The secondary winding of that transformer was composed of three separate coils, one per each phase of the stator. Each supplied an equal current to each of the phases. The cables used to deliver the current to the stator had a section of 25 mm^2 while the three phases combined had a section significantly lesser. Greater section area of the cables limited the heat dissipated outside of the stator windings. Figure 3-22 illustrates the heating system. The bottleneck of the system was the primary winding of the transformer. The nominal value of current was 10 A. In the preliminary trials the autotransformer knob was set to a value that assured that the primary current would not exceed the 10 A value. On secondary side the transformer outputted 150 A for a cold stator and the value dropped to about 130 A after the copper heated up.

The phases were led to the outside of the oven with wires as it was done for the passive heating case. The difference was that the wires were not soldered onto terminals but incorporated into the link between the windings and the cable delivering current into the stator. Also, in order to measure the conductor's degradation, the current supply was turned off from the experimental set-up for security reasons. A test was a matter of a few minutes. The time was not long enough for the temperature to drop a lot (from 10 °C to 15 °C only).

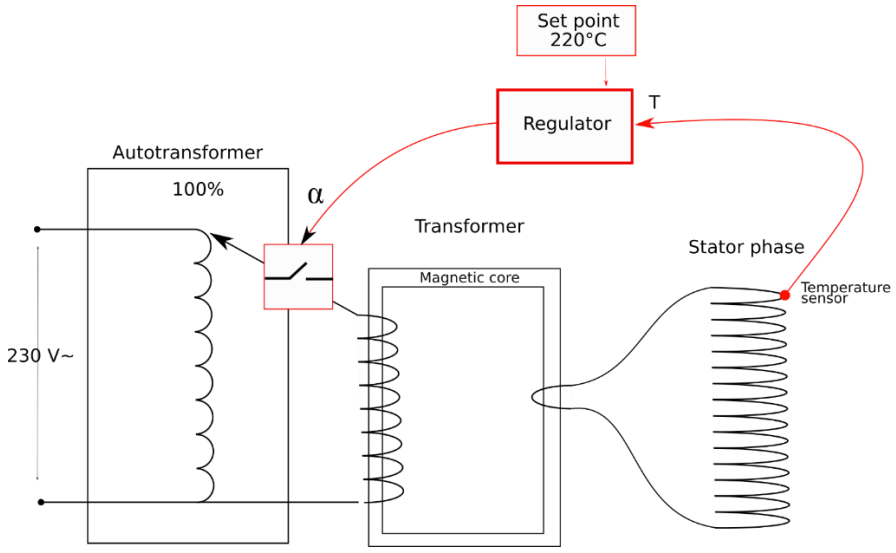

Figure 3-22 Electric scheme of the heating set-up. Only one phase shown on the secondary side.

The temperature profile envisioned for this test was supposed to be as similar to the previous profile as possible. Setting of a current which maintained the 220 °C in open loop would be too small to rise the temperature as fast as the oven. Current high enough to reproduce the ramp of oven heating would produce much higher temperature than required. For this reason, the temperature was regulated in a close loop. A simple bistable regulator with hysteresis was connected. The temperature at end-winding was measured with a thermocouple, the value relayed to the regulator. The regulator controlled an electromagnetic

relay at the primary winding of the transformer, after the autotransformer as shown in Figure 3-22. Figure 3-23 presents the realisation of this schema.

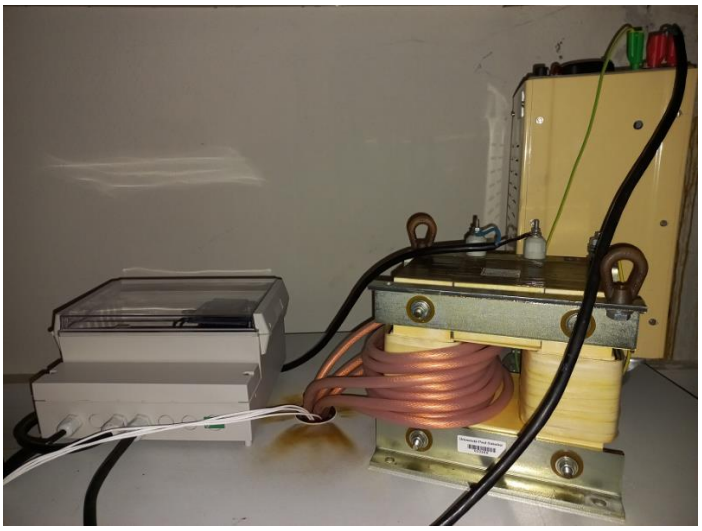

Figure 3-23 The heating set-up: from the right the autotransformer, the transformer (with winded secondary cables disappearing in the oven), and the box with the regulator. The opening at the top of the oven also lets out four white wires – for the connection to the phases and the ground.

When achieving the temperature set value (or slightly over that) the relay switched off and the stator started to cool down. Then again, when the temperature had dropped under a degree under the set value the regulator started the heating. Each cycle was 12 hours of elevated temperature followed by 12 hours at 40 °C. The regulator had a timer and it cut off the current from the stator after 12 hours. Then the temperature was maintained by the oven which was always set up at the required 40 °C.

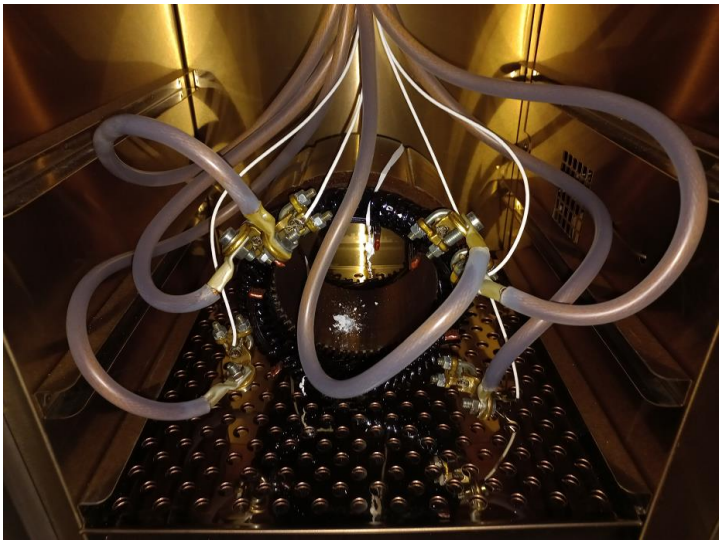

Figure 3-24 The stator inside the oven chamber. A pair of cables lead to each phase, they are winded on the transformer as the secondary winding. The insulation on the cables is made of silicon that can withstand the 220 °C present in the oven.

3.3.4 Thermal distribution modelling

To ensure that the temperature of the insulation is really the envisioned 220°C it was important that the measurement relayed to the regulator was taken at a correct spot. It has been chosen that the measurement should be done in a place where the temperature represents the highest temperatures experienced by the stator. Otherwise, the ageing could not be then compared to the first test in the oven. To make that choice, a simplified thermal model of the stator was simulated. Also, a representative sample of one machine slot was manufactured and the results were confirmed experimentally.

3.3.4.1 Thermal model of an insulated wire in a machine slot

To calculate the temperature of the copper a linear model was chosen. The main concern was if the highest temperature point is in the middle of the stator, covered by steel. Using the linear model was sufficient for this purpose. By simulating distribution of produced heat, the model could answer where, over the length of the wire, the highest temperature would occur.

The created simulation divided the wire into multitude of small parts of copper. Each particle like that has its own dimensions, temperature and it interacted with neighbour particles and its own surroundings.

Temperature of a copper particle was established by taking into account:

- Heat diffusion between copper particles – every step of the simulation the discrete heat diffusion equation is resolved for whole length of the wire.

$$T_i^{n+1} = T_i^n + \Delta t \frac{TD}{l^2}\left(T_{i-1}^n - 2T_i^n + T_{i+1}^n\right) \tag{3.5}$$

$$T_i^n - temperature\ of\ part\ i\ at\ moment\ n$$

$$\Delta t\ - \text{time step}$$

$$TD\ - thermal\ diffusivity\ for\ copper$$

$$l - length\ of\ a\ part$$

- Heat dissipated by passing current – resistance was calculated from the dimension of a single particle, copper resistivity corrected by the changing temperature. Resistivity of conductors rises with temperature.

$$\rho(T) = 0.0171 * \left(1 + 0.00393 * (T - 20)\right) \tag{3.6}$$

$$\rho - resistivity$$

$$T\ - temperature$$

- Heat transferred through the insulation into the steel – for the particles inside the steel.

$$q = \frac{kA}{d}\Delta T \tag{3.7}$$

$$q\ -heat\ flow$$

$$\Delta T\ -temperature\ difference$$

$$k\ -thermal\ conductivity\ of\ the\ insulation$$

$$A - surface$$

$$d - layer\ width$$

- Heat transferred through the insulation into air – for the particles located in the wire sticking out of the metallic part.

$$q = UA\Delta T \tag{3.8}$$

$$U\ -overall\ heat\ transfer\ coefficient, calculated\ as:$$

$$\frac{1}{U} = \sum \frac{k_n}{d_n} + \frac{1}{h_o} \tag{3.9}$$

$$k_n\ -thermal\ conductivity\ of\ layer\ n$$

$$d_n\ -width\ of\ layer\ n$$

$$h_o\ -convection\ heat\ transfer\ coefficient\ for\ air$$

Every step of the simulation the amount of heat produced and conducted was calculated. For every particle it presents as follows in Figure 3-25.

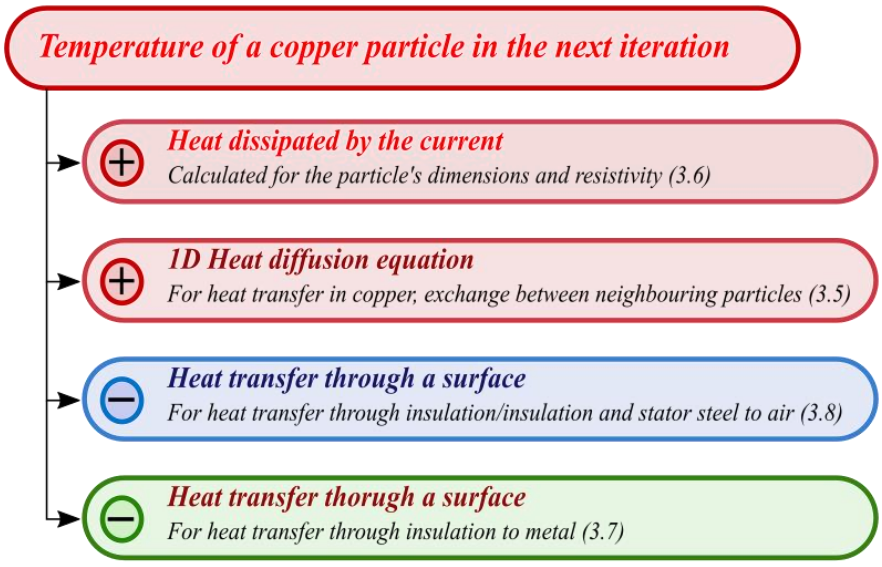

Figure 3-25 Diagram of temperature evaluation for next steps in the simulation.

Simultaneously the heat transferred into the steel is converted to the rise of its temperature with relation to its mass. The conduction of heat from this part is neglected as insignificant.

That heat was related to the mass of the particle to obtain the change of temperature from that additional heat. In next step the change of temperature was added to the heat diffusion form neighbouring particles. The simulation considers the extremities as if they were connected to the particle second to last, for stability reasons.

The script running the simulation created a wire of 70 cm divided into 70 copper particles. More points would result in finer temperature resolution but augment the running time of the simulation. 70 points, so, 1 cm long particles were chosen as a compromise between the resolution and performance. The middle 12 cm of the wire was modelled to be enclosed with the metallic block. It changes its mechanism of heat exchange with its neighbourhood. The particles outside of the enclosure were exchanging their heat with air through the insulation, while the ones inside transferred their heat to the steel and then to air.

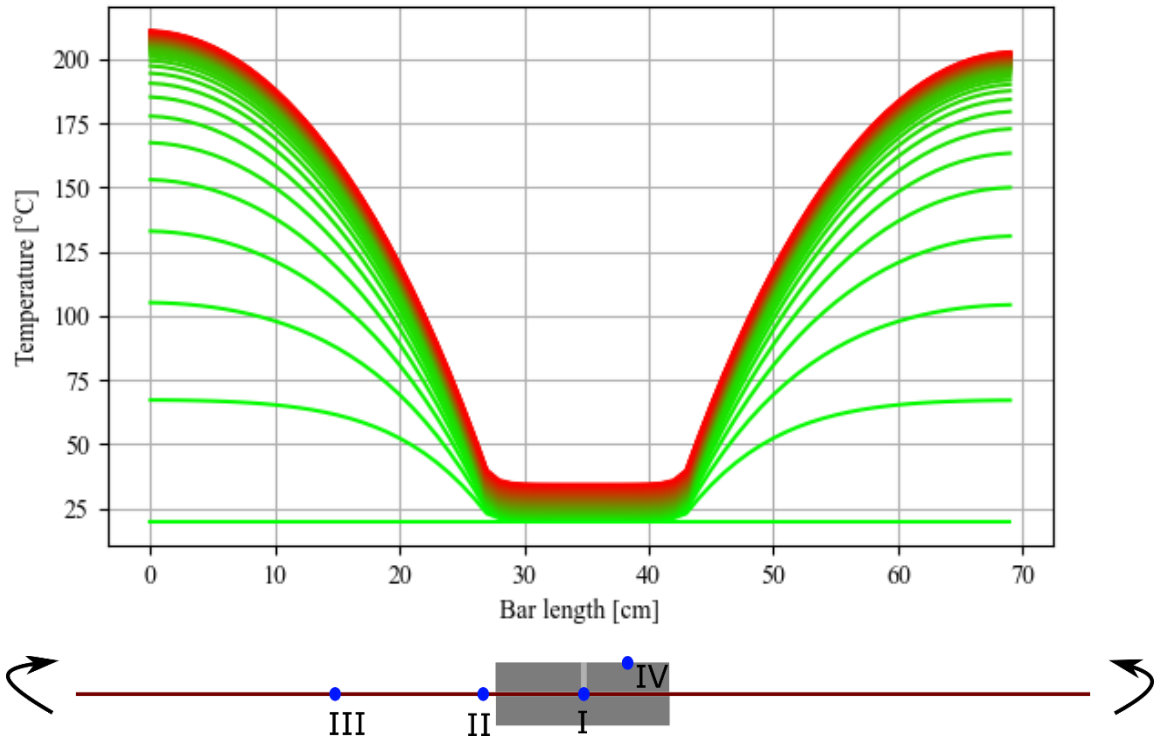

Figure 3-26 Simulation of wire temperature inside the slot maquette. The corresponding slot maquette illustrated at the bottom. Every line signifies temperatures over the length of the wire, the earliest in green to the latest in red. The total simulation time was one hour.

The simulation results in Figure 3-26 clearly show the impact of the metallic block on temperature dynamics in the wire. The simulation starts with all the elements at 20 °C. Then a current of 70 A starts to run through the wire. The simulation operates on a time step of 0.03 s but the drawn temperature lines are separated by 60 s. The exposed parts of the wire quickly, within a few minutes, achieve elevated temperature, while the particles enclosed by the steel stay relatively cool. Temperature rises only by 13 °C in an hour.

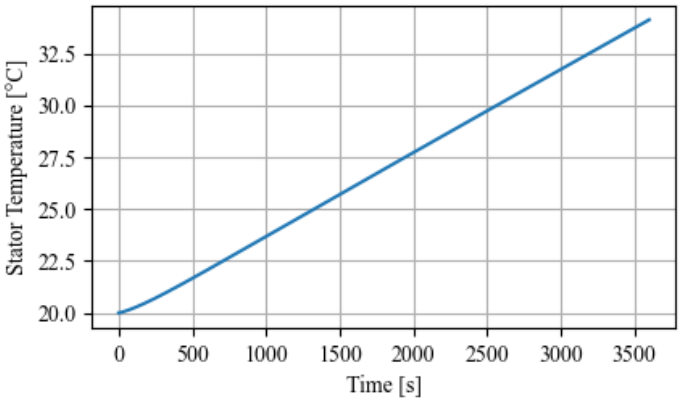

Figure 3-27 Temperature of the metallic part of the simulated slot maquette.

The simplified maquette has one wire and comparatively big steel enclosure. A question may arise, why does it heat up so slow and if the temperature inside is so low, do we have the accelerated ageing? There is much more copper wire in the actual stator and comparatively less steel. The rate of heating for the stator is much higher. The model heats up by 13 °C in an hour, whilst the stator achieves over 200 °C at similar time.

The simulation has shown that the part of conductor hidden by the steel part of the stator is not the hottest point. Quite the opposite is true, the stator works as a heat sink. It takes time to heat up the mass of the steel. In the meantime, it keeps the hidden parts of the winding in a lower temperature than those outside that are only in contact with the air. The winding in the stator loops outside of the slot and comes back into another. The point in the middle of that loop would be the highest temperature point and that is where the temperature would be the highest.

3.3.4.2 Measurement of thermal distribution in an experimental emulator of a slot

The simulation results were simultaneously confirmed with a mock-up slot. Two physical experimental emulators of a slot were created. Each one consisted of two blocks of steel, length of the stator. One of the blocks had a slot carved into it. One version had smaller slot, for one rectangular conductor (presented in Figure 3-29). The second version had place for three wires. Later, it was decided to drill three narrow passages into the slot from the side of the block. This way it became possible to monitor the temperature of the conductor inside more easily as standard thermocouple wire would not fit into the slot with the rectangular conductors.

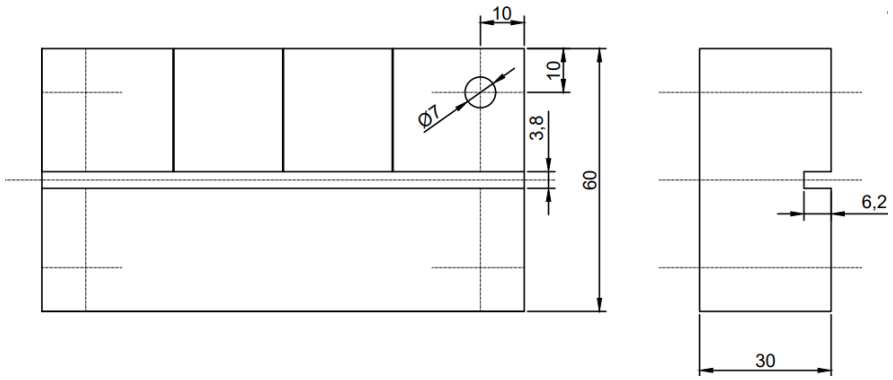

Figure 3-28 The drawing of the lower part of the slot emulator with the slot dimensions.

Figure 3-29 The slot maquette. Two metallic plates, one with a groove to imitate the slot of a stator in an electrical machine. A thermocouple was introduced into the middle of the slot to measure the temperature inside.

The wire in the slot emulator was heated up by copper losses. High current of 100 A was inducted by the components later used for active heating of the stator. One loop of the wire was introduced into the transformer as the secondary winding. Four thermocouples measured the temperatures, one about 20 cm away from the slot opening, second 5 mm away. The third one measured the temperature down the drilled hole, the temperature of the surface of insulation inside the slot. The last one measured the surface of the metallic plate.

Table 3-8 Example measurement of temperatures measured in the slot emulator.

Measurement point (location in Figure 3-26 **)**	**Temperature after 10 min [°C]**
Far (10 cm away from the slot) (III)	149.7
Close (5 mm away from the slot) (II)	96.7
Inside the metal (I)	28.9
Surface of the metal (IV)	23.8

Table 3-8 records one temperature measurement point of the slot model. The temperatures were registered after 10 minutes after the introduction of the heating factor (the current), when the far point temperature stopped rising rapidly. At that point, the wire was exchanging the heat with the surrounding air at a rate that prevented the internal heating from further rise of temperature. At the same time, the part of the wire in contact with the steel of the 'stator', deep inside, was heating it up slowly. The steel could absorb a lot of heat before the temperature of the wire could rise. It is visible by the fact that the temperature closer to the steel was 50 °C lower and the temperature inside still not much hotter than the surface.

3.3.4.3 Temperature during the test

The temperature was monitored during the ageing test. Three thermocouples were used with equipment that recorded the gathered data. One was placed at the end-winding on the inside where the highest temperature was identified. Another on the surface inside the stator. In fact, the windings are not directly accessible in the stators of the design used. A layer of steel of about one millimetre encloses the space where the opening of the slot would be.

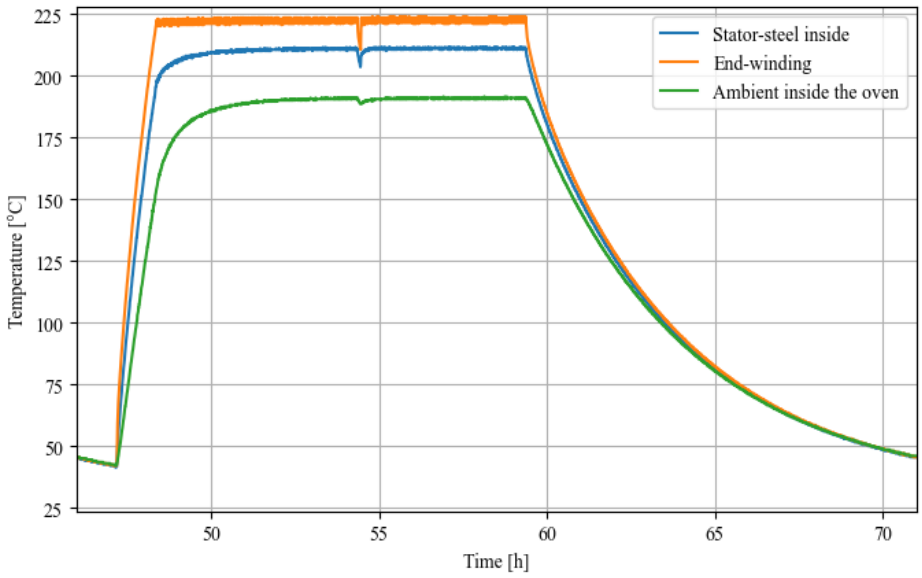

Figure 3-30 Temperature during each cycle, at the end-winding, on the inside of the stator on the steel enclosure of the stator and in the air in the oven chamber.

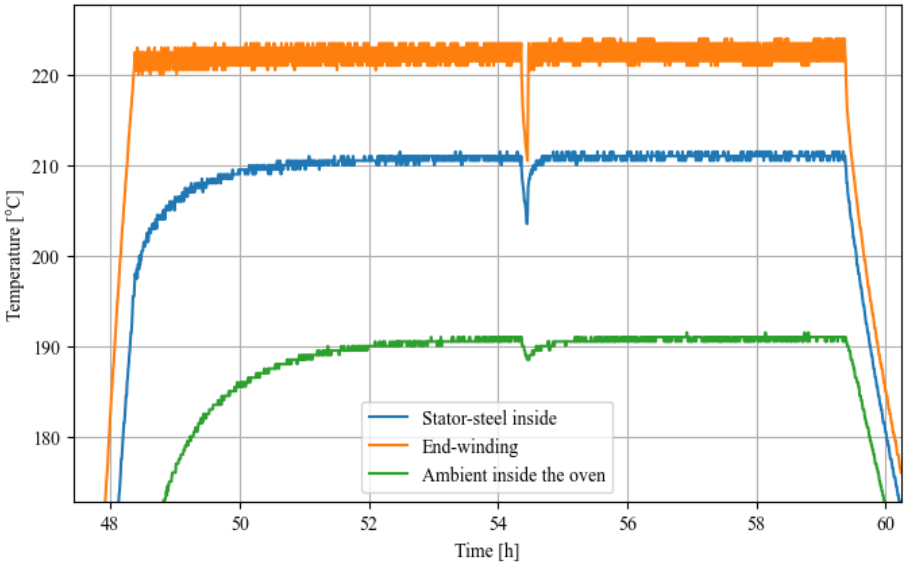

Figure 3-31 Close-up of temperatures in the higher temperatures range in Figure 3-30..

The temperature of the end-winding is the highest, as expected. Its value was regulated at 220 °C. In can be observed in Figure 3-30 as the regulator maintains the temperature. Once the set value is achieved the heating is periodically turned on and off. The temperature of steel just above the wire in the slot is about 10 °C lower. For one the heat once transferred from the insulation to the metal gets conducted quickly and distributed throughout the stator. The stator exchanges heat with the air and some thermal equilibrium is found after some time. The same is true for the air in the oven. There are ways in which the heat escapes the chamber. That is why the entire system achieves thermal exchange equilibrium and temperature of stator and air stabilises. The measured temperature shows a dip about 7 h point into the cycle (in Figure 3-31 visible after the 54th hour). The heating was stopped for the duration necessary to do the electrical rigidity tests (described in section 3.4.1).

3.3.5 Stator cycling experimental results

3.3.5.1 Passive and Active stator cycling comparison.

In the case of passive heating, the oven was set up to continue the cycles every day, whether weekday or weekend. The tests were run during the week and sometimes due to various unforeseen reasons not even then. For active heating it was the opposite. To make the measurements, one had to restart the regulator manually so that it performed one cycle. So, the stator was not cycled during the weekends and when there was a day without a measurement – it was forcibly also a day without a thermal cycle. That created a situation where the results are not imminently comparable when simply using the number of days till end-of-life. In Figure 3-32 the active cycling last twice as long as the passive cycling. Yet,

that conclusions would be wrong since much less ageing factor was applied on the second stator, than the first would have experienced in the longer time.

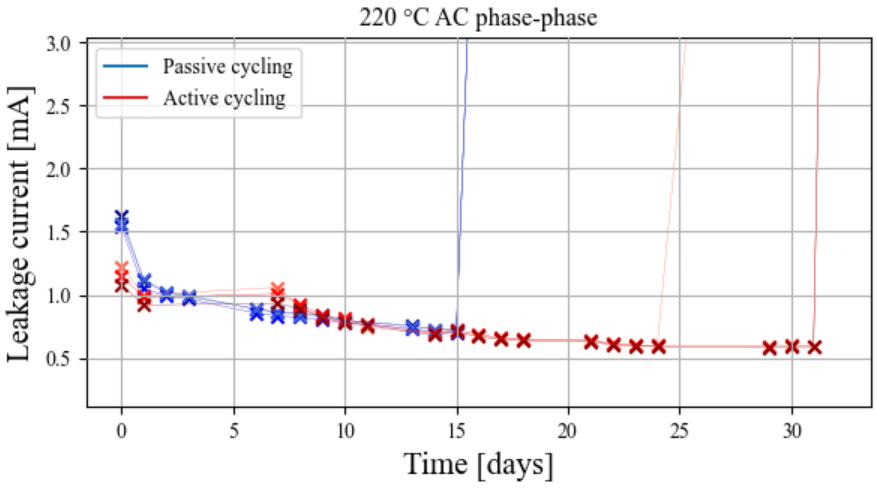

Figure 3-32 AC leakage current of passive heating stator test (in blue) and active heating stator test (in red). Three measurements per point in time for three phases. In time domain.

Rather than looking at number of days passed, it was more sensible to consider the number of cycles. Figure 3-33 and Figure 3-32 show the same data, the vital difference being that the latter switches to the number of the 24h cycles on the abscissa. That erases the days without a cycle from the picture.

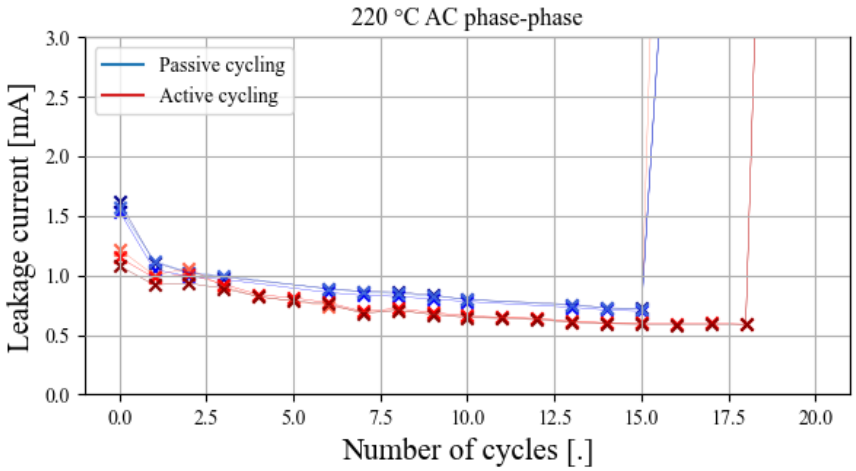

Figure 3-33 Active thermal ageing vs passive thermal ageing. Number of cycles instead of days on the abscissa.

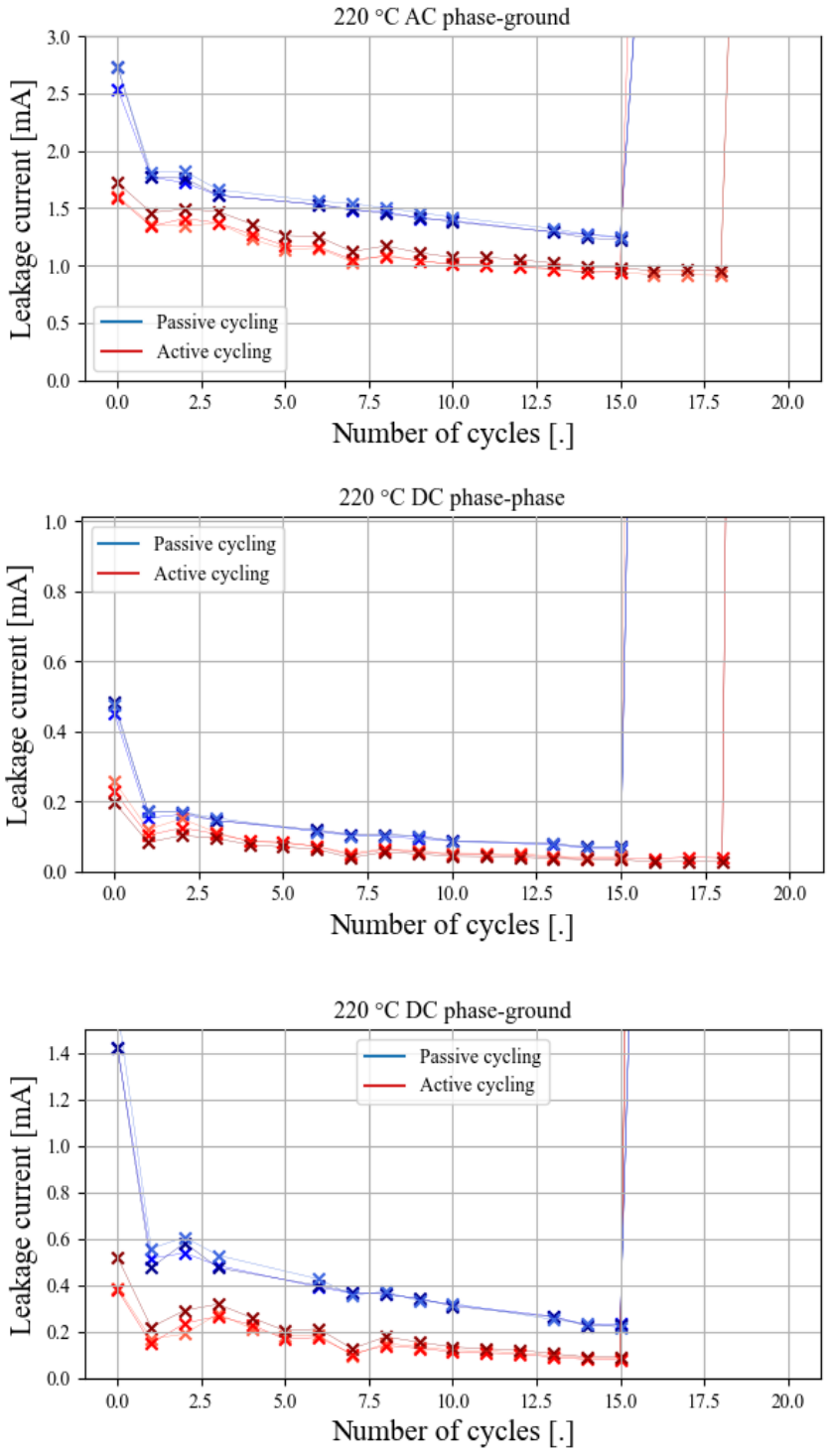

Figure 3-34 Active thermal ageing vs passive thermal ageing. Results for AC phase-to-ground, DC phase-to-phase and phase-to-ground.

Two sets of measurements were done daily. One at 40 °C and a second at 220°C. The low temperature values did not change over time or the change was below the perception of the equipment. The impedance of the insulator heated up to 220°C was a few orders of magnitude lower than that of insulator at ambient temperature (compare DC measurements in Figure 3-34 with DC measurements in Figure 3-35).

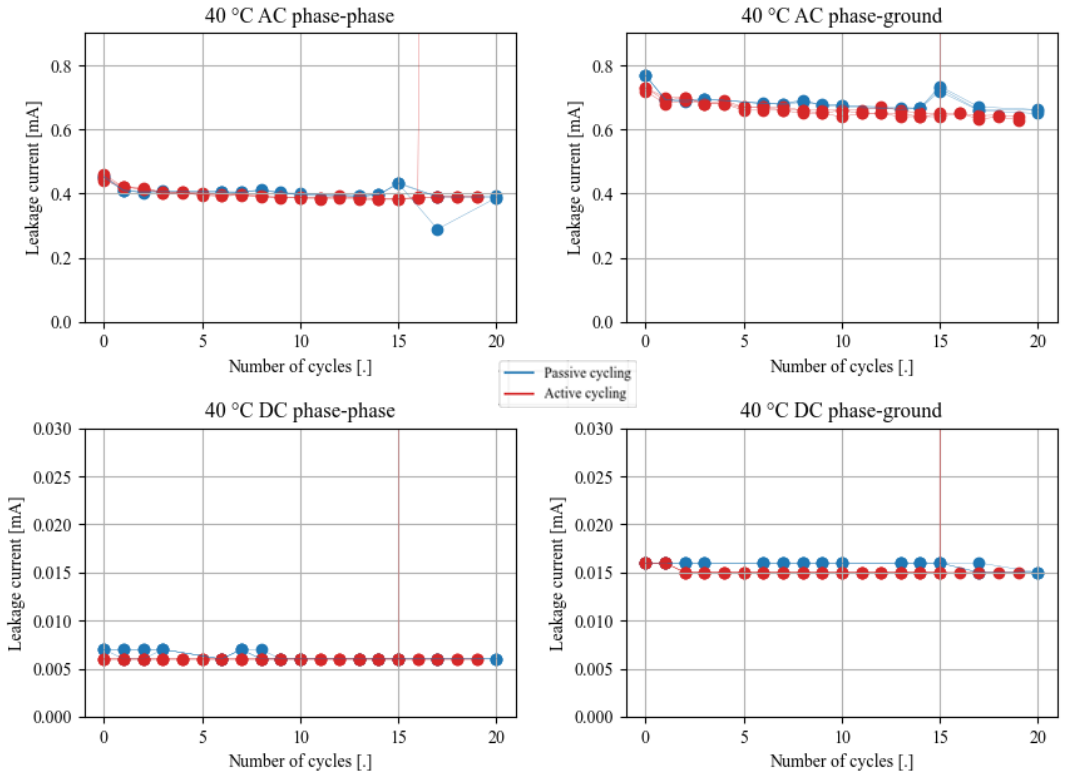

Figure 3-35 Comparison of measurements taken at 40 °C. Little to no measurable change.

The first stator, passively cycled, lasted 15 days, the second, cycled actively, 18 days. It is interesting to note that there was no significant spread between the trios of measurements (three phase-to-phase and three phase-to-ground tests). Also, if one phase was dead the others were dead the same or the day after – here the spread was equally low. Even though the system is quite complex all the three samples (a sample being a phase of which are three in the stator) died at the same time.

Table 3-9 Mean difference between passive heating ageing and active heating ageing.

Test type	Average of measured values of the leakage current in active heating as a percentage of the average values in passive heating
AC phase-to-phase at 220 °C	87.0 %
AC phase-to-ground at 220 °C	58.5 %
DC phase-to-phase at 220 °C	81.7 %
DC phase-to-ground at 220 °C	52.2 %

The stators were identical, expectedly they followed the same pattern of evolution of the measured values. Between the two stators there was not that much difference in ageing.

They survive similar amount of time and the evolution of the values is not significantly different. Comparison of values of the two tests are in Table 3-9. The fraction of leakage current value in active heating to the value in passive heating for each number of cycles was then averaged and presented as percentage in the table. The phase-to-phase measurements values in active heating are between 80-90 % of corresponding tests in passive heating. The phase-to-ground tests are just above 50%. It is hard to draw any conclusions from these facts as only two stators were tested.

The observed leakage current was decreasing every day. The suspected reason is the initial process acute to curing of the insulation rather than actual degradation. It was additionally cured by the elevated temperature hence gained on rigidity.

3.3.5.2 Additional tests on back-to-back samples

Another test tries to establish purely thermal ageing on the wire. Ten back-to-back samples were put in the oven. Every three days two were taken out of the oven. Those samples also await testing. At the end of the test a question arose whether the tests itself were not destructive to the insulation. A test was developed where the same kind of wire as in the windings of the stator was fabricated into back-to-back samples. They were aged in an oven, some of them were tested daily and the control group was left alone. To further develop the tests in this matter is left to whoever picks up the work after me, it is a perspective for another research activity.

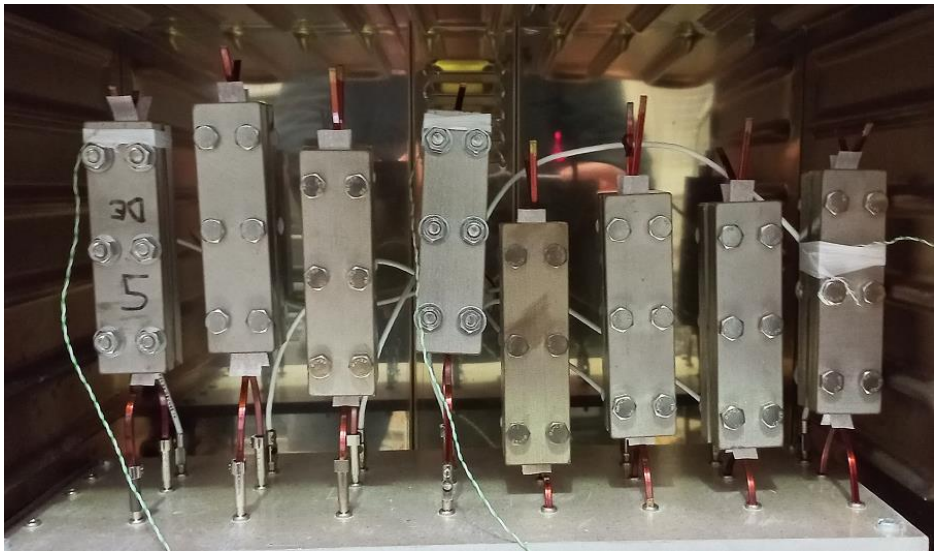

Figure 3-36 The back-to-back rectangular wire samples fixed in an oven.

The initial idea was to test the samples for their Breakdown Voltage after the periods of thermal ageing. But during the test when the DC Voltage was ramped up to a value around 10 kV the sample was shorted thorough the air on the surface of the enamel as shown in Figure 3-37.

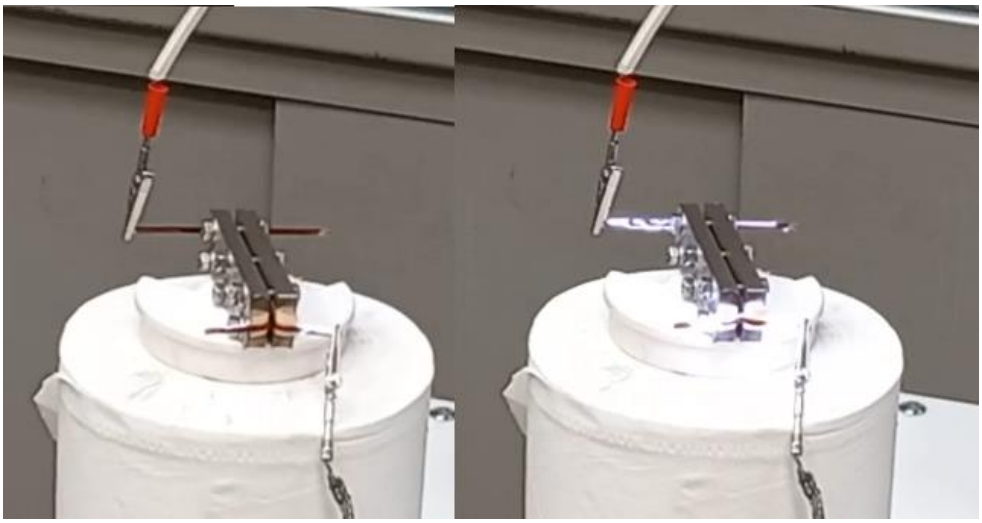

Figure 3-37 Surface discharge between two conductors of a rectangular wire sample in a back-to-back configuration.

3.3.6 Leakage current evolution during the test

3.3.6.1 Literature review

There are four components in current measurements of insulation in DC test [21]. Notably the mentioned study puts more emphasis on high-voltage machines, but the observations remain valid for low-voltage machines.

- Capacitive current: it is a high charging current that decreases exponentially. It depends on insulation system dimensions and material; in other words, it depends on its capacity. It decays to zero in a few seconds after a voltage step.
- Conduction current: the charge carriers (electrons and/or ions) move across the insulation under the electric field effect. It may be increased with contamination, impurities and additives.
- Leakage surface current: a current that flows on the surface of the insulation through contamination by oil or moisture with dust and other particles. Ideally it is equal to zero.
- Absorption current (or polarization current): current appearing due to the reorganization/movement of electrons, polar molecules and polymer chain arms inside of the material. The process may persist for a long time – depending on what is moving into the insulator. Another effect that adds to absorption current is due to electron trappings at high voltage laminated insulation.

The measurement of Insulation Resistance is based on those currents. Two measurements of the same value can differ by order of magnitude with mere difference of 10°C. Leakage current depends on temperature.

Leakage current, as the current that appears at a voltage step, was used as a diagnostic tool to predict remaining lifetime of insulation. [61]. Magnitude of overshoot in the transient response of the leakage current was measured. With degradation both capacitance and resistance decrease which in turn lowers the leakage current overshoot. The publication says that value of that overshoot starts at some level, then increases rapidly, then decreases exponentially over time and when it reaches below the value from the beginning of life, the insulation would arrive at the end-of-life. The study relates to [107] as source of confirmation of changes of resistance. There, an accelerated ageing test of thermal cycling was performed on motorettes of round enamelled wire (Figure 3-38 Motorette with cooling canals in the 'stator' [107]. Resistance was decreasing over time as in Figure 3-39, which does not conform to the obtained results. In our data the leakage current decreased over time, hence the resistance increased.

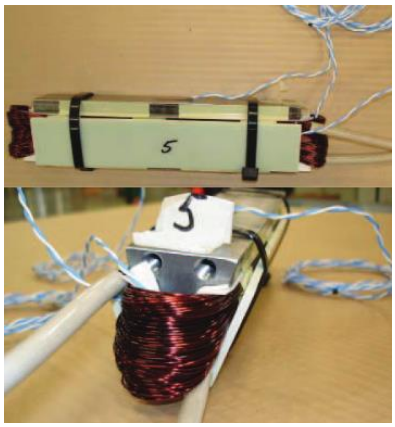

Figure 3-38 Motorette with cooling canals in the 'stator' [107]

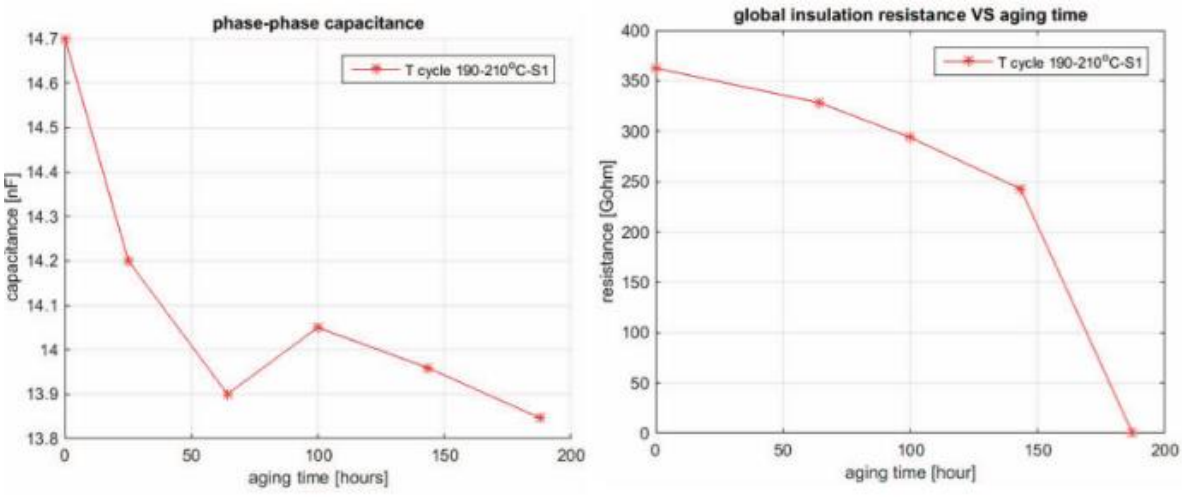

Figure 3-39 Capacitance and resistance measurements of motorettes over time while under accelerated thermal ageing. [107]

In a preliminary study, rectangular wire of 3 mm by 1.8 mm was used [143]. The leakage current was measured with a FI 9015 HT (the same equipment used for our measurements). The applied test voltage was 1.75 kV AC. The rectangular enamelled

conductors were immersed in metallic balls of diameter of 2mm, shown in Figure 3-40 The standardised test for rectangular enamelled wires immersed in metal balls.. The test voltage was applied between the wire and the mass, represented by the little balls. Fault criterion was set as 1 mA. The set-up was subjected to a temperature of 240°C for 336h. Every 24h the test was performed. During this experiment, the leakage current stayed at the same level, only increased slightly at the end of life.

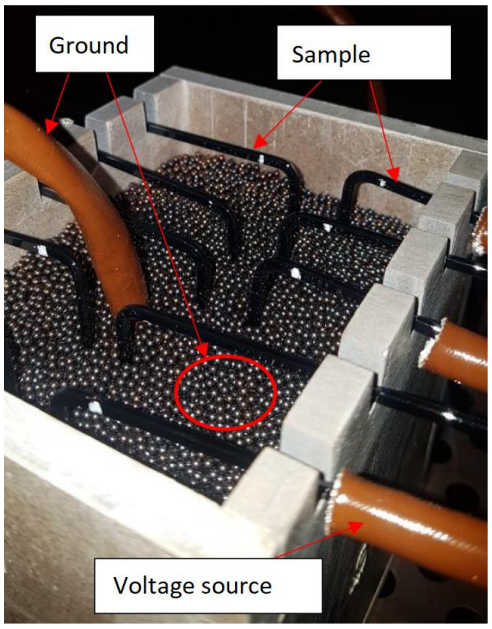

Figure 3-40 The standardised test for rectangular enamelled wires immersed in metal balls.

It was interestingly remarked that after rupture of insulation the copper was exposed to elevated temperatures and air which caused quickened apparition of oxide layer. That layer was responsible for regaining of some residual insulating properties after total short circuit.

A method for online measurement of dissipation factor, insulation capacitance and resistance was developed [144]. The method utilised differential current transformers clamped on each phase and its corresponding neutral point sinks (in Y configuration). A simple insulation system model was used to construct a set of equations that permitted to find values of the indicators based on the measured leakage currents. A RC parallel circuit models the behaviours of the insulation. Leakage current was divided into its resistive and capacitive part (as it would be for Dissipative Factor calculation).

Concerning the evolution of the leakage current with thermal ageing it was supposed that the resistances will decrease, while the capacitance would decrease only by 1%. It was simulated in the study by introducing variable resistances between the phases. Actual thermal ageing tests are not a part of the study.

One of the co-authors of the paper described above, applied the same method experimentally in another paper [123]. The study builds upon the developed theory by performing the test on a complete machine. It traced the indicators during its thermal ageing.

The single motor in the study was loaded from no load to 200% of nominal load every 5 minutes, it heated up to 255°C. The test was stopped for the night (hence the peaks in Figure 3-41).

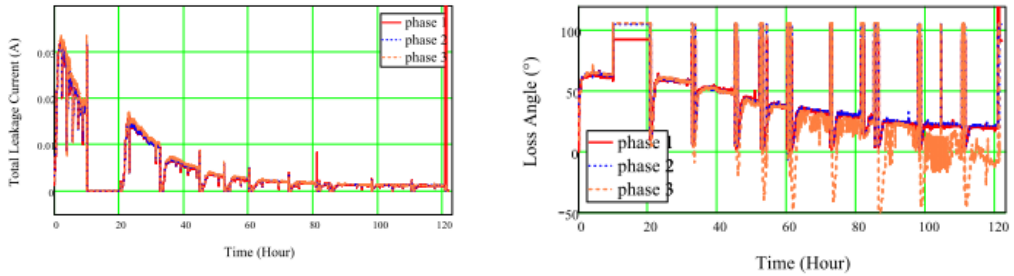

Figure 6. Long term trend of the total insulation leakage current in Amperes for each winding phase during the entire thermo-mechanical aging duration (day1 to day10).

Figure 7. Long term trend of the loss angle delta for each winding phase during the entire thermo-mechanical aging duration (day1 to day10).

Figure 3-41 [123] The data from thermal ageing test. Measurement of leakage current and the dissipation factor.

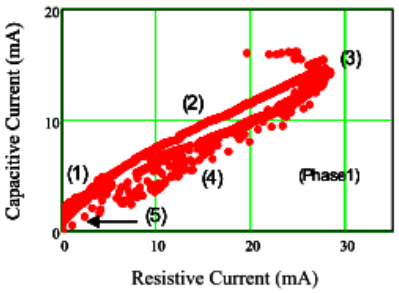

Figure 8. Phasor diagram of Phase-1 insulation leakage current during accelerated life motor aging. The highlighted different life stages of the motor insulation are identified and explained in the previous section.

Figure 3-42 Evolution of leakage current resolved on resistive and capacitive part [123]

"*Stage (1) is about 1 hour, the insulation showed an increase in capacitance and loss angle delta. This is due to a thermally activated insulation conductivity and permittivity. Stage (2) is a longer-term stage lasting about 10 hours (The described increase does not seem like 10h in the figure). It is characterized by a continued increase in the overall leakage current and at a constant loss angle. Stage (3) shows a peaking of the leakage current followed by a steep decrease. This can be due to resin volatile evaporation and weight loss. Stage (4) started after about 60 hours and is a period when the motor insulation is losing resin mass at a substantial rate. Stage (5) represents the motor end of life with an electrical breakdown between phase 1 and the stator grounded core.*" The description to the evolution is presented in Figure 3-42.

The initial rise in capacitance was ascribed to thermally activated permittivity and the rise of loss angle delta due to the rise of conductivity (so a decrease in resistance). The subsequent decrease of leakage current was due to resin mass loss (weight loss causes rise of resistance).

Another article [145], contrary to the previous examples, presents results for inverter-fed machine. The previous ones were subjected to mains-fed machine. The authors make a claim that in case of inverter-fed setup additional higher frequency components change the repartitions of the leakage current. The method utilizes an additional current transformer. The sensor is clasped on all three phases together between the inverter and the motor. Even though the article is among ones most relevant and similar to the experiments performed in this thesis, the question of projected evolution of the leakage current or other measured indicators is not commented on.

In [146] two previous methods, one with insulation current (or the leakage current) and one with transient current [147] are cited. The author aims to amalgamate them. According to the study the insulation paper is the dominant insulation in determining the insulation current and the epoxy's impact is negligible. A 2D FEM simulation of conductors in slots gives values of capacity and resistance. Then the materials' characteristics (permittivity) were changed to simulate ageing. Capacity decreases and the resistivity increases. The measurement of the insulation current was done by subtraction of current measurements at both sides of motor phase. There are resistors of small and precise resistance in series with the phase. One before and another after the motor armature. Voltage drop on the resistors was measured by oscilloscopes. Voltage of 20 V in square wave of 10 kHz was applied onto the phase. The study cites [123] for used model of leakage current evolution over time.

Interestingly in [147] it was found that a transient current peak at the beginning of a commutation decreases with degradation. The value of that peak was used as an ageing indicator, not the leakage current.

Overall, the evolution of the leakage current over time in accelerated ageing of insulation is not a topic that was explored in detail. The results, decrease in leakage current, so increase of resistance, were counter-intuitive and a look into literature did not offer much in terms of clarification. Expectations as to what happens to the value of leakage current in a stator of an electrical machine vary. Experimental studies discovered similar evolution, yet do not provide physical models of why it is happening.

3.4 Cycling and static test comparison

Once again, we are faced with the problem of comparing two different kinds of tests in order to determine the impact of an additional factor – namely cycling. In order to compare the two, cycling and static tests, a form of equivalent thermal ageing method had to be applied. It is assumed that cycling is an ageing factor. To quantify its impact we must insulate it, deconvolute from the thermal ageing. It can be done with both Arrhenius' and Miner's rule. The methodology used is described in 2.4.5. The thermal impact on degradation is calculated with a model obtained with a constant temperature test. Then, if the lifetime of a stator in a

cycling test does not conform to the purely thermal ageing model, we can deduce impact of the cycling and try to quantify it.

In this part, data obtained by Emotors on early experimental prototype samples was used. They performed standard thermal ageing tests at three elevated temperatures to use them in an Arrhenius' Model. The temperatures were 190 °C, 210 °C and 230 °C. For each temperature there was between four and five stators. Each stator has three phases, each phase was treated as separate sample for the purpose of statistical analysis. The samples were tested twice every day, at the instant of a failure of one of the tests (same tests as in Table 3-7) they were considered at the end-of-life.

Table 3-10 Lifetime data of stators (Weibull's values)

Temperature	**Alpha – Lifetime [h]**	**Beta**	**R^2 of fit**
190 °C	3277	24.28	0.949
210 °C	2839	46.23	0.982
230 °C	2829	39.52	0.834

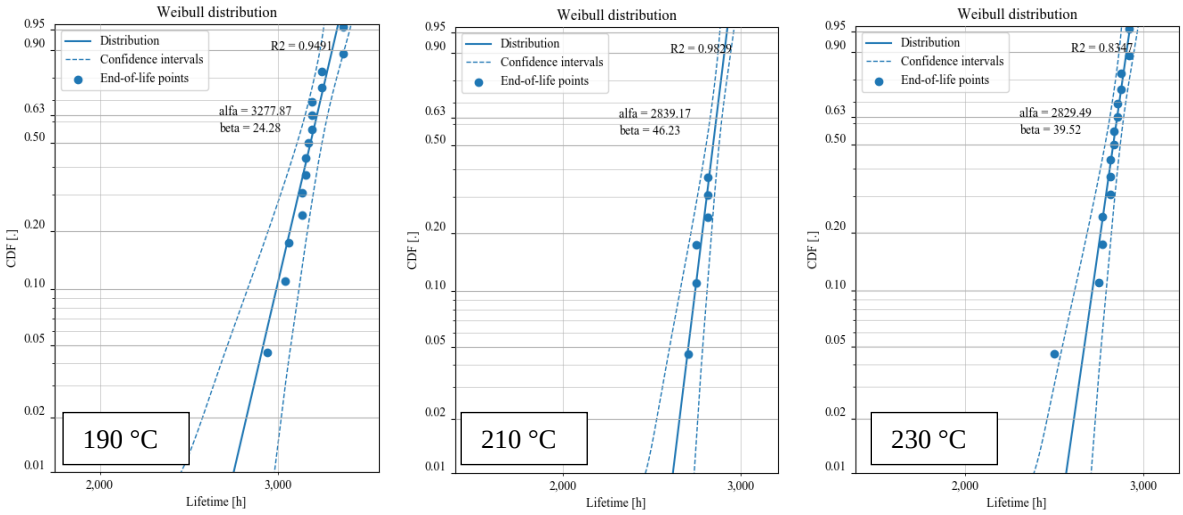

Figure 3-43 Weibull's plots of lifetimes of stator phases. From left to right at 190 °C,210 °C and 230 °C.

Figure 3-43 shows the distributions at the three temperatures. Only about 40% of samples at 210 °C arrived at the end of life. The test was terminated before they died. Their resistance to succumb to degradation is unexpected, with the logic of the test they should all arrive at the end of life at least before the last samples of 190 °C batch. Regardless of the exact reason for that, it is problematic for the model as illustrated in Figure 3-44. The 210 °C points do not lay on the same line as the two other points, also their dispersion (expressed as the beta parameter of Weibull distribution, higher number means less dispersion) is lower.

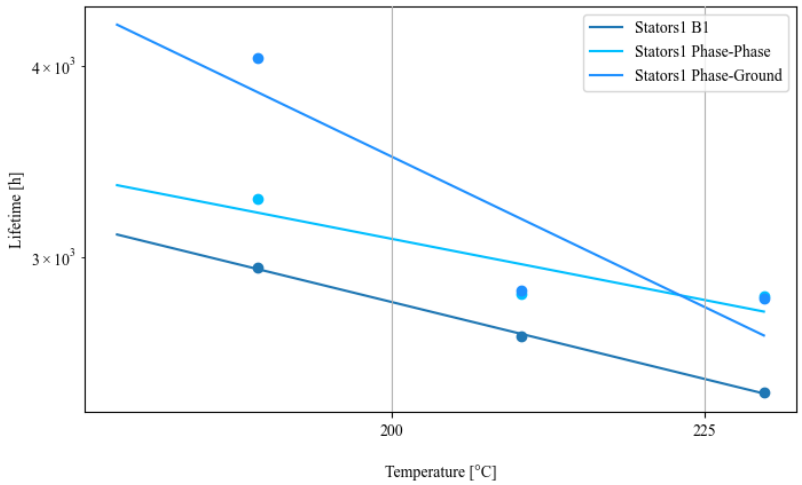

Figure 3-44 Arrhenius law for stator's insulation end of life. The point in the middle at 210 °C too low due to unexpected resistance of some of the samples.

The constant temperature tests were stopped abruptly at about 2800 hours. As a result of brief electrical blackout, the ovens stopped heating up the stators and the temperature dropped to ambient in a few hours. When the test bench was brought back online, the samples experienced unexpected and premature end-of-life.

Another set of tests was done, on different stators, at temperatures higher than in the first set, 230 °C, 250 °C and 260 °C.

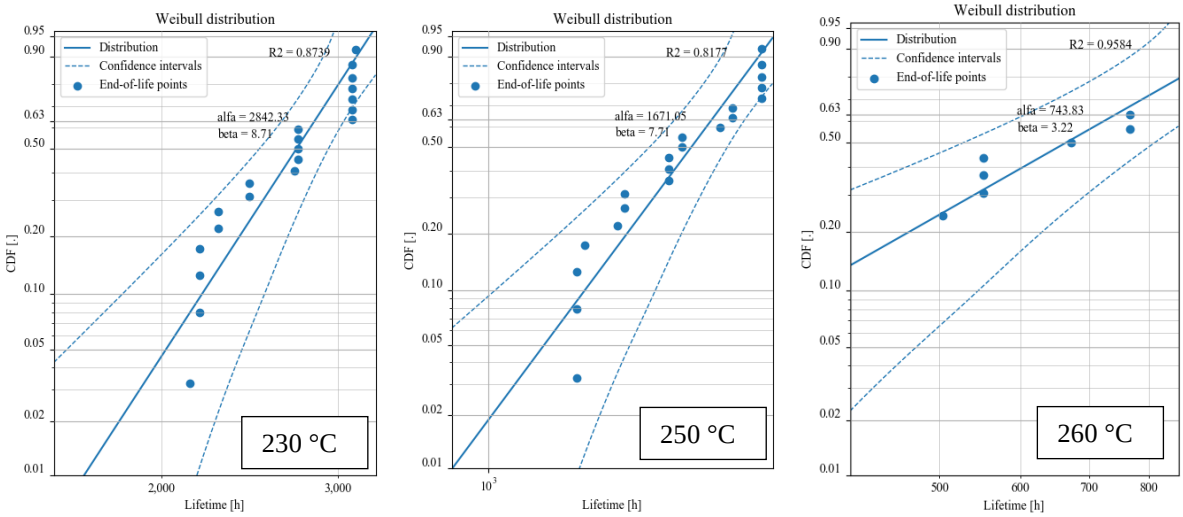

Figure 3-45 Weibull distributions of lifetimes of stator phases. From left to right at 230 °C,250 °C and 260 °C.

The beta parameter (also known as shape parameter) of Weibull distribution for these results is almost one order of magnitude lower than for those of the previously presented tests. Lower beta parameter means more dispersion. In Figure 3-45 that fact can be observed. This distribution is something that we expect from complex system which a stator is. In the

previous experience, the lower dispersion was caused by the sudden dip in temperature at the end of the test. This observation was a powerful hint that cycling may have an important role in degradation of electrical insulation system.

Table 3-11 Lifetime data of stators as Weibull distribution. Second set of stators.

Temperature	**Alpha – Lifetime [h]**	**Beta**	**R^2 of fit**
230 °C	2842	8.75	0.873
250 °C	1671	7.71	0.817
260 °C	743	3.32	0.985

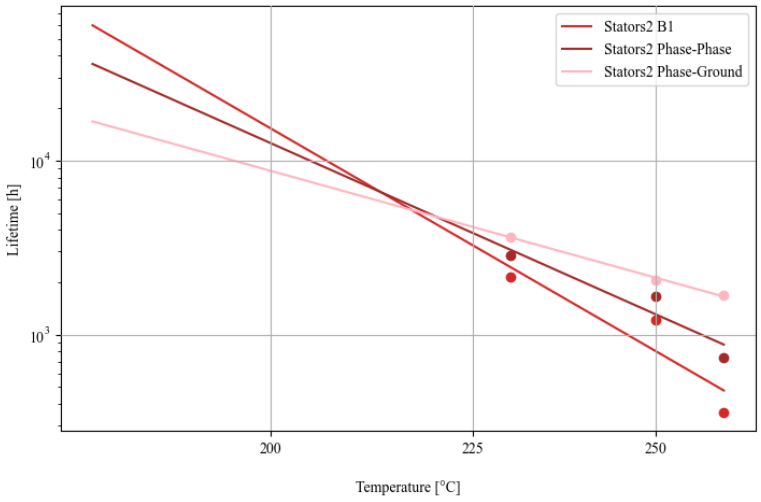

Figure 3-46 Arrhenius law for stator's insulation end of life. Red lines represent the model fitted onto Weibull's α parameter of phase-to-phase and phase-to-ground data.

When comparing the two obtained ageing models it can be noticed (in Figure 3-47) that the end of life for the two lower temperatures happened prematurely. The 210 °C point, which two tests share, had the same lifetime, while the lower temperatures had lifetimes comparable to the most severe conditions. This was caused by the accidental cycle, related to electrical blackout, that happened about the end-of-life mark of the 210 °C ageing.

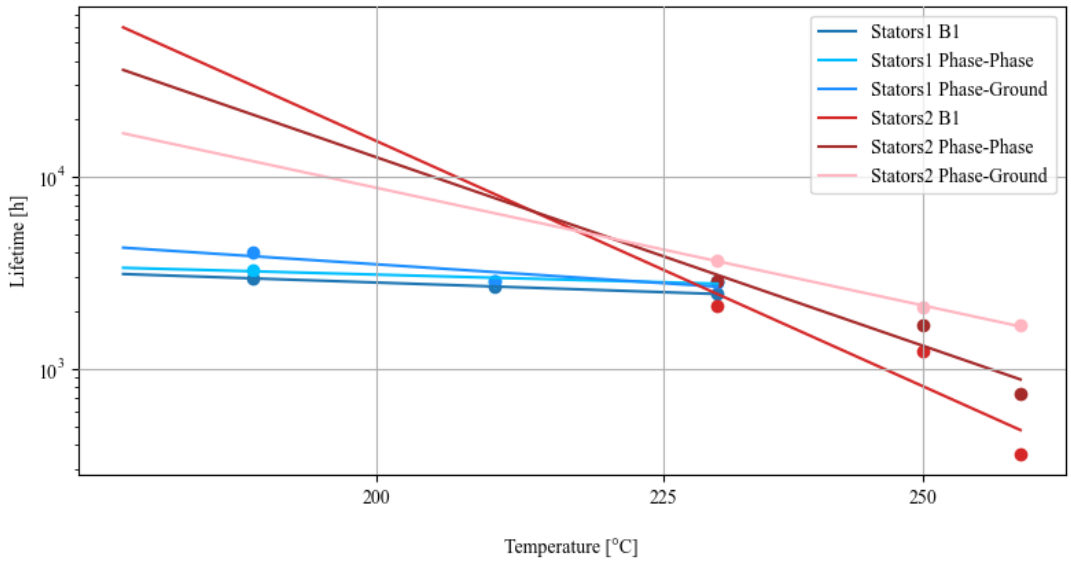

Figure 3-47 Comparison between resulting Arrhenius law lines of first batch of tests (in blue) with the second one (in red).

The thermal loss of life is modelled with Arrhenius Law (3.10).

$$Arrhenius\ Law\colon\ L(T) = A\, e^{\frac{B}{T}} \tag{3.10}$$

If applied to a temperature profile, one can obtain the cumulative damage also known as the loss of life. It is calculated as a sum of fractions of time passed at a temperature by time to end-of-life at that temperature, expressed in equation (3.11).

$$Loss\ of\ Life = \int_0^{t_{eol}} \frac{dt}{L(T(t))} \tag{3.11}$$

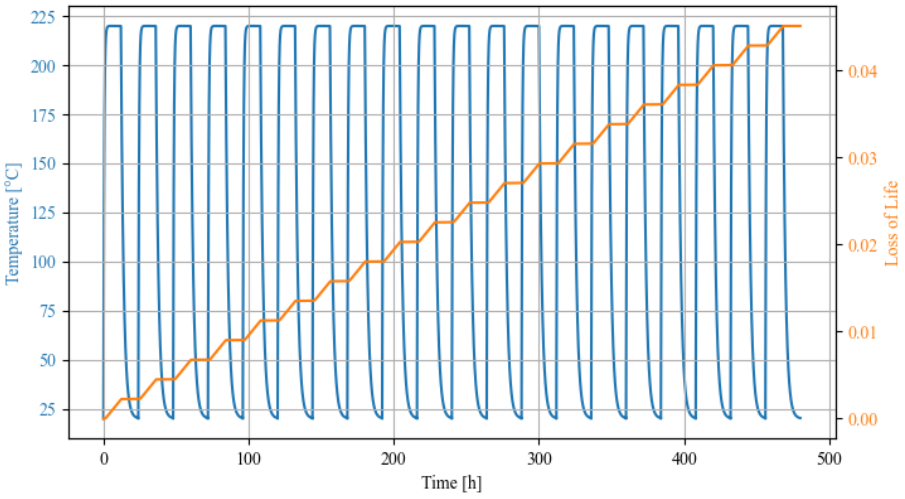

Figure 3-48 Temperature profile and corresponding loss of life.

Figure 3-48 presents a cycling profile, one really performed on a set of stators. The end of life in this experiment arrived after 480 h. There were 20 cycles overall. The thermal

loss of life was calculated with (3.11) where the model (3.10) was established with data from Table 3-11. At that point, the loss of life was only 4.51%, yet the insulation started failing diagnostic tests. In a naïve fashion we can calculate the amount of loss of life caused by cycling and divide it by number of cycles (as in Table 3-12). But it is highly probable that the more degraded the insulation, the more rigid it is, and the impact of a cycle would be more important. The primary mechanism of cycling is the thermo-mechanical degradation – more rigid insulation is more susceptible to tearing by strain caused by rapid temperature change.

Table 3-12 Cycling data and quantification of ageing by cycle.

Cycling lifetime [h]	480
Number of cycles	20
Loss of Life by thermal ageing [%]	4.51
Loss of Life by cycling [%]	100 – 4.51 = 95.48
Loss of Life per cycle average [%]	95.48 / 20 = 4.77

3.5 Conclusions

The chapter discloses results of cycling tests performed on different kinds of samples. In the first part multi-factor accelerated ageing tests were done on twisted pairs of enamelled wire. This kind of wire is commonly used as magnet wire in electrical machines.

The accelerated ageing tests with Partial Discharges were used to establish impact of voltage, frequency and thermal cycling. No voltage or frequency impact was confirmed. The experiments were an opportunity to consider the question of comparing constant stress ageing and cyclic stress ageing. The Arrhenius-Miner method provides this functionality. Once a model of ageing is confirmed with constant stress ageing tests the model can be applied to calculate equivalency between different stress profiles.

Results for thermal cycling were more promising. Two ranges of temperature, around 15 °C and 123 °C were considered. Around the 123 °C point two amplitudes of cycling were tested. It was concluded that higher amplitudes of temperature, of 100 °C, resulted in significantly shorter lifetimes of the sets of twisted pair samples. The research is quite original and there is not much to compare with, only the impact of cycling in temperatures above Temperature Index was investigated and demonstrated.

Electrical motors for application in electric vehicles are a developing domain. No emphasis has been placed so far on cycling tests in the process of design or qualification of the electrical low-voltage machines. Historically the main part of qualification is the static tests in an oven.

The objective of part 3.4 was to decide whether the standard oven thermal tests are representative or such tests should be done with active heating. The Table 3-9 shows a difference in averaged measured leakage current throughout the ageing. Nevertheless, the

stators whether aged with passive or active heating survived almost identical number of cycles. It was concluded that whether the stator is subjected to external or internal heat does not make a difference. To assure conditions as similar as possible between the two heating modes, the active heating was done in an insulated interior of an oven. However, in order to approach the reality of automotive application, one can imagine a test where the actively heated winding is surrounded by lower or even ambient temperature. It would be interesting to perform an experiment in these conditions to see how it compares to a situation with the controlled high temperature in the oven.

Part 3.5 deals with the comparison of cycling and constant temperature tests. By applying data obtained with constant temperature standard test an ageing model was created. That model was then used to quantify the amount of degradation caused by cycling. The most important conclusion from this part is that the lifetime of a stator under cyclic temperature profile is much shorter than it would result from pure thermal ageing. A clear impact of cycling was observed. Still, the findings require confirmation and further investigation of thermal cycling.

Chapter 4.

Degradation of magnet wire modelling by PDIV evolution data

4.1 Introduction

This chapter describes the research done on degradation of enamel of magnet wire in form of twisted pairs. The twisted pair is the simplest approximation of turn-to-turn insulation. Enameled wire is commonly used in electrical motors as magnet wire. The objective of this research was to determine if PDIV can be considered as an ageing indicator and used to predict lifetime. For this purpose, the samples of insulation were subjected to degrading factors that accelerated the ageing. PDIV was measured periodically during the process over weeks of ageing, the results were recorded and analysed. The choice of degradation levels was informed by the Design of Experiments methodology which permitted to create a model of evolution of PDIV as a function of those factors. This is a first step in the aim of predicting the lifespan of electric machines in EV under different operating constraints.

The chapter consists of a part about the ageing indicators in general and an explanation of what led to the choice of PDIV for the research. It is followed by a review of the PDIV measurement methods. Further on the method used during this thesis is described, both the test bench and the details of the measurement process. Then the collected data is summarized and some decisions on the data treatment are mentioned. Some of the experiments were a part of a Design of Experiments plan, the plans and the corresponding factors' levels are disclosed. Finally, the methodology on how the ageing data was applied to create a model of evolution of PDIV is described.

4.2 Ageing indicators

We perform equipment tests with two main objectives in mind. One is to qualify a designed product whether it can withstand the envisioned lifetime. The other reason is to determine the state of an appliance after some exploitation in order to determine the level of degradation and make a maintenance decision. Whether to fix, replace or leave as is. It is important in all branches of the industry as most of them employ rotating electrical machines. For electrical machines in vehicles, we would like to at least be able to detect incoming failure during a periodical check-up. That could be achieved by determining which measurable insulation characteristic or set of those characteristics is indicative of an imminent end of life.

That could be done with offline test with additional equipment. Another matter is to equip the machine with self-diagnostic measures that would inform the user of the problems.

In the process of designing an electrical insulation system designers need feedback about emerging system's capability to perform its envisioned function. Technical standards describe a range of tests and practices for validation of such a system. As the empirical knowledge and understanding of ageing phenomena grow the standards change as well. Advancements in technologies and corresponding research on them also necessitate changes. An example is the introduction of inverters for driving electric motors which has evolved over the last decades. Low-voltage machines are equipped with Type I insulation systems, which is defined as one containing material that cannot sustain the destructive impacts of long-term Partial Discharges (PD). Yet, if confronted with overvoltage from rapidly changing, high dv/dt PWM inverter output, sometimes increased as a result of long cables, the system may experience PD. The effect is even more pronounced when fast-switching new generation SiC components are used [148].

Validation tests can provide theoretical information about the envisioned time a system should survive. They are not aimed at finding a way to evaluate a system in operation, ascertaining how much life it has left and predicting with some uncertainties when it will fail. What is more, the standards put more emphasis on comparative nature of their tests. They compare the beginning of life results of a field-validated system with those of a new one. This may be problematic in the case of systems with largely different designs.

One of the ways to predict the remaining life of a system is to find a proper ageing indicator. In an ideal world, the indicator must be robust but sensitive, fast, cheap and simple. It may be a measurable value that monotonously decreases or increases while the system is in operation. Then, beyond a specific value of that indicator, the system could be considered to be at its end of life. If a model, which describes the change over time of that indicator, is found, it is then possible to extrapolate the indicator's value into the future and have some information about when the system may fail.

As of now, the lifetime prediction methods are not well developed. There are numerous tests that can be performed on insulation systems [21], but there is no consensus yet on which tests are universal and provide robust indicators of health [140][94].

4.2.1 Diagnostic measurements for electrical machines

4.2.1.1 Insulation Resistance

Insulation Resistance (IR) according to a relevant standard [149] is measured between the copper of a winding and the stator. Consequently, resistance of several elements of the insulation system is measured, the enamel, the insulating paper and the resin. The resistance between two phases or two turns may as well be a diagnostic test carrying

information about the state of health of the machine. In those cases, phase-to-phase or turn-to-turn, the test is more complicated to perform. One would need to physically disconnect parts of the winding. While for two phases it may be only problematic, for interturn insulation it is practically not doable. That is the reason for which the standards stay in the scope of resistance between the carcass and winding.

After the same standard [149], for low voltage (below 1 kV) electrical machines, the test voltage is 500 V. The current passing through the insulation is recorded after one minute from the moment the voltage was applied. The resistance is then, of course, calculated from the Ohm's law, voltage to current relation.

What is more, the standard proposes corrective multipliers for temperatures above 40°C. The measurement is highly dependent on the temperature, unless one is sure of thermal state of the equipment under test during every test, two measurements are not comparable. This is problematic when we need a reliable method to trace changes of a characteristic value that serves as an ageing indicator.

4.2.1.2 Polarisation Index

The Polarisation Index (PI) is defined as ratio of IR after ten minutes to IR after one minute. The requirement to measure resistance after some time have passed stems from the fact that the current that runs through the insulation has multiple components. Some of these components are temporary, caused by the voltage step, they diminish after a few seconds to a few minutes. The period is characteristic to the process that causes the current and the size of the insulations system. As an example, for smaller machines insulation polarisation is a much faster process. The time of measurement can be reduced to six seconds and one minute after the voltage pulse. The idea of summing the different currents passing through the insulation is illustrated in the Figure 4-1.

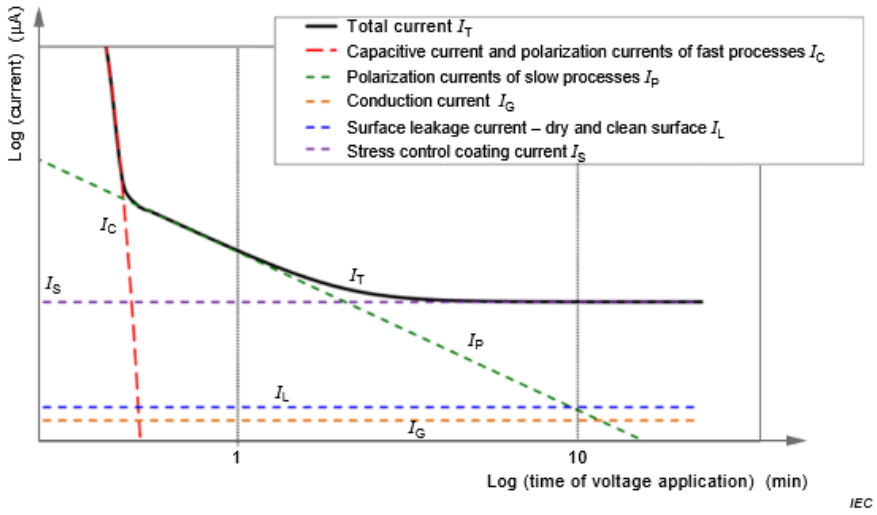

Figure 4-1 Currents present in the insulation after a voltage step is applied [141].

An advantage of PI over simple IR is that it is invulnerable to the temperature's impact. The PI is a ratio of two resistance measurements. Whatever the temperature during the test, the coefficient from temperature cancels out, so it does not have to be known or accounted for. Results from tests performed in different temperatures are comparable. According to the literature, the commonly applied practical diagnostic indicator is the value of 2 for the PI ratio [21]. PI lower than 2 is an indication of contamination or presence of moisture.

The PI or IR provide rather general evaluation of the insulation. It can detect serious problems or contamination. However, it does not provide quantitative information about the state of health. The results of both measurements depend highly on the environmental conditions, whether it is temperature of humidity. For those reasons IR and PI are not strong candidates to be used for prognostics.

4.2.1.3 Dissipation Factor (DF) or tanδ (tangent-delta)

Dissipation Factor (complementary to Power Factor) is a measure of the dielectric losses of the insulation. Under the AC voltage normally applied to the windings, the insulation between two phases behaves like a capacitor from a theoretical point of view. However, it is not an ideal capacitor, the insulation would heat up a bit, the energy is not only stored but also dissipated. That is modelled by a resistance in parallel with the capacitance as shown in Figure 4-2. The physical explanation for the phenomenon is that the polar molecules of the insulation oscillate with frequency of the applied AC voltage. That oscillation creates friction that creates heat.

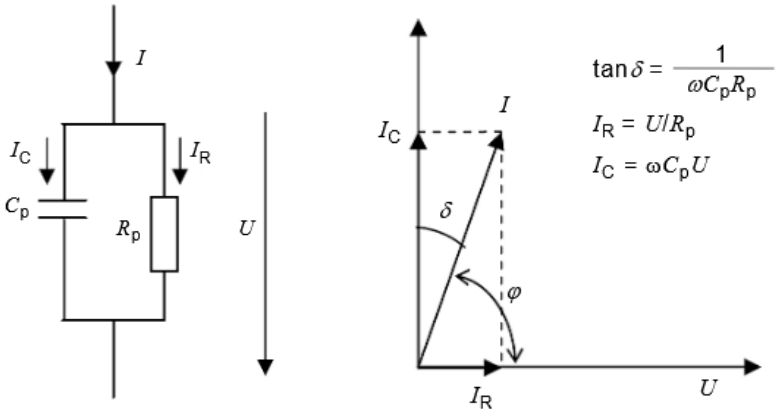

Figure 4-2 Model of insulation and current phase diagram IEC 60034-27-3.

Capacity C_p represents the lossless capacitance of the insulation while the resistance R_p stands for all the different kinds of dielectric losses. The capacitive current is 90 degrees ahead of resistive current in the phase diagram. The DF is the tangent of the angle between the vector of capacitive current and the sum of the resistive and capacitive currents' vectors. The value is represented as a unitless number or, somewhat confusingly, as a percentage. In

fact, it is then the value of the tangent multiplied by a hundred. The DF is measured with an instrument where a central piece is a bridge. One arm of the bridge consists of a capacity and a resistance, the other is connected to the motor winding (shown in Figure 4-3, R_x and C_x are the insulation capacity and resistance values). The resistance and the capacity are balanced in a way that would result in the same voltage and phase angle as those of the motor winding [21]. The DF measurement is sensitive to ambient relative humidity [150].

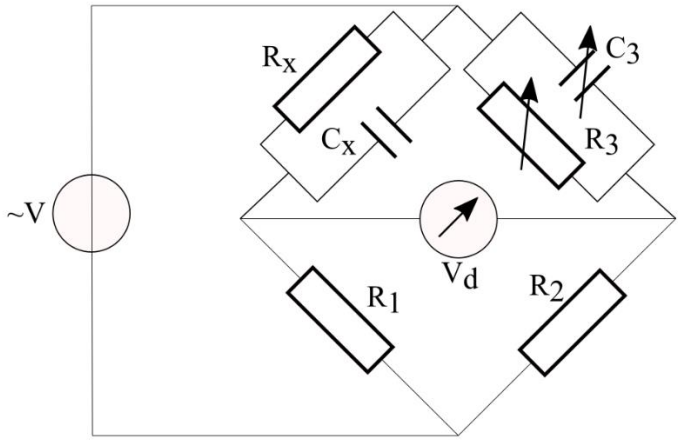

Figure 4-3 An example of a schema of DF measurement bridge.

4.2.1.4 Insulation Capacitance

Insulation Capacitance (IC) is the value of capacitance, for an electric machine's stator, between the winding and the ground. Capacitance tests may be employed for tests during manufacturing. It can test whether the resin properly penetrated the slots. A stator whose winding is not properly impregnated would deviate from standard measured IC. The measurement is also used in systems with water cooling. A rise in capacitance signifies appearance of moisture in the insulation, which, in turn, signifies a leakage from the cooling system. On the other hand, the capacitance decreases from thermal degradation [21]. Even though the IC is a tool to detect moisture in the insulation, it is not sensitive to ambient relative humidity [150].

For all the mechanisms that influence the Insulation Capacitance, the increase or the decrease is rather minuscule, on the level of magnitude of 0.1% [21]. For this reason, it requires instrumentation above a basic capacitance meter for the measurement to be meaningful. Moreover, the fact that it does not change significantly and that two different factors may cancel out each other's impact makes the test unusable for the purposes of degradation tracing or predictive modelling.

4.2.1.5 Dissipation Factor Tip-Up

The Dissipation Factor Tip-Up is a difference between DF measured at a low voltage and at a high voltage. What is understood as a low voltage for this indicator is 0.1 to 0.3 of the rated voltage of the machine under test. The high voltage is then 0.6 to 1 of the rated voltage.

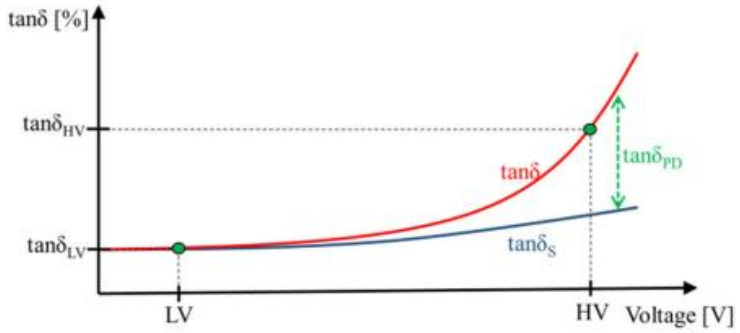

Figure 4-4 Change of DF tip-up over time illustrated. In blue - the early moments of life of an insulation, in red - after some ageing. The aged insulation is subject to Partial Discharges, and it shows in rising DF tip-up. [150]

According to the literature, the DF tip-up is mostly a qualitative indicator of the apparition of Partial Discharges. An electrical machine tested over the course of its life may show a rise in the value of DF tip-up. Historically the test is mostly used for type II insulation systems, where the insulation is PD resistant. The test may show evolution of the degradation of this kind of system, as development of various problems, e.g., delamination will result in rising PD activity. For low voltage machines and type I insulation the test is not viable as shortly after PDs start appearing repetitively such a system quickly deteriorates and arrives at the end of life.

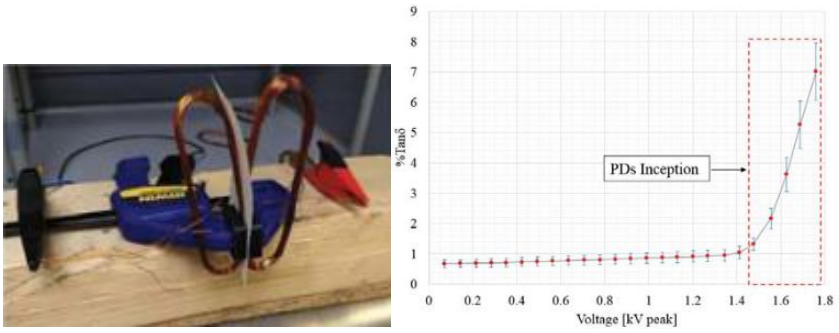

Figure 4-5 The phase-to-phase samples and the Dissipation Factor value from [150]. The rising DF indicates the inception of PD.

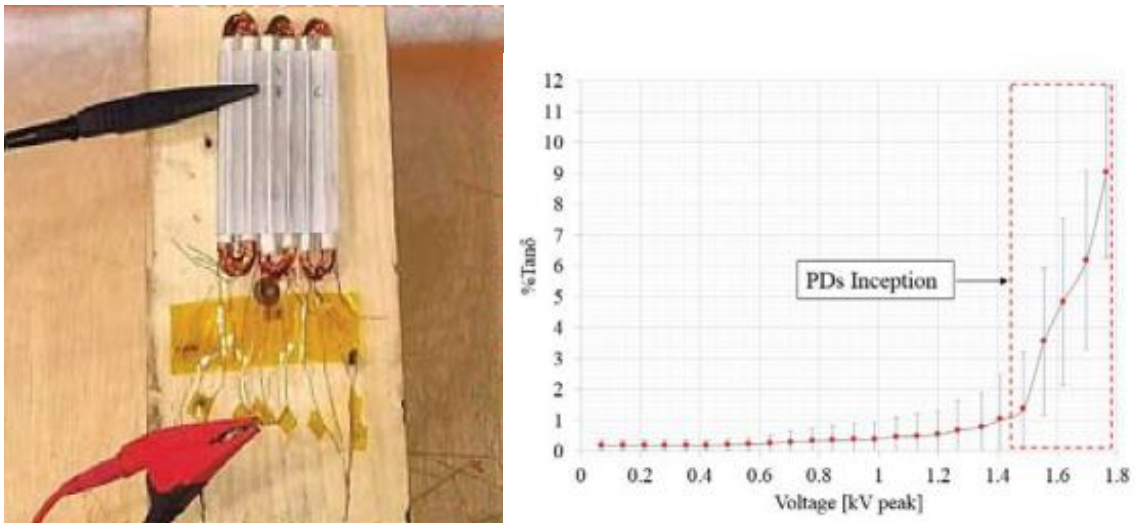

Figure 4-6 The coils in a slot sample and corresponding DF evolution from [150]. The rising DF indicates the inception of PD.

The DF tip-up test can be used differently than in the case of type II EIS for low voltage machines. It was used as a PDIV level determination tool, both for the phase-to-phase (Figure 4-5) and phase-to-ground (Figure 4-6) insulation in [150]. The system in the described study consists of round-section random-wound enameled wires packed into a stator's slots maquette. When the DF tip-up exceeds a certain threshold while the voltage is being increased, the PDIV level is recorded. A follow up study [151] contains many significant insights into the viability of different aforementioned diagnostic tests. Accelerated thermal ageing of a type I insulation system was performed with simultaneous tests of IC, DF and DF tip-up. It turned out that capacitance rises with thermal ageing (contrary to the cited knowledge for high-voltage machines), and that DF does not change when applied voltage is below PDIV. For the test voltages above PDIV, both IC and DF increase with the applied thermal ageing. The findings are illustrated in Figure 4-7. The graphs show the evolution of IC and DF over voltage. Each curve represents a different point in the time of ageing. The more ageing cycles performed, the higher the capacitance and the higher the rise of both capacitance and DF in higher voltages.

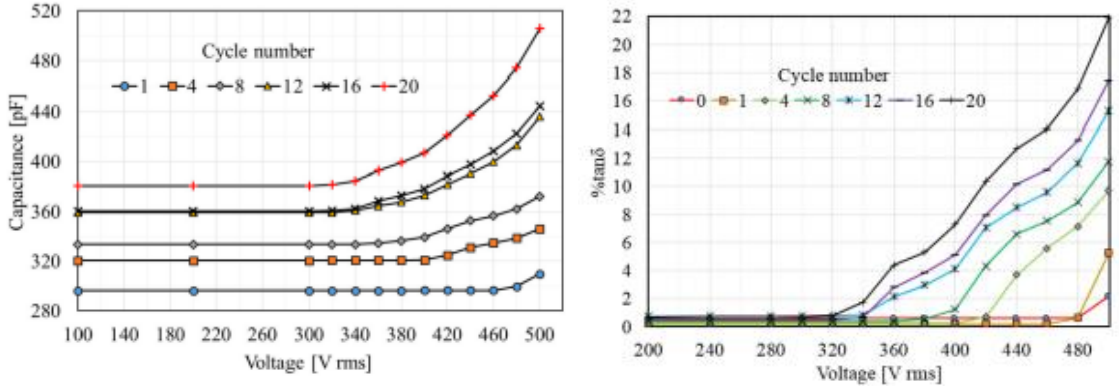

Figure 4-7 The evolution of Capacitance and Dissipation Factor from [150]. The numbers in legends indicate number of thermal ageing cycles.

In the paper the tests were used as PDIV level indirect measurements. The PDIV was also measured directly in order to validate the approach. The resulting measured values of PDIV were accurate when compared to a commercial PD detector. Therefore, the method was deemed to be appropriate, comparison of the methods is illustrated in Figure 4-8.

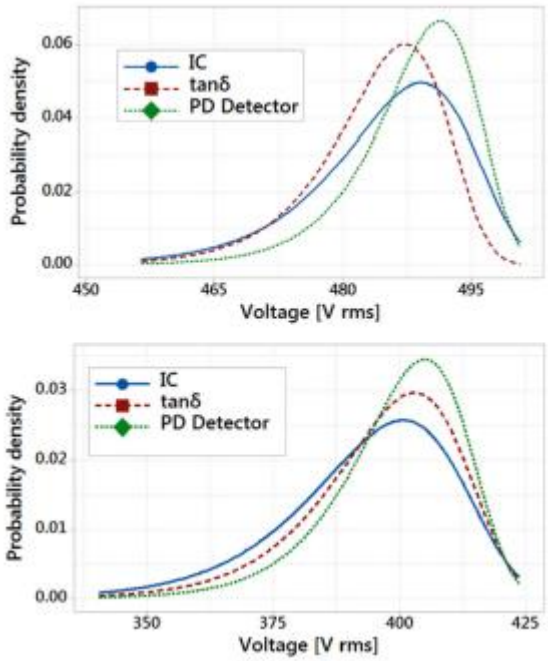

Figure 4-8 Difference between the direct PDIV measurement (PD detector) and the experimental methods (IC and tan-delta). The upper figure represents Weibull probability distribution at the beginning of life, the lower shows the distribution after thermal cycling ageing in high temperatures. [150]

4.2.2 Conclusions for ageing indicators

None of the methods mentioned is deemed a good ageing indicator. In a publication from 2010 [140] multiple lifetime prognostic methods were evaluated. Each of the methods uses some specific diagnostic measurements in order to predict remaining lifetime. The authors present other research and cross examination of the methods that prove their inability to perform the claimed task. What is more, the authors made an observation, that since there are so many possible failure mechanisms of an insulation system, it is not pertinent to expect one single indicator to cover them all. Other publications already tried to correlate evolution of some diagnostic measurement with thermal ageing, among them, the mentioned [150] [151]. At the time of writing of this thesis the PDIV evolution is not a vastly covered topic. It is known that PDIV will decrease with ageing, but it remains to be discovered how it occurs over time. In [152] both capacitance and PDIV are measured over time, both indicators appear to be decreasing, yet there were too few measurements to resolve the exact trend. In the scope of this thesis, it was decided to evaluate how the level of PDIV behaves under simultaneous multiple factor stress ageing and whether it would be useful as an indicator of that ageing.

4.3 PDIV measurement methods state of art

The Partial Discharge Inception Voltage is defined as the level of alternative voltage that causes the insulation system to experience Partial Discharges. A complementary characteristic to PDIV is the Partial Discharge Extinction Voltage (PDEV). It marks the voltage where the partial discharges stop. The existence of the two markers is, for one, indicative of the existence of hysteresis. The PDEV is usually lower than PDIV. What is more, the two values are noted because of the way the test is made. The voltage on the tested system is gradually increased and when the PDs are detected, the PDIV is recorded. Then, in turn, the voltage is gradually decreased and when there are no more PDs, that is the PDEV. To sum up, the PDIV measurement is in fact a PD detection and measurement. Hence, when we talk about PDIV measurement methods, in fact, we speak of PD measurement.

4.3.1 Partial discharge measurement methods classification

The IEEE guide on online and offline PD measurement methods [153] presents multiple methods for off-line and online testing of stator windings, among them:

- Multiple different Electrical Pulse Sensing Mechanisms: a category of methods where some equipment, an electric circuit, is connected directly to the Machine Under Test. The current pulses created by the PD pass through elements of the measurement equipment are registered. The time of occurrence and, sometimes, amplitude of the PD impulse are recorded.
- Radio Frequency radiation sensing: a PD impulse creates a high frequency electro-magnetic distortion. Suitably sensitive equipment, when antenna is close to the PD occurrence, can pick up on that PD induced distortion.
- Dissipation Factor Tip-up: the diagnostic measurement, as already mentioned in 4.2.1.5 can serve as an indicator of PD appearance.
- Ozone detection: Partial Discharge is a phenomenon where the air in between layers of insulation undergoes electric breakdown. The discharge ionizes the air. Some free oxygen particles are created, they join in with oxygen 0_2 molecules creating ozone. Ozone itself is abrasive for the insulation. On the other hand, its appearance in a test chamber indicates that the PDs are present.
- Acoustic and ultrasonic detection: a discharge heats up the air in its immediate vicinity. The change in heat changes pressure, the change in pressure propagates as a sound wave. The sound has components in spectrum sensed by human ear, the sound associated with sparks. Yet, the spectrum has its peak at ultrasounds of 40 kHz and continues up to 150 kHz.

- Visual detection (Black-out test): the PDs emit electromagnetic waves also in visible spectrum - light. A stator can be put into a darkened chamber with a light detector and tested by ramping up voltage between winding and ground. Detected light would indicate apparition of PD. Unfortunately, the method works for discharges on the surface, may be blind to internal discharges.

Quantifiable values representing PD activity:

- Partial Discharge Inception Voltage: lowest voltage at which PD appears in insulation system while voltage is being gradually increased.
- Partial Discharge Extinction Voltage: highest voltage at which PD stops occurring when voltage is gradually descending. Hysteresis exists between PDIV and PDEV. PDEV is normally lower than PDIV.
- Repetitive Partial Discharge Inception Voltage: voltage level when PD is present during each 5 out of 10 pulses. Whether the pulses are half-periods of a sinusoidal voltage or square-wave impulses.
- Maximum magnitude of discharge expressed either in pC, mA or mV.

Standards do not provide any acceptance criteria for PD tests. It is emphasized that PD data serves comparative purposes only. That is, it does not compare with other objects but with itself over time.

4.3.2 Partial discharge electrical measurement – basic principle

A paper exploring the standardised PD measurements describes two options present in the standard [154]: a capacitor in parallel or an impedance on the ground side of the object. The current that passes through the external circuit (order of milliamperes) is measured on the impedance (in millivolts). The magnitude of the detected pulse depends on the capacitance of the stator. With higher capacitance more current will be shorted out within the test object and less will pass through the external circuit to be measured. The measurement for this method is often translated into electrical charge (picocoulombs). The apparatus must be calibrated first. Known amount of charge is injected into the test object and corresponding reading in mV or mA is used to derive a measurement ratio.

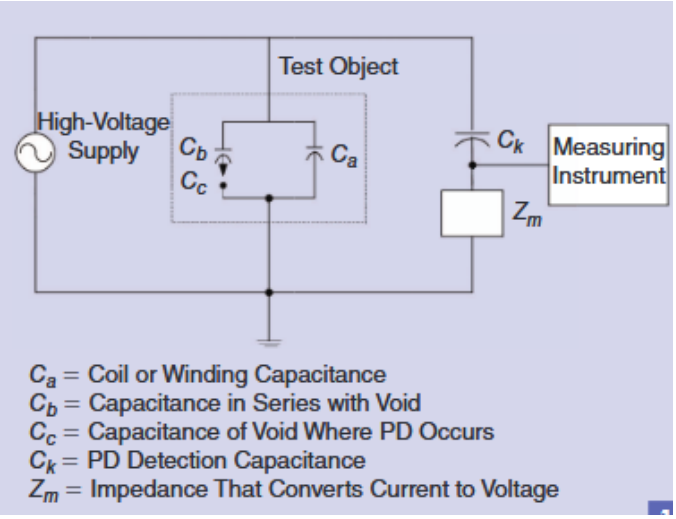

Figure 4-9 The basic quantitative partial discharge test. A capacitor in parallel with the test object.[154]

4.3.3 Phase Resolved Partial Discharge

The detected PD can be visualised on a Phase Resolved PD plot. It shows PD pulses' magnitudes appearing over a period of alternating voltage (sinusoidal or PWM-style). The plot shows the discharges' magnitudes in pC. The colour indicates the density of discharges at that point over a course of a period of a sinusoid. The warmer the colour the more discharges at that magnitude, at that moment of period. The shape of the discharge mapping provides information on types of problems occurring in the insulation Figure 4-11. It carries both information on what kind of fault is developing but may also indicate the placement, for example whether a delamination is appearing deeper in the slot or closer to the end-winding. The pattern changes over time as can be seen in the example in Figure 4-10, where a high-voltage machine with type II insulation undergoes accelerated thermal ageing in 'cycles' of multiple days at constant high temperature (over TI).

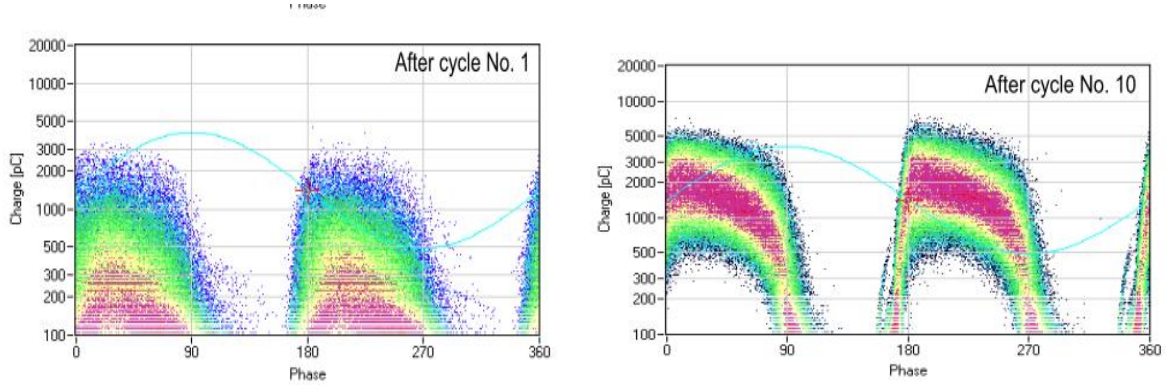

Figure 4-10 An example of PRPD plot, it shows change in PD pattern after accelerated thermal ageing [30].

4.3.3.1 Partial discharge pattern classification

As it was already mentioned certain parts of the discharge pattern can be attributed to different PD phenomena but also some noise from various sources can be present in the signal. Some papers focus on developing methods for classifying groups present in PD pattern in order to provide more complete diagnostic information [155], [156].

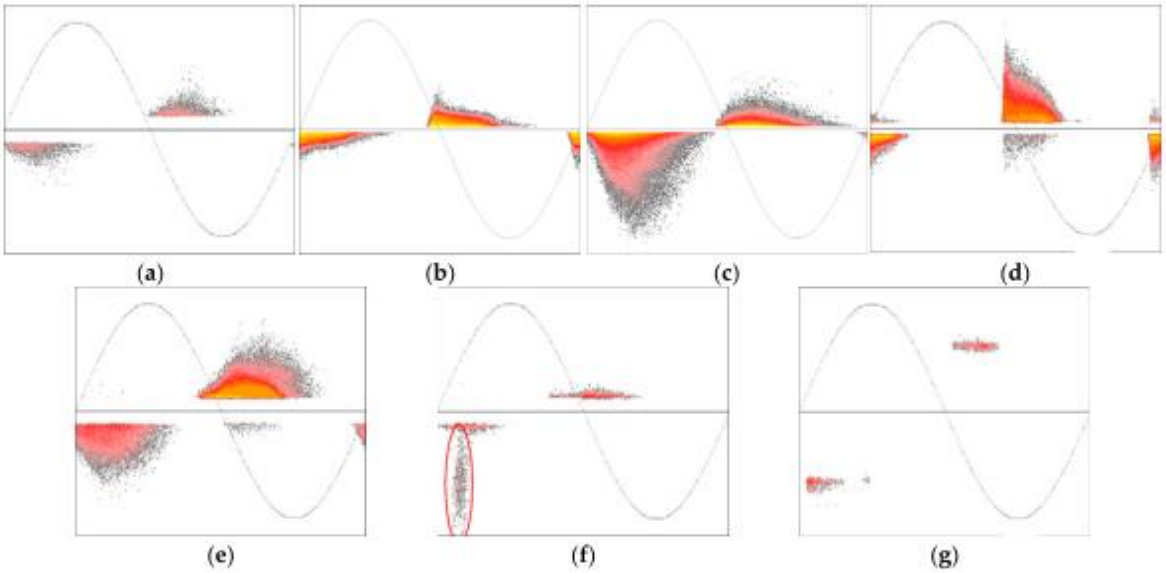

Figure 4-11 Examples of different PD patterns which are symptomatic of the following insulation problems: a) Internal voids; b) Internal delamination; c) Delamination between conductor and insulation; d) Slot discharge; e) End-winding corona; f) Surface tracking; g) Phase-to-phase discharge. [155]

The classification is understood as making a decision whether one or multiple model shapes associated with a particular problem are present in a real pattern, and to do it despite measurement noise. Among the classifying methods we count Fuzzy Classifiers [155] and various Neural Network or Deep Learning methods [156]. The methods often concern type II machines. Applying a PD analysis method to type I machines would be interesting from the perspective of diagnostics. The problem is that the PD are destructive to this type of insulation and may deteriorate too quickly under test, when the test is performed periodically.

4.4 PDIV as an ageing indicator

Some researchers measure PDIV for the purposes of diagnostics during ageing [157] [122] [158] [159]. In [122] one measurement of PDIV for a low-voltage machine was taken at the beginning of life. Then the stators were subjected to a few thermo-electrical ageing periods. After that, the PDIV was measured again in order to check if it had decreased below a certain threshold. The research did not provide many data points, for some the PDIV decreased, while for a few stators it appeared to be rising. Similarly, in [158], evolution of

PDIV was traced in a thermo-electrical ageing experiment. The study also aimed at evaluating the influence of frequency of sinusoidal voltage on insulation lifetime. The test temperature was constant and the applied electrical stress was above PDIV, the PDs were present, hence the lifetime measured only up to tens of hours. However, the authors were able to observe the decreasing PDIV and modelled it with Inverse Power Model. High-temperature accelerated ageing on twisted-pairs was performed in [159]. PDIV measurements with sine wave voltage were taken multiple times every minute. A decrease in PDIV was observed during the lifetime, having an initial drop over the course of the first hour and then slower linear decrease for a few tens of hours until breakdown.

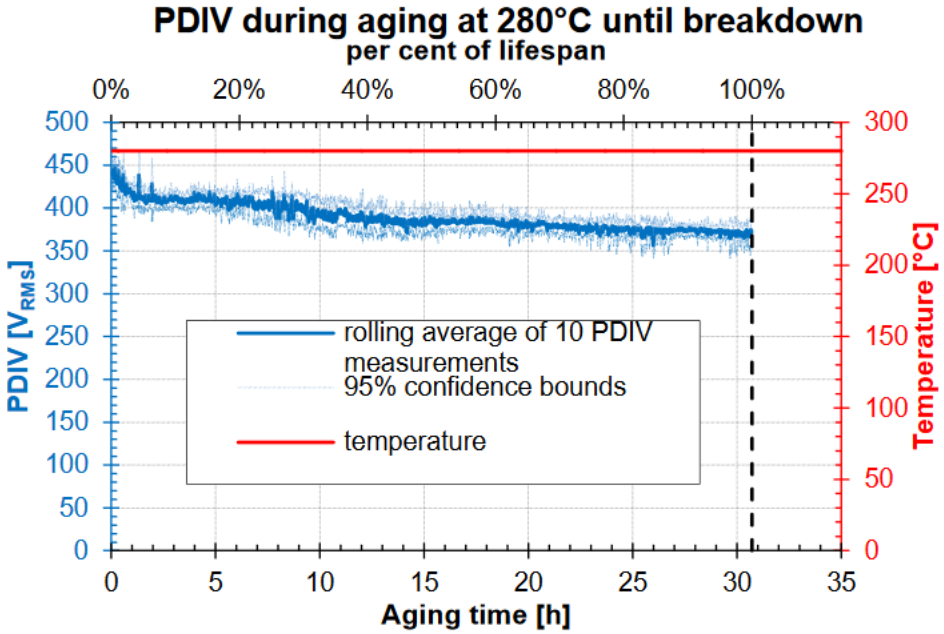

Figure 4-12 Evolution of PDIV of twisted pairs samples in ageing in high temperature and inverter voltage over PDIV. [159]

The second study [159] falls within the scope of research on multi-factor tests and lifetime prediction of insulation systems for electrical machines. It is an attempt to find an indicator of state or remaining life of an insulation system for inverter fed electric motors. Samples of twisted pairs are subjected to high temperature and inverter voltage over long periods of time. Partial Discharge Inception Voltage (PDIV) is measured over the course of their life. The article contains the description of the experimental test bench, method of PDIV measurement and a method of analysis and modeling of the obtained PDIV evolution over time. Changes of PDIV over time are observed. The found evolution of PDIV is modeled with Inverse Power Model with a prediction error of a few percent.

4.5 PDIV measurement with square-wave bipolar voltage

In the scope of multi-factor tests, several directions have already been explored. Previous iterations of the research include work done on ageing with influence of PD [160].

The next step was to perform ageing below Partial Discharge Inception Voltage (PDIV). The advantage of test with PD is that they do not take a lot of time, i.e. lifetime ranges from minutes to a couple of hours. On the other hand, it does leave any time to trace evolution of any potential indicators.

The PDIV measurements in this work are performed with square-wave voltage emulating inverter. It was discovered [11] [161] that the standard test with sinusoidal form may return different results. Thus, it is better to evaluate the PDIV with the same form of waveform that the samples experience during ageing.

An experiment is set up in this work to follow PDIV while applying multiple ageing factors on the samples. The obtained data could then be utilized for modelling the evolution of PDIV. And afterward, to construct a model which extrapolates the evolution model for different sets of stress factors' levels.

4.5.1 Samples and experimental set-up

The tests performed for this research were done on twisted pairs of enameled wires of 0.5 mm in diameter and Temperature Index of 210°C. The samples were prepared according to relevant standard [141]. A table included in the standard informs how many times the sample is turned and how much force (normally in the form of an attached weight) must be applied on the free end of the pair. In the case of a 0.5 mm diameter the number of turns is sixteen and the weight is 50 g. The appliance used to produce the twisted pairs is shown in Figure 4-13.

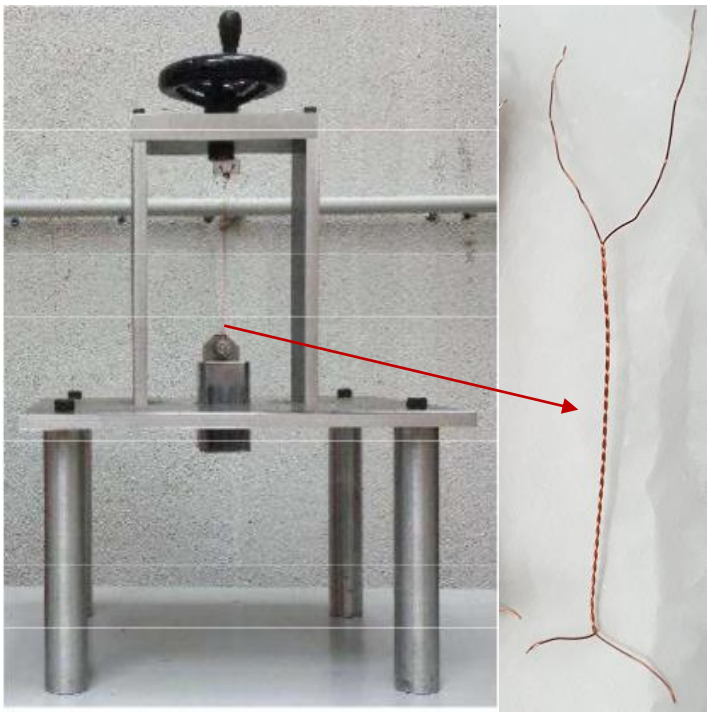

Figure 4-13 Device employed in twisted pair manufacturing process.

The twisted pair is a useful sample of turn-to-turn insulation if it is carefully prepared. One needs to take precautions to assure proper repeatability of production process and reduce dispersion in the results. From previous experience with twisted pair production the following additions to the protocol were added:

- The magnet wire and the produced pairs were handled in latex gloves.
- The endings were shed of enamel before twisting. To do so after would very likely disturb the form of the pair.
- Before twisting the wire was wiped with ethanol.
- Before putting the pairs in the oven, they were also wiped with ethanol-soaked tissue.

Each experimental batch of samples that was stressed with a specific factor level combination consisted of eight twisted pairs. The standard considers that five samples per trial is the minimum to be statistically significant, but the more the better. In this case one trial is limited to eight samples since the test bench is designed for eight samples, from eight places on the sample supports to eight time-counters. To try to design the test bench for more samples would make it technically problematic, so it was settled at eight.

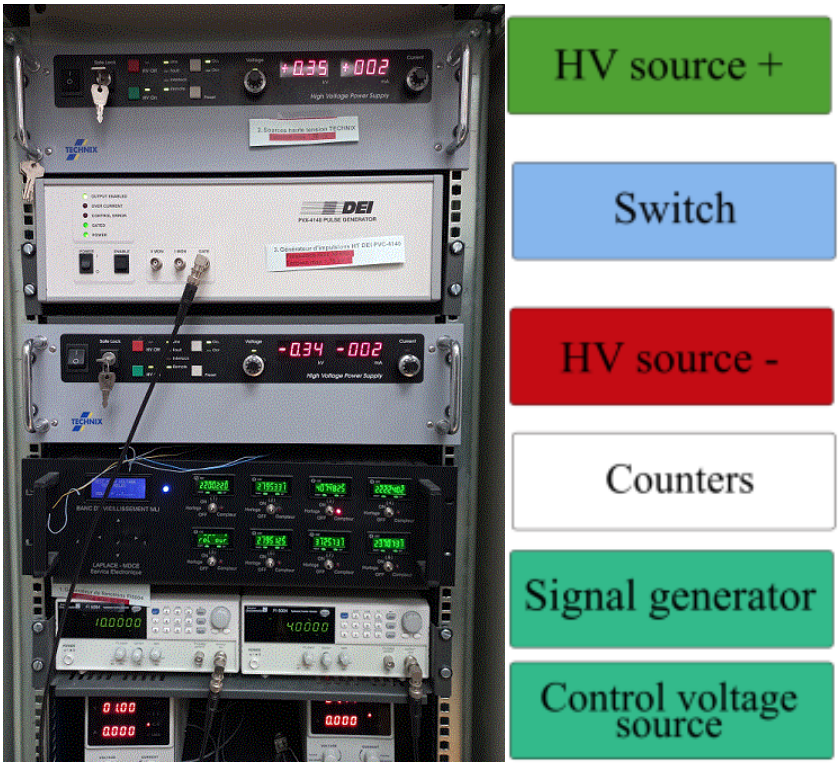

Figure 4-14 The test bench photo, the square-wave inverter style source emulator with elements described. [44]

The test bench (shown in Figure 4-14) allows emulating the voltage form that is experienced by inverter-fed machines. It consists of two high voltage sources, a switch, a function generator and eight counters on a control panel. The sources provide voltage of opposite polarities but equal in value into the switch inputs. The switch, which is gated with a

signal from the function generator, outputs either the positive or the negative voltage values. This output is applied onto the pairs through relays on one side. The other leg of the pair is connected directly to the switch's ground. The test bench simulates square-wave bidirectional voltage and permits to set the values of voltage amplitude and frequency. An additional voltage source allows setting the level of applied voltage in real time. Temperature is also controlled as the samples are kept in an oven during the ageing.

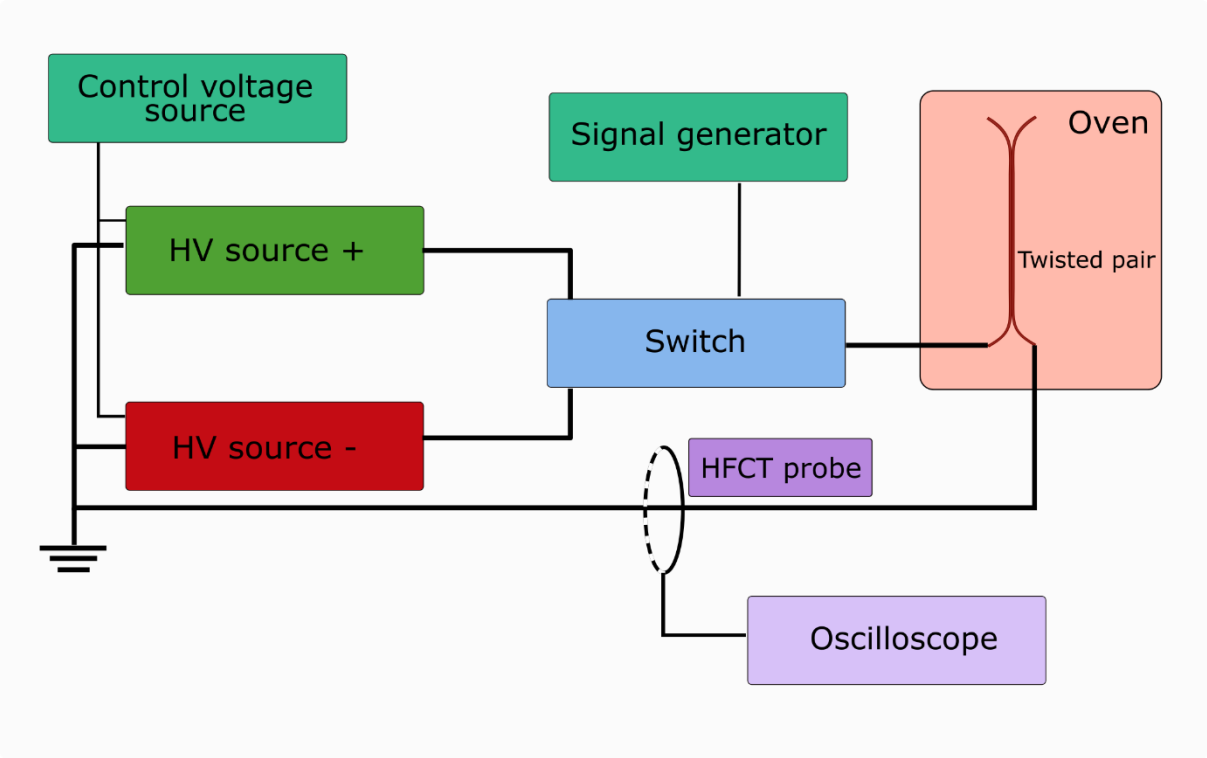

Figure 4-15 The test bench schema. The system responsible for maintaining the temperature, the voltage, and its frequency. The same parts serve the purpose of PDIV measurement.

4.5.2 The measurement of PDIV

A High Frequency Current Transformer (HFCT) is inserted on the return wire between the twisted pairs and the sources' mass (Figure 4-15). The HFCT is a Pearson Electronic Current Monitor Model 6585 with a large working bandwidth (400Hz to 250MHz). The signal is observed by an oscilloscope, a Tektronic MSO5204. During each commutation, both current and its FFT are observed. The shape of the current is highly repeatable and characteristic for each pair. During a measurement the level of the applied voltage is increased step by step and the oscilloscope's display is set on the image of the current. This current is the sum of the whole circuit response to pulse voltage (feeding cable, connectors, twisted pair) and, if existing, PD. At some level of voltage PDs start to appear. PD may be identified by their HF signature. The sudden change in both temporal and FFT current signature from a critical voltage value has been attributed to PD and has been verified by using an ozone detector put at the top of the twisted pairs. As soon as the recorded signal changes (sudden

level change in some frequency bands), the sensor detects ozone, which allows to validate the method. Figure 4-16 displays experimental data with and without PD. The sensitivity of our PD measuring method has been estimated to be about 1pC. This calibration has been performed with another PD measuring test bench using a traditional detection (coupling capacitor and measuring impedance), a sinus applied voltage and a calibration device. The HFTC has been added to the circuit and the sensitivity could then be estimated by comparing the (calibrated) signal measured by the conventional measuring circuit and our current probe.

The fact of achieving the level over PDIV during the test may be a concern whether an additional destructive factor was introduced. In [159] the PDIV measurements were fully automated and done with much greater frequency and sinusoidal signal. One extra sample was placed in the test conditions with intention to not perform the PDIV measurements on it. The lifetime of the control sample was not longer than the lifetime of the ones under constant measurements. It leads to the conclusion that the measurements were not significantly destructive. The experiments were conducted with only two samples hence hesitation to draw strong conclusions.

As for the measurements done in the research presented here, they are much less frequent (one per day vs. a few per minute) yet the voltage is controlled 'by hand'. The voltage is always lowered as fast as possible as soon as the PDs are spotted. Still, the reaction time of a human being would not be as fast as an automatic programmed response in [159]. The measurements do not seem to be an additional stressor. Moreover, if the impact exists all the samples receive a similar 'dose'. A PDIV measurement on a single pair was done only once a day. It was not repeated so only one value was measured and recorded. Preliminary tests of the method with multiple repetitions proved that the spread for one specimen was minimal – no more than one step of voltage resolution of 3.5 V for a few tests taken one after another.

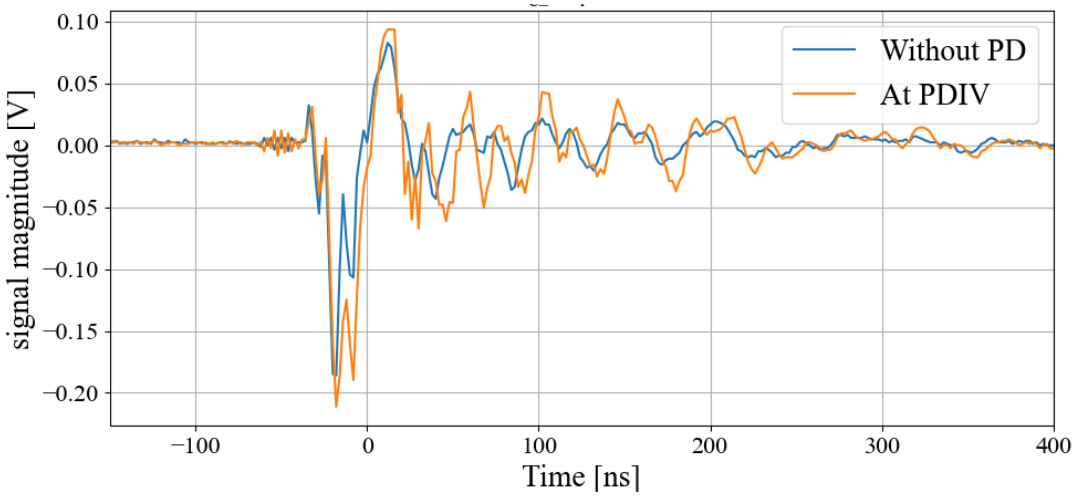

Figure 4-16 The temporal view of the measured currents at the instant of commutation between the two sources. Signal shown in Volts corresponds 1 V : 1 A for the measured current.

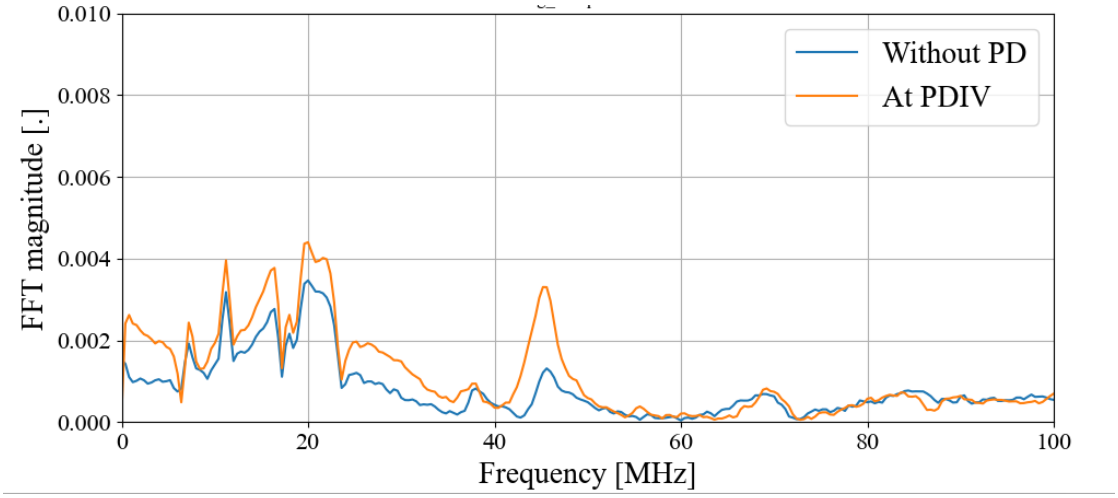

Figure 4-17 The spectra of the current signals from Figure 4-16, changes are visible in the peak magnitude between 40 and 60 MHz.

The signal and its spectrum are monitored live during measurements. The value of voltage level of the initial appearance of change of form of the temporal signal and the spectrum is recorded as the PDIV. The qualitative change of the observed signal appeared much more clearly in its spectrum shown in Figure 4-17. A rise in frequencies between 40 and 60 MHz can be observed.

To recapitulate, Figure 4-16 and Figure 4-17 show respectively the signal that is an image of the current measured at the commutation instant and the spectrum of that signal. The current is the charge passing though caused by changing of polarity of the electric filed applied onto the insulation. Both images show two cases, with and without PD. The case below PDIV is straightforward to show, the temporal form (so also the spectrum) remains stable. Between many square-wave pulses the signal stays almost identical. The shift that happens once the PDIV is achieved is hard to illustrate in a picture. The temporal form is no longer stable, it starts to shift randomly. No two forms are the same, due to the additional current passing – the PDs. The PDs create stochastic distortions in the signal. In the figures one example is presented, but the full picture of what happens would be visible only on a video. It is important to stress the fact that the instant of the crossing into PD regime is clear on site and the key element – the shifting – is missing in the pictures.

4.5.3 Voltage overshoot at commutation

A short investigation of the possible overvoltage occurring at the commutation was done to achieve a few goals. To confirm that the value of voltage displayed on the sources' displays is actually the value of the electric field experienced by the insulation. Additionally, to evaluate the commutation voltage overshoot and observe how it changes with rising voltage.

That was achieved by attaching a high voltage probe to the terminals of a twisted pair connected to its support, hence to the inverter emulator. That is the point closest to the insulation. Such a placement of the probe assures the minimum of impact of the equipment between the source and the sample on the voltage measurement. The twisted pair used for this experiment was enameled with different material, in this case the PDIV is higher, over 800 V.

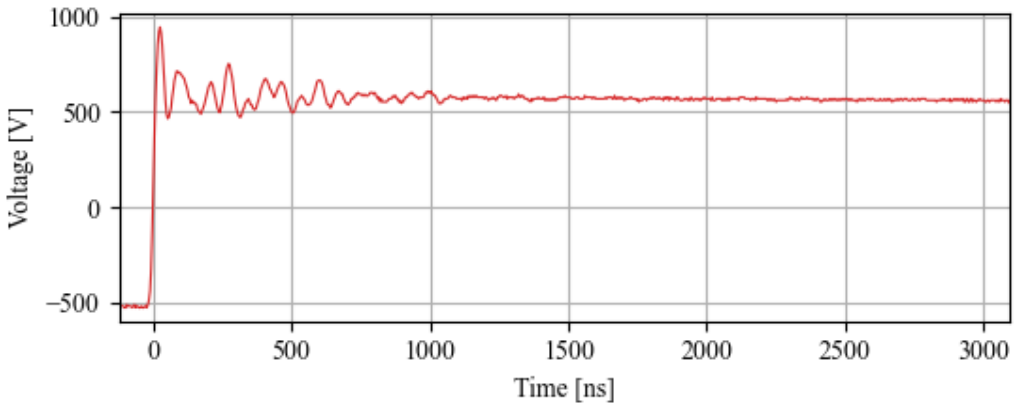

Figure 4-18 Voltage applied on the samples. The overshoot at the moment of the commutation from - 500 V to 500 V. The voltage stabilises after 1 millisecond.

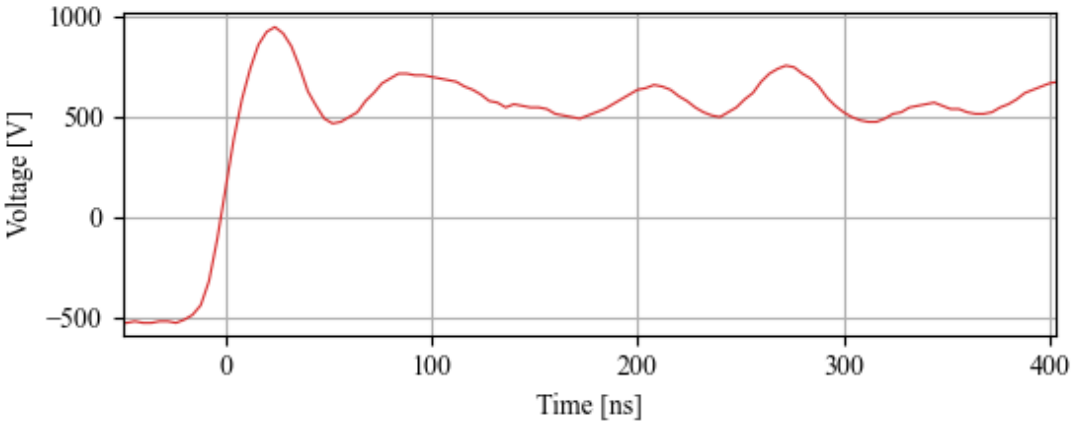

Figure 4-19 The commutation between negative and positive voltage, the overshoot visible. The voltage rise ramp at 50 V/ns.

Figure 4-18 shows a signal captured by the oscilloscope fed by the probe performing the measurement. It is the voltage at the commutation instant. It shows the initial overshoot and continues till full stabilisation. The same signal is presented in Figure 4-19 but zoomed at the initial part with overshoot. It shows the rate at which the voltage increases, it's about 50 V/ns. With the test bench we are not able to control the rise rate, we cannot set any ramp we wish. The rise time is another factor that influences the ageing [58], [162]–[164]. The steeper ramps influence lifetime negatively. Luckily, the test bench is capable of delivering only one value of V/ns and the value stays within the same order of magnitude. For now, we are not considering impact of different ramp rates in the scope of this thesis, but it is an interesting question indeed.

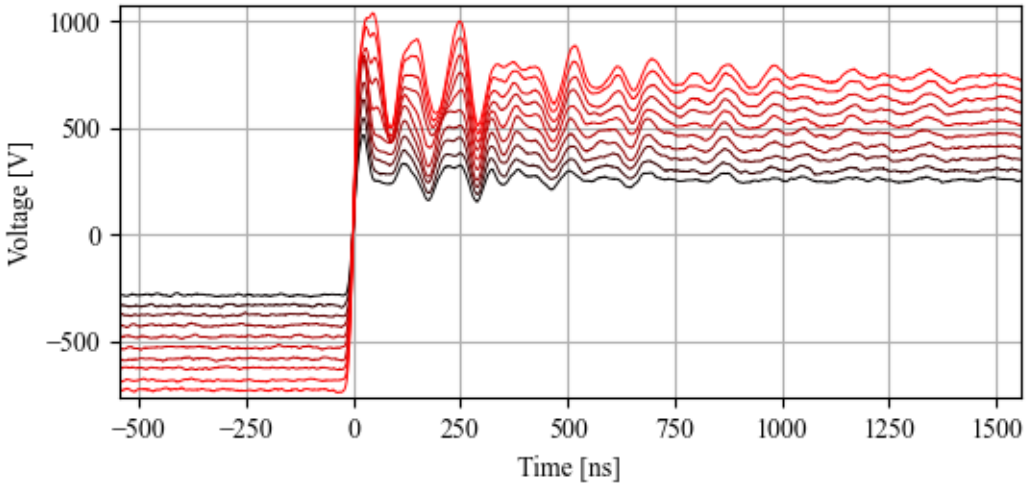

Figure 4-20 Multiple voltage signals at the instant of the commutation. The different hues of the colour red show the rising voltage.

The overvoltage test was repeated for multiple voltages. It was started at 250 V and increased by an interval of 50 V until it reached 700 V. At each value of the voltage an image of the measured signal was captured. All the signals are shown in Figure 4-20. The oscilloscope was set to high rate of sampling, hence the noise on the measurement. The data was smoothed with an average filter of a narrow window (25 points) and when treated later, it is the averaged values that are used.

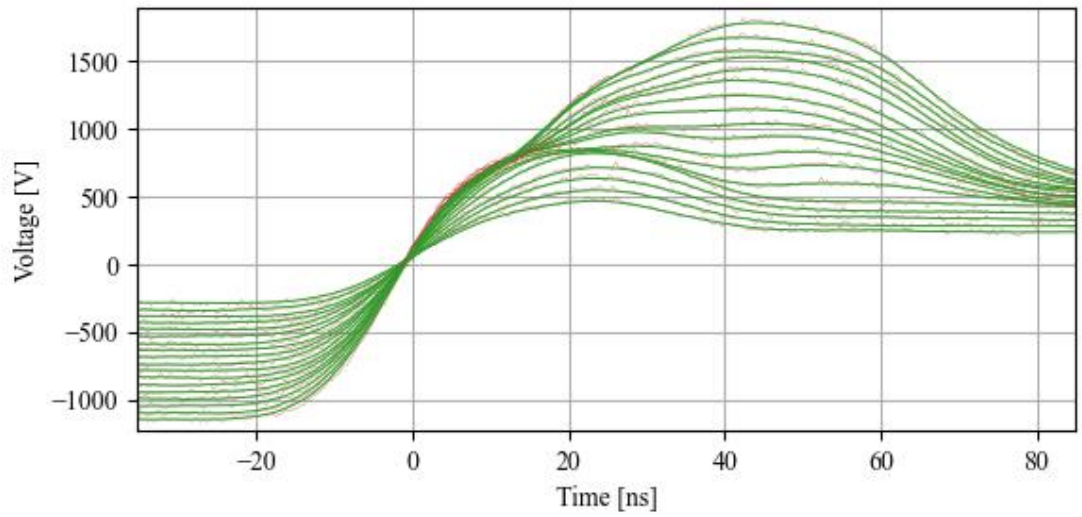

Figure 4-21 A close-up of the initial moments after the commutation, the same data as in Figure 4-20 with addition of measurements up to 1100 V.

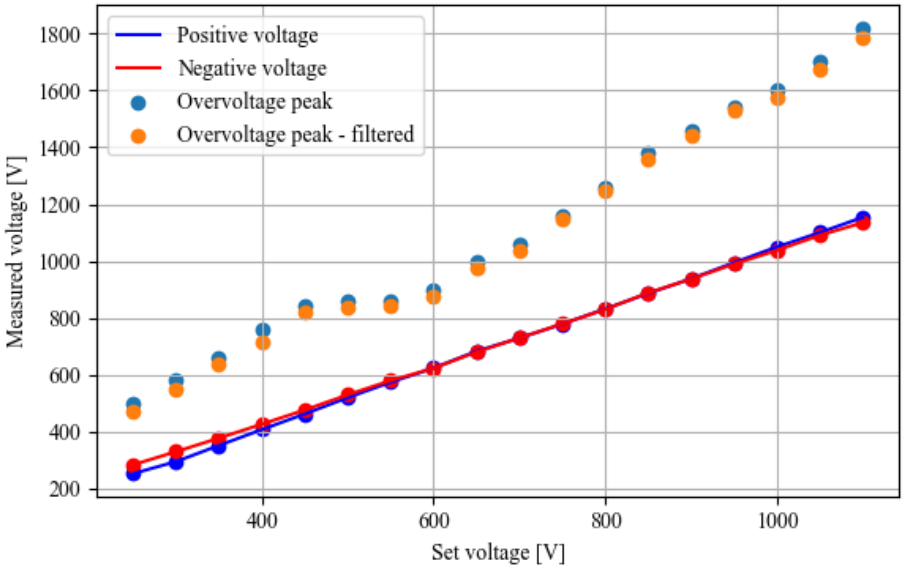

Figure 4-22 The voltages set compared with the negative voltage before the commutation (blue), the steady-state positive voltage after the commutation (red) and the voltage overshoot.

The set voltage, the one shown at the display of the high-voltage source, differs by a few percent (2-3%) from the measured value. It is not a random error that changes between measurements but rather a steady bias. This is not something to be concerned about in later treatment. The function of measured value by set value stays linear; the bias is not proportional to the value of the voltage.

The tests were done up to 1100 V, yet the interesting part is up to 600 V. Interesting part meaning the part useful for our purposes. The PDIV for the samples used in research later in the chapter starts at maximum 600 V at the beginning of life and ends at 350 V at the end of life. We try to demonstrate that the test bench behaviour is independent of the voltage level and that the overshoot is constant. Then we can proceed without reservation whether the voltage displayed on the source reflects the stress that we want to apply on the samples.

Figure 4-23 shows the relevant part of the data. The overvoltage in this domain stays at the value of 35% of peak-to-peak value of the emulated inverter signal. In Figure 4-23 the real PDIV is between ‘Measured voltage’ and a value opposite of ‘Measured voltage’, hence the overvoltage is related to value of twice the ‘Measured voltage’.

During ageing and during PDIV measurements it is the same test bench and the same emulator that acts upon the samples. The form of applied voltage does not differ between the ageing and test. The PDIV is recorded as the value displayed on the voltage source’s panel. We can do that because the voltage overshoot remains constant. Therefore, if we decided to record PDIV as the value of overshoot, we would end up with proportionally identical results, the overshoot multiplier would cancel itself out.

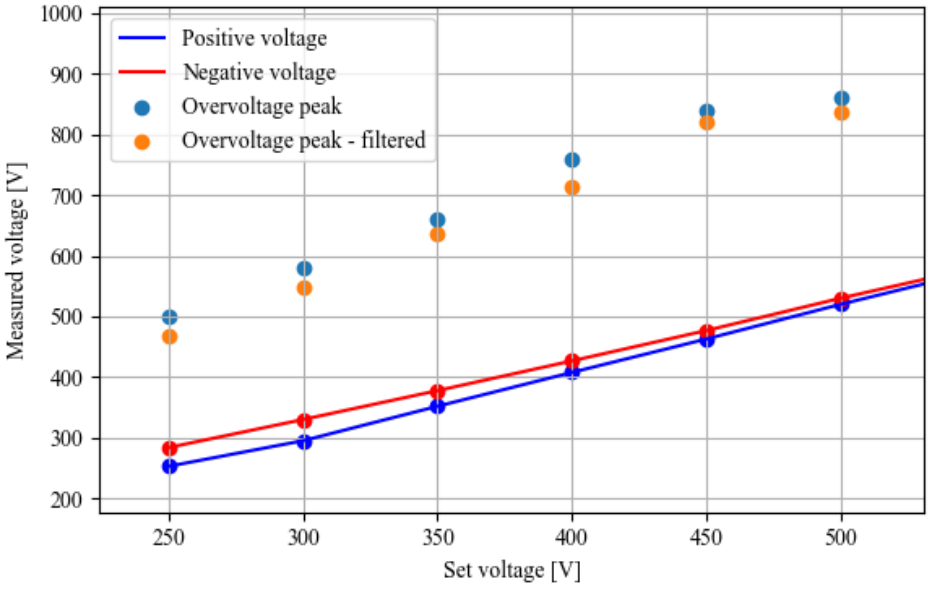

Figure 4-23 Overshoot test data up to 550 V. A close-up of data relevant to the tests performed during the thesis. Collected ageing data.

In this part reasoning for the choice of the ageing factors levels for the experiments is explained. Then all the combinations of factors that were tested are presented and how they fit into the modelling that was done later.

4.5.4 Preliminary runs

To choose the factor's levels for the experimental runs some preliminary tests were done. The objective was to find temperatures, voltages and frequencies that would accelerate the ageing but at the same time permit the experiment to runs for a significant amount of time of weeks or months. We want to maximise the impact of the factors on PDIV evolution yet avoid early breakdown.

4.5.4.1 Frequency levels choice

The frequency of the bipolar square-wave voltage produced by the test bench was effectively limited to about 15 kHz. Above that value the switch would detect overcurrent (it has a limit of an average current permissible), and the tests would be stopped by the automatic counters. An inverter in a typical automotive application operates at 10 kHz. Considering that and the fact that frequency is the least significant factor when it comes to ageing [44] (at least ageing with inception of PDs) the value of frequency was settled at 10 kHz and another level at 4 kHz.

4.5.4.2 Temperature levels choice

The Thermal Index (TI) of the used enamel material was 210 °C. What it means is that the material should survive 20000 h if held at the temperature called its TI. The TI of a material or of an insulation system in a standardized test. Three or four constant thermal ageing tests are done at three temperatures above the suspected TI. The samples are aged till they break down. Then an Arrhenius Law is fitted onto achieved lifetime data. Where the model's extrapolation crosses the 20000 h line, the TI is marked. In practice, it can be approximated that raising the temperature by 10 °C divides the lifetime by half.

Initially some trials were done in ambient temperature, the data shown in Figure 4-24. Voltages below PDIV alone were considered not degrading enough and the test was stopped after some 1000 h.

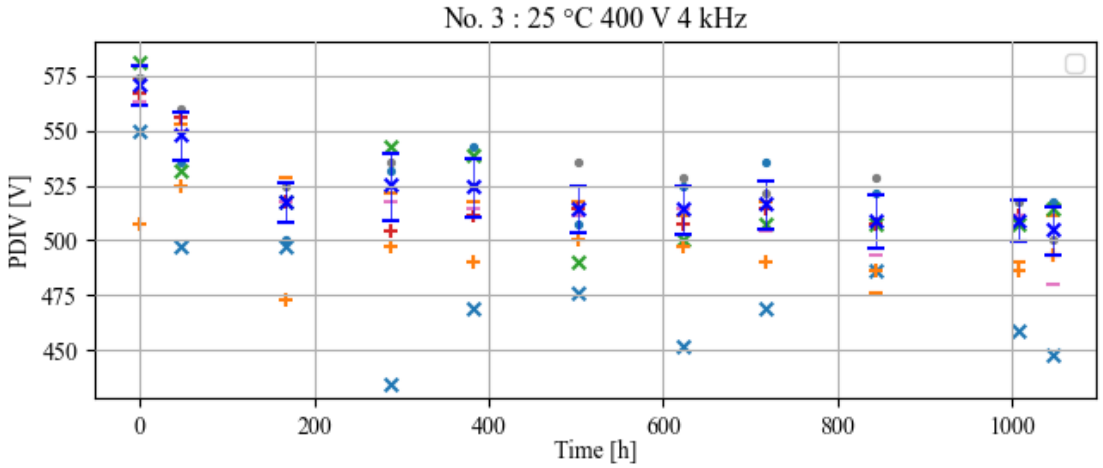

Figure 4-24 Data for ageing at 25 °C. The shapes in various colours represent the PDIV of the individual samples. The dark blue cross represents the scale parameter of their Weibull's distribution and the blue bars show the confidence interval.

In parallel, tests at 100 °C (Figure 4-25) and 200 °C (Figure 4-26) were done. Similarly, as in the test at ambient temperature, the perceived evolution of PDIV at 100 °C was not visible. On the other hand, at 200 °C more change in PDIV was observed.

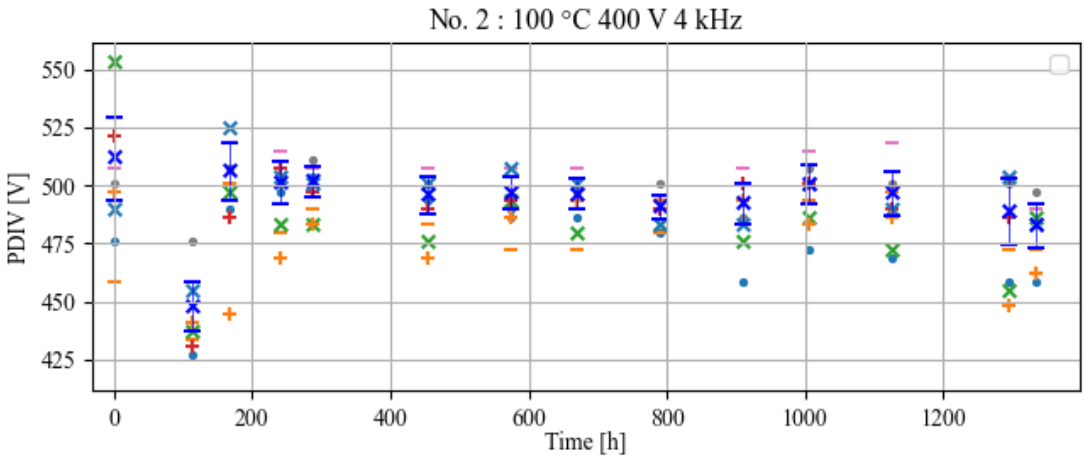

Figure 4-25 Data for ageing at 100 °C. The shapes in various colours represent the PDIV of the individual samples. The dark blue cross represents the scale parameter of their Weibull distribution and the blue bars show the confidence interval.

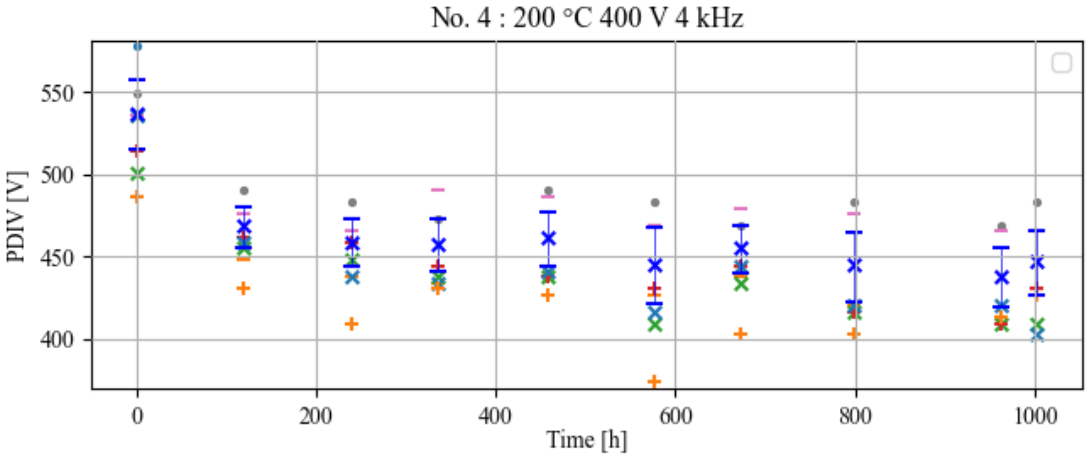

Figure 4-26 Data for ageing at 200 °C. The shapes in various colours represent the PDIV of the individual samples. The dark blue cross represents the scale parameter of their Weibull distribution and the blue bars show the confidence interval.

More tests were performed at 200 °C and the other level was chosen as 220 °C. Later, the set of temperatures was fixed at 220 and 250 °C, because the temperature of 200 °C was, in the end, deemed not degrading enough.

At that stage of research, it was envisioned to use both the evolution of PDIV and the samples' lifetimes for the purpose of modelling. Hence the objective was to degrade the samples till their end of life considered as electrical breakdown of the enamel.

Ultimately, the usage of the lifetime data was abandoned. The insulation while degrading has its PDIV gradually decreased. Because the voltage was chosen to be quite close the PDIV at some point the imposed voltage was greater than the decreasing PDIV hence the ageing was significantly accelerated (Twisted pairs with non-PD-resistant enamel last from

minutes to a couple of hours with PDs). Ageing from the three factors was now coupled with the ageing from the PD impact, the idea to use the lifetime data was discarded.

4.5.4.3 Voltage levels choice

It was decided that the voltage level should be as high as possible in order to make its potential degrading influence as pronounced as possible. In this case the test bench capabilities were not an issue, the assembly was capable of providing signal up to 1.5 kV where the switch was the bottleneck. For the twisted pairs used at the beginning of life and at ambient temperature the PDIV was about 600 V. The PDIV depends on the temperature, so rise in the temperature decreases the PDIV. The first tests were done at 500 V (Figure 4-27). There were no signs of PDs inception after a couple tens of hours. Then the PDIV decreased below 500 V and the samples were broken down.

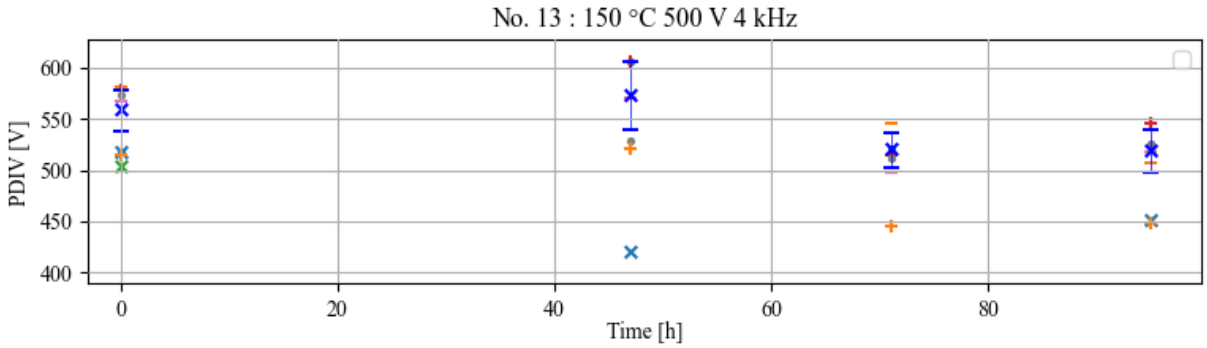

Figure 4-27 The ageing data at 500 V. The samples all break down after three days.

Another test at 480 V was done with ultimately similar results. The upper level of voltage was fixed at 450 V and the lower level at 400 V. Later, after many hours of ageing at 450 V in multiple configurations it was discovered that the PDIV continues to decrease throughout the lifetime and in the end the 450 V is enough to incept PDs. For this reason, an alternative set of factor levels, namely 350 V and 400 V was added.

4.5.5 Collected data overview

Overall, thirty-seven experiments at different sets of factor levels were launched. Some of them broke down quickly. Some were stopped because the ageing acceleration factor was too low and the suspicion was that the samples would survive many months more. Some were stopped due to the lab summer maintenance period. A few of the factor levels' combinations were repeated – mostly the ones that were stopped due to external reasons or some that gave dubious results. For the sake of completeness all the factor combinations are presented in Table 4-1.

Table 4-1 All degradation experimental data points (values of voltage, frequency and temperature).

No	Voltage [V]	Frequency [Hz]	Temperature [°C]	Lifetime [h]	
2	400	4	100	1336	Stopped
3	400	4	25	1048	Stopped
4	400	4	200	1002	Stopped
5	500	10	250	0	Early EoL
6	500	10	250	0	Early EoL
7	500	10	220	0	Early EoL
8	500	10	200	24	Early EoL
9	500	4	200	24	Early EoL
10	500	10	200	24	Early EoL
11	450	4	150	1247	EoL
12	450	4	200	576	EoL
13	500	10	150	93 D	Early EoL
14	480	10	200	432	EoL
15	400	10	250	74 D	Early EoL
16	450	10	250	24	Early EoL
17	480	10	250	0	Early EoL
18	450	10	250	74 D	Early EoL
19	480	10	250	25 D	Early EoL
20	350	10	250	862	EoL
21	400	10	250	573	EoL
22	400	10	220	741	EoL
23	450	4	220	160 D	Early EoL
24	480	4	220	160 D	Early EoL
25	400	4	250	246 T	Stopped
26	450	10	250	246 T	Stopped
27	450	10	220	246 T	Stopped
28	400	4	200	2610	EoL
29	350	4	220	2610	EoL
30	450	10	220	352	EoL
31	450	4	220	430	EoL
32	400	4	220	1586	EoL
33	350	10	220	1224	EoL
34	400	10	250	741	EoL
35	400	4	220	2258 D	EoL
36	350	10	250	1897	EoL
37	350	10	250	891 T	Stopped
38	400	10	40	261 T	Stopped

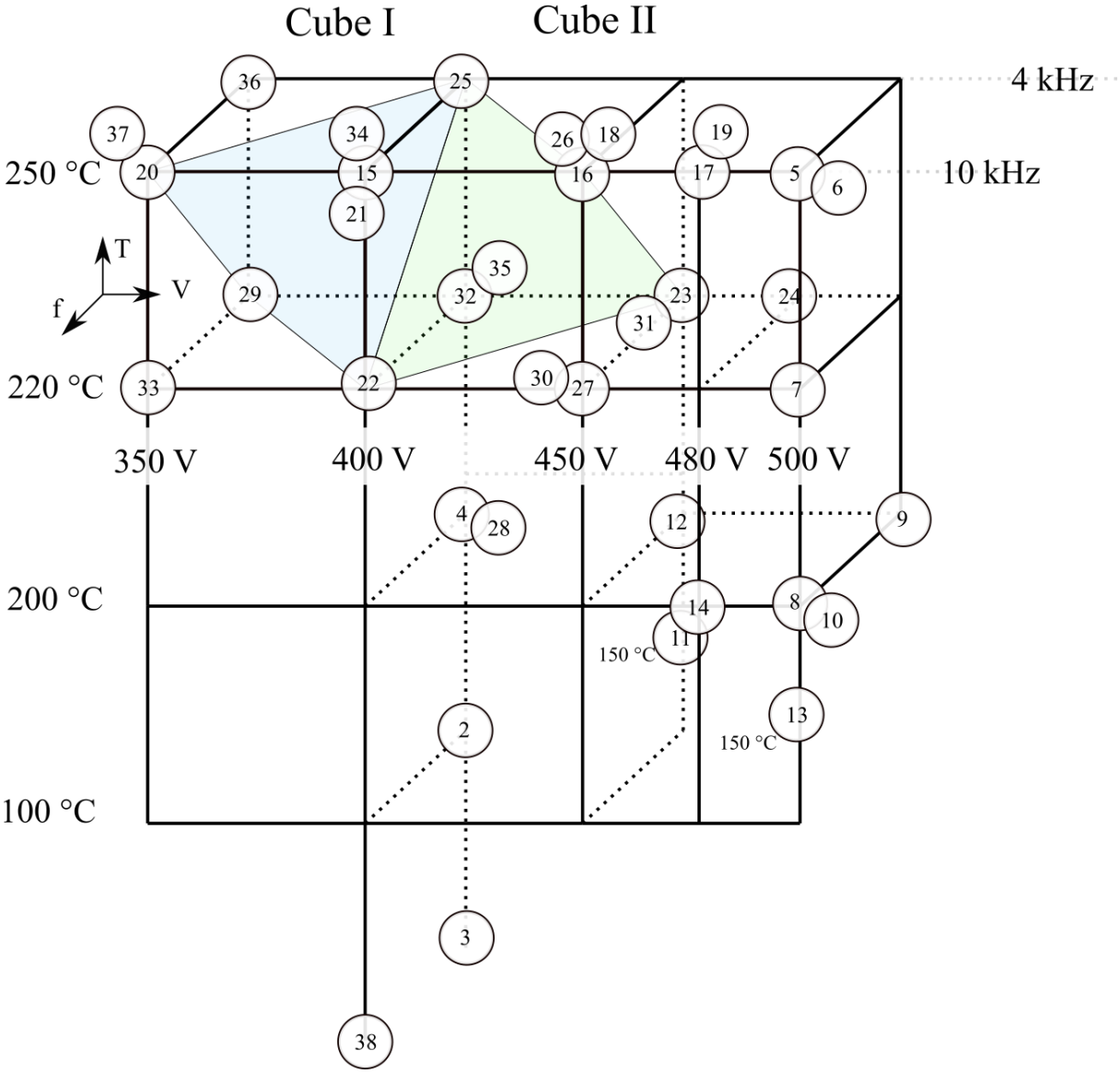

Figure 4-28 Every experiment presented on a three-dimensional grid. The temperatures are presented vertically, the values of voltage horizontally and the frequencies in the third direction.

Figure 4-28 is another way of presenting the information included in Table 4-1. Instead of the chronological order, the points are placed in a space where coordinates represent factors' levels. Also, it illustrates which experiments were repeated.

4.6 Design of Experiments for PDIV evolution experiments

4.6.1 Design of Experiments

Some of the objectives of the domain called Design of Experiments (DoE) [45], [165] are to minimize the number of experimental runs and to obtain a model of an output as a

function of experimental factors. In our case the output being PDIV or rather of PDIV evolution model's parameters.

The method applies to many fields. Notably it was used in the past for insulation lifetime modelling [50]. It is required that the output is linearly dependent on each factor. For this purpose, a general form of a model of relation output (Y)-factor (X) needs to be known and then linearized, which can be achieved thanks to non-linear operators. Additionally, the factor levels are normalized so that their influence in the final model can be directly compared. In case of two factors with two levels each, in order to obtain full information four experiments are required (as shown in an example in Figure 4-29).

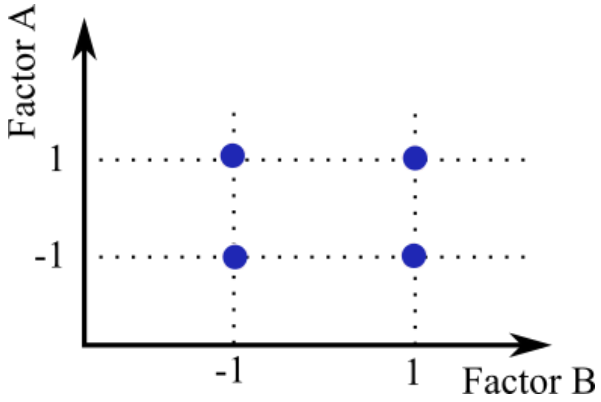

Figure 4-29 An example of a full experimental plan for two factors and two levels of the factors. The values of the levels are normalised into -1 and 1 in this example.

The four experiments can be described in a matrix form:

$$\begin{bmatrix} Y_1 \\ Y_2 \\ Y_3 \\ Y_4 \end{bmatrix} = \begin{bmatrix} 1 & -1 & -1 & 1 \\ 1 & -1 & 1 & -1 \\ 1 & 1 & -1 & 1 \\ 1 & 1 & 1 & -1 \end{bmatrix} \begin{bmatrix} M \\ E_A \\ E_B \\ I_{AB} \end{bmatrix} \quad (4.1)$$

Where the vector on the right contains values of results of the experiments, the matrix signifies the levels of the factors, and the right vector consists of resulting factor effects. M is the mean value of output Y; E_A, E_B are the main effects of the factors A and B; I_{AB} is the effect of interaction between A and B. Once the effect vector is calculated from (4.1) it can be used to create a model of output Y for any other combination of the factor levels (4.2).

$$Y = M + X_A * E_A + X_B * E_B + X_A X_B I_{AB} \quad (4.2)$$

In (4.2) X_A and X_B are normalized levels of factors. They take values from <-1;1> but the model may be valid for extrapolation beyond that set.

4.6.2 The experimental plan

Effects of three factors were studied, namely temperature, voltage level and voltage frequency. Values of the chosen levels are specified in Figure 4-30. These levels were specifically chosen, as explained in 4.5.4, in order to have some accelerated ageing from thermal ageing and to be just below PDIV which maximizes potential electrical ageing impact.

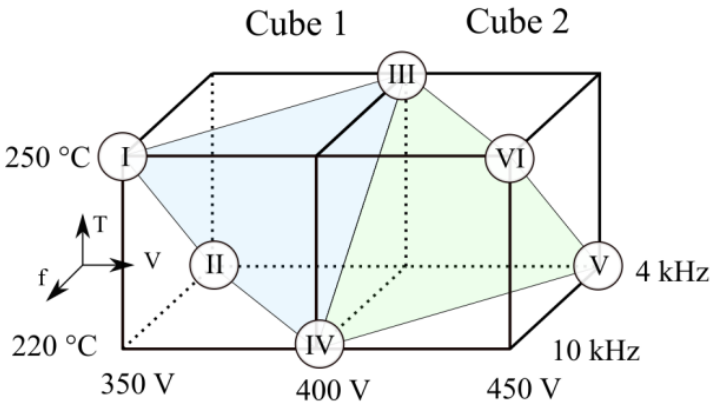

Figure 4-30 Two designs of experiment (Cube 1 and Cube 2). Both cubes have three factors and two levels each. The fractional plans are marked with the coloured shapes.

Here, only partial designs are considered (4 experiments among the 8 possible configurations) in order to accelerate the experimental process. The main consequence is the inability to model the interactions between the different factors which could reduce the modelling accuracy. Points I to IV were used to model creation in later sections and points V, VI were employed to evaluate the Cube I model extrapolation.

4.6.3 Methods in PDIV evolution modelling

4.6.3.1 Weibull distribution

Each experimental run consisted of eight samples so eight measurements for each combination of the factor's levels. The samples were identical but some variability in the population is inevitable, for this reason the data were treated with the Weibull distribution.

In order to apply the distribution, the values of PDIV, in ascending order, were assigned a cumulative probability fraction based on Benard's Approximation. Then those values were transformed into scales corresponding to Weibull graph and modelled with linear regression. Parameters of this model, when retransformed into linear scales are connoted as; scale (α) and shape (β) parameters of Weibull Distribution respectively. The confidence intervals for the values are calculated with methodology presented in the standard [142]. PDIV at each point in time for the purposes of modelling was then considered to be equal to

the α-Weibull scale parameter. Multiple identical specimens permit to get a better idea of an average value. Weibull distribution is well adapted to describing lifetime or degradation process – the weakest specimens have less impact on the average result. For tests with less than twenty specimens it is assured by introduction of discrimination weights for the samples with the shortest lifespans.

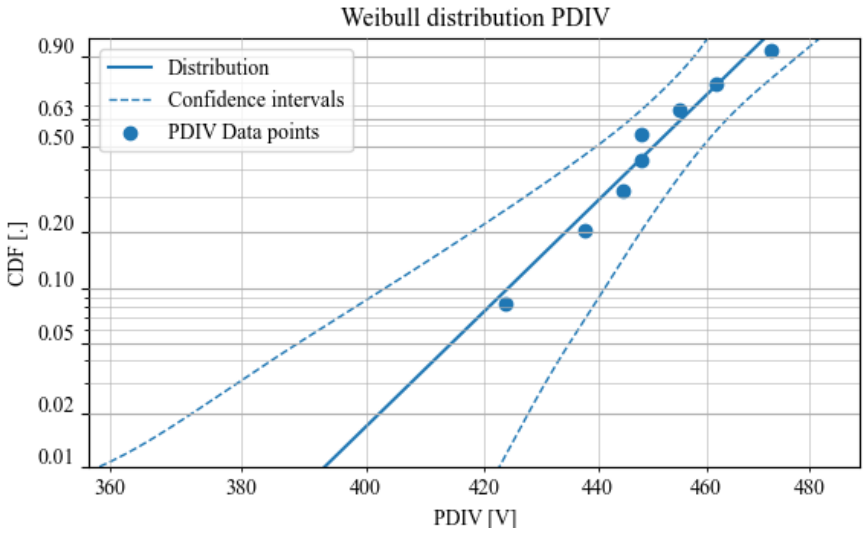

Figure 4-31 Example of cumulative distribution function (CDF) of Weibull's distribution on Weibull graph. The α-Weibull at 0.63 of CDF, section at that value used as the confidence intervals.

4.6.3.2 Degradation model

The samples undergoing accelerated ageing are treated with high temperature and square-wave voltage. During ageing PDIV is measured periodically. The recorded PDIV is always the value of the voltage displayed on the positive source when PDs are detected. One could argue that the actual PDIV is either the peak-to-peak value or at least the amplitude measured from the negative value to the positive value. As explained in 4.5.3 the peaks are not a factor. The PDIV is marked as the value of the voltage at positive source for consistency reasons.

The measurement campaign resulted with sets of data for every chosen factor combination. Each set contains many days of measurements. Each day's data has up to eight values of PDIV for the samples at that day. The day's sets were treated as Weibull distribution, the distribution's parameters were established for each set. That resulted in series of α-Weibull of PDIV in time. These data were modelled with two different models, the exponential model and the inverse power model. These are presented as:

The assumed form of the Inverse Power Model (IPM):

$$PDIV_{IPM}(t) = Kt^{-n} \tag{4.3}$$

The form of Exponential Model:

$$PDIV_{exp}(t) = Ke^{-nt} \tag{4.4}$$

And of the Exponential 3-parameter Model:

$$PDIV_{exp2}(t) = Ke^{-nt} + M \tag{4.5}$$

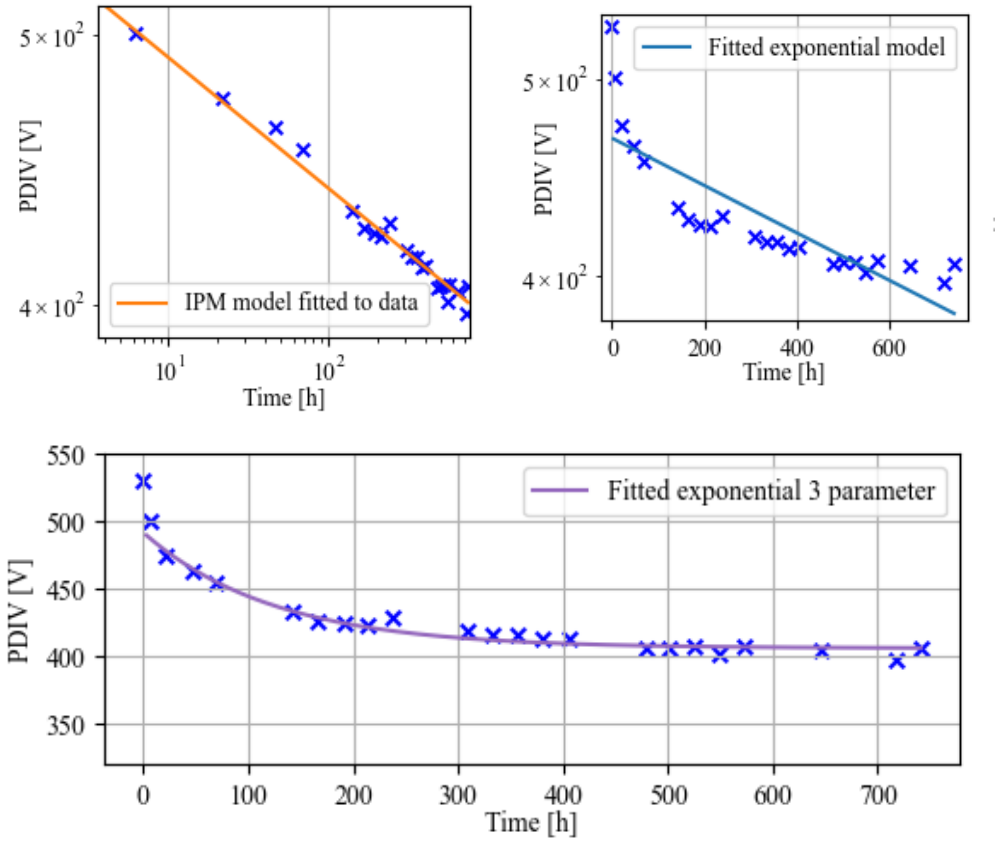

Figure 4-32 The comparison of IPM and exponential model using the data of ageing at Point IV. Log-log scale in the IPM plot and linear-logarithmic in the exponential model plot.

Models shown in (4.3) and (4.4) are functions of PDIV over time with two constants K and n which were determined by fitting the model to the data. The data were transformed into logarithmic scales and fitted with linear regression. The model with three parameters (4.5) was fitted in a process of optimization. From the values of the coefficient of determination (R^2) presented in Table 4-2 and visual evaluation of Figure 4-32 the IPM and the three parameter exponential models were better at explaining the data. IPM was chosen as the one with fewer parameters hence better suited to the following steps involving modelling of the parameters in function of the values of the factors.

Table 4-2 R^2 values for modelling by means of the two considered models.

Point	**Model R^2**		
	IPM (4.3)	***Exponential (4.4)***	***Exponential 3-parameter (4.5)***
I	**0.69**	0.16	0.85
II	**0.91**	0.72	0.94
III	**0.39**	0.50	0.51
IV	**0.99**	0.69	0.94
V	**0.92**	0.83	0.92
VI	**0.81**	0.86	0.93
VII	**0.80**	0.70	0.89
VIII	**0.94**	0.87	0.93
IX	**0.91**	0.83	0.96
X	**0.77**	0.85	0.89
Average	**0.813**	0.701	0.876

4.6.3.3 Dealing with premature end of life in modelling

One of the problems that had to be considered was that a few twisted pairs died prematurely. That caused the spread of the times till the end of life to be significant in many cases. Naturally the first pairs to die off were those that manifested lower PDIV from the start. Consequently, the population in some cases may give impression of rising PDIV. The pairs with lowest PDIV are removed from the calculation – the average (or rather the α-Weibull|) rises.

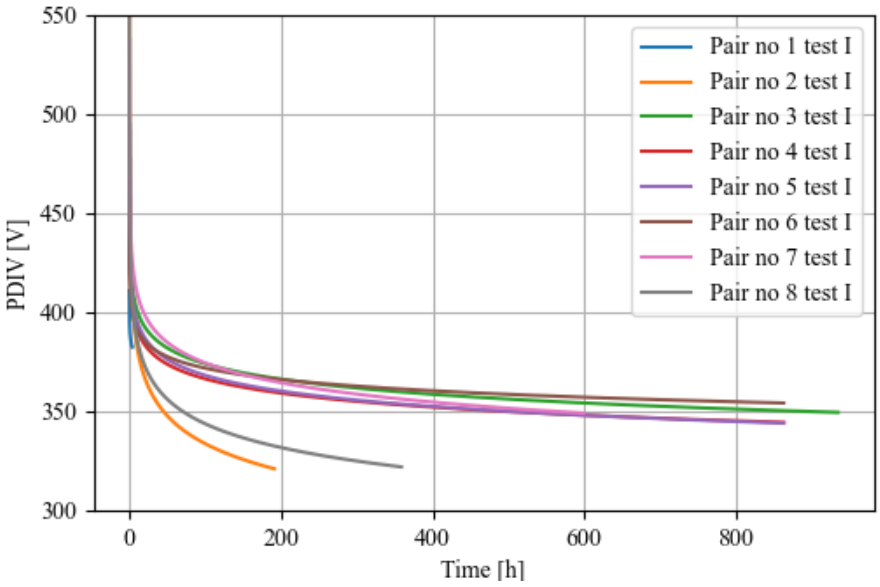

Figure 4-33 Inverse Power Model fitted to the PDIV data of the individual samples. The curves stretch as far as the lifetime of the particular sample.

In order to take this effect into account a different approach is proposed. The model was fitted to the data of the individual samples (rather than to the scale parameter, α-Weibull of all the remining samples). The individual models' curves can be observed in Figure 4-33. Then a weighted average was applied in order to merge the models of all the samples. The weight of a model was proportional to its lifetime. Results of that original method are presented in Figure 4-34 for the extreme case of Point I (point aged at 250°C, 350 V and 10 kHz).

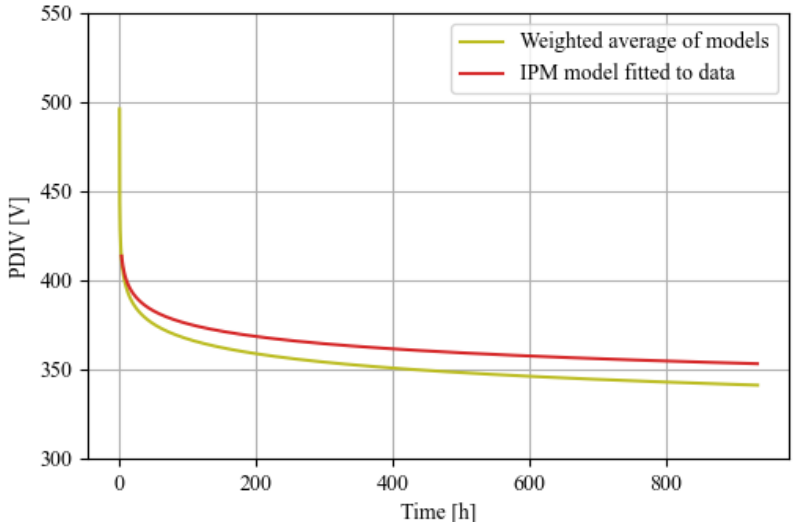

Figure 4-34 Comparison of the model calculated purely for α-Weibull parameters of the surviving samples (in red) and the averaged model created from the individual models. The second approach takes into account the shorter lifespans of some of the samples.

4.7 Modelling of PDIV evolution

4.7.1 Factor levels and collected data

Figure 4-35 and *Figure 4-36* show the experimental data with fitted IPM models' curves obtained from long ageing below PDIV. The measurements were carried out until the last sample of the run broke down (except for points III and VI which were deliberately stopped because the test benches were not available any longer). Table 4-3 shows the levels of factors applied the values correspond to the plan shown in 4.6.2. Table 4-4 beside restating the values of factors also shows model parameters of IPM, n and K, as in equation (4.3).

Table 4-3 Factor levels

Cube I (II)	**Factor levels**	
	Minimum level (-1)	***Maximum level (+1)***
Voltage (below PDIV)	350 V (400 V)	400 V (450 V)
Frequency	4 kHz	10 kHz
Temperature	220°C	250°C

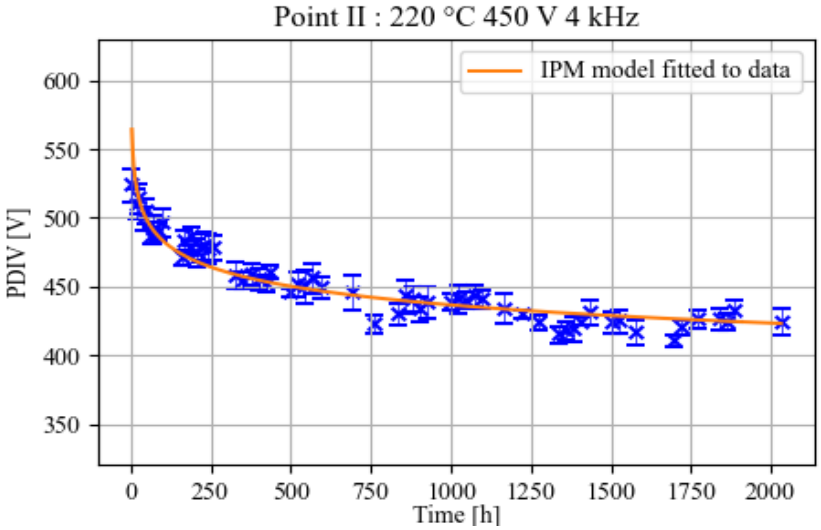

Figure 4-35 Data and models of evolution of PDIV at Point II.

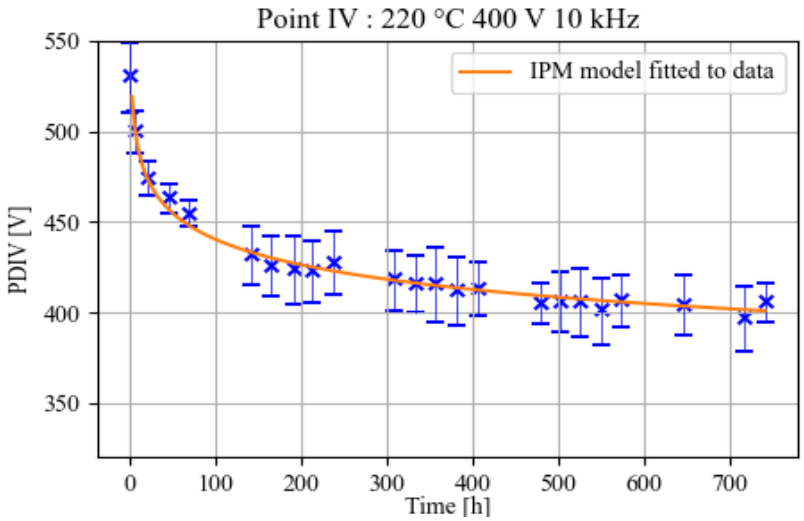

Figure 4-36 Data and models of evolution of PDIV at Point VI.

Table 4-4 IPM parameters per point.

Point	**Factor values**			**Parameter**	
	V [V]	***f [kHz]***	***T [°C]***	***K***	***n***
I	350	10	250	426	0.0275
II	350	4	220	592	0.0441
III	400	4	250	475	0.0104
IV	400	10	220	546	0.0468
V	450	4	220	533	0.0303
VI	450	10	250	502	0.0184
VII	400	10	250	546	0.0468
VIII	400	4	220	559	0.0418
IX	350	4	250	535	0.0482
X	350	10	220	547	0.0323

4.7.2 PDIV evolution model extrapolation

For some of the experimental points over 2000 h of electro-thermal ageing was conducted. The long lifetime presents an opportunity to check how much data is needed to predict accurately the future evolution of PDIV. The modeling was performed with data from the first 200, 400 and 600 hours. Then the models resulting from partial data were extrapolated as far as the actual data and these were compared to that reality.

The errors are calculated from the difference between α-Weibull and modeled value at the point in time. Then that difference is divided by the α-Weibull actual PDIV and converted to percentage.

Table 4-5 The Extrapolation error

Mean % error of model compared to all collected data		**Time considered for the model**			
	Time of data collection [h]	***All***	***600 h***	***400 h***	***200 h***
Point I	930	3.17	3.77	4.96	4.32
Point II	2031	1.46	2.32	3.10	4.45
Point III	245	1.45	-	-	1.50
Point IV	740	0.63	0.64	0.65	0.65
Point V	445	0.92	-	0.92	1.06
Point VI	245	0.92	-	-	1.03
Point VII	742	1.04	1.08	1.09	1.27
Point VIII	2258	1.01	1.80	2.17	2.81
Point IX	1896	1.69	2.56	2.95	3.07
Point X	1224	1.69	2.17	2.88	2.76

Table 4-5 presents relative errors (in %) between the value of α-Weibull and extrapolated model at four points in time.

Taking Point II as an example of an interesting case - the data were collected for a long period of time, much beyond 600 h. Using 200 h of PDIV evolution data (10% of total collected data) provides with model that describes the PDIV with an error of 4.45% on average. Additional 400 h of tests importantly reduces the gap between the model and real values (Table 4-5), but it still represents only 30% of collected data. Error of model constructed from 600 h of data (2.32%) is comparable to the error of model calculated from all the data at 2031 h (1.46%). A similar situation can be observed for Points VIII and IX.

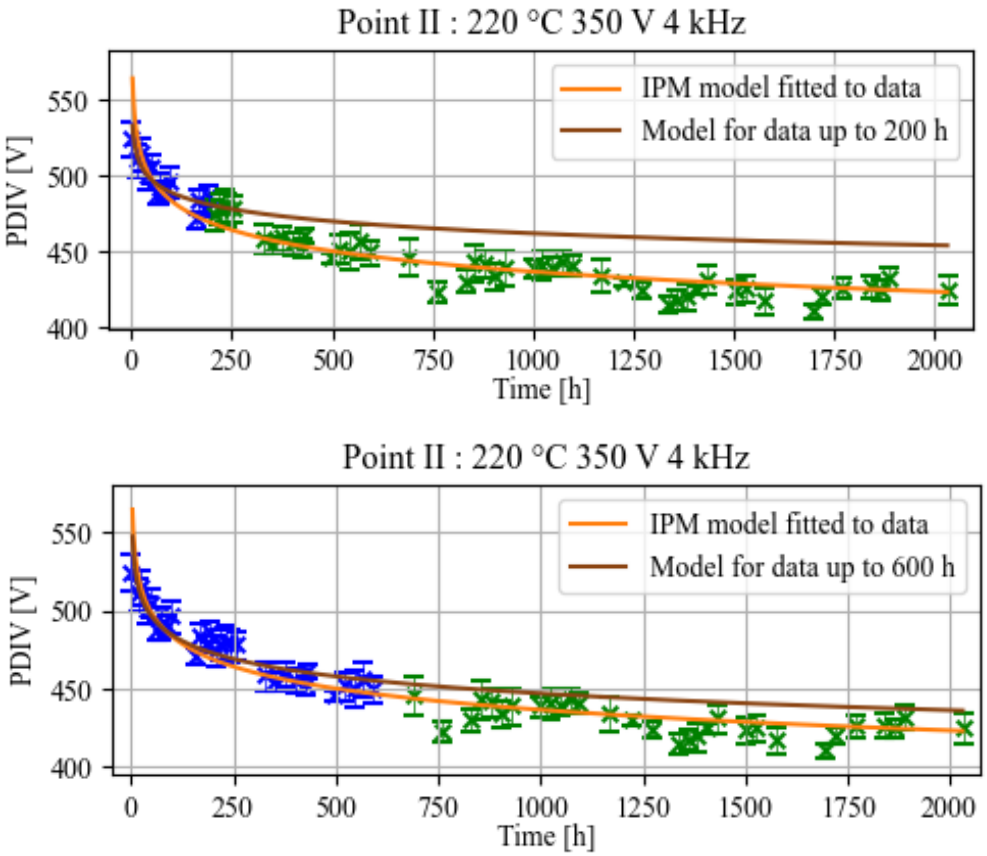

Figure 4-37 Comparison of IPM model from limited data and model with all the data. 'Training set' in blue and the remaining data in green.

4.7.3 Fractional plan model

Once the evolution of PDIV over time is expressed as a two-parameter model, the next step is to try to find a way to extrapolate the evolution to different conditions.

The two vectors of results for parameter *K* and *n* from Table 4-4 can be then implanted into equation similar to (4.1). As in (4.5) where the output vector is substituted with the values of the parameter *K* for the four models based on the ageing at the four experimental points according to the established plan.

$$\begin{bmatrix} K_1 \\ K_2 \\ K_3 \\ K_4 \end{bmatrix} = \begin{bmatrix} 1 & -1 & -1 & 1 \\ 1 & -1 & 1 & -1 \\ 1 & 1 & -1 & 1 \\ 1 & 1 & 1 & -1 \end{bmatrix} \begin{bmatrix} M \\ E_A \\ E_B \\ I_{AB} \end{bmatrix} \tag{4.5}$$

This equation, when solved, provides the main effects of the factors. Since it is not a full experimental design, we do not get the interactions between factors.

$$K = M_K + X_v * E_{KV} + X_f * E_{Kf} + X_T * E_{KT} \tag{4.6}$$

$$n = M_n + X_v * E_{nV} + X_f * E_{nf} + X_T * E_{nT} \tag{4.7}$$

Each of the parameters has three main effect coefficients, one for every factor (Voltage, frequency, temperature). *Xs* take values of corresponding factor in normalized form. The models (4.6) and (4.7) make it possible to calculate PDIV curve parameters *K* and *n* for any combination of factors' levels for values between the minimum and maximum as in Table 4-1.

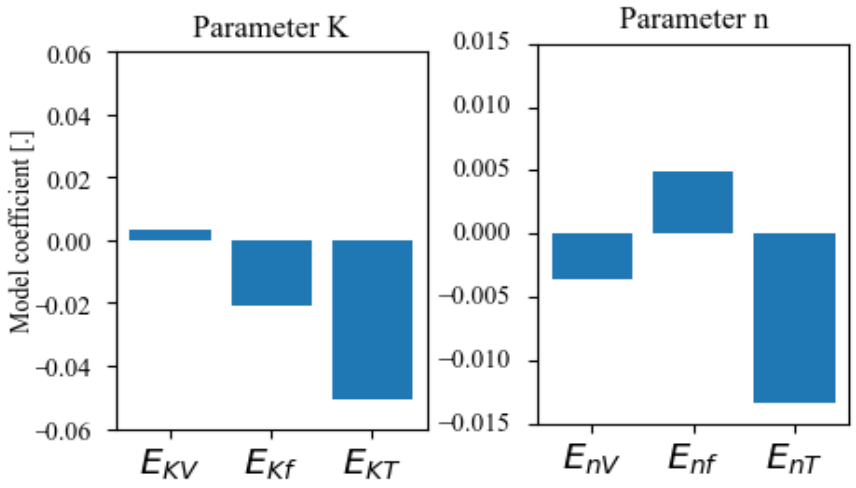

Figure 4-38 Main effects of voltage, frequency and temperature on parameter K (left) and n (right) of equation (4.3) for models of PDIV evolution.

Figure 4-38 presents the qualitative impact of the factors on the model of evolution of PDIV. Parameter *K*, which is responsible for describing the initial value, is most influenced by temperature. The relation is negative, thereby signifying that the higher the temperature, the lower the initial PDIV. Similar case applies to frequency, but the impact is comparatively smaller. The voltage applied during the ageing does not influence the initial value of PDIV which is not surprising because it does not influence the first measurements.

Parameter *n*, which is responsible for the shape of the curve, is again strongly influenced by the temperature and to a smaller degree by frequency and voltage. The temperature over Temperature Index of the material of the enamel is the main ageing factor in this case.

The work up to this point involved half of the tests needed for a full DoE plan. The analysis lacks the impact of the interactions.

4.7.4 Full plan model

Initially only the fractional plan experiments were conducted. Later, in order to discover the importance of the interactions between the factors, all the points of the cube were added. The factor levels of the additional points are complementary to the levels of the previously treated points and presented in Figure 4-39 as points VII to X.

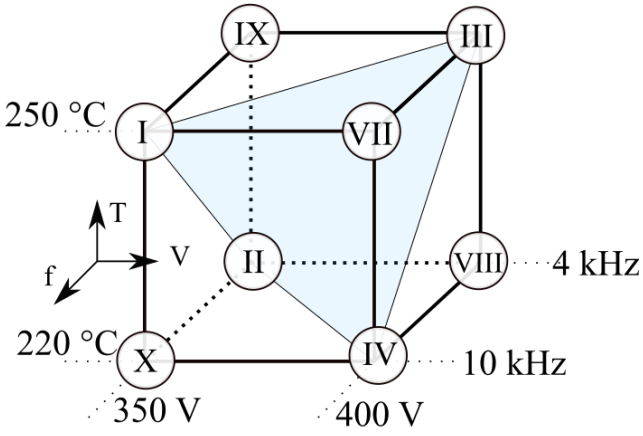

Figure 4-39 The full experimental plan for three factors and two levels per factor, overall, there are $2^3 = 8$ experimental points.

When there are eight points instead of four the equation becomes the equation (4.8). The effect vector gains the variables responsible for the interactions' impacts, I_{AB}, I_{AC}, I_{BC} and I_{ABC}.

$$\begin{bmatrix} Y_1 \\ Y_2 \\ Y_3 \\ Y_4 \\ Y_5 \\ Y_6 \\ Y_7 \\ Y_8 \end{bmatrix} = \begin{bmatrix} +1 & -1 & -1 & -1 & +1 & +1 & +1 & -1 \\ +1 & -1 & -1 & +1 & +1 & -1 & -1 & +1 \\ +1 & -1 & +1 & -1 & -1 & +1 & -1 & +1 \\ +1 & -1 & +1 & +1 & -1 & -1 & +1 & -1 \\ +1 & +1 & -1 & -1 & -1 & -1 & +1 & +1 \\ +1 & +1 & -1 & +1 & -1 & +1 & -1 & -1 \\ +1 & +1 & +1 & -1 & +1 & -1 & -1 & -1 \\ +1 & +1 & +1 & +1 & +1 & +1 & +1 & +1 \end{bmatrix} \begin{bmatrix} M \\ E_A \\ E_B \\ E_C \\ I_{AB} \\ I_{AC} \\ I_{BC} \\ I_{ABC} \end{bmatrix} \tag{4.8}$$

Like in the process described in the previous part we determined the values of the *n* and *K* parameters of the four additional models of evolution of PDIV. Then the values are used in the equation (4.8) as the output vector. The equation can be solved in order to calculate the values of the effects vector. Once the values are known they can be used in an equation that describes the two parameters as functions of the three parameters. The equations are (4.9) for K parameter and (4.10) for n parameter.

$$\begin{aligned} \boldsymbol{K}(X_V, X_f, X_T) = M_K + \boldsymbol{E_{VK}} X_V + \boldsymbol{E_{fK}} X_f + \boldsymbol{E_{TK}} X_T + I_{VfK} X_v X_f \\ + I_{VTK} X_V X_T + I_{fTK} X_f X_T + I_{VfTK} X_v X_f X_T \end{aligned} \tag{4.9}$$

$$\begin{aligned} \boldsymbol{n}(X_V, X_f, X_T) = M_n + \boldsymbol{E_{Vn}} X_V + \boldsymbol{E_{fn}} X_f + \boldsymbol{E_{Tn}} X_T + I_{Vfn} X_v X_f \\ + I_{VTn} X_V X_T + I_{fTn} X_f X_T + I_{VfTn} X_v X_f X_T \end{aligned} \tag{4.10}$$

The values of the effect vectors, that are at the same time coefficients of the models (4.9) and (4.10) are presented in Figure 4-40.

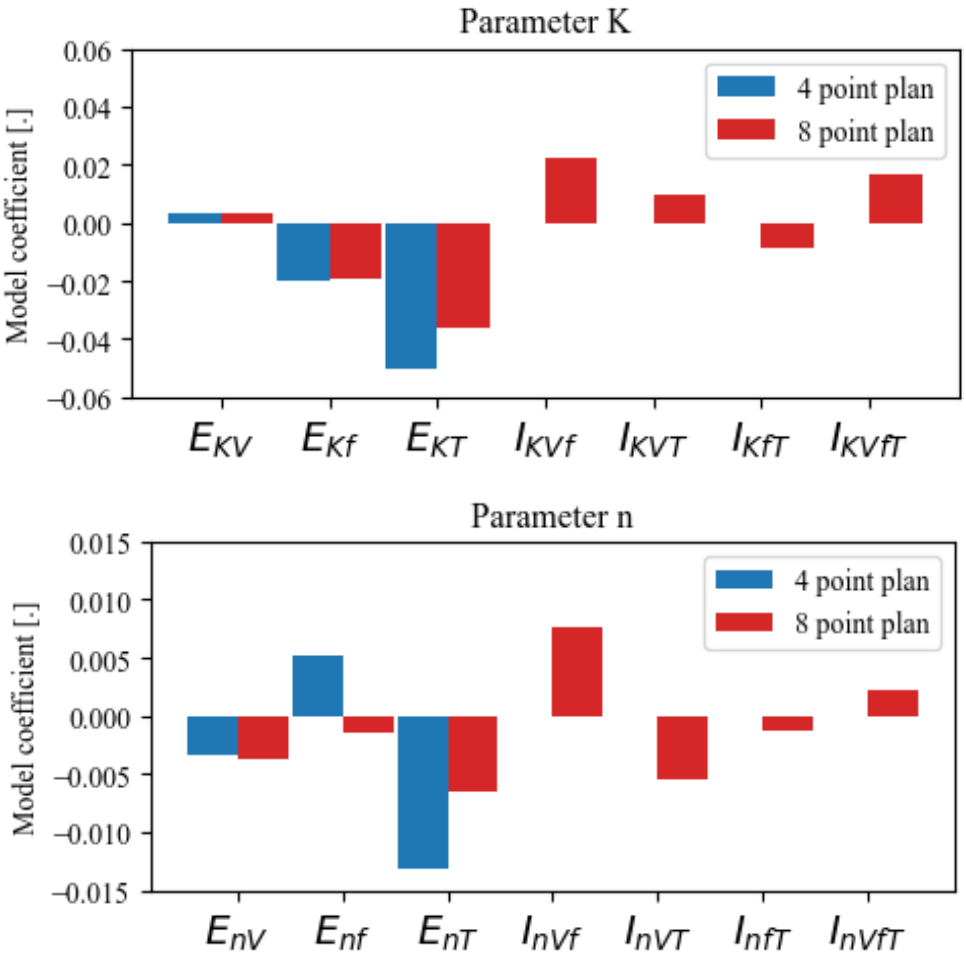

Figure 4-40 The values of main factors calculated for fractional plan and full plan.

Figure 4-40 shows the difference between the values of the model parameter *K* and *n*. The information is repeated in Table 4-6. The comparison is possible only between the main effects coefficients as the first model lacks the interaction coefficients.

Table 4-6 The comparison between numerical values of the model coefficient of fractional (4 point) and full (8 point) plan.

	K 4-point	***K 8-point***	***n 4-point***	***n 8-point***
M	2.7039	2.712	0.032	0.033
X_v	0.0035	0.0033	-0.0034	-0.0036
X_f	-0.0202	-0.0189	0.0051	-0.0013
X_T	-0.0504	-0.0363	-0.013	-0.0065
I_{Vf}	-	0.0222	-	0.0076
I_{VT}	-	0.0009	-	-0.0054
I_{fT}	-	-0.008	-	-0.0013
I_{VfT}	-	0.016	-	0.0021

The change in parameter *K* is not qualitatively significant. The values of the main effects have the same sign and similar values corrected by the addition of the interactions. The parameter n experienced change of sign for frequency's effect and addition of important impact of interaction of frequency and voltage. This parameter is responsible for the slope of the evolution. When ageing over PDIV, the higher frequency the more destructive PDs occur. When the ageing is done without PDs the frequency itself has marginal impact on lifetime. Yet, change of frequency with higher voltage made the evolution slower. There were only two levels of frequency in this study so the exact impact and the causes behind this phenomenon remain unexplained.

Some of the interactions' coefficients are positive, they add to the calculated values of the parameters. That seems counter-intuitive, as the ageing factors should be harmful and their interactions, if any, should be even more degenerative. This particularity stems from the fact that the outputs that had been used were not a direct measure of destructiveness of the factors. It would have been expected all the coefficients to be negative if it had been the lifetime that had been used as the model's output. However, the parameters *K* and *n* are connected. When *K*, the starting point decreases, the n may need to increase, yet both depend on the same three factors.

4.7.5 Model extrapolation to other factor values

In order for the model to have a practical application it needs to be able to predict the actual evolution of PDIV. It should perform this task within the boundaries marked by the experimental levels. It would be even better if it were able to do that beyond those boundaries. In this section the ability of the model to extrapolate is tested.

Two points at higher voltages were used to demonstrate the accuracy of the extrapolation. The ageing tests had been conducted; hence the real model of the evolution was known for that combination of factors' levels.

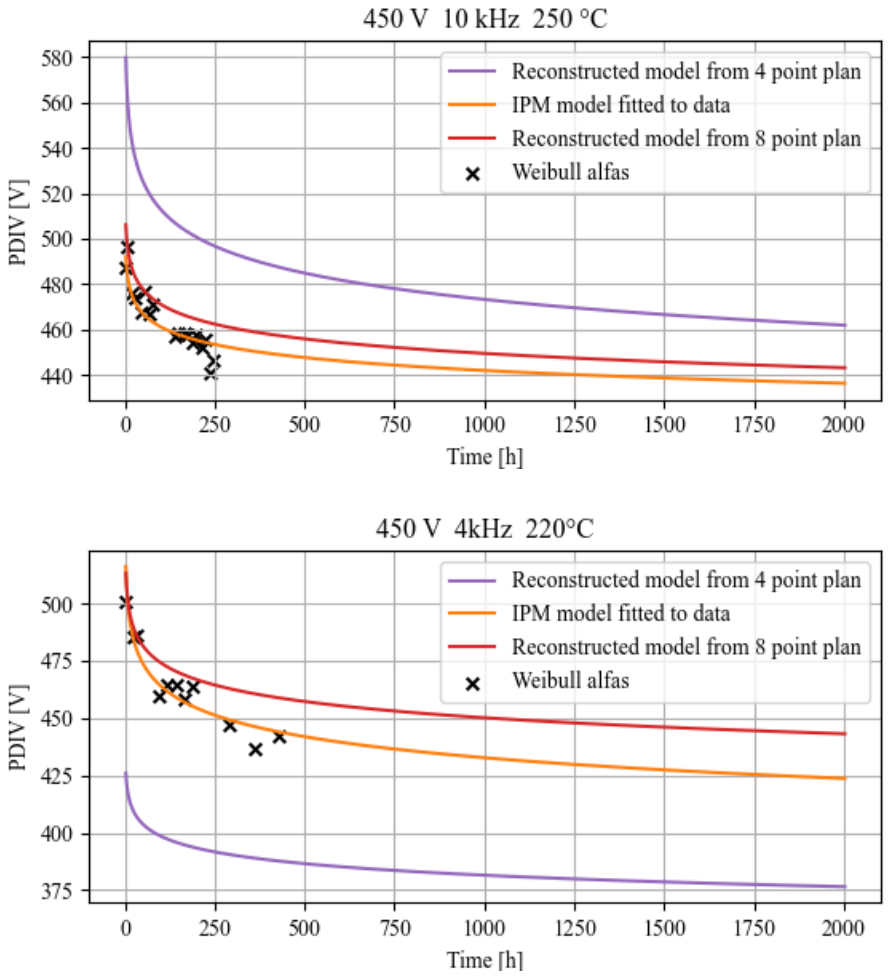

Figure 4-41 The results of the extrapolation. The measurements are shown as the black crosses, corresponding fitted model as the orange curve. The curve in blue is calculated from the model from the fractional plan, the red curve – the full plan model.

Figure 4-41 shows how much the introduction of the impact of the interaction added to the model's accuracy. The first model widely misses the actual model, whereas the full plan model is reasonably accurate. The distance between the domain of factor levels used in establishing the model and the value of voltage at the extrapolation point is as wide as the domain itself. To be exact, the voltages in the test for model are 350 V and 400 V, the distance between them is thus 50 V, and 450 V is again 50 V beyond that domain.

Two points at higher voltages were used to demonstrate the accuracy of the extrapolation. The ageing tests had been conducted; hence the real model of the evolution was known for that combination of factors' levels. The results are shown in figure 22 and 23, the models obtained with 8-point plan are significantly closer to the model fitted to data.

Result of application of the model to another test at a lower temperature is shown in Figure 4-42. The full plan gives worse results than the fractional plan. Moving away by 20 °C beyond the factor domain already worsens the result of the extrapolation.

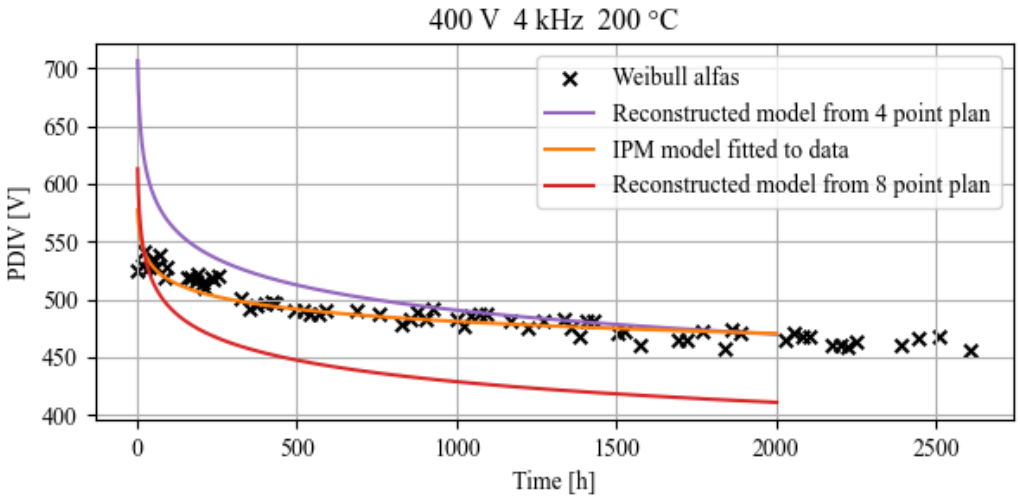

Figure 4-42 Model extrapolation to point at 200 °C. Comparison of fractional and full experimental plan. Introduction of additional points negatively impacted the extrapolative ability.

4.8 Conclusions

The obtained data show some promise as to PDIV's utility as an ageing indicator. In most cases the trend of the evolution in time is monotonous. The inverse power model was identified as the one that best describes the evolution of PDIV. The method of PDIV measurement is not a standard one. Usually, the PDIV is measured with an AC voltage not a square-wave form. The new method turned out to be sufficiently robust.

The standard way to apply DoE would be to use lifetimes instead of degradation model parameters. It is not possible because at the instant when a PDIV of a sample goes under the level of voltage stress, the main ageing factor changes. The two failure mechanisms act at the same time and there is no way to separate those impacts.

The objective of the modelling of the PDIV evolution is to predict time till the end of life of real-life electrical machine. In this chapter methods to measure the PDIV, to model its evolution and then to extrapolate the shape of that evolution into other values were presented. All that in an effort to gain knowledge on how the PDIV describes degradation of insulation. An interesting fact was found that evolution can be described with inverse power equation. In theory we could extrapolate the PDIV curve to lower values of factors, such as they are for a machine in its nominal operation. That curve again extrapolated would give us a moment in time when the PDIV falls below the operational voltage. But that is often not the case that the end of life arrives when the PDIV arrives at values so low. There are other mechanisms of failure. The work to follow up this research could be to try to find maybe a threshold, maybe a percentage of loss of PDIV that would mean imminent failure of the insulation. But that is beyond me for now.

What is more, this study made use of twisted pair of round enameled wire, which is the most basic of samples. In order to gain more holistic results, one needs to perform tests on different kinds of samples, such as motorettes or complete stators.

Conclusions and Perspectives

In the initial periods of the PhD thesis, during the bibliographic research, the problematic of cycling was introduced as an ageing factor. The discovered state of knowledge in the domain of cycling of different ageing factors showed that it is a field not well explored, which, to some extent, is remedied by the work done during the thesis.

The research in the direction of thermal cycling brought actual benefits into the work done on testing of the stator insulation. Methodology developed for quantifying impact of thermal cycling with simultaneous impact of accelerated thermal ageing helps the decision-making process. In the scope of the PhD thesis two stators were subjected to accelerated ageing with thermal cycling. It was done in order to establish whether the heating mode is a factor influencing the degradation of the insulation. Two different modes of heating were applied, passive and active, where in the passive one the stator is heated by an oven and in the active mode the heat is created by the current running through the stator's windings. The heating current was an AC one, it would be pertinent for the sake of completeness to perform the same ageing with DC heating. Also, in perspective, the experience could be repeated with a greater number of stators or with another type of sample, like the back-to-back sample. The active heating test was performed with the stator encapsulated in an oven to keep the heat in, in another research axis, we could imagine tests where the stator is in an ambient temperature or even is ventilated. This kind of test would be even closer to the real application.

The research on thermal cycling is one thing, the results of cycling on stators and twisted pairs show that it is pertinent to continue work in this direction, to develop better tests and methodologies. On the other hand, in the domain of cycling of other factors a vacuum remains. The voltage and frequency cycling done does not show significance of the cycling factor in the form that it was introduced during this PhD thesis. However, it is not conclusive on the question whether an impact exists, especially for electrical insulation in automotive, where the cyclic aspect of the ageing stresses is quite apparent. First steps were made in this direction, it would be a perspective opened by this thesis to continue research in this domain, with different factors, cycling amplitudes and profiles, for different samples.

Large amounts of data of PDIV evolution in multi-factor ageing of twisted-pair samples were gathered. The work done on degradation monitoring demonstrates the adequacy of the PDIV measurement method and shows promise as to usefulness of PDIV as an ageing indicator. The measurement method that observes the spectrum of the transitional current from an inverter is something that could be automatised. The question of exact nature of the spectral changes over PDIV are an interesting research topic in itself.

A lot of effort and time was dedicated to measurements of twisted pair samples. At the beginning of the thesis, we started the experiments with twisted pairs. The reason for that

is that the experimental infrastructure dedicated for them was already available at the lab. Even though, there was an intention to shift to rectangular enamelled wire, we never transitioned into it. For one, as the amount of ageing data for twisted pair grew, it was becoming less practical to start from scratch. More importantly, the existing infrastructure was not easily adaptable to the different kind of sample. The back-to-back samples were bigger in size and its enamel sturdier. Measurements of the PDIV for the new samples were much less obvious that for the twisted pairs. For one the PDIV was higher, closer to the voltage limits of the test bench. The observed spectrum never showed the shift observed when measuring the PDIV of the twisted pairs. The conclusion is that if we wanted to research a new kind of wire, we should have started developing the dedicated infrastructure from the beginning.

Bibliography

[1] ‘Commercial materials of Nidec PSA Emotors, https://emotors.com/products’. 2023.
[2] ‘IEC 60034-18-41:2014 Rotating electrical machines - Part 18-41 : Partial discharge free electrical insulation systems (Type I) used in rotating electrical machines fed from voltage converters - Qualification and quality control tests’. 2014.
[3] G. Singh, M. Matuonto, J. Amos, and K. Sundaram, ‘System of Systems Strand Tilt Analysis Perspective on MediuMHigh Voltage Stator Bar and a Non-Destructive Testing Case Study’, in *2019 IEEE International Systems Conference (SysCon)*, Orlando, FL, USA: IEEE, Apr. 2019, pp. 1–8. doi: 10.1109/SYSCON.2019.8836934.
[4] M. D. Bradfield, ‘manufacturing method of inserting hairpin conductors in a core having deformable tooth tips’, EP1463184A2, Sep. 29, 2004
[5] ‘https://www.elektrisola.com/fr/Products/Enamelled-Wire/Types’. 2022.
[6] Essex Furukawa, ‘How Thermal Classes are Derived - NEMA Magnet Wire Thermal Class Ratings and Corresponding Film Insulation Applications Explained’, *2022*.
[7] M. Chapman, N. Frost, and R. Bruetsch, ‘Insulation Systems for Rotating Low-Voltage Machines’, in *Conference Record of the 2008 IEEE International Symposium on Electrical Insulation*, Jun. 2008, pp. 257–260. doi: 10.1109/ELINSL.2008.4570323.
[8] X. Chen, J. Wang, A. Griffo, and A. Spagnolo, ‘Thermal Modeling of Hollow Conductors for Direct Cooling of Electrical Machines’, *IEEE Trans. Ind. Electron.*, vol. 67, no. 2, pp. 895–905, Feb. 2020, doi: 10.1109/TIE.2019.2899542.
[9] ‘IEC 60505:2011 Evaluation and qualification of electrical insulation systems’. 2011.
[10] R. Acheen, C. Abadie, T. Lebey, T. Billard, and S. Duchesne, ‘Comparison of the Electrical Ageing Under Sinusoidal and Square-Wave Stresses’, in *2018 IEEE Electrical Insulation Conference (EIC)*, Jun. 2018, pp. 353–356. doi: 10.1109/EIC.2018.8481024.
[11] P. Wang, A. Cavallini, and G. C. Montanari, ‘Endurance testing of rotating machines insulation systems: Do sinusoidal and square voltage waveforms provide comparable results?’, in *2013 IEEE International Conference on Solid Dielectrics (ICSD)*, Jun. 2013, pp. 310–313. doi: 10.1109/ICSD.2013.6619823.
[12] E. Persson, ‘Transient effects in application of PWM inverters to induction motors’, in *Conference Record of 1991 Annual Pulp and Paper Industry Technical Conference*, Jun. 1991, pp. 228–233. doi: 10.1109/PAPCON.1991.239644.
[13] R. J. Kerkman, D. Leggate, and G. L. Skibinski, ‘Interaction of drive modulation and cable parameters on AC motor transients’, *IEEE Trans. Ind. Appl.*, vol. 33, no. 3, Art. no. 3, May 1997, doi: 10.1109/28.585863.
[14] T. Wakimoto, H. Kojima, and N. Hayakawa, ‘Fluctuation and change of partial discharge inception voltage under high humidity for rectangular wire motors’, in *2015 IEEE Conference on Electrical Insulation and Dielectric Phenomena (CEIDP)*, Oct. 2015, pp. 59–62. doi: 10.1109/CEIDP.2015.7351997.
[15] P. Wang, Y. Li, A. Cavallini, J. Zhang, E. Xiang, and K. Wang, ‘The Influence of Relative Humidity on Partial Discharge and Endurance Features under Short Repetitive Impulsive Voltages’, in *2018 IEEE Conference on Electrical Insulation and Dielectric Phenomena (CEIDP)*, Cancun: IEEE, Oct. 2018, pp. 506–509. doi: 10.1109/CEIDP.2018.8544905.
[16] ‘IEC 60085:2008 Electrical insulation - Thermal evaluation and designation’. 2008.
[17] ‘IEC 60216-1:2013 Electrical insulating materials - Thermal endurance properties - Part 1: Ageing procedures and evaluation of test results’. 2013.
[18] ‘IEC 60172:2021 Test procedure for the determination of the temperature index of enamelled and tape wrapped winding wires’. 2021.
[19] ‘IEC 61857-1:2008 Electrical insulation systems - Procedures for thermal evaluation - Part 1: General requirements - Low-voltage’. 2008.

[20] ‘IEC 60034-18-31:2012 Rotating electrical machines - Part 18-31: Functional evaluation of insulation systems - Test procedures for form-wound windings Thermal evaluation and classification of insulation systems used in rotating machines’. 2012.
[21] G. C. Stone, Ed., *Electrical insulation for rotating machines: design, evaluation, aging, testing, and repair*. in IEEE Press series on power engineering. Piscataway, NJ : Hoboken, NJ: IEEE ; Wiley-Interscience, 2004.
[22] Z. Huang, ‘Modeling and Testing of Insulation Degradation due to Dynamic Thermal Loading of Electrical Machines’, 2017.
[23] P. Mancinelli, S. Stagnitta, and A. Cavallini, ‘Lifetime analysis of an automotive electrical motor with hairpin wound stator’, in *2016 IEEE Conference on Electrical Insulation and Dielectric Phenomena (CEIDP)*, Oct. 2016, pp. 877–880. doi: 10.1109/CEIDP.2016.7785538.
[24] P. Mancinelli, S. Stagnitta, and A. Cavallini, ‘Qualification of Hairpin Motors Insulation for Automotive Applications’, *IEEE Trans. Ind. Appl.*, vol. 53, no. 3, Art. no. 3, May 2017, doi: 10.1109/TIA.2016.2619670.
[25] J. Chen and L. Ruan, ‘Comparative study on thermo-mechanical insulation aging of evaporative cooled and air cooled stator bar’, in *2015 18th International Conference on Electrical Machines and Systems (ICEMS)*, Pattaya, Thailand: IEEE, Oct. 2015, pp. 1234–1240. doi: 10.1109/ICEMS.2015.7385228.
[26] ‘IEC 60034-18-21:3013 Rotating electrical machines - Part 18-21 : functional evaluation of insulation systems - Test procedures for wire-wound windings - Thermal evaluation and classification’. 2013.
[27] W. Chen and G. Gao, ‘Using multi-stress aging test to evaluate and improve medium-voltage stator insulation for adjustable speed drive applications’, in *2011 Record of Conference Papers Industry Applications Society 58th Annual IEEE Petroleum and Chemical Industry Conference (PCIC)*, Toronto, ON, Canada: IEEE, Sep. 2011, pp. 1–7. doi: 10.1109/PCICon.2011.6085877.
[28] H. Provencher, C. Hudon, and E. David, ‘Thermal and thermo-mechanical aging of epoxy-mica insulated stator bars’, in *2013 IEEE Electrical Insulation Conference (EIC)*, Jun. 2013, pp. 248–252. doi: 10.1109/EIC.2013.6554243.
[29] M. Farahani, H. Borsi, E. Gockenbach, and M. Kaufhold, ‘Investigations on characteristic parameters to evaluate the condition of the insulation system for high voltage rotating machines’, in *Conference Record of the 2004 IEEE International Symposium on Electrical Insulation*, Sep. 2004, pp. 4–7. doi: 10.1109/ELINSL.2004.1380418.
[30] M. Farahani, E. Gockenbach, H. Borsi, K. Schäfer, and M. Kaufhold, ‘Behavior of machine insulation systems subjected to accelerated thermal aging test’, *IEEE Trans. Dielectr. Electr. Insul.*, vol. 17, no. 5, Art. no. 5, Oct. 2010, doi: 10.1109/TDEI.2010.5595537.
[31] B. Jokanović, M. Bebić, and N. Kartalović, ‘The influence of combined strain and constructive solutions for stator insulation of rotating electrical machines on duration of their reliable exploitation’, *Int. J. Electr. Power Energy Syst.*, vol. 110, pp. 36–47, Sep. 2019, doi: 10.1016/j.ijepes.2019.02.041.
[32] V. N. Höpner and V. E. Wilhelm, ‘Insulation Life Span of Low-Voltage Electric Motors—A Survey’, *Energies*, vol. 14, no. 6, Art. no. 6, Jan. 2021, doi: 10.3390/en14061738.
[33] T. W. Dakin, ‘Electrical Insulation Deterioration Treated as a Chemical Rate Phenomenon’, *Trans. Am. Inst. Electr. Eng.*, vol. 67, no. 1, Art. no. 1, Jan. 1948, doi: 10.1109/T-AIEE.1948.5059649.

[34] C. Rusu-Zagar *et al.*, 'Method for estimating the lifetime of electric motors insulation', in *2013 8TH INTERNATIONAL SYMPOSIUM ON ADVANCED TOPICS IN ELECTRICAL ENGINEERING (ATEE)*, May 2013, pp. 1–6. doi: 10.1109/ATEE.2013.6563466.
[35] 'IEC 60034-18-42:2017 Rotating electrical machines - Part 18-42 : partial discharge resistant electrical insulation systems (Type II) used in rotating electrical machines fed from voltage converters - Qualification tests'. 2017.
[36] V. I. J. Kokko, 'Ageing due to thermal cycling by start and stop cycles in lifetime estimation of hydroelectric generator stator windings', in *2011 IEEE International Electric Machines & Drives Conference (IEMDC)*, Niagara Falls, ON, Canada: IEEE, May 2011, pp. 318–323. doi: 10.1109/IEMDC.2011.5994867.
[37] A. C. Gjaerde, 'Multi Factor Ageing Models - Origin and Similarities', p. 6, 1997.
[38] G. C. Montanari and L. Simoni, 'Aging phenomenology and modeling', *IEEE Trans. Electr. Insul.*, vol. 28, no. 5, Art. no. 5, Oct. 1993, doi: 10.1109/14.237740.
[39] G. Mazzanti, G. C. Montanari, L. Simoni, and M. B. Srinivas, 'Combined electro-thermo-mechanical model for life prediction of electrical insulating materials', in *Proceedings of 1995 Conference on Electrical Insulation and Dielectric Phenomena*, Oct. 1995, pp. 274–277. doi: 10.1109/CEIDP.1995.483716.
[40] M. B. Srinivas and T. S. Ramu, 'Multifactor aging of HV generator stator insulation including mechanical vibrations', *IEEE Trans. Electr. Insul.*, vol. 27, no. 5, Art. no. 5, Oct. 1992, doi: 10.1109/14.256476.
[41] T. S. Ramu, 'Degradation of HV generator insulation under mechanical, electrical and thermal stresses', in *IEEE International Symposium on Electrical Insulation*, Jun. 1990, pp. 21–24. doi: 10.1109/ELINSL.1990.109699.
[42] J.-P. Crine, C. Dang, and J.-L. Parpal, 'Electrical aging of extruded dielectric cables: a physical model', in *Conference Record of the 1996 IEEE International Symposium on Electrical Insulation*, Jun. 1996, pp. 646–649 vol.2. doi: 10.1109/ELINSL.1996.549428.
[43] C. Kaijiang, W. Guangning, Z. Liren, G. Xiaoxia, L. Kegang, and G. Bo, 'Insulation life-span models for electrical and thermal aging under continuous high square impulses voltage', in *2009 IEEE 9th International Conference on the Properties and Applications of Dielectric Materials*, Jul. 2009, pp. 285–288. doi: 10.1109/ICPADM.2009.5252428.
[44] M. Szczepanski, 'Development of methods allowing the test and the comparison of low-voltage motors insulation systems running under partial discharges (fed by inverter)', 2019.
[45] F. Selmeh, 'Méthodes de modélisation statistique de la durée de vie des composants en génie électrique', 2016.
[46] V. Divljakovic, J. Kline, J. Akers, and K. Theis, 'Multifactor aging of electrical machines energized by standard PWM drives', in *Proceedings of Conference on Electrical Insulation and Dielectric Phenomena - CEIDP '96*, Millbrae, CA, USA: IEEE, 1996, pp. 808–812. doi: 10.1109/CEIDP.1996.564631.
[47] N. Lahoud, J. Faucher, D. Malec, and P. Maussion, 'Electrical Aging of the Insulation of Low-Voltage Machines: Model Definition and Test With the Design of Experiments', *IEEE Trans. Ind. Electron.*, vol. 60, no. 9, Art. no. 9, Sep. 2013, doi: 10.1109/TIE.2013.2245615.
[48] N. Lahoud, M. Q. Nguyen, P. Maussion, D. Malec, and D. Mary, 'Lifetime model of the inverter-fed motors secondary insulation by using a design of experiments', *IEEE Trans. Dielectr. Electr. Insul.*, vol. 22, no. 6, pp. 3170–3176, Dec. 2015, doi: 10.1109/TDEI.2015.005202.

[49] T. G. Arora and M. V. Aware, ‘Life Model for PWM Controlled Induction Motor Insulation using Design of Experiments Method’, *Electr. Power Compon. Syst.*, vol. 47, no. 1–2, pp. 153–163, Jan. 2019, doi: 10.1080/15325008.2019.1566843.
[50] M. Szczepanski, D. Malec, P. Maussion, B. Petitgas, and P. Manfé, ‘Use of Design of Experiments (DoE) predictive models as a method of comparison of enameled wires used in low voltage inverter-fed motors’, in *2018 IEEE Industry Applications Society Annual Meeting (IAS)*, Sep. 2018, pp. 1–8. doi: 10.1109/IAS.2018.8544548.
[51] M. Szczepanski, D. Malec, P. Maussion, B. Petitgas, and P. Manfé, ‘Design of Experiments (DoE) predictive models as a tool for lifespan prediction and comparison for enameled wires used in low voltage inverter-fed motors’, *IEEE Trans. Ind. Appl.*, pp. 1–1, 2020, doi: 10.1109/TIA.2020.2970855.
[52] T. Liu, Q. Li, G. Dong, M. Asif, X. Huang, and Z. Wang, ‘Multi-factor model for lifetime prediction of polymers used as insulation material in high frequency electrical equipment’, *Polym. Test.*, vol. 73, pp. 193–199, Feb. 2019, doi: 10.1016/j.polymertesting.2018.11.006.
[53] P. Maussion, A. Picot, M. Chabert, and D. Malec, ‘Lifespan and aging modeling methods for insulation systems in electrical machines: A survey’, in *2015 IEEE Workshop on Electrical Machines Design, Control and Diagnosis (WEMDCD)*, Mar. 2015, pp. 279–288. doi: 10.1109/WEMDCD.2015.7194541.
[54] G. Jones, N. Frost, and A. Mosier, ‘Introduction to Predictive Models for Motor Dielectric Aging’, in *2022 IEEE Electrical Insulation Conference (EIC)*, Jun. 2022, pp. 276–279. doi: 10.1109/EIC51169.2022.9833207.
[55] N. Hayakawa, H. Inano, Y. Nakamura, and H. Okubo, ‘Time variation of partial discharge activity leading to breakdown of magnet wire under repetitive surge voltage application’, *IEEE Trans. Dielectr. Electr. Insul.*, vol. 15, no. 6, pp. 1701–1706, Dec. 2008, doi: 10.1109/TDEI.2008.4712674.
[56] P. Wang and A. Cavallini, ‘The influence of repetitive square wave voltage parameters on PD statistical features’, in *2013 Annual Report Conference on Electrical Insulation and Dielectric Phenomena*, Oct. 2013, pp. 1282–1285. doi: 10.1109/CEIDP.2013.6748195.
[57] P. Wang, A. Cavallini, and G. C. Montanari, ‘The influence of impulsive voltage frequency on PD features in turn insulation of inverter-fed motors’, in *2014 IEEE Conference on Electrical Insulation and Dielectric Phenomena (CEIDP)*, Des Moines, IA, USA: IEEE, Oct. 2014, pp. 35–38. doi: 10.1109/CEIDP.2014.6995876.
[58] P. Wang, A. Cavallini, and G. C. Montanari, ‘The effects of square wave voltage rise time on PD statistics in time and frequency domain’, in *2015 IEEE Electrical Insulation Conference (EIC)*, Jun. 2015, pp. 262–265. doi: 10.1109/ICACACT.2014.7223552.
[59] Peng Wang, Hongying Xu, Jian Wang, A. Cavallini, and G. C. Montanari, ‘The effects of asymmetry repetitive square wave voltages on PD statistics and endurance’, in *2016 IEEE International Conference on Dielectrics (ICD)*, Jul. 2016, pp. 693–696. doi: 10.1109/ICD.2016.7547710.
[60] V. Nguyen, J. Seshadrinath, D. Wang, S. Nadarajan, and V. Vaiyapuri, ‘Model-Based Diagnosis and RUL Estimation of Induction Machines Under Interturn Fault’, *IEEE Trans. Ind. Appl.*, vol. 53, no. 3, Art. no. 3, May 2017, doi: 10.1109/TIA.2017.2669195.
[61] W. R. Jensen, E. G. Strangas, and S. N. Foster, ‘Online estimation of remaining useful life of stator insulation’, in *2017 IEEE 11th International Symposium on Diagnostics for Electrical Machines, Power Electronics and Drives (SDEMPED)*, Aug. 2017, pp. 635–641. doi: 10.1109/DEMPED.2017.8062421.
[62] W. R. Jensen, E. G. Strangas, and S. N. Foster, ‘A More Robust Stator Insulation Failure Prognosis for Inverter-Driven Machines’, in *2019 IEEE International Electric Machines*

& Drives Conference (IEMDC), San Diego, CA, USA: IEEE, May 2019, pp. 203–209. doi: 10.1109/IEMDC.2019.8785359.
[63] M. A. Vogelsberger, C. Zoeller, T. M. Wolbank, and H. Ertl, 'Insulation Health State Monitoring of Traction Machines Based on Online Switching Transient Exploitation', in *PCIM Europe 2017; International Exhibition and Conference for Power Electronics, Intelligent Motion, Renewable Energy and Energy Management*, May 2017, pp. 1–6.
[64] C. Zoeller, M. Vogelsberger, M. Bazant, H. Ertl, and T. M. Wolbank, 'Diagnostic Technique for Traction Motor Insulation Condition Monitoring by Transient Signal Assessment', in *PCIM Europe 2018; International Exhibition and Conference for Power Electronics, Intelligent Motion, Renewable Energy and Energy Management*, Jun. 2018, pp. 1–8.
[65] 'IEEE Recommended Practice for Thermal Cycle Testing of Form-Wound Stator Bars and Coils for Large Rotating Machines', *IEEE Std 1310-2012 Revis. IEEE Std 1310-1996*, pp. 1–30, May 2012, doi: 10.1109/IEEESTD.2012.6204190.
[66] Z. Huang, 'Modeling and Testing of Insulation Degradation due to Dynamic Thermal Loading of Electrical Machines', 2017.
[67] A. Khazanov, A. Gegenava, and B. Nindra, 'Practical Experience with Thermal Cycling per IEEE 1310–2012. Alternative Approach to Monitor Copper Temperature and to Efficient Cooling Air Flow', in *2018 IEEE Electrical Insulation Conference (EIC)*, Jun. 2018, pp. 465–468. doi: 10.1109/EIC.2018.8481023.
[68] M. J. da Silva *et al.*, 'Facts and Artifacts from IEEE 1310-2012', in *2018 IEEE Electrical Insulation Conference (EIC)*, San Antonio, TX: IEEE, Jun. 2018, pp. 170–174. doi: 10.1109/EIC.2018.8481073.
[69] M. Istad, M. Runde, and A. Nysveen, 'A Review of Results From Thermal Cycling Tests of Hydrogenerator Stator Windings', *IEEE Trans. Energy Convers.*, vol. 26, no. 3, pp. 890–903, Sep. 2011, doi: 10.1109/TEC.2011.2127479.
[70] T. Brügger, 'A new test method for assessing the impact of thermal cycling on hydrogenerator stator insulation', in *2010 Annual Report Conference on Electrical Insulation and Dielectic Phenomena*, West Lafayette, IN: IEEE, Oct. 2010, pp. 1–4. doi: 10.1109/CEIDP.2010.5724097.
[71] A. Ruf, J. Paustenbach, D. Franck, and K. Hameyer, 'A methodology to identify electrical ageing of winding insulation systems', in *2017 IEEE International Electric Machines and Drives Conference (IEMDC)*, May 2017, pp. 1–7. doi: 10.1109/IEMDC.2017.8002305.
[72] G. C. Montanari, A. Cavallini, F. Ciani, and A. Contin, 'Accelerated aging, partial discharges and breakdown of Type II turn-to-turn insulation system of rotating machines', in *2016 IEEE Electrical Insulation Conference (EIC)*, Jun. 2016, pp. 190–193. doi: 10.1109/EIC.2016.7548692.
[73] A. Rumi and A. Cavallini, 'The Influence of Short-Width SiC Pulses on the Partial Discharge Inception Voltage of Turn-Turn Insulation', in *2022 IEEE Conference on Electrical Insulation and Dielectric Phenomena (CEIDP)*, Oct. 2022, pp. 447–450. doi: 10.1109/CEIDP55452.2022.9985315.
[74] A. Rumi, L. Lusuardi, A. Cavallini, M. Pastura, D. Barater, and S. Nuzzo, 'Partial Discharges in Electrical Machines for the More Electrical Aircraft. Part III: Preventing Partial Discharges', *IEEE Access*, vol. 9, pp. 30113–30123, 2021, doi: 10.1109/ACCESS.2021.3058090.
[75] A. Cimino, F. Jenau, and C. Staubach, 'Causes of cyclic mechanical aging and its detection in stator winding insulation systems', *IEEE Electr. Insul. Mag.*, vol. 35, no. 3, Art. no. 3, May 2019, doi: 10.1109/MEI.2019.8689434.

[76] H. Mitsui, K. Yoshida, Y. Inoue, and K. Kawahara, ‘Mechanical Degradation of High Voltage Rotating Machine Insulation’, *IEEE Trans. Electr. Insul.*, vol. EI-16, no. 4, Art. no. 4, Aug. 1981, doi: 10.1109/TEI.1981.298369.
[77] R. Soltani, L. Lafortune, R. Draper, and A. Khosravi, ‘Qualification test results on stator bars of large hydro generators’, in *2012 IEEE International Symposium on Electrical Insulation*, Jun. 2012, pp. 596–600. doi: 10.1109/ELINSL.2012.6251540.
[78] G. C. Stone, B. K. Gupta, J. F. Lyles, and H. G. Sedding, ‘Experience with accelerated aging tests on stator bars and coils’, in *IEEE International Symposium on Electrical Insulation*, Jun. 1990, pp. 356–360. doi: 10.1109/ELINSL.1990.109772.
[79] A. Anton, ‘New developments in resin rich insulating systems for high voltage rotating machines’, in *Proceedings: Electrical Insulation Conference and Electrical Manufacturing and Coil Winding Conference*, Sep. 1997, pp. 607–618. doi: 10.1109/EEIC.1997.651263.
[80] R. Bartnikas and R. Morin, ‘Multi-Stress Aging of Stator Bars With Electrical, Thermal, and Mechanical Stresses as Simultaneous Acceleration Factors’, *IEEE Trans. Energy Convers.*, vol. 19, no. 4, pp. 702–714, Dec. 2004, doi: 10.1109/TEC.2004.832060.
[81] Yue Bo, Li Jian, Cheng Yonghong, and Hengkun Xie, ‘Study on the multi-stress aging of stator insulation based on fingerprint parameters’, in *Proceedings of 2001 International Symposium on Electrical Insulating Materials (ISEIM 2001). 2001 Asian Conference on Electrical Insulating Diagnosis (ACEID 2001). 33rd Symposium on Electrical and Ele*, Nov. 2001, pp. 729–732. doi: 10.1109/ISEIM.2001.973781.
[82] Yue Bo, Chen Xiaolin, Sun Xiang, and Hengkun Xie, ‘Study on the aging condition of stator bar based on Ultra-wideband PD detection technique’, in *Proceedings of the 7th International Conference on Properties and Applications of Dielectric Materials (Cat. No.03CH37417)*, Jun. 2003, pp. 220–223 vol.1. doi: 10.1109/ICPADM.2003.1218392.
[83] J. M. Braun, G. C. Stone, and H. G. Sedding, ‘Application of dynamic mechanical analysis to endurance testing of generator stator bars’, in *Conference Record of the 1992 IEEE International Symposium on Electrical Insulation*, Jun. 1992, pp. 469–472. doi: 10.1109/ELINSL.1992.246956.
[84] Y. Cao, L. Wang, H. Zhu, J. Wu, and Y. Yin, ‘Research of Generator Stator Bar Insulation Detection based on Isothermal Relaxation Current Method’, in *2013 Annual Report Conference on Electrical Insulation and Dielectric Phenomena*, Oct. 2013, pp. 1058–1061. doi: 10.1109/CEIDP.2013.6748110.
[85] S. Hirabayashi, K. Shibayama, S. Matsuda, and S. Ito, ‘Development of new mica paper epoxy insulation systems for high voltage rotating machines’, in *1973 EIC 11th Electrical Insulation Conference*, Sep. 1973, pp. 90–91. doi: 10.1109/EIC.1973.7468651.
[86] Song Jiancheng, Yue Bo, and Xie Hengkun, ‘Aging diagnosis of large generator stator winding insulation based on digital discharge detection’, in *Proceedings of the 6th International Conference on Properties and Applications of Dielectric Materials (Cat. No.00CH36347)*, Jun. 2000, pp. 765–769 vol.2. doi: 10.1109/ICPADM.2000.876342.
[87] Song Jiancheng, Yue Bo, and Xie Hengkun, ‘New estimating techniques for multi-stress aging test of large generator stator winding insulation’, in *Proceedings of the 6th International Conference on Properties and Applications of Dielectric Materials (Cat. No.00CH36347)*, Jun. 2000, pp. 951–956 vol.2. doi: 10.1109/ICPADM.2000.876388.
[88] Song Jiancheng, Cheng Yonghong, Xie Hengkun, Hao Junfang, and Li Haiying, ‘Aging diagnosis of large generator stator winding insulation based on AC dielectric characteristic parameters’, in *Proceedings of 2001 International Symposium on Electrical Insulating Materials (ISEIM 2001). 2001 Asian Conference on Electrical*

Insulating Diagnosis (ACEID 2001). 33rd Symposium on Electrical and Ele, Nov. 2001, pp. 709–712. doi: 10.1109/ISEIM.2001.973776.
[89] W. Ladstätter, G. Lemesch, and R. Mlecnik, 'Limits of off-line PD measurement to assess quality and condition of HV insulation windings for rotating machines', in *2017 INSUCON - 13th International Electrical Insulation Conference (INSUCON)*, May 2017, pp. 1–6. doi: 10.23919/INSUCON.2017.8097189.
[90] Y.-S. Lee, J. K. Nelson, H. A. Scarton, D. Teng, and S. Azizi-Ghannad, 'An acoustic diagnostic technique for use with electric machine insulation', *IEEE Trans. Dielectr. Electr. Insul.*, vol. 1, no. 6, Art. no. 6, Dec. 1994, doi: 10.1109/94.368645.
[91] H. Mitsui, K. Yoshida, Y. Inoue, and S. Kenjo, 'Thermal Cyclic Degradation of Coil Insulation for Rotating Machines', *IEEE Trans. Power Appar. Syst.*, vol. PAS-102, no. 1, Art. no. 1, Jan. 1983, doi: 10.1109/TPAS.1983.317999.
[92] A. Nakayama, 'Evaluation of mechanical characteristics for a new vacuum pressure impregnation insulation system', in *Proceedings of 1995 International Symposium on Electrical Insulating Materials*, Sep. 1995, pp. 503–506. doi: 10.1109/ISEIM.1995.496619.
[93] H. Provencher, C. Hudon, and E. David, 'Thermal and thermo-mechanical aging of epoxy-mica insulated stator bars', in *2011 Electrical Insulation Conference (EIC).*, Jun. 2011, pp. 483–487. doi: 10.1109/EIC.2011.5996203.
[94] G. C. Stone, H. G. Sedding, B. A. Lloyd, and B. K. Gupta, 'The ability of diagnostic tests to estimate the remaining life of stator insulation', *IEEE Trans. Energy Convers.*, vol. 3, no. 4, pp. 833–841, Dec. 1988, doi: 10.1109/60.9359.
[95] G. C. Stone, J. F. Lyles, J. M. Braun, and C. L. Kaul, 'A thermal cycling type test for generator stator winding insulation', *IEEE Trans. Energy Convers.*, vol. 6, no. 4, Art. no. 4, Dec. 1991, doi: 10.1109/60.103645.
[96] M. Tari, L. Yoshida, S. Sekito, R. Brutsch, J. Allison, and A. Lutz, 'HTC insulation technology drives rapid progress of indirect-cooled turbo generator unit capacity', in *2001 Power Engineering Society Summer Meeting. Conference Proceedings (Cat. No.01CH37262)*, Jul. 2001, pp. 1427–1432 vol.3. doi: 10.1109/PESS.2001.970285.
[97] R. Morin and R. Bartnikas, 'Multistress Aging of Stator Bars in a Three-Phase Model Stator Under Load Cycling Conditions', *IEEE Trans. Energy Convers.*, vol. 27, no. 2, Art. no. 2, Jun. 2012, doi: 10.1109/TEC.2012.2187902.
[98] H. Akahori, Y. Inoue, T. Yamada, H. Mitsui, and H. Yoshida, 'Considerations on aging tests of the class H post impregnated insulation system for rotating machines', in *1984 IEEE International Conference on Eletrical Insulation*, Jun. 1984, pp. 266–270. doi: 10.1109/EIC.1984.7465194.
[99] H. Zhu, C. Morton, and S. Cherukupalli, 'Quality evaluation of stator coils and bars under thermal cycling stress', in *Conference Record of the 2006 IEEE International Symposium on Electrical Insulation*, Jun. 2006, pp. 384–387. doi: 10.1109/ELINSL.2006.1665338.
[100] H. Zhu, D. Kung, M. Cowell, and S. Cherukupalli, 'Acoustic monitoring of stator winding delaminations during thermal cycling testing', *IEEE Trans. Dielectr. Electr. Insul.*, vol. 17, no. 5, Art. no. 5, Oct. 2010, doi: 10.1109/TDEI.2010.5595542.
[101] J. C. G. Wheeler and M. L. Lissenburg, 'The effect of ageing on the thermal conductivity of stator coil overhangs in medium generators', in *1988 Fifth International Conference on Dielectric Materials, Measurements and Applications*, Jun. 1988, pp. 375–378.
[102] J. Williams, B. McDermid, T. Reid, and M. Nikrandt, 'A comparison of the electrical performance of various turn and strand insulation systems before and after rapid thermal

cycling', in *2014 IEEE Electrical Insulation Conference (EIC)*, Jun. 2014, pp. 407–411. doi: 10.1109/EIC.2014.6869419.
[103] I. Kremza, S. Bomben, T. Black, and A. Shaikh, 'Qualification test results on multi-turn coils of large hydrogenerators', in *2014 IEEE Electrical Insulation Conference (EIC)*, Jun. 2014, pp. 434–439. doi: 10.1109/EIC.2014.6869425.
[104] S. Ul Haq, R. Omranipour, G. Hanna, W. Lucas, and M. Znidarich, 'Flexible medium voltage stator coil insulation system for on-site winding', in *2012 IEEE International Symposium on Electrical Insulation*, Jun. 2012, pp. 291–295. doi: 10.1109/ELINSL.2012.6251475.
[105] S. U. Haq and R. Omranipour, 'Accelerated life testing of high voltage stator coils with enhanced PET-mica insulation system', in *2011 Electrical Insulation Conference (EIC).*, Jun. 2011, pp. 479–482. doi: 10.1109/EIC.2011.5996202.
[106] V. Madonna, P. Giangrande, L. Lusuardi, A. Cavallini, and M. Galea, 'Impact of thermal overload on the insulation aging in short duty cycle motors for aerospace', in *2018 IEEE International Conference on Electrical Systems for Aircraft, Railway, Ship Propulsion and Road Vehicles & International Transportation Electrification Conference (ESARS-ITEC)*, Nottingham: IEEE, Nov. 2018, pp. 1–6. doi: 10.1109/ESARS-ITEC.2018.8607539.
[107] Z. Huang, A. Reinap, and M. Alaküla, 'Dielectric properties modeling and measurement of single tooth coil insulation system under accelerated degradation test', in *2016 XXII International Conference on Electrical Machines (ICEM)*, Sep. 2016, pp. 2698–2703. doi: 10.1109/ICELMACH.2016.7732903.
[108] B. K. Gupta, 'Effectiveness of thermo-mechanical stress in accelerated aging of turn insulation in motor coils', in *Conference Record of the 1992 IEEE International Symposium on Electrical Insulation*, Jun. 1992, vols vols 79–82. doi: 10.1109/ELINSL.1992.247047.
[109] B. K. Gupta, W. T. Fink, and R. M. Boggia, 'Use of thermal cycling as type test for turn insulation in motor coils', in *Proceedings of 1994 IEEE International Symposium on Electrical Insulation*, Jun. 1994, pp. 107–110. doi: 10.1109/ELINSL.1994.401456.
[110] M. R. M. Fernando, W. L. B. Naranpanawa, R. H. M. Rathnayake, and G. Jayantha, 'Condition assessment of stator insulation during drying, wetting and electrical ageing', *IEEE Trans. Dielectr. Electr. Insul.*, vol. 20, no. 6, Art. no. 6, Dec. 2013, doi: 10.1109/TDEI.2013.6678856.
[111] W. McDermid, 'Experience with thermal cycling of stator coils and bars', in *Conference Record of the 2006 IEEE International Symposium on Electrical Insulation*, Jun. 2006, pp. 344–345. doi: 10.1109/ELINSL.2006.1665328.
[112] W. McDermid, 'Experience with accelerated aging and related diagnostic tests for stator coils and bars of rotating machines', in *2014 ICHVE International Conference on High Voltage Engineering and Application*, Sep. 2014, pp. 1–5. doi: 10.1109/ICHVE.2014.7035383.
[113] L. Lusuardi, A. Cavallini, V. Madonna, P. Giangrande, and M. Galea, 'Unconventional accelerated thermal ageing test for traction electric motors in vehicles', in *2020 IEEE Electrical Insulation Conference (EIC)*, Jun. 2020, pp. 212–216. doi: 10.1109/EIC47619.2020.9158744.
[114] P. Giangrande, V. Madonna, and M. Galea, 'Reliability Oriented Design of Low Voltage Electrical Machines Based On Accelerated Thermal Aging Tests', in *2020 International Symposium on Power Electronics, Electrical Drives, Automation and Motion (SPEEDAM)*, Jun. 2020, pp. 448–453. doi: 10.1109/SPEEDAM48782.2020.9161974.

[115] C. Gerada, M. Galea, P. Giangrande, and C. Sciascera, ‘Lifetime Consumption and Degradation Analysis of the Winding Insulation of Electrical Machines’, in *8th IET International Conference on Power Electronics, Machines and Drives (PEMD 2016)*, Glasgow, UK: Institution of Engineering and Technology, 2016, p. 5 .-5 . doi: 10.1049/cp.2016.0231.

[116] V. Boucher, P. Rain, G. Teissedre, and P. Schlupp, ‘Mechanical and Dielectric Properties of Glass-Mica-Epoxy Composites along Accelerated Thermo-Oxidative Aging’, in *2007 IEEE International Conference on Solid Dielectrics*, Jul. 2007, pp. 162–165. doi: 10.1109/ICSD.2007.4290778.

[117] B. Gupta, I. Kremza, J. Williams, K. Alewine, and W. McDermid, ‘A proposed procedure for endurance testing of turn insulation in rotating machine coils’, in *2016 IEEE Electrical Insulation Conference (EIC)*, Jun. 2016, pp. 252–255. doi: 10.1109/EIC.2016.7548706.

[118] Young-Jun Lee and Young-Ho Ju, ‘An assessment of insulation condition for generator rotor windings’, in *2008 International Conference on Condition Monitoring and Diagnosis*, Apr. 2008, pp. 543–545. doi: 10.1109/CMD.2008.4580345.

[119] V. Peesapati *et al.*, ‘Impact of thermal cycling on high voltage coils used in marine generators using FEA methods’, in *2015 IEEE Electrical Insulation Conference (EIC)*, Jun. 2015, pp. 434–437. doi: 10.1109/ICACACT.2014.7223543.

[120] I. Preda, J. Figueroa, S. Noël, B. Soulieres, and E. David, ‘Thermal modeling of a stator bar - Influence of geometry and material properties’, in *2015 IEEE Electrical Insulation Conference (EIC)*, Jun. 2015, pp. 166–171. doi: 10.1109/ICACACT.2014.7223555.

[121] A. Griffo, I. Tsyokhla, and J. Wang, ‘Lifetime of Machines Undergoing Thermal Cycling Stress’, in *2019 IEEE Energy Conversion Congress and Exposition (ECCE)*, Baltimore, MD, USA: IEEE, Sep. 2019, pp. 3831–3836. doi: 10.1109/ECCE.2019.8913216.

[122] J. Richnow, P. Stenzel, A. Renner, D. Gerling, and C. Endisch, ‘Influence of different impregnation methods and resins on thermal behavior and lifetime of electrical stators’, in *2014 4th International Electric Drives Production Conference (EDPC)*, Sep. 2014, pp. 1–7. doi: 10.1109/EDPC.2014.6984406.

[123] K. Younsi *et al.*, ‘Online capacitance and dissipation factor monitoring of AC motor stator insulation’, in *2010 IEEE International Power Modulator and High Voltage Conference*, May 2010, pp. 530–533. doi: 10.1109/IPMHVC.2010.5958411.

[124] X. Liu, T. Zhang, Y. Bai, X. Ding, and Y. Wang, ‘Effects of accelerated repetitive impulse voltage aging on performance of model stator insulation of wind turbine generator’, *IEEE Trans. Dielectr. Electr. Insul.*, vol. 21, no. 4, Art. no. 4, Aug. 2014, doi: 10.1109/TDEI.2014.004363.

[125] M. J. da Silva *et al.*, ‘Evaluation of Roebel bars aged under service conditions in large hydrogenerators’, in *2015 IEEE Electrical Insulation Conference (EIC)*, Jun. 2015, pp. 479–482. doi: 10.1109/ICACACT.2014.7223617.

[126] M. Uno and K. Tanaka, ‘Accelerated ageing testing and cycle life prediction of supercapacitors for alternative battery applications’, in *2011 IEEE 33rd International Telecommunications Energy Conference (INTELEC)*, Amsterdam, Netherlands: IEEE, Oct. 2011, pp. 1–6. doi: 10.1109/INTLEC.2011.6099720.

[127] P. Giangrande, V. Madonna, S. Nuzzo, and M. Galea, ‘Moving Towards a Reliability-Oriented Design Approach of Low-Voltage Electrical Machines by Including Insulation Thermal Aging Considerations’, *IEEE Trans. Transp. Electrification*, pp. 1–1, 2020, doi: 10.1109/TTE.2020.2971191.

[128] D. Barater *et al.*, ‘Multistress Characterization of Fault Mechanisms in Aerospace Electric Actuators’, *IEEE Trans. Ind. Appl.*, vol. 53, no. 2, Art. no. 2, Mar. 2017, doi: 10.1109/TIA.2016.2633948.
[129] L. F. Coffin, ‘A Study of the Effects of Cyclic Thermal Stresses on a Ductile Metal’, *J. Fluids Eng.*, vol. 76, no. 6, pp. 931–949, Aug. 1954, doi: 10.1115/1.4015020.
[130] S. Manson, ‘Behavior of materials under conditions of thermal stress’, Jul. 1953. Accessed: May 10, 2023. [Online]. Available: https://www.semanticscholar.org/paper/Behavior-of-materials-under-conditions-of-thermal-Manson/25e2ebf0c1b5240d7687b6f497f7220ef6f3e03f
[131] K. C. Norris and A. H. Landzberg, ‘Reliability of Controlled Collapse Interconnections’, *IBM J. Res. Dev.*, vol. 13, no. 3, pp. 266–271, May 1969, doi: 10.1147/rd.133.0266.
[132] H. Cui, ‘Accelerated temperature cycle test and Coffin-Manson model for electronic packaging’, in *Annual Reliability and Maintainability Symposium, 2005. Proceedings.*, Jan. 2005, pp. 556–560. doi: 10.1109/RAMS.2005.1408421.
[133] M. A. Miner, ‘Cumulative Damage in Fatigue’, *J. Appl. Mech.*, vol. 12, no. 3, pp. A159–A164, Mar. 2021, doi: 10.1115/1.4009458.
[134] D. Huger and D. Gerling, ‘An advanced lifetime prediction method for permanent magnet synchronous machines’, in *2014 International Conference on Electrical Machines (ICEM)*, Sep. 2014, pp. 686–691. doi: 10.1109/ICELMACH.2014.6960255.
[135] G. Mazzanti, ‘Including the calculation of transient electric field in the life estimation of HVDC cables subjected to load cycles’, *IEEE Electr. Insul. Mag.*, vol. 34, no. 3, Art. no. 3, May 2018, doi: 10.1109/MEI.2018.8345358.
[136] ‘IEC 60216-2: Electrical insulating materials - Thermal endurance properties - Part 2: Determination of thermal endurance properties of electrical insulating materials Choice of test criteria’. 2005.
[137] IEC 60216-1, ‘Electrical insulating materials – Thermal endurance properties – Part 1: Ageing procedures and evaluation of test results’. 2013.
[138] L. GopiReddy, L. M. Tolbert, B. Ozpineci, and J. O. P. Pinto, ‘Rainflow Algorithm Based Lifetime Estimation of Power Semiconductors in Utility Applications’, p. 8.
[139] J. Leffler and P. Trnka, ‘Failures of Electrical Machines - Review’, in *2022 8th International Youth Conference on Energy (IYCE)*, Jul. 2022, pp. 1–4. doi: 10.1109/IYCE54153.2022.9857519.
[140] G. C. Stone and I. Culbert, ‘Prediction of stator winding remaining life from diagnostic measurements’, in *2010 IEEE International Symposium on Electrical Insulation*, San Diego, CA, USA: IEEE, Jun. 2010, pp. 1–4. doi: 10.1109/ELINSL.2010.5549791.
[141] ‘IEC 60851-5:2008 Winding wires Test methods Part 5: Electrical properties’, 2008.
[142] ‘IEC/IEEE Guide for the Statistical Analysis of Electrical Insulation Breakdown Data (Adoption of IEEE Std 930-2004)’, *IEC 62539 First Ed. 2007-07 IEEE 930*, pp. 1–53, 2007, doi: 10.1109/IEEESTD.2007.4288250.
[143] S. Barranco, ‘Development of test methods for multi-stress testing and lifetime modelling of insulated copper wires in electric motors used in future hybrid and all-electric automobiles’, 2019.
[144] Sang Bin Lee, Jinkyu Yang, K. Younsi, and R. M. Bharadwaj, ‘An online groundwall and phase-to-phase insulation quality assessment technique for AC-machine stator windings’, *IEEE Trans. Ind. Appl.*, vol. 42, no. 4, Art. no. 4, Jul. 2006, doi: 10.1109/TIA.2006.876077.

[145] P. Zhang, K. Younsi, and P. Neti, ‘A novel online stator ground-wall insulation monitoring scheme for inverter-fed AC motors’, in *2013 IEEE Energy Conversion Congress and Exposition*, Sep. 2013, pp. 3541–3547. doi: 10.1109/ECCE.2013.6647167.
[146] A. S. Babel and E. G. Strangas, ‘Condition-based monitoring and prognostic health management of electric machine stator winding insulation’, in *2014 International Conference on Electrical Machines (ICEM)*, Sep. 2014, pp. 1855–1861. doi: 10.1109/ICELMACH.2014.6960436.
[147] P. Nussbaumer, M. A. Vogelsberger, and T. M. Wolbank, ‘Exploitation of induction machine’s high-frequency behavior for online insulation monitoring’, in *2013 9th IEEE International Symposium on Diagnostics for Electric Machines, Power Electronics and Drives (SDEMPED)*, Aug. 2013, pp. 579–585. doi: 10.1109/DEMPED.2013.6645773.
[148] R. Acheen, C. Abadie, T. Lebey, and S. Duchesne, ‘Electrical stress mapping in a Type II machine supplied by inverters using Si and SiC-based components’, *IET Electr. Power Appl.*, vol. 14, no. 6, Art. no. 6, Jun. 2020, doi: 10.1049/iet-epa.2019.0345.
[149] ‘IEC 60034-27-4 Rotating electrical machines - Part 27-4: Measurement of insulation resistance and polarization index of winding insulation of rotating electrical machines’. 2018.
[150] V. Madonna, P. Giangrande, and M. Galea, ‘Evaluation of strand-to-strand capacitance and dissipation factor in thermally aged enamelled coils for low-voltage electrical machines’, *IET Sci. Meas. Technol.*, vol. 13, no. 8, Art. no. 8, 2019, doi: 10.1049/iet-smt.2019.0071.
[151] V. Madonna *et al.*, ‘Reliability vs. Performances of Electrical Machines: Partial Discharges Issue’, in *2019 IEEE Workshop on Electrical Machines Design, Control and Diagnosis (WEMDCD)*, Apr. 2019, pp. 77–82. doi: 10.1109/WEMDCD.2019.8887809.
[152] S. Dreuilhe, S. Pin, L. Fetouhi, S. Stemmer, G. Belijar, and L. Albert, ‘Ageing in aircraft electromechanical chain: design of thermal cycling bench for winding elements’, in *2021 IEEE Electrical Insulation Conference (EIC)*, Jun. 2021, pp. 42–46. doi: 10.1109/EIC49891.2021.9612334.
[153] ‘IEEE Guide for the Measurement of Partial Discharges in AC Electric Machinery’, IEEE, Dec. 2019. doi: 10.1109/IEEESTD.2014.6973042.
[154] G. C. Stone, M. K. W. Stranges, and D. G. Dunn, ‘Common Questions on Partial Discharge Testing: A Review of Recent Developments in IEEE and IEC Standards for Offline and Online Testing of Motor and Generator Stator Windings’, *IEEE Ind. Appl. Mag.*, vol. 22, no. 1, Art. no. 1, Jan. 2016, doi: 10.1109/MIAS.2015.2458337.
[155] A. Contin, A. Cavallini, G. C. Montanari, G. Pasini, and F. Puletti, ‘Digital detection and fuzzy classification of partial discharge signals’, *IEEE Trans. Dielectr. Electr. Insul.*, vol. 9, no. 3, Art. no. 3, Jun. 2002, doi: 10.1109/TDEI.2002.1007695.
[156] Barrios, Buldain, Comech, Gilbert, and Orue, ‘Partial Discharge Classification Using Deep Learning Methods—Survey of Recent Progress’, *Energies*, vol. 12, no. 13, Art. no. 13, Jun. 2019, doi: 10.3390/en12132485.
[157] P. Yuan *et al.*, ‘Deterioration of Stator Winding Insulation in Inverter-Fed Traction Motors’, in *2020 IEEE Electrical Insulation Conference (EIC)*, Jun. 2020, pp. 457–460. doi: 10.1109/EIC47619.2020.9158656.
[158] L. Briano, F. Gallesi, F. Guastavino, and E. Torello, ‘Variation Over Time of Partial Discharge Inception Voltage Due to Combined Electrical and Thermal Stress on Twisted Pairs’, in *2021 IEEE Conference on Electrical Insulation and Dielectric Phenomena (CEIDP)*, Dec. 2021, pp. 543–546. doi: 10.1109/CEIDP50766.2021.9705328.
[159] M. Szczepanski, L. Fetouhi, M. Sabatou, S. Pin, and G. Belijar, ‘PD energy as a marker of low-voltage insulation aging’, in *2021 IEEE Electrical Insulation Conference (EIC)*, Jun. 2021, pp. 377–380. doi: 10.1109/EIC49891.2021.9612374.

[160] P. Pietrzak *et al.*, ‘Effect of voltage and frequency cycling on the lifetime of enameled wires for low voltage inverter-fed motors’, in *2021 IEEE Conference on Electrical Insulation and Dielectric Phenomena (CEIDP)*, Dec. 2021, pp. 163–166. doi: 10.1109/CEIDP50766.2021.9705459.
[161] G. C. Montanari, A. Cavallini, F. Ciani, and A. Contin, ‘Accelerated aging, partial discharges and breakdown of Type II turn-to-turn insulation system of rotating machines’, in *2016 IEEE Electrical Insulation Conference (EIC)*, Jun. 2016, pp. 190–193. doi: 10.1109/EIC.2016.7548692.
[162] G. C. Montanari and P. Seri, ‘The effect of inverter characteristics on partial discharge and life behavior of wire insulation’, *IEEE Electr. Insul. Mag.*, vol. 34, no. 2, Art. no. 2, Mar. 2018, doi: 10.1109/MEI.2018.8300442.
[163] M. S. Moonesan, S. Jayaram, E. Cherney, R. Omranipour, and S. Ul Haq, ‘Effect of voltage rise time on time-to-failure of form-wound stator coil enamelled turn insulation’, in *2014 IEEE Electrical Insulation Conference (EIC)*, Jun. 2014, pp. 167–171. doi: 10.1109/EIC.2014.6869368.
[164] A. Rumi, A. Cavallini, and L. Lusuardi, ‘Impact of WBG Converter Voltage Rise-Time and Switching Frequency on the PDIV of Twisted Pairs’, in *2020 IEEE 3rd International Conference on Dielectrics (ICD)*, Jul. 2020, pp. 902–905. doi: 10.1109/ICD46958.2020.9341897.
[165] D. C. Montgomery, *Design and analysis of experiments*, Eighth edition. Hoboken, NJ: John Wiley & Sons, Inc, 2013.

List of Figures

List of Tables